WIND-TUNNEL INVESTIGATION OF THE

RUCK-A-CHUCKY SUSPENSION BRIDGE

by

J. E. Cermak*, B. Bienkiewicz** and
J. A. Peterka***

for

T. Y. Lin International
315 Bay St.
San Francisco, CA 94133

Fluid Dynamics and Diffusion Laboratory
College of Engineering
Colorado State University
Fort Collins, Colorado 80523

* Director, Fluid Dynamics and Diffusion Laboratory.
** Research Assistant, Fluid Mechanics and Wind Engineering Program, Department of Civil Engineering.
*** Associate Professor, Fluid Mechanics and Wind Engineering Program Department of Civil Engineering.

July 1977

CER77-78JEC-BB-JAP11

RUCK-A-CHUCKY BRIDGE

ACKNOWLEDGMENTS

Support for this study was provided by T. Y. Lin International. Construction of the section bridge model was accomplished by personnel of the Engineering Research Center Machine Shop. Mr. James A. Garrison made motion and still pictures of flow visualization. Data collection was facilitated by the assistance of Mr. Don Patzer.

Advice on formulation of the testing program and initial design of the model by Dr. R. H. Scanlan, Princeton University, and Mr. H. R. Bosch, Fairbank Research Laboratory, U.S. Federal Highway Administration, was very helpful.

ABSTRACT

A section model of the proposed Ruck-A-Chucky Bridge and a topographic model of its site were used in the wind tunnel study. Freely oscillating section models of the original and modified bridge decks were applied to investigate aerodynamic derivatives. Steady drag, lift and pitching moment were measured for the rigidly supported model.

Wind parameters (velocity profiles and turbulence characteristics) for the bridge site were measured on the topographic model.

Flow visualization for both the section and topographic model was used to determine nature of the flow field and detect regions of separation and vortex formation.

The aerodynamic derivatives indicate stable behavior of the proposed bridge decks, although the smooth bridge deck (without fences and railings) shows slight coupling between flexural and torsional modes.

Further analysis for the entire bridge, using the wind tunnel derived aerodynamic coefficients, is necessary to predict its overall aerodynamic stability.

TABLE OF CONTENTS

LIST OF SYMBOLS

Symbol	Description
λ_L	geometrical scale
λ_v	velocity scale
U	mean velocity
N	frequency, cps.
δ_n	logarithmic decrement of damping for n cycles
A_n	amplitude of motion after n cycles
A_o	initial amplitude of motion
ζ	damping ratio--actual/critical
n	number of cycles
a	decay coefficient
A_i, H_j	aerodynamic derivative (i = 2,3, j = 1)
ζ_α (ζ_h)	damping ratio for angular (vertical) degree of freedom
ω_α (ω_h)	circular frequency for undamped oscillations in angular (vertical) mode
A_i^*, H_j^*	nondimensional aerodynamic derivative (i = 2,3, j = 1)
I	deck moment of inertia about c.g. per unit span
m	deck mass per unit span
ρ	mass density of air
B	deck width
ω	net circular frequency
F_L(F_D)	steady lift (drag) force
M	steady pitching moment
C_L(C_D)[C_M]	lift (drag) [moment] coefficient per unit span
S	projected crosswind area
L(h)	deck length (depth)

LIST OF FIGURES

LIST OF TABLES

1. INTRODUCTION

Wind loading is a very important factor in an analysis of long-span suspension bridges. Wind characteristics depend on a site and are affected by geographical latitude, topography and location relative to large bodies of water. A bridge response is governed by its structural properties and geometry. Interaction between wind loading and structure response presents an aeroelastic problem. Its analysis cannot be conducted in a purely analytical way and some experimental work is needed. Physical modeling in wind tunnels fulfills a gap between existing theoretical models and techniques necessary to solve complex practical problems. Aerodynamic analysis of suspension bridges represents one of them.

A wind-engineering study, reported herein, has been performed for the proposed Ruck-A-Chucky Bridge, California. The main purpose of this work was to find--by means of modeling in a wind tunnel--aerodynamic derivatives (of self-excited motions) for the proposed bridge decks.

A freely oscillating, mechanically sprung, section model (a short length of the bridge deck between end plates) was used. An approach developed by Scanlan (1-5) was adopted to obtain dynamic characteristics of the bridge.

Scales of turbulence usually realized in wind tunnels imply that the model scales should be very small for bridges in order for the ratio of the turbulence integral scale to deck width to be equal to prototype values. Since a large geometrical scale (1:40) was selected for the Ruck-A-Chucky Bridge section model, laminar flow with constant wind velocity was used in accordance with common procedure. Although recent work by Lin (6) indicates influence of the free-stream turbulence upon the aerodynamic derivatives, section-model testing under laminar flow may generally be considered to give conservative results, Scanlan (4).

The aerodynamic derivatives, defined by Scanlan (3), were obtained for the original and slightly modified bridge decks. Steady drag, lift and pitching moment were measured for the rigidly supported model.

Wind parameters (velocity profiles and turbulence characteristics) for the bridge site were measured on the topographic (1:1920 geometrical scale) model.

Flow visualization for both the section and topographic model as well as direct observation of the section-model dynamic behavior completed the presented wind tunnel study.

The main part of this report is devoted to the section-model investigations. Experimental configurations, testing procedures, instrumentation and data acquisition are presented below. In Appendix A, detailed results referring to aerodynamic characteristics of bridge decks for different configurations is collected. A brief description of testing procedures and results for the topographic model tests is given in Appendix B.

2. EXPERIMENTAL CONFIGURATIONS

2.1 Wind Tunnel Facility

The experiments reported herein were conducted in the Industrial Aerodynamics Wind Tunnel located in the Fluid Dynamics and Diffusion Laboratory at Colorado State University.

The Industrial Aerodynamics Wind Tunnel shown in Figure 1 is a closed circuit facility driven by a variable-pitch propeller. The test section is nominally 6 ft square and approximately 62 ft long with flow entering through a contraction having a 4-to-1 contraction ratio. The mean velocity is adjustable continuously from 1 to 65 fps.

2.2 General Assumptions

The section model is geometrically and dynamically similar to a short section of the prototype bridge deck. Although the Ruck-A-Chucky Bridge as shown by Figure 2 is curved in a plane, a straight section was modeled since it represents a length of the whole bridge, small relative to the radius of curvature. Wind perpendicular to the model centerline was assumed to be the most critical for stability. The model was constructed in such a way that an angle of attack could be changed from -6 to +6 degrees. Since laminar flow was assumed, the model together with a supporting frame, were placed at the test section entrance of the wind tunnel as shown in Figure 1 where the turbulence intensity is very low and scales are small compared to the bridge section width.

2.3 Model Scaling

A section of the bridge shown in Figure 3 was modeled at a geometrical scale λ_L of 1:40. The velocity scale λ_V, according to the Froude number equality for the model and a prototype is given by the following relationship:

$$\lambda_v = \lambda_L^{1/2}$$

The mass scale λ_m implied by the geometrical scale is

$$\lambda_m = \lambda_L^3$$

Elastic properties of the model (represented by supporting springs) were calculated on the basis of a reduced velocity equivalence

$$\left(\frac{U}{NB}\right)_{model} = \left(\frac{U}{NB}\right)_{prototype}$$

where U = mean velocity, N = frequency in Hertz, and B = deck width. In the previous dynamic calculations for the prototype bridge, the first mode shown in Figure 4 was used for vertical motion and the sixth mode shown in Figure 5 for torsional (angular) motion--T. Y. Lin (7). Values of particular parameters for the prototype and the "exact" model are given in Table 1. These "exact" values are compared with those actually achieved for the model (the original, modified and "smooth" bridge decks). The comparative values are given in Table 2 and show a large discrepancy between the "exact" and realized frequency for angular motion. However, as shown by Scanlan (5) such a difference is permissible and does not affect conclusions on stability. No attempt was undertaken to duplicate a particular value of prototype damping. However, the model was constructed to have a damping ratio lower than is estimated for full-scale suspension bridges.

2.4 Some Model Details

The section model was made of a dense styrofoam core bonded to a thin aluminum skin. Almost all structural elements were constructed of aluminum. The end plates were composed of two materials: magnesium (the smaller plates), and balsa wood (the larger, external plates), as shown in Figures 6(a) and 6(b) respectively.

The suspension system shown in Figure 7 consisted of supporting beams, pre-tensioned coil springs, strain gauge transducers and turnbuckles attached to the rigid frame. This frame was dynamically isolated from wind-tunnel vibrations. The strain-gauge transducers for measurement of vertical and torsional motion are described in section 4.1. The section model was constructed in such a way that it was possible to modify the bridge deck geometry by replacing bridge deck fairings, fences and railings. Details of the deck configurations studied are given by Figures 8 and 9.

3. TESTING PROCEDURES

3.1 Aerodynamic Derivatives

The basic parameters involved in aerodynamic derivative calculations are damping and frequency of the freely oscillating model. These two parameters may be calculated from time-history records of the model vibrating respectively in a vertical and angular mode without coupling. In the case of coupling between these two modes a phase shift between them is an additional parameter that can be also calculated from the records of motion decay.

Since no coupling (except slight coupling for the "smooth" model) was observed during experiments with the Ruck-A-Chucky Bridge section model, aerodynamic coefficients were calculated only for uncoupled motions. For a vertical (angular) motion the model was released from its initial vertical (angular) displacement and its free damped oscillations were recorded. Experiments were repeated at different wind velocities for the bridge decks shown in Figure 8 and model configurations shown in Figure 10.

3.2 Drag, Lift and Pitching Moment

During drag, lift and pitching moment measurements the suspension system was modified and the model was rigidly supported. Data taken were averaged and drag, lift and moment coefficients were computed. Experiments were performed for the modified bridge deck (c.f. Figure 8) in a range of an angle of attack from -3 to +3 degrees. Measurements were repeated for three different wind velocities to determine if these coefficients were Reynolds number dependent.

4. INSTRUMENTATION

4.1 Model Arrangement for Measurement of Aerodynamic Response

The two strain-gauge systems shown in Figure 11 were used to detect a vertical and an angular motion. The signals from both sides of the model were averaged. By this means the influence of rolling motion of the model (rotation about a model axis of symmetry parallel to the air stream), observed in some range of wind velocity, was reduced. Amplified signals from the strain-gauge bridges were recorded by strip recorders. The strain gauges were mounted on channels as indicated by Figure 12 to eliminate an influence of spring torsion upon strain readings. The calibration of both the strain-gauge systems indicated a linear relationship between input and output. A typical example of the calibration--for vertical motion--is shown in Figure 13.

4.2 Model Arrangement for Measurement of Drag, Lift and Pitching Moment

The same strain-gauge systems used for aerodynamic response measurements were employed for lift force and pitching moment measurements. For these measurements the model was rigidly supported by attaching stiff rods to the suspension springs as indicated in Figure 14. As an example, a calibration curve for the lift force is shown in Figure 15. Lift force and pitching moment were measured at the same time. The special support for drag-force measurements is shown in Figure 16 with the associated strain-gauge wiring given in Figure 17. As well as for the lift and moment, only averaged steady values of the drag force were obtained, from which nondimensional coefficients were calculated. The calibration for the drag force is presented in Figure 18.

5. DATA ACQUISITION AND RESULTS

5.1 Aerodynamic Derivatives

Time-history records of motion (typical records for different velocities are shown in Figure 19) were used to calculate aerodynamic derivatives. Each record was divided into three sections. For each section logarithmic decrement of damping for n cycles

$$\delta_n = \ell n \left(\frac{A_n}{A_o}\right)$$

where A_n = amplitude of motion after n cycles, A_o = initial amplitude of motion, and the ratio of actual to critical damping (damping ratio)

$$\zeta = \frac{1}{\sqrt{1 + \left(\frac{2\pi n}{\delta_n}\right)^2}}$$

were calculated. Mean values of δ_n, ζ (taken over mentioned above three record sections) were employed. The aerodynamic derivatives are given by the following formulas for the vertical deflection h and the torsional rotation α as formulated by Scanlan (3):

$$\ddot{h} + 2\zeta_h \omega_h \dot{h} + \omega_h^2 h = H_1 \dot{h} + H_2 \dot{\alpha} + H_3 \alpha$$

$$\ddot{\alpha} + 2\zeta_\alpha \omega_\alpha \dot{\alpha} + \omega_\alpha^2 \alpha = A_1 \dot{h} + A_2 \dot{\alpha} + A_3 \alpha .$$

When the motion is uncoupled, stability (or instability) can be established by determination of the aerodynamic derivatives H_1, A_2 and A_3.

These three coefficients are related to physical properties of the system as follows:

$$A_2 = 2\,(a + \zeta_\alpha \cdot \omega_\alpha)\ ,$$

$$A_3 = \omega_\alpha^2 - \omega^2 - a^2 \quad \text{and}$$

$$H_1 = 2(a + \zeta_h \cdot \omega_h)\ .$$

In these expressions

$$a = -\zeta\ \omega_i \qquad (i = \alpha, h)$$

$$\omega = \omega_i \sqrt{1 - \zeta^2} \qquad (\ i = \alpha, h)$$

ω_i = circular frequency for undamped oscillations,

$(\ )_\alpha$ = quantity referring to angular motion in still air, and

$(\ )_h$ = quantity referring to vertical motion in still air.

Their nondimensional counterparts are defined by Scanlan (3) as follows:

$$A_2^* = \frac{A_2 \cdot I}{\rho \cdot B^4 \cdot \omega}\ ,$$

$$A_3^* = \frac{A_3 \cdot I}{\rho \cdot B^4 \cdot \omega^2} \quad \text{and}$$

$$H_1^* = \frac{H_1 \cdot m}{\rho\ B^2\ \omega}$$

where B = deck width, I = deck moment of inertia about c.g. per unit span, m = deck mass per unit span, ρ = density of air, and ω = circular frequency.

The nondimensional derivatives A_2^*, A_3^*, H_1^* (denoted as A2S, A3S, H1S) were evaluated for the different bridge decks shown in Figure 8 and the different configurations illustrated in Figure 10. Final results for the modified, original and smooth bridge decks are collected respectively in Appendices A.1, A.2 and A.3. They were slightly smoothed to reduce scattering caused by imperfect damping evaluation. In Appendix A.4, a typical aerodynamic derivative before and after smoothing is shown as an example.

5.2 Drag, Lift and Moment Coefficients

The drag force, lift force and moment were nondimensionalized on the basis of a projected crosswind area of the bridge model as follows:

$$C_i = \frac{F_i}{1/2\rho U^2 S} \qquad (i = L,D) \text{ and}$$

$$C_M = \frac{M}{1/2\rho U^2 SB}$$

where $F_D(F_L)$ = drag (lift) force,

M = pitching moment,

$C_D(C_L)[C_M]$ = steady drag (lift) [moment] coefficient,

$S = Lh$ = projected crosswind area (based on smooth deck depth as defined by Fig. 20),

B = deck width, and

ρ = mass density of air.

Measurements were performed for the modified bridge deck (see Fig. 8) for angles of attack in a range from -3 to +3 degrees. They were repeated for three different wind velocities. The Reynolds number based on the bridge deck width varied from 1.9 to 3.4 x 10^5. For each configuration a series of 10 single measurements was taken. The mean values of these measurements were the basis for calculations of drag, lift and moment coefficients. Their final values (c.f. Figs. 21-23) are averages of the values for different Reynolds numbers. Previous investigations--Scanlan (4)--have shown that the drag coefficient becomes independent of Reynolds number at the values for this investigation.

It was observed during experiments that drag force, lift force and moment forces were highly unsteady. It is obvious that averaging process over 10 values series is only a rough estimation of an expectation. Therefore drag, lift and moment coefficients (shown in Figs. 21-23) should be considered as an approximation of their true steady values.

6. FLOW VISUALIZATION

In an effort to determine the nature of flow over the bridge deck smoke (titanium chloride) was introduced at several critical locations near and on the model. A permanent record of the flow for study of the relationships between flow characteristics and model response was obtained by both still and motion-picture photography.

Flow visualization was performed for the most part on the modified bridge deck shown in Figure 8 although some visualizations were repeated for the smooth deck (configuration B, 0° angle of attack). The representative configuration B (c.f. Fig. 10) was chosen for different angles of attack (-3°, 0°, +3°) with the model rigidly supported and with the model freely oscillating. For the oscillating bridge deck the smoke source was attached to the model.

Both still and movie pictures taken during the flow visualization are a supplemental part of this report. Figures 24-29 show features of flow patterns around the still bridge (modified) deck. Vortex formation at the leading and trailing edge as well as flow separation along upper and lower surface of the deck can be observed. The Figures 30-31 were taken for the model oscillating in a vortical mode. These photographs show clearly, vortex formation at the trailing edge (Fig. 30) and a wake behind the model (Fig. 31). More information regarding flow characteristics of the oscillating as well as the fixed model is given by the movie pictures. A 470 ft, 13 minutes film is included as a part of this report. A listing of contents of the film is given in Table 3. The motion pictures reveal more clearly the unsteady character of airflow around the bridge deck both in the case of the still and oscillating model. Again, almost steady vortex shedding can be observed.

7. CONCLUSIONS

1. No instability for the oscillating section model (all the bridge decks) was observed in a range of reduced velocity from 0 to 6.

2. The original bridge deck was unstable (flutter) at very high reduced velocity ($V/NB \approx 9.5$).

3. Variation of the aerodynamic coefficient A_2^* with reduced velocity for all cases confirms Conclusion 1. However, further analytical analysis is necessary for predicting the full-bridge aerodynamic response.

4. No coupling between the vertical and angular modes was observed in case of the modified and original bridge deck. Slight coupling was observed for the smooth bridge deck.

5. Analysis of aerodynamic derivatives indicates a possibility of vortex-shedding induced vibrations at low wind speed.

6. Drag force, lift force, and pitching moment (for modified bridge deck) are highly unsteady. The steady nondimensional values for lift and pitching moment show higher dependence on an angle of attack than for drag which can be roughly assumed constant for angles of attack in the range -3 to 3 degrees.

8. REFERENCES

1. Sabzevari, A., Scanlan, R. H., "Aerodynamic Instability of Suspension Bridges," Jnl. Eng. Mech. Div., ASCE, vol. 94, No. EM2, April 1968.

2. Scanlan, R. H., Sabzevari, A., "Experimental Aerodynamic Coefficient in the Analytical Study of Suspension Bridge Flutter," Jnl. Mech. Eng. Science, Institution of Mech. Engrs., London, Vol. 11, No. 3, 1969.

3. Scanlan, R. H., Tomko, J. J., "Airfoil and Bridge Deck Flutter Derivatives," Jnl. Eng. Mech. Div., ASCE, Vol. 97, No. EM6, December, 1971.

4. Scanlan, R. H., "Recent Methods in the Application of Test Results to the Wind Design of Long, Suspended-Span Bridges," Report No. FHWA - RD 75-115, October, 1975.

5. Scanlan, R. H., "Theory of the Wind Analysis of Long-Span Bridges Based on Data Obtainable from Section Model Tests, Proc. of the 4th Int'l. Conf. Wind Effects on Buildings and Structures," London, 1975.

6. Lin, W. H., "Forced and Self-Excited Responses of a Bluff Structure in a Turbulent Wind," Doctoral Dissertation, Princeton University, December, 1976.

7. Lin, T. Y., International "Ruck-A-Chucky Steel Bridge, General Information," (Unpublished) September, 1976.

9. FIGURES

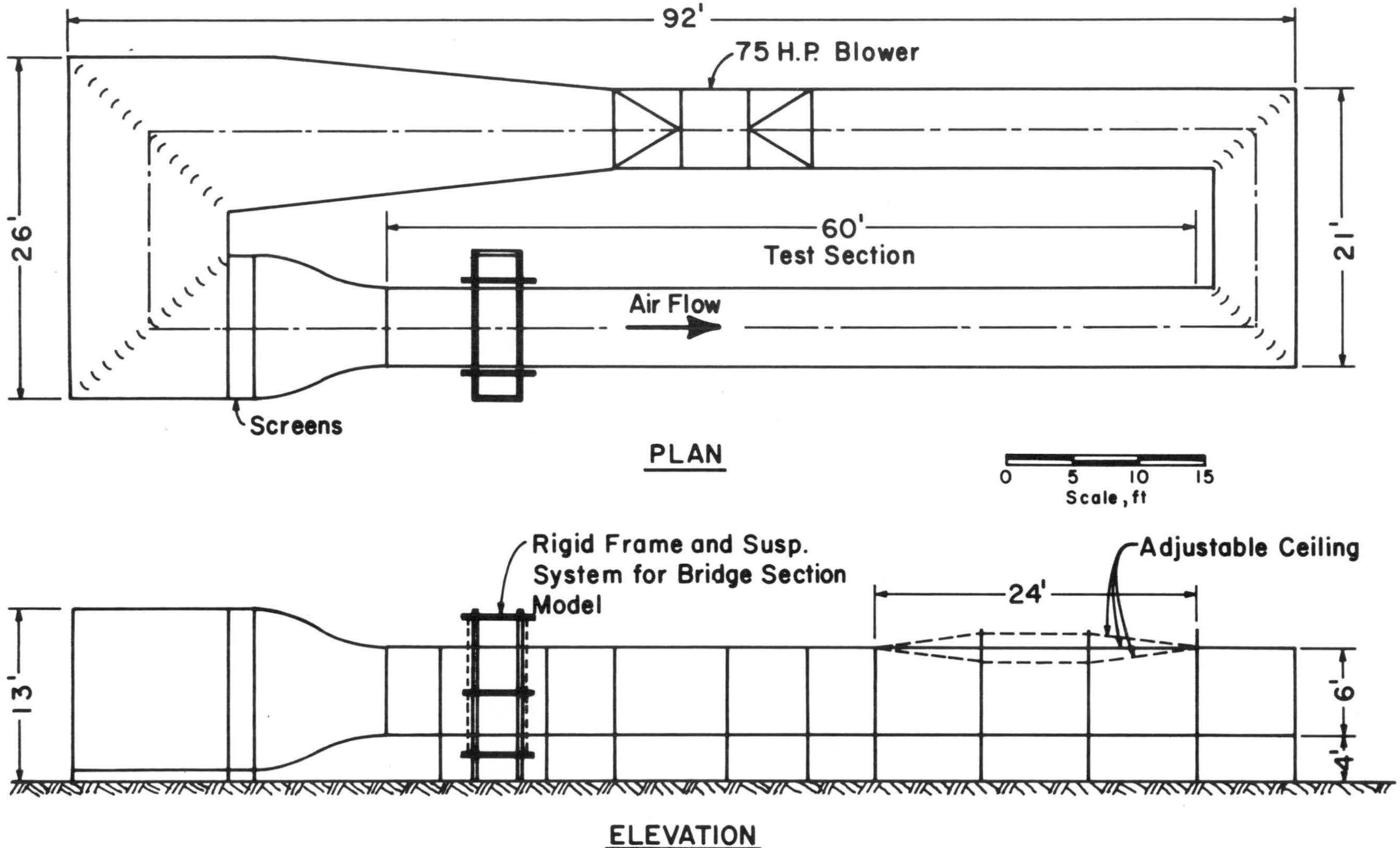

Fig. 1. Industrial Aerodynamic Wind Tunnel

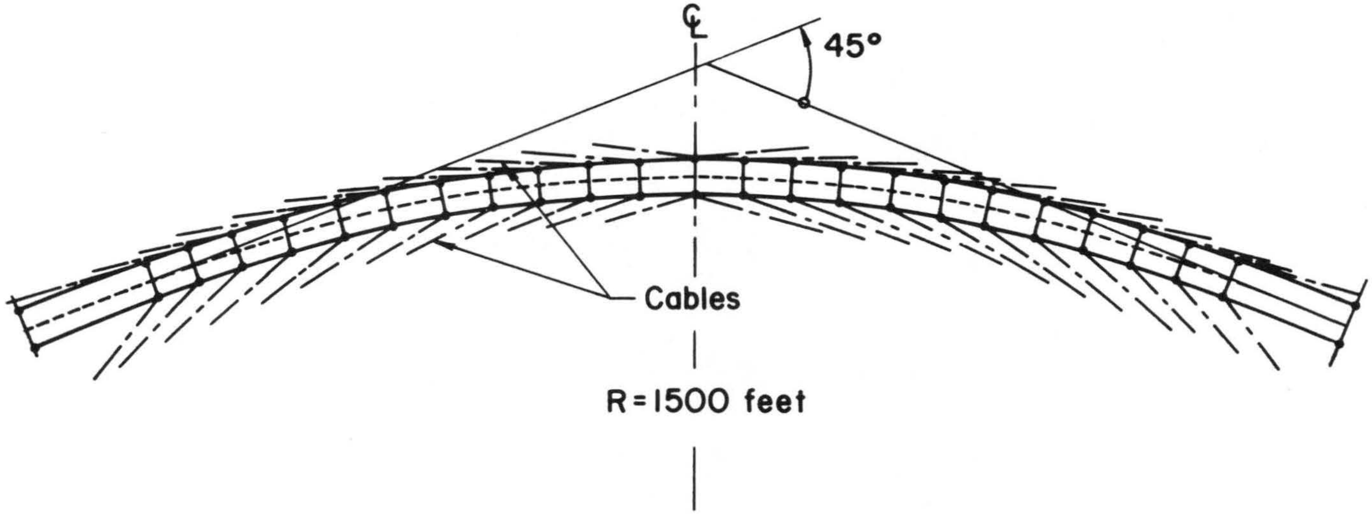

Fig. 2. Plan View of Ruck-A-Chucky Bridge Deck

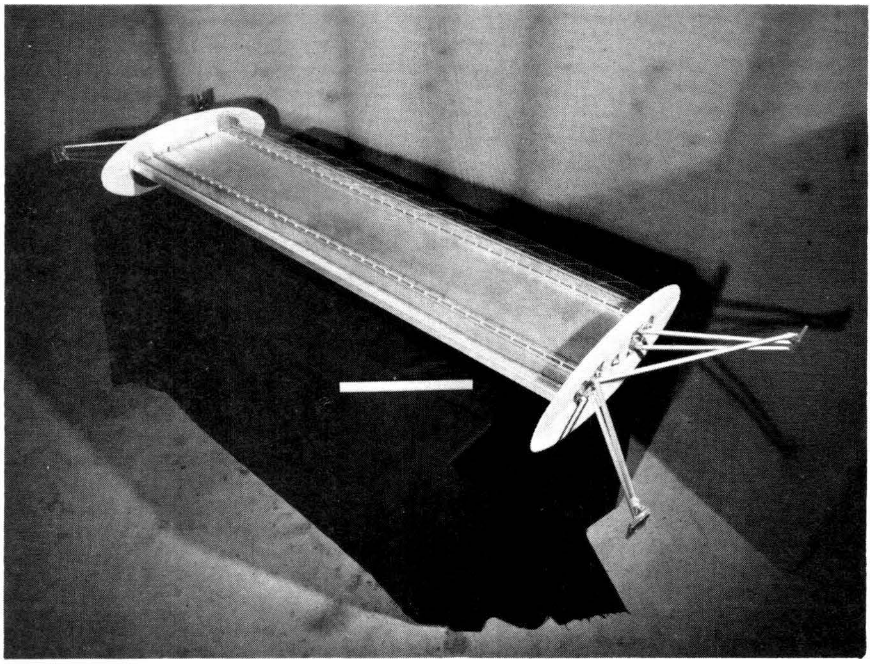

Fig. 3. Section Model of Bridge

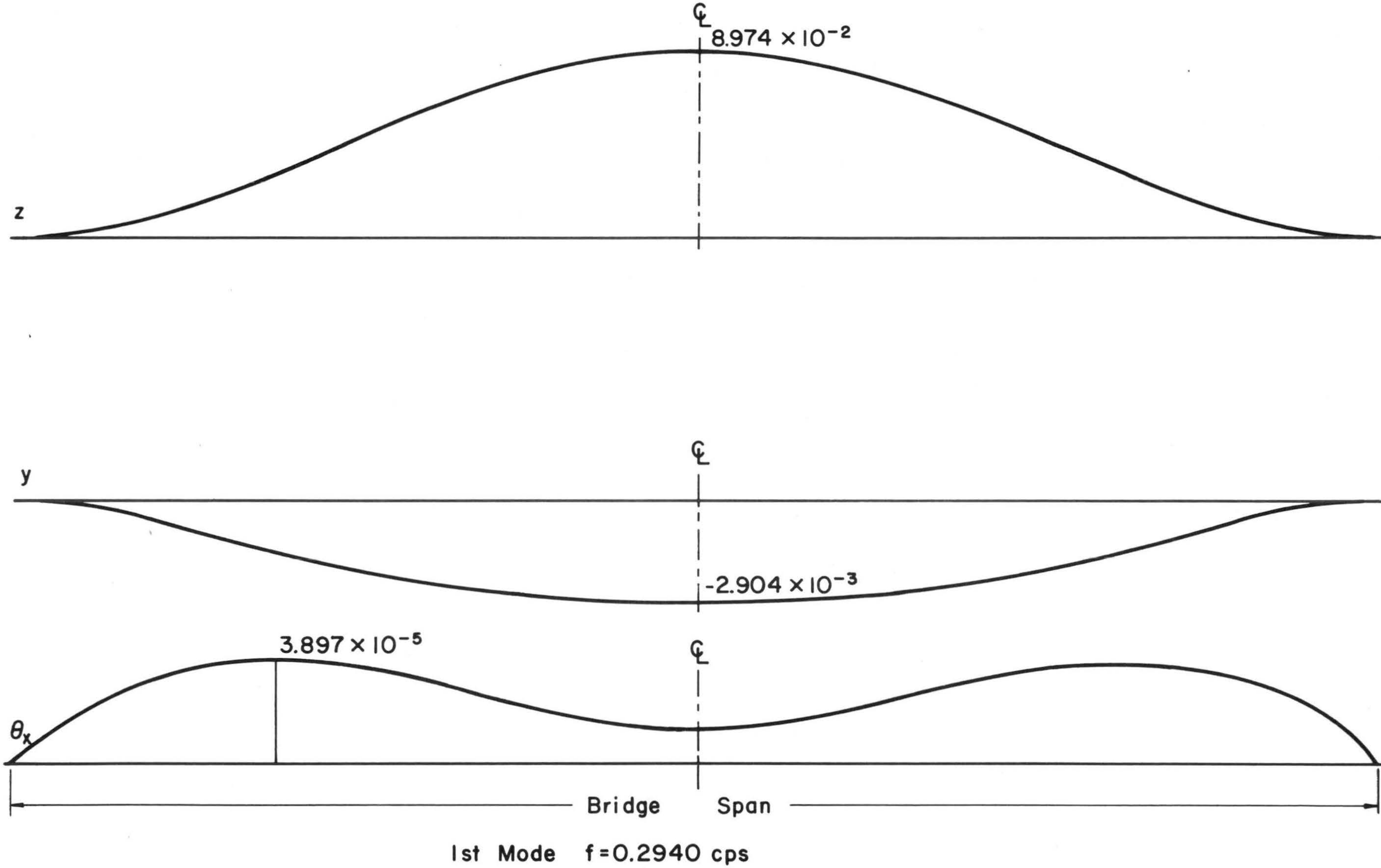

Fig. 4. Fundamental Bending Bridge Mode

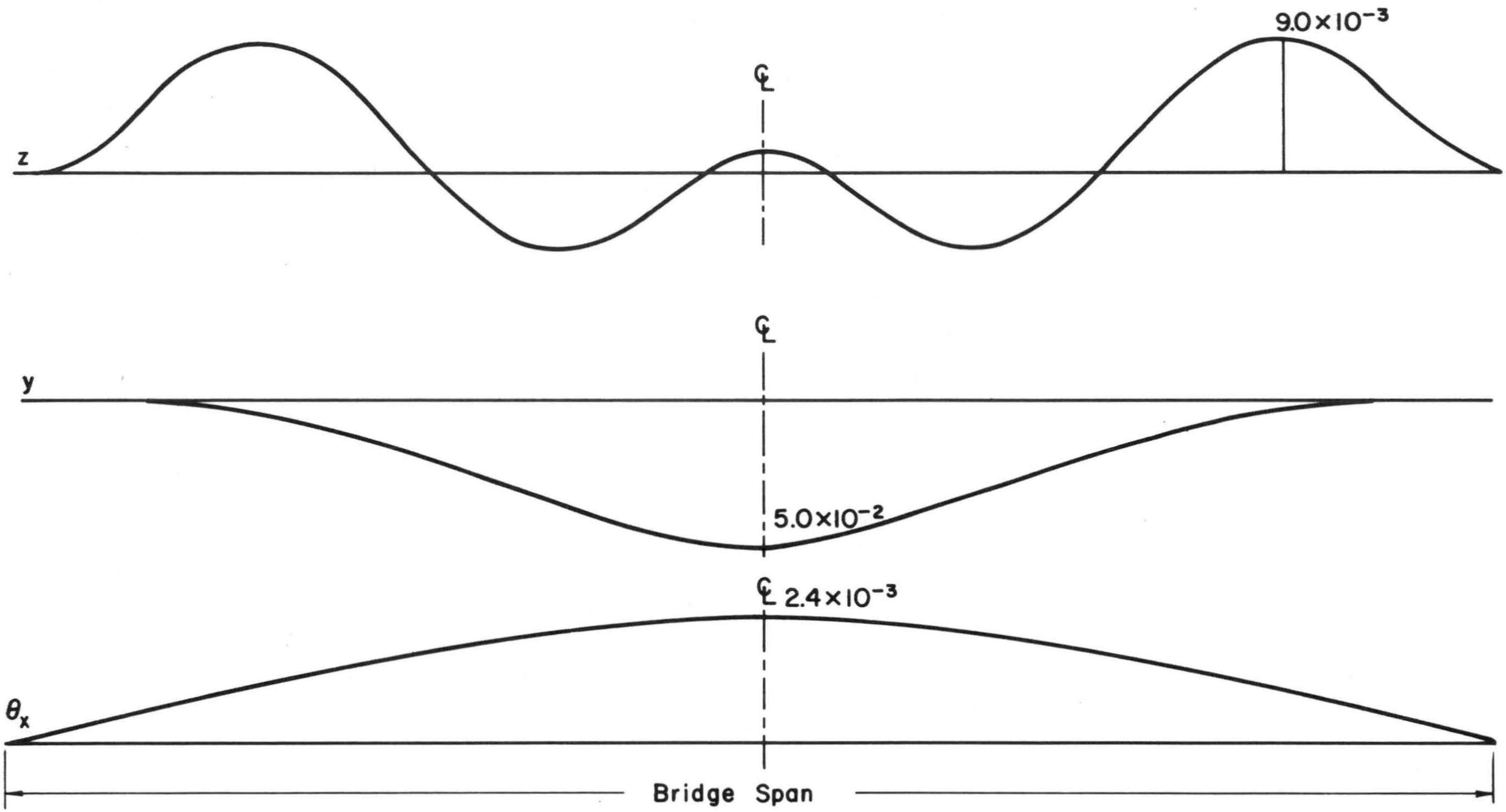

6th Mode f=0.9840 cps

Fig. 5. Fundamental Torsional Bridge Mode

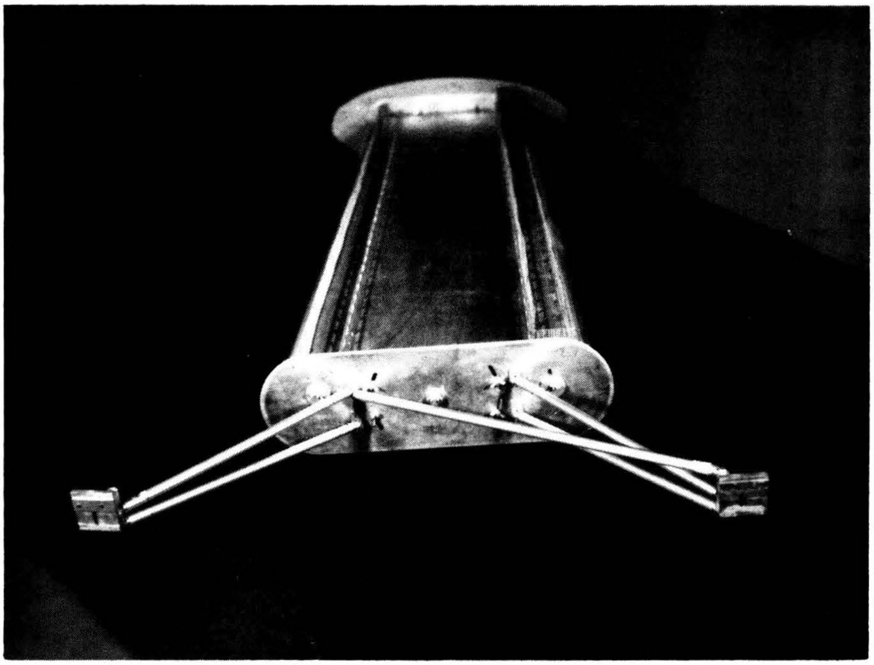

(a)

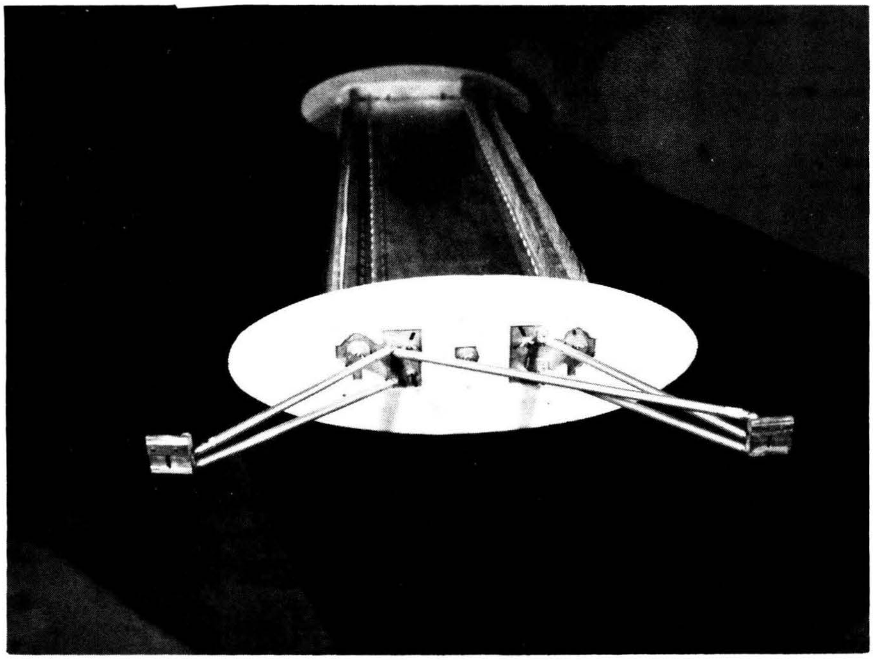

(b)

Fig. 6. End Plates

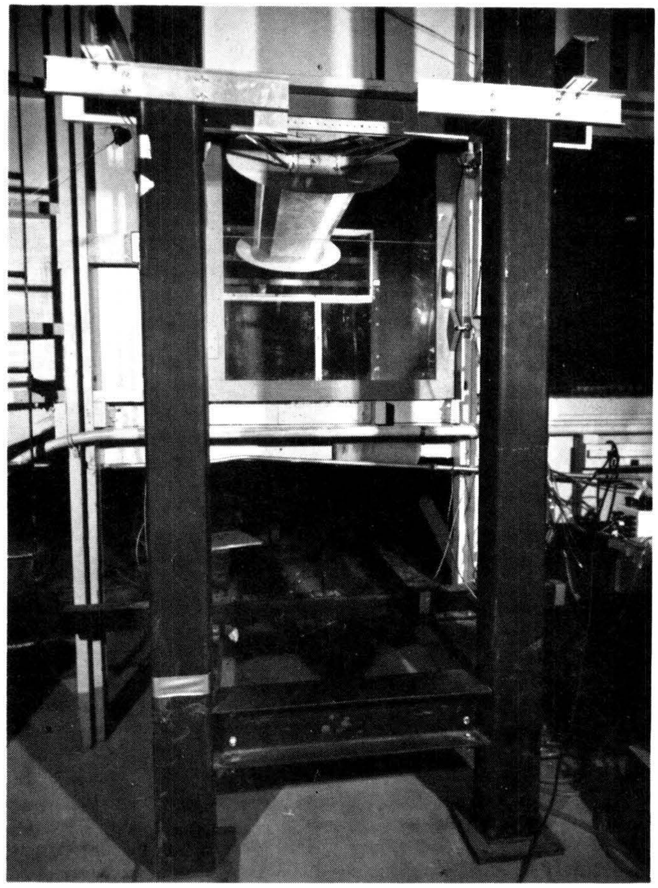

(a)

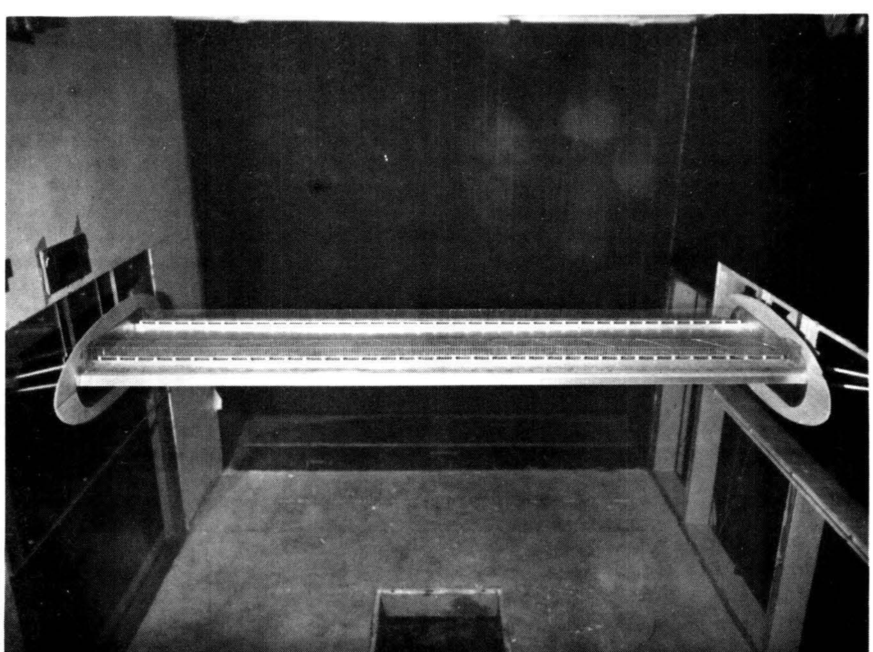

(b)

Fig. 7. General View of Model and Supporting Frame

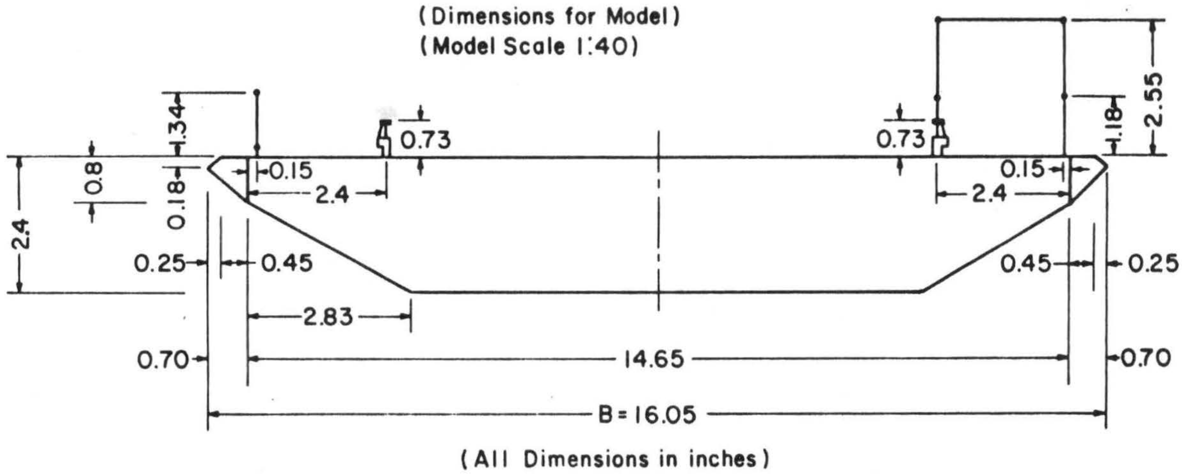

a. Original Deck

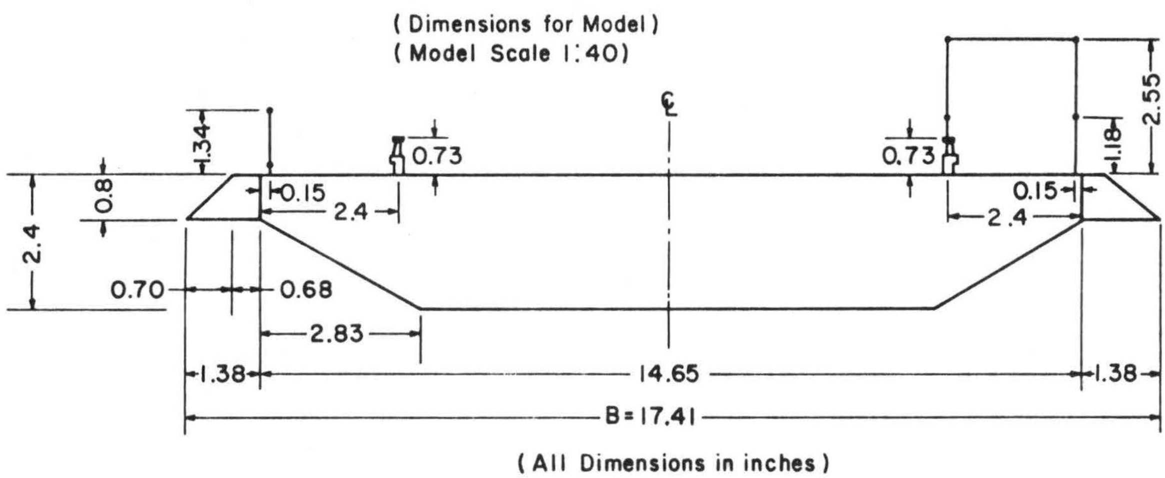

b. Modified Deck

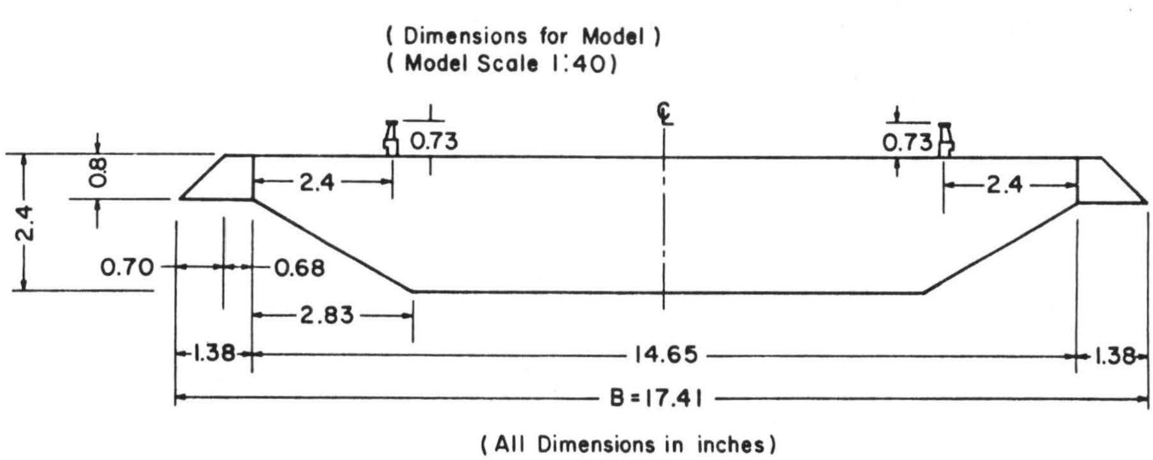

c. Smooth Deck

Fig. 8. Model Bridge Decks

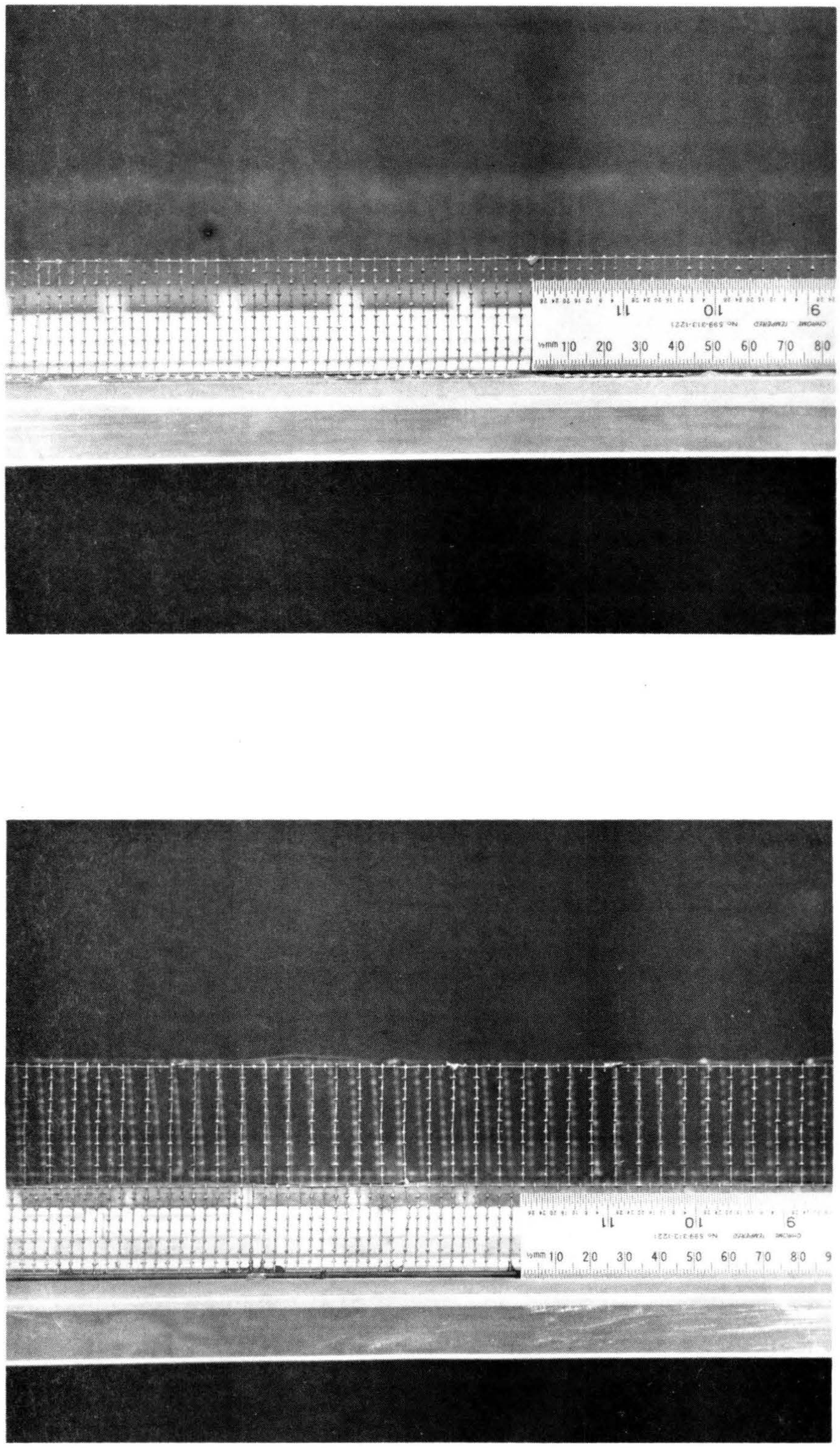

Fig. 9. Details of Fences

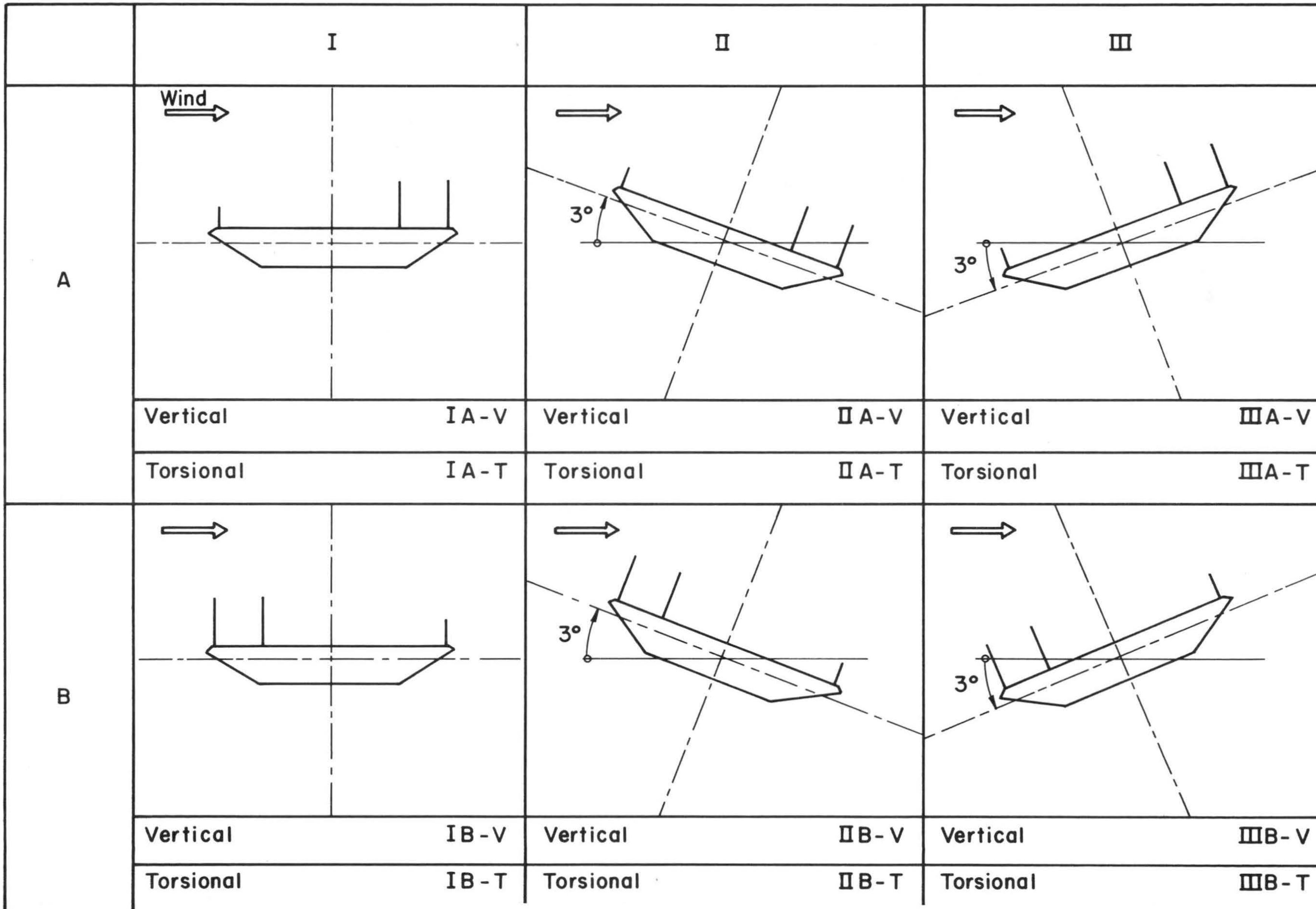

Fig. 10. Experimental Configurations

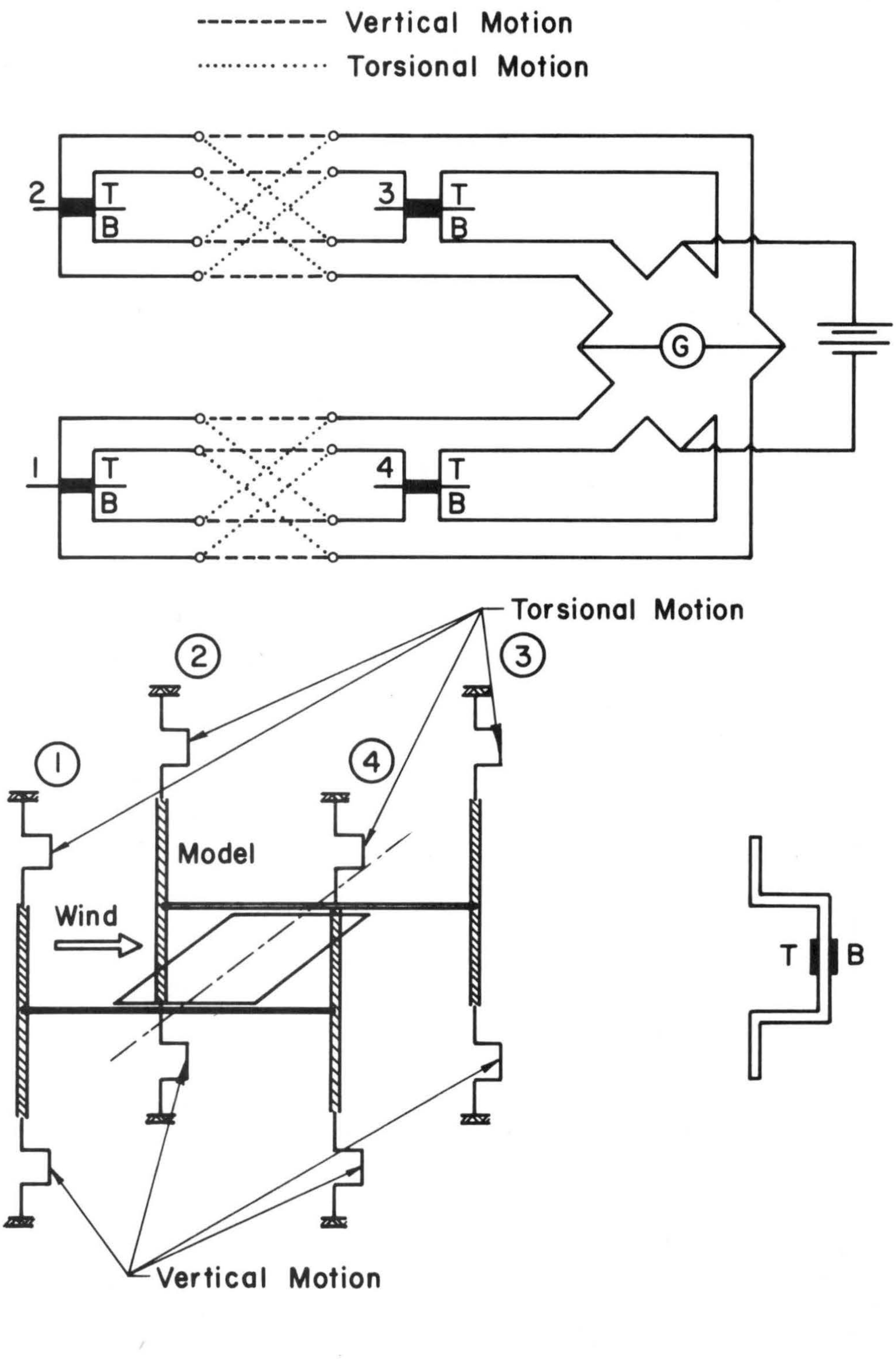

Fig. 11. Arrangement for Aerodynamic Measurements

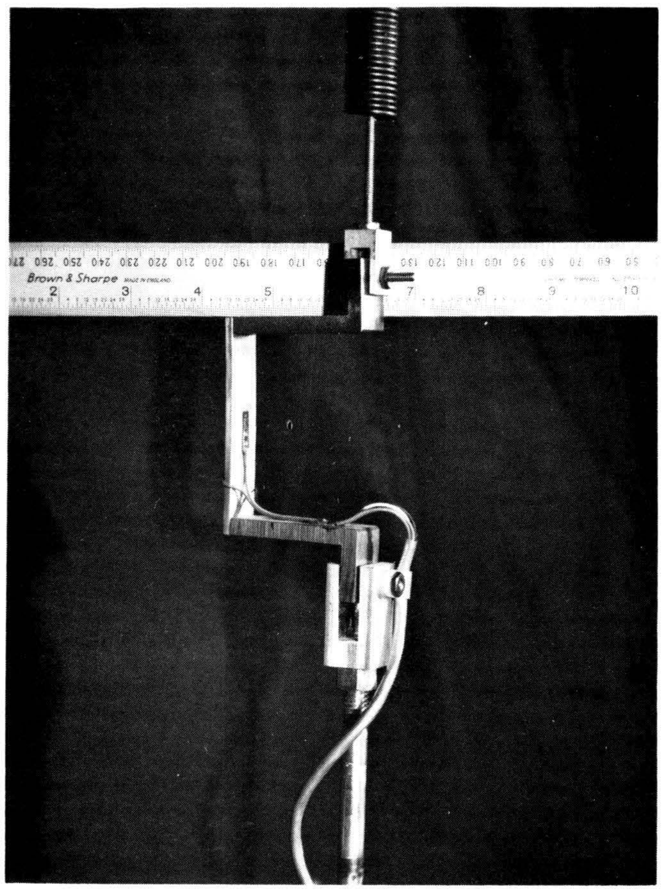

Fig. 12. Strain Transducer

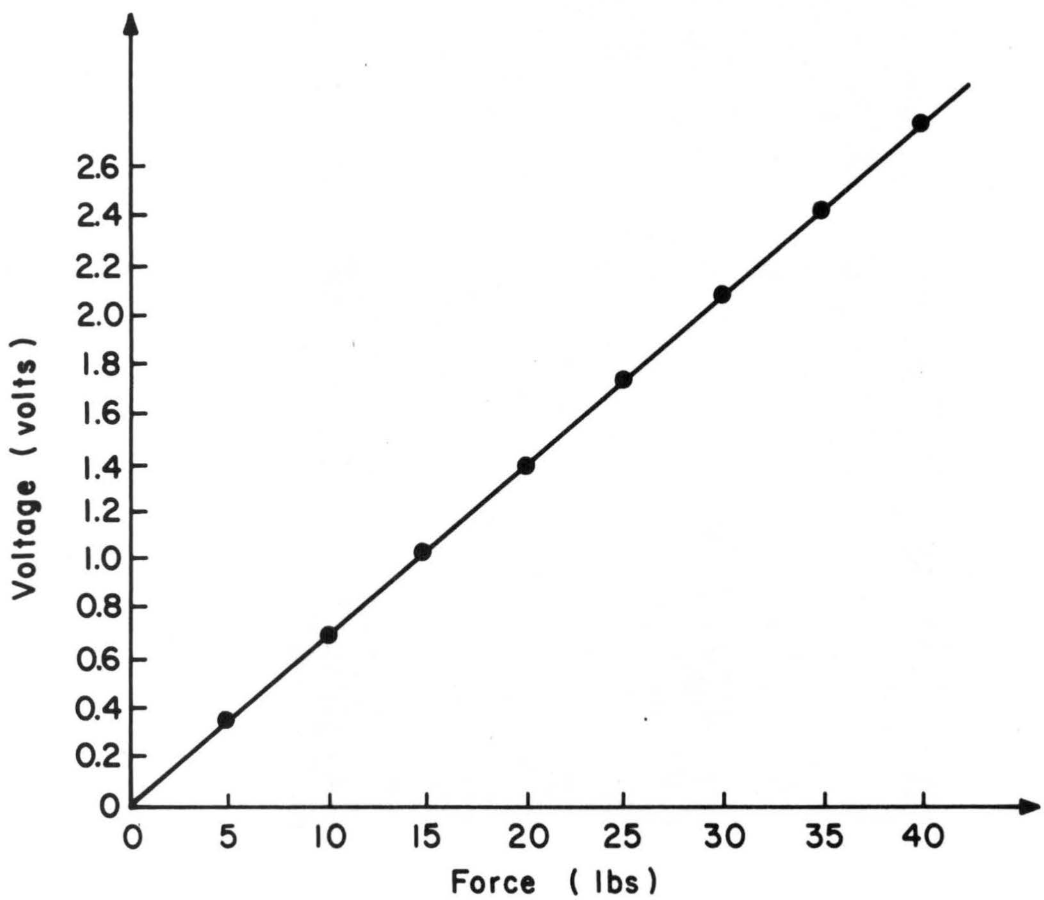

Fig. 13. Calibration for Aerodynamic Measurements (Vertical Mode)

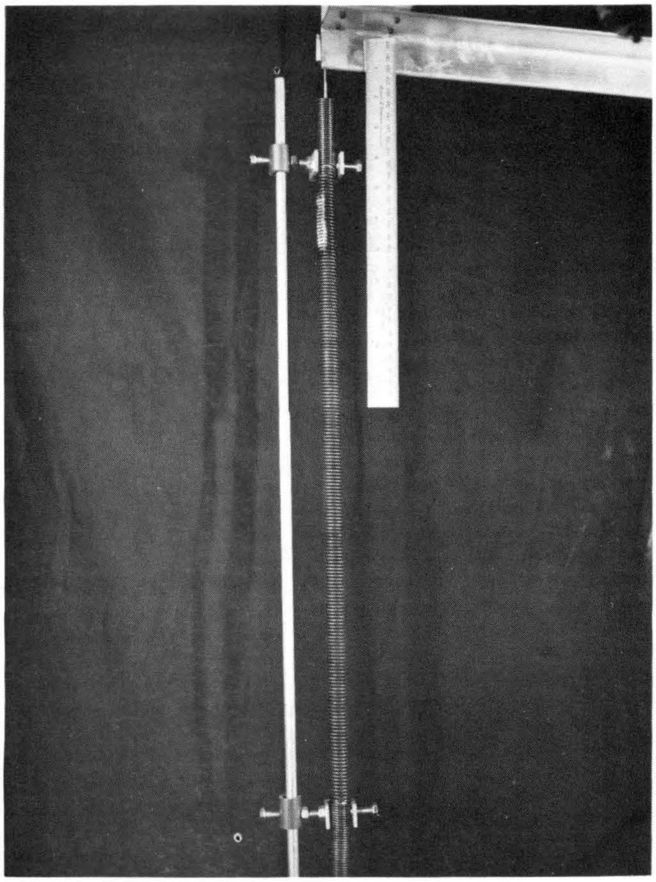

Fig. 14. Spring Stabilizer

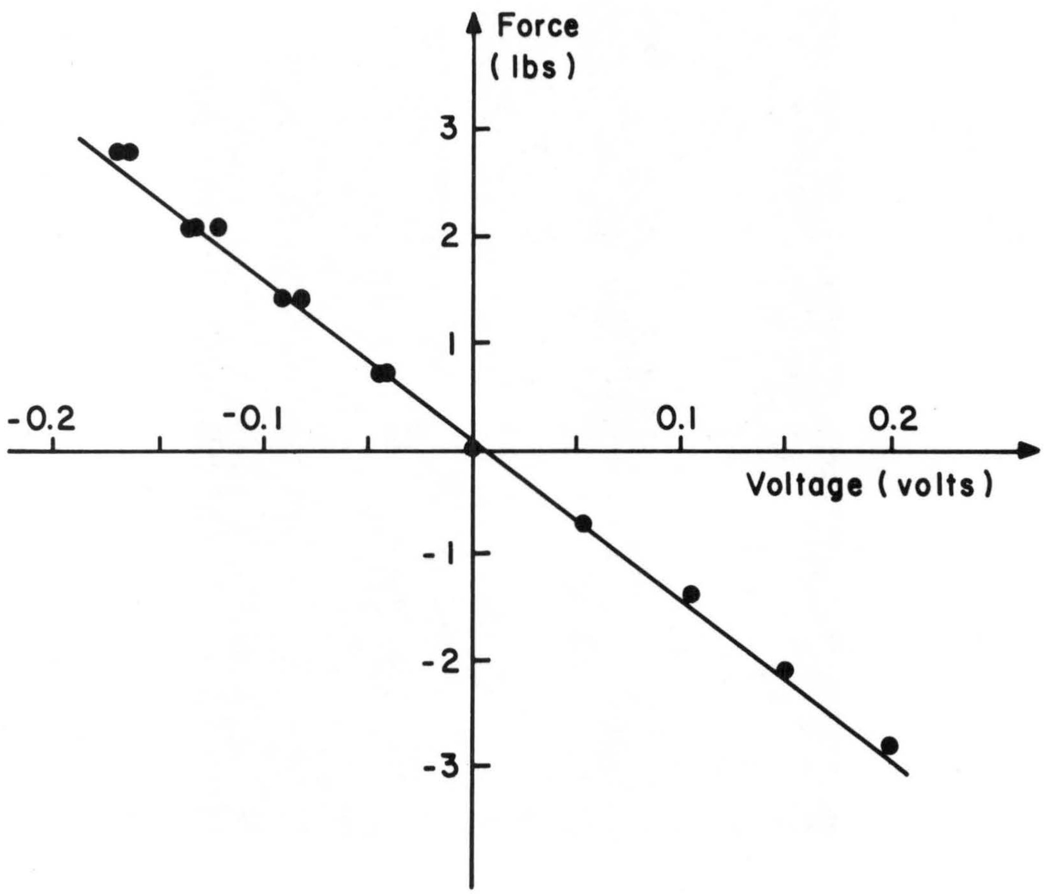

Fig. 15. Lift-Force Calibration

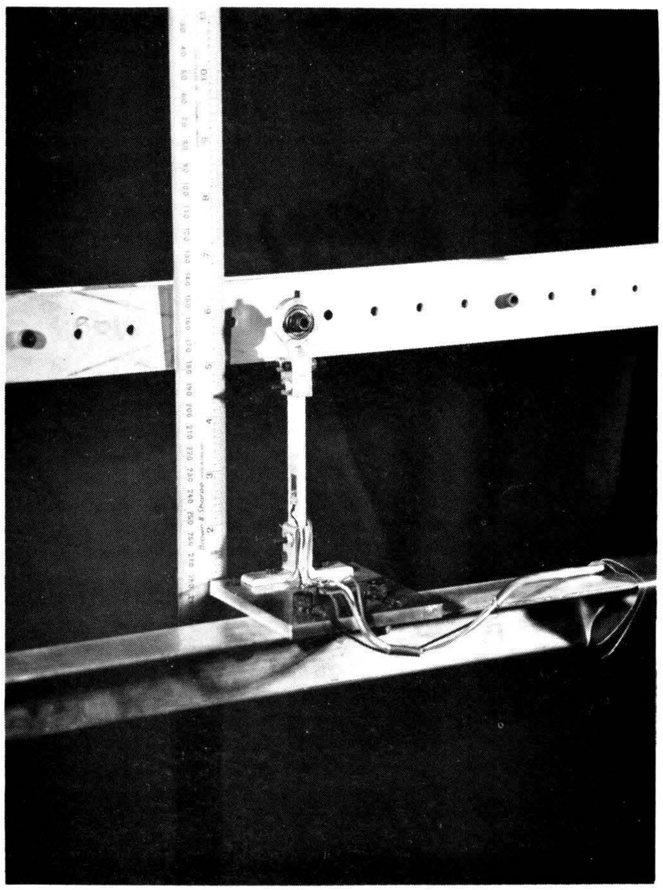

Fig. 16. Drag-Force Transducer

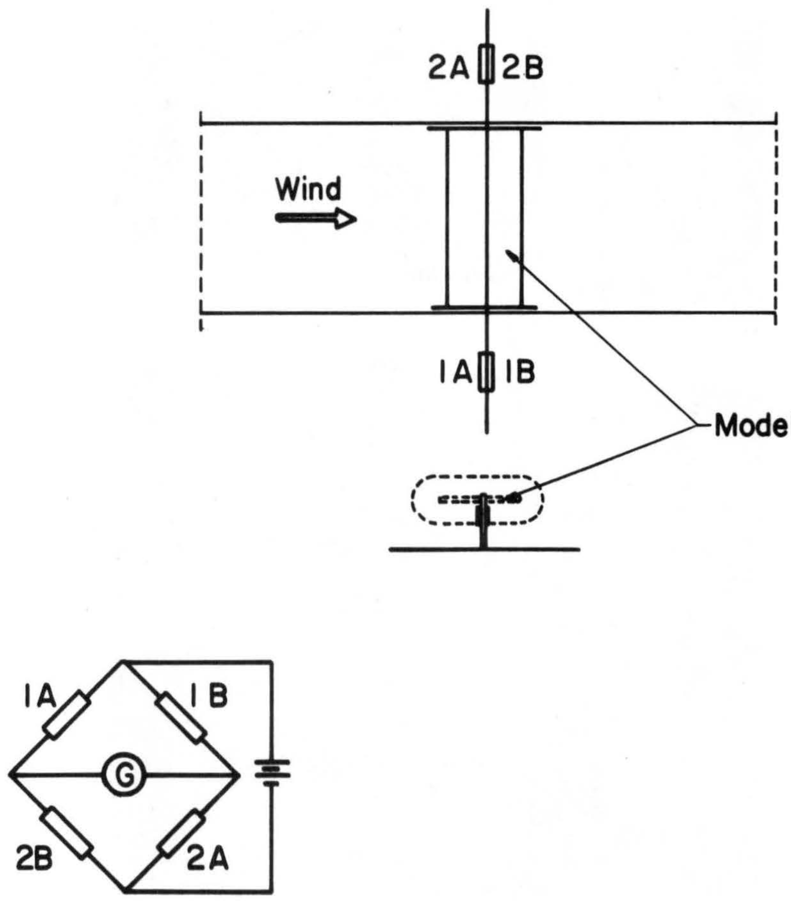

Fig. 17. Arrangement for Drag-Force Measurements

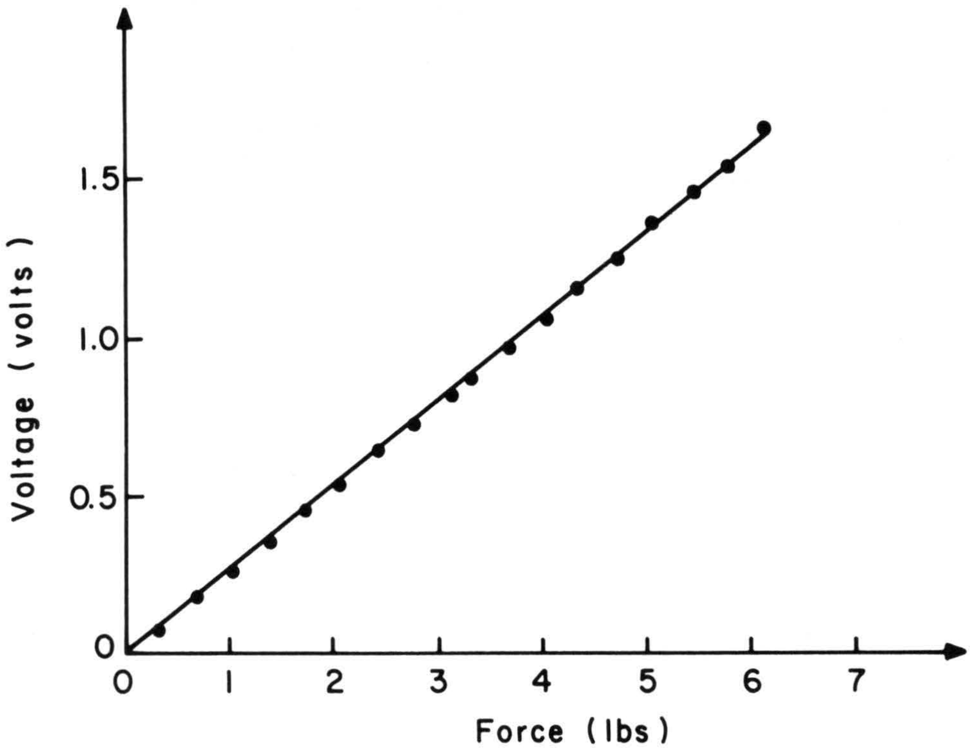

Fig. 18. Drag-Force Calibration

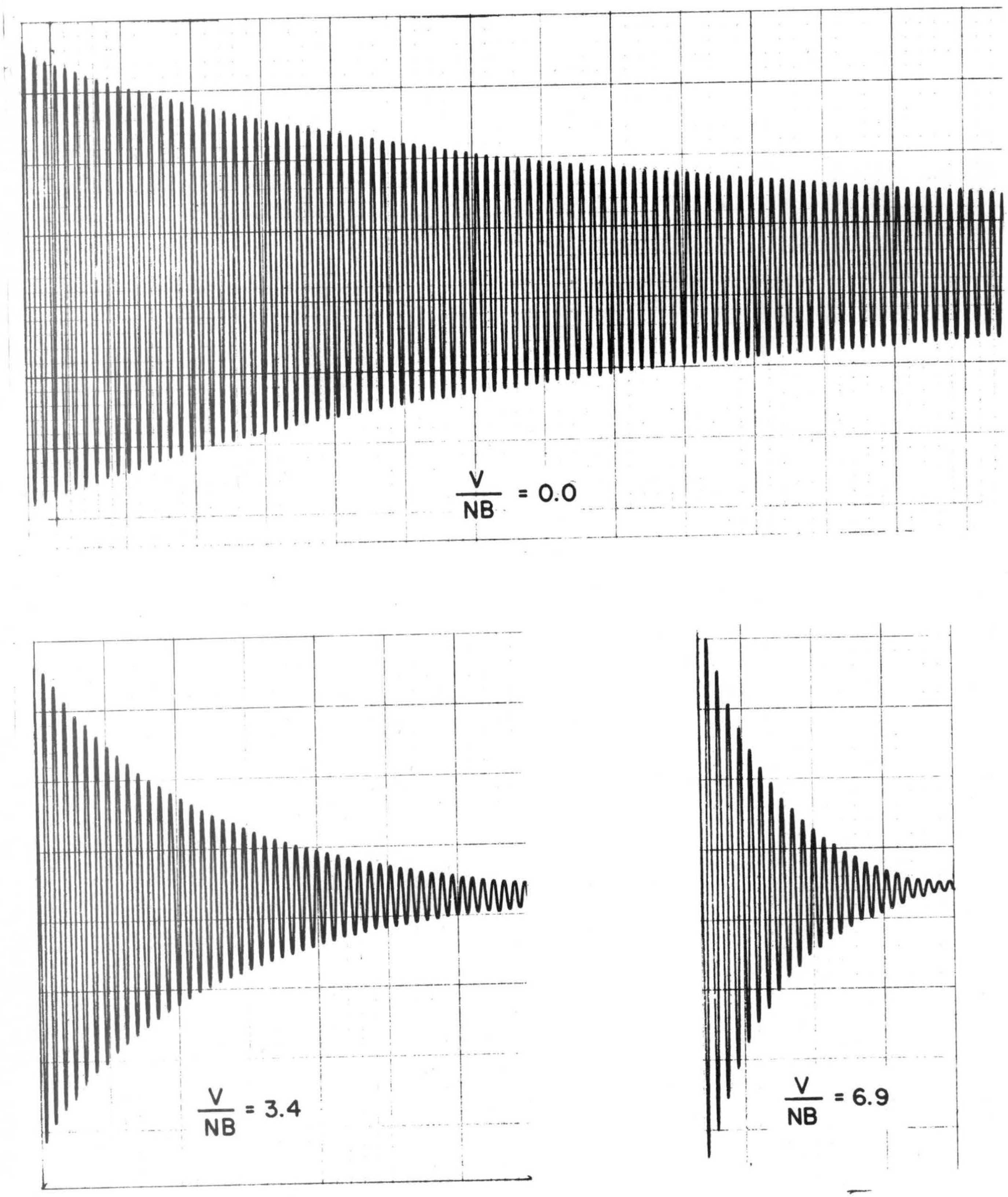

Fig. 19. Typical Records of Model Oscillations
(Vertical Motion)

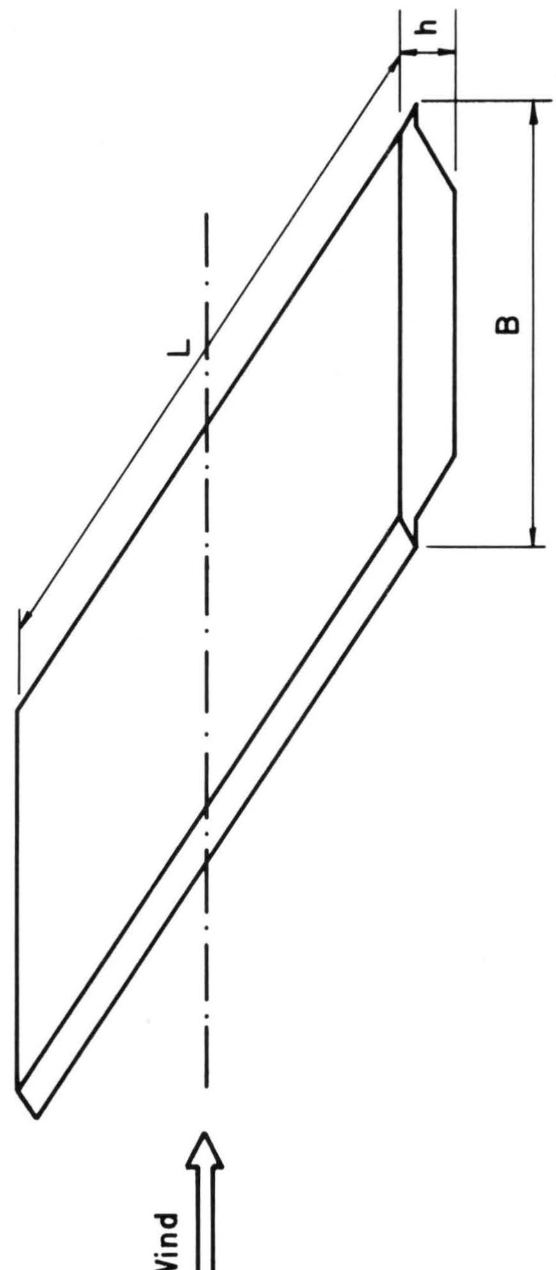

Fig. 20. Smooth Deck Model

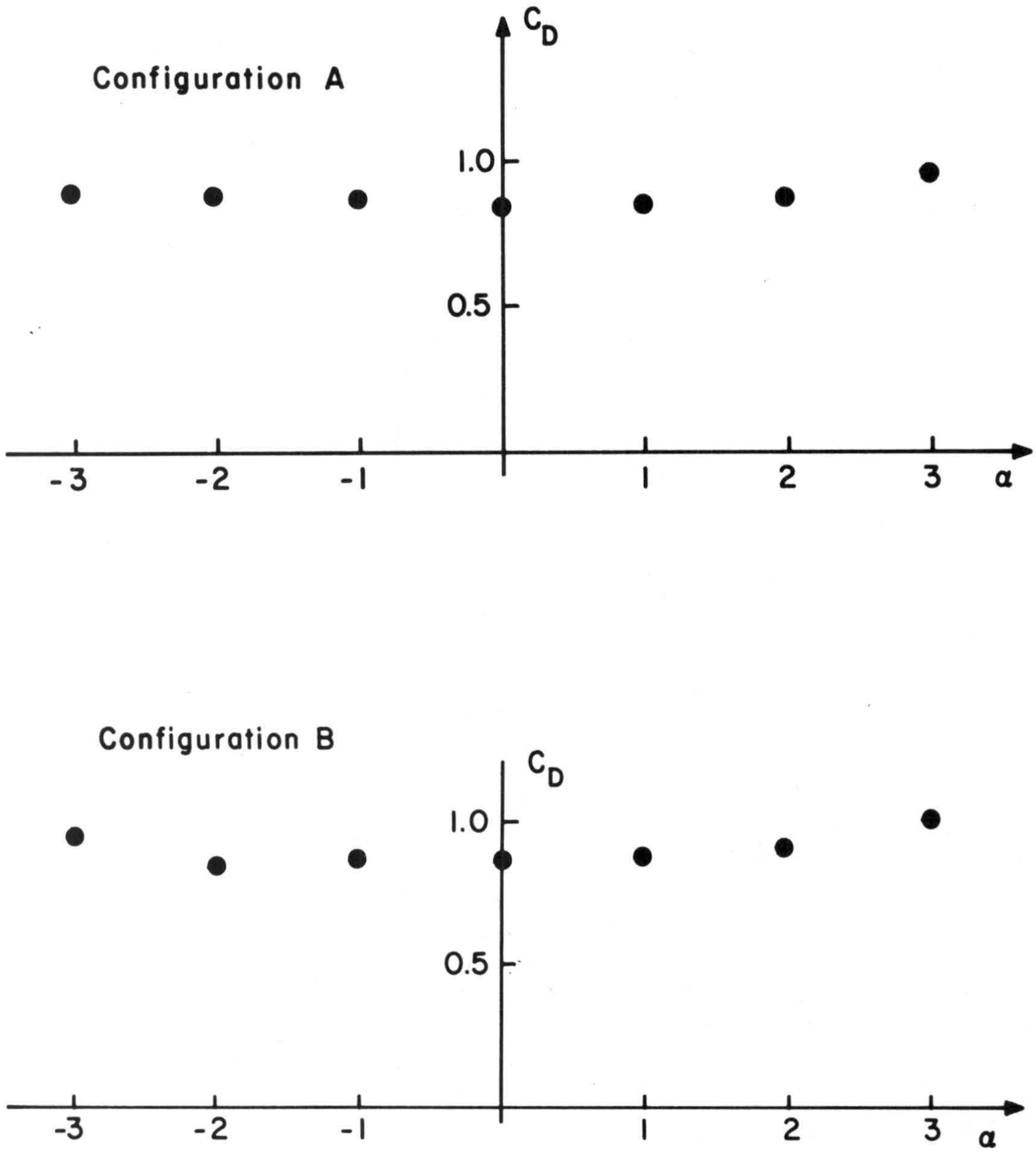

Fig. 21. Drag Coefficient (versus Angle of Attack)

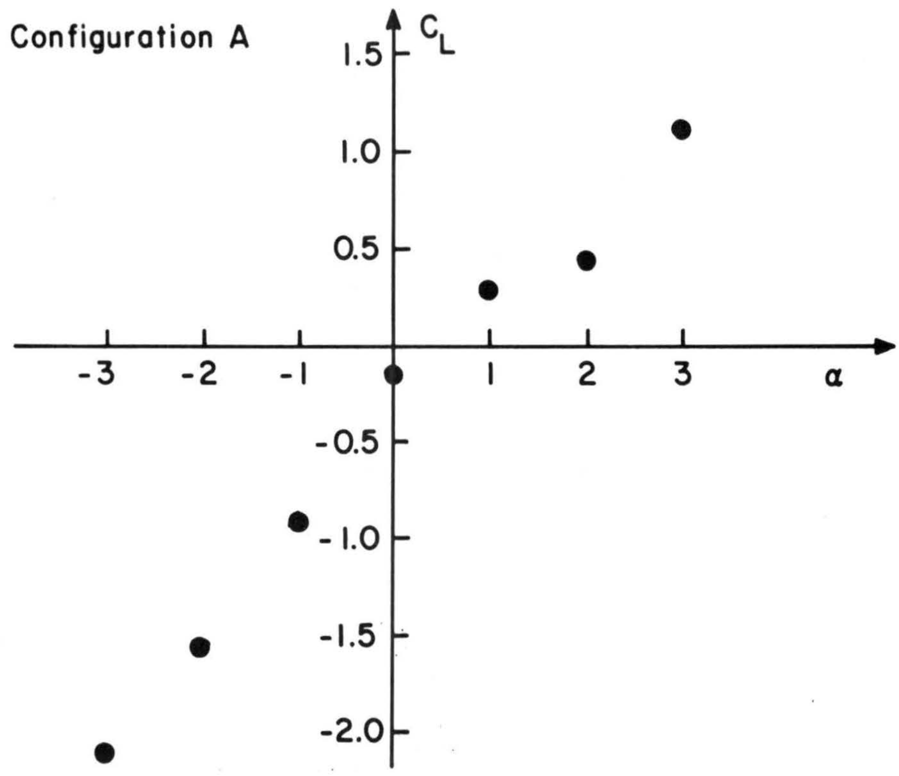

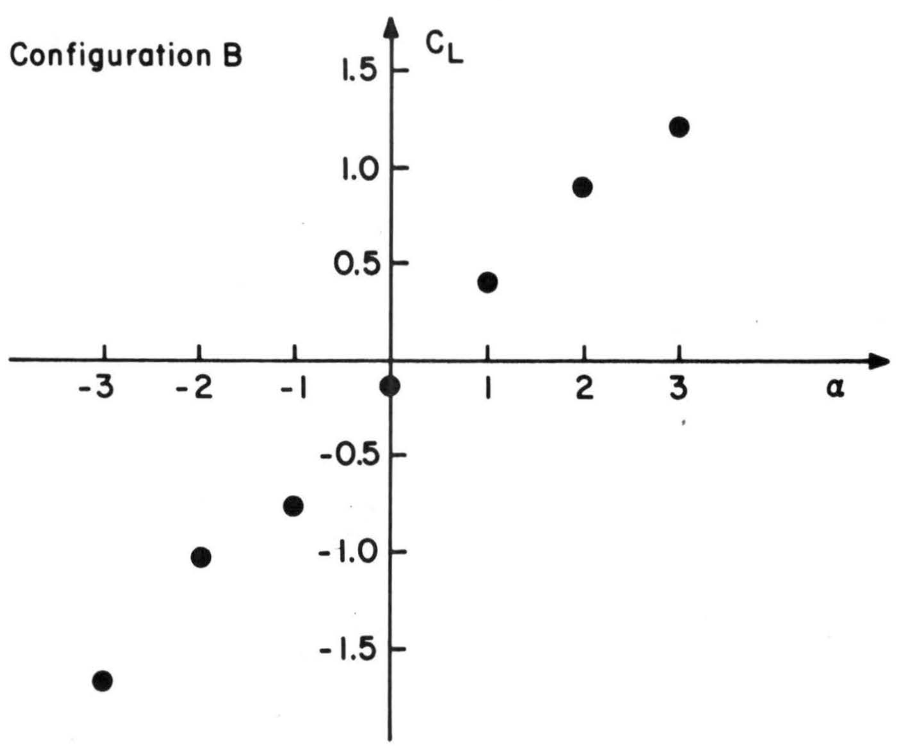

Fig. 22. Lift Coefficient (versus Angle of Attack)

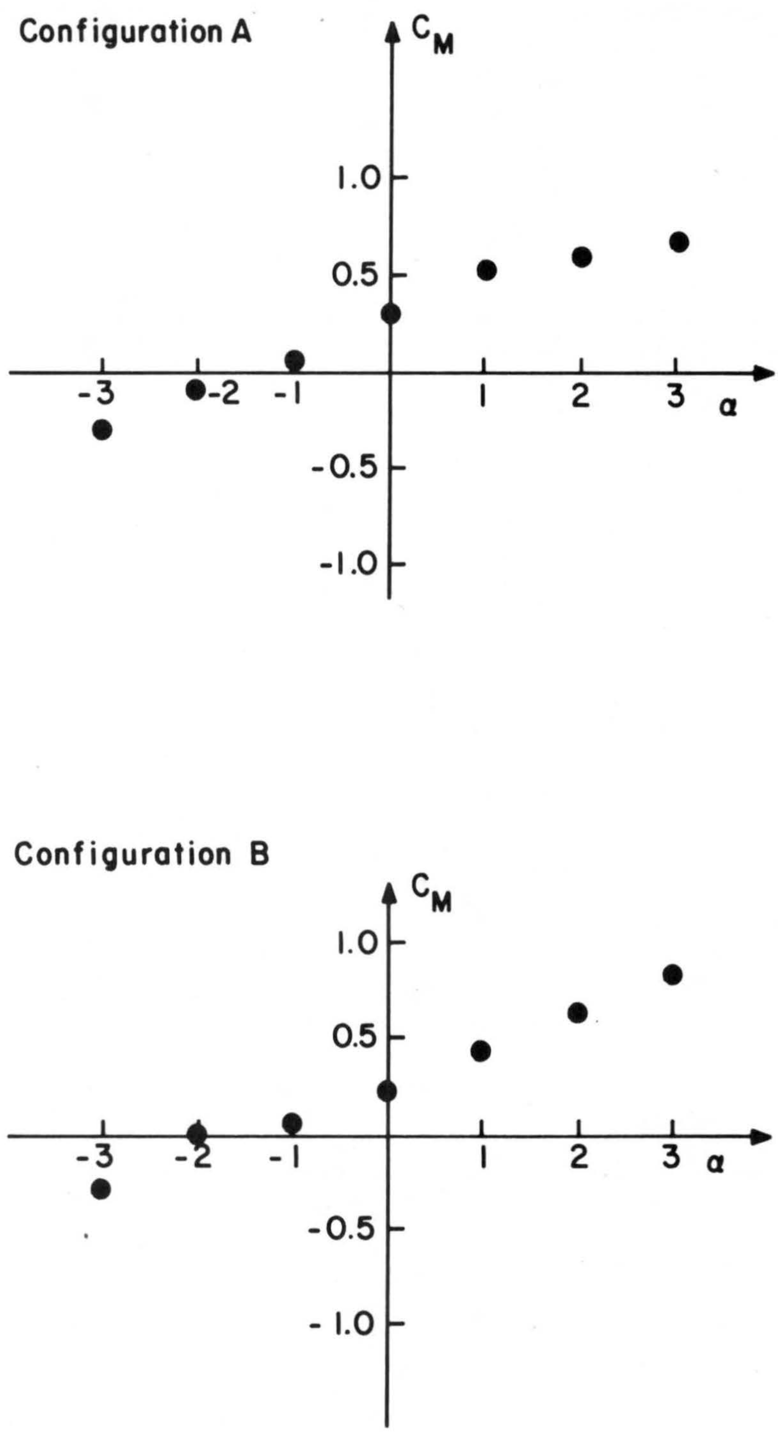

Fig. 23. Moment Coefficient (versus Angle of Attack)

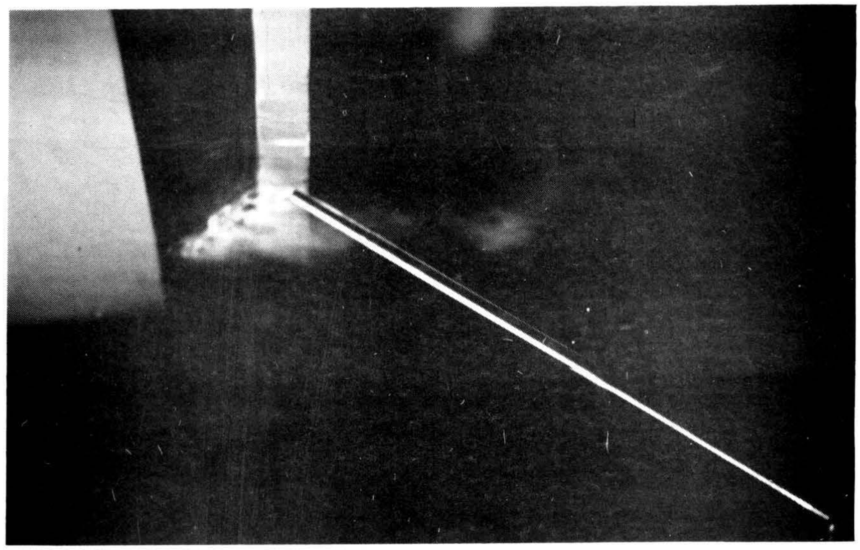

($\alpha \simeq +3°$)

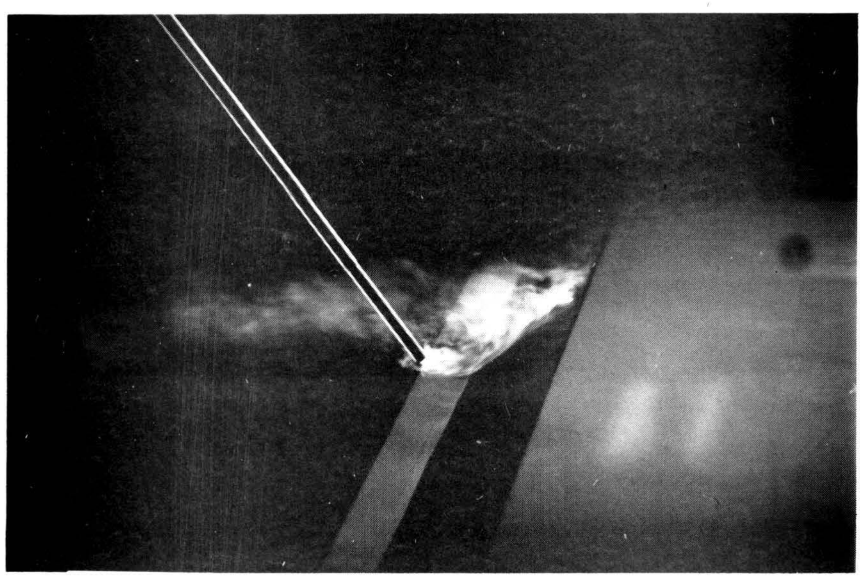

($\alpha = 0°$)

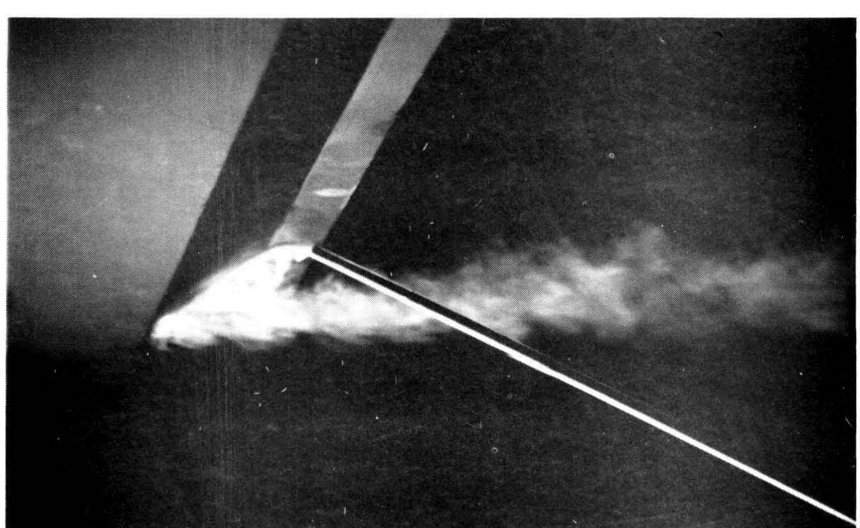

($\alpha = -3°$)

Fig. 24. Flow Visualization; Still Model--Trailing Edge

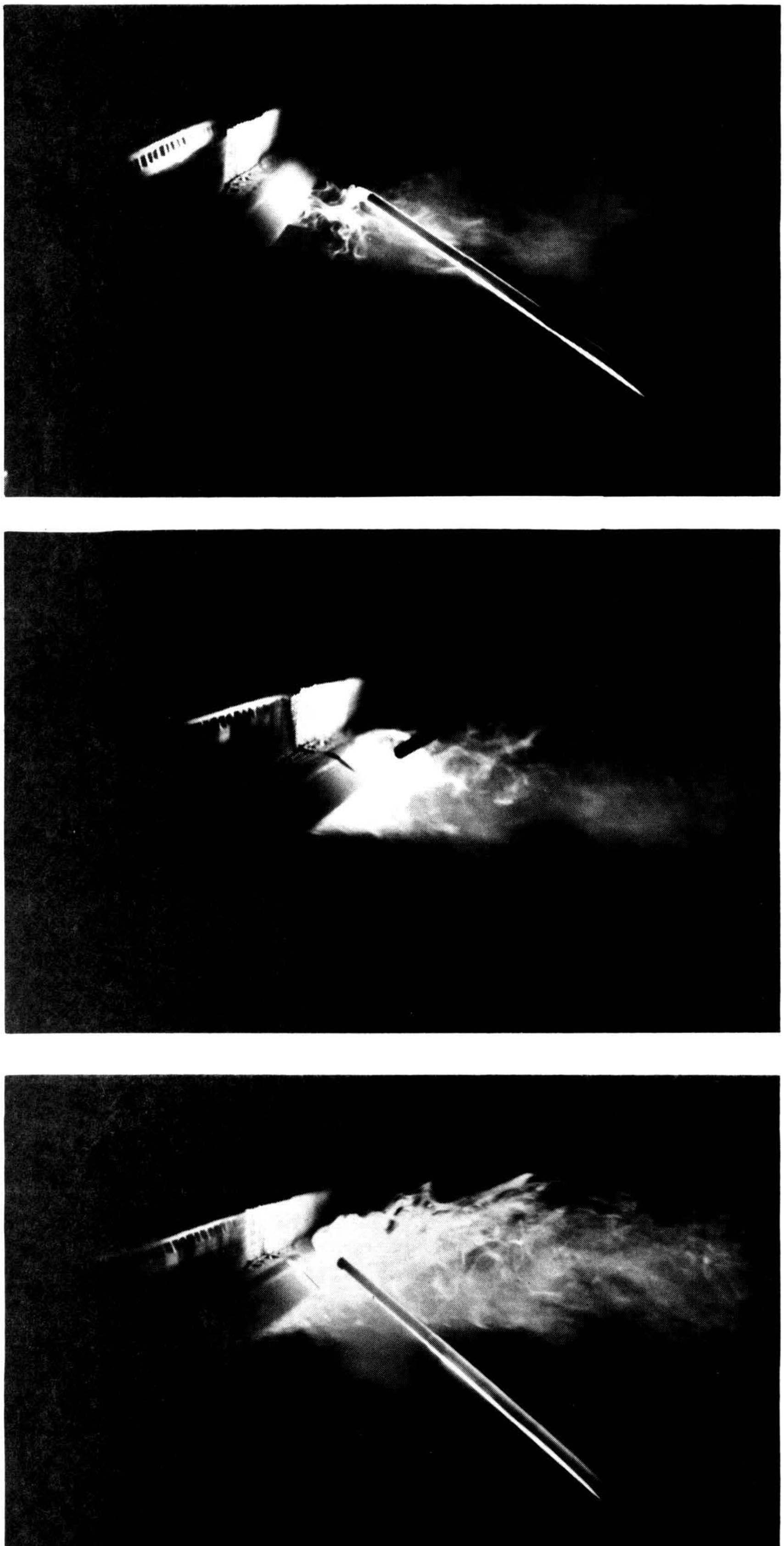

(α=+3°)

(α=0°)

(α=-3°)

Fig. 25. Flow Visualization; Still Model--Trailing Edge

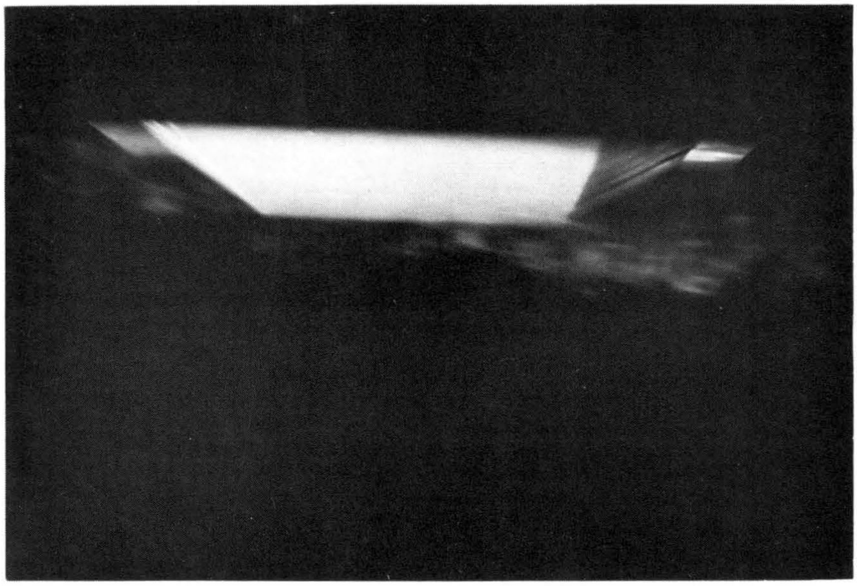

(α=+3°)

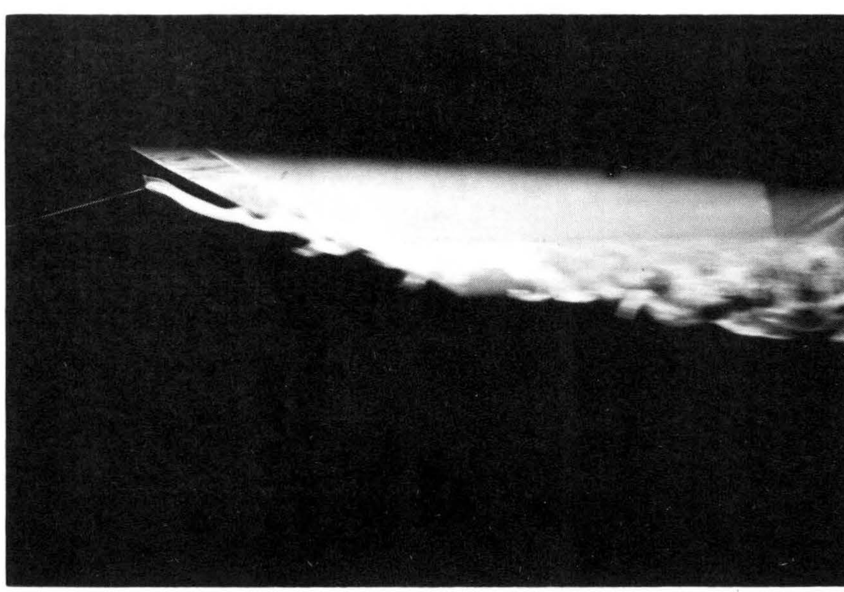

(α=-3°)

Fig. 26. Flow Visualization; Still Model--Lower Surface

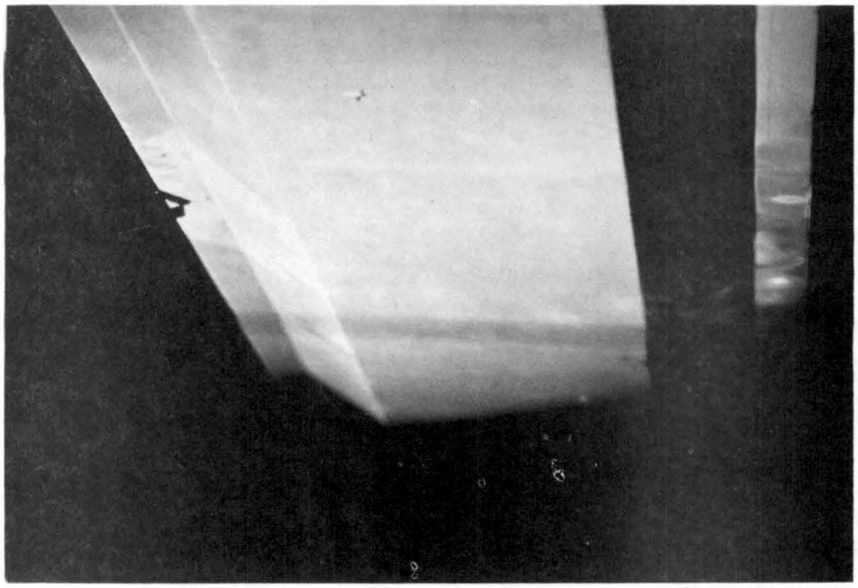

(α=+3°)

(α=0°)

Fig. 27. Flow Visualization; Still Model--Leading Edge

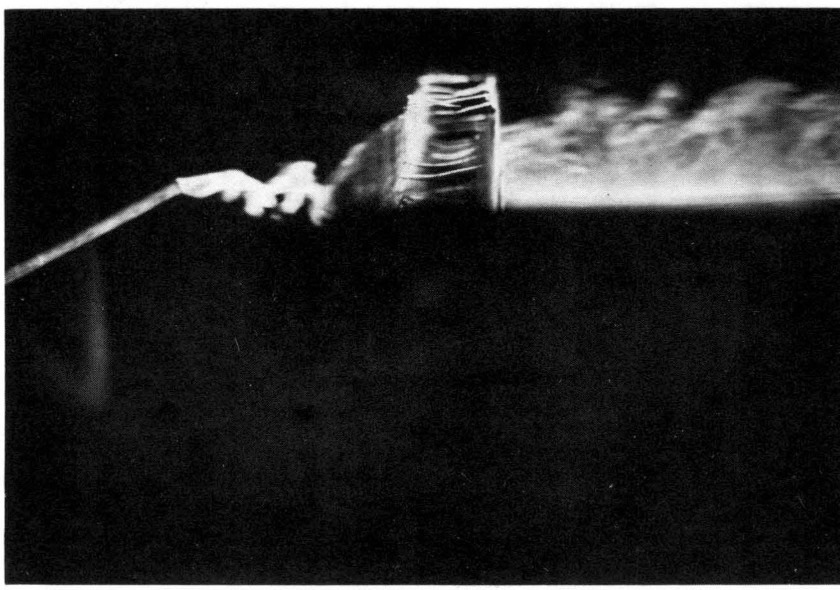

(α=-3°)

Fig. 28. Flow Visualization; Still model--Upper Surface

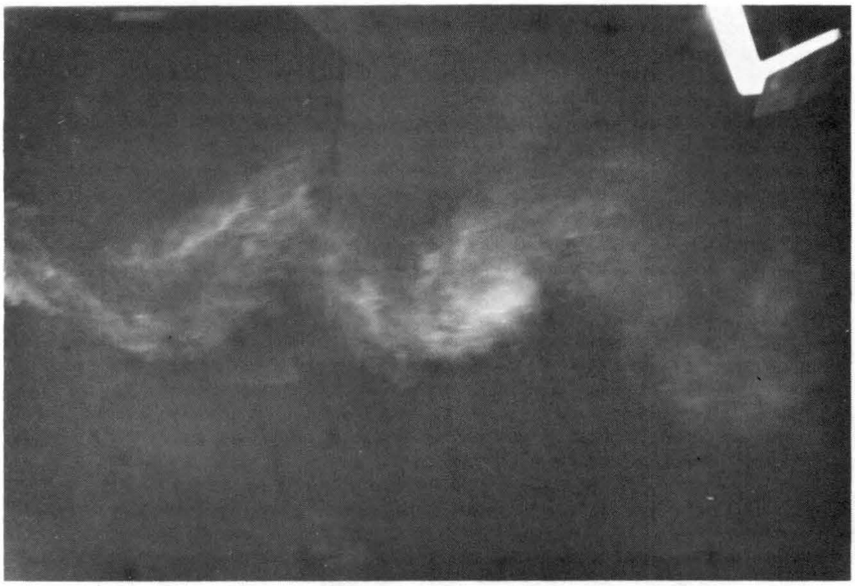

($\alpha=+3°$)

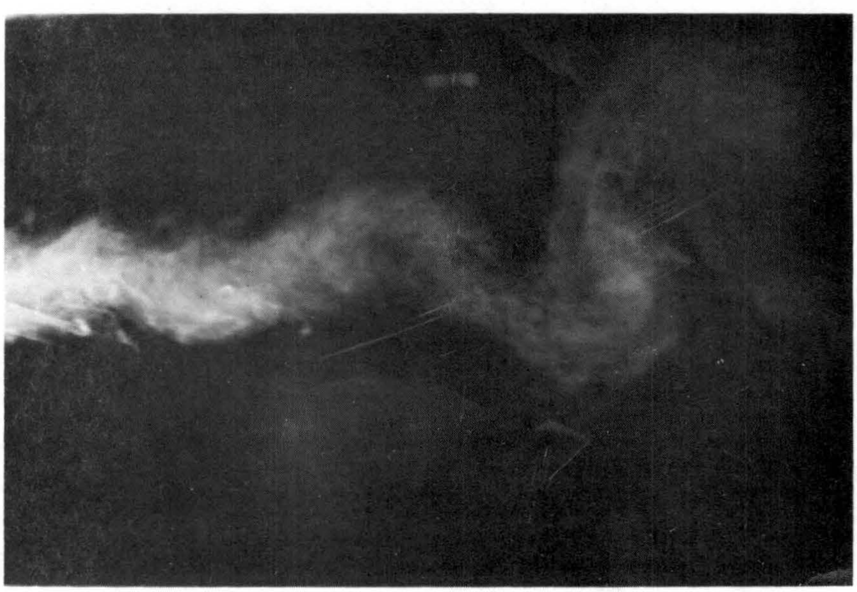

($\alpha=-3°$)

Fig. 29. Flow Visualization; Still Model--Wake behind Model

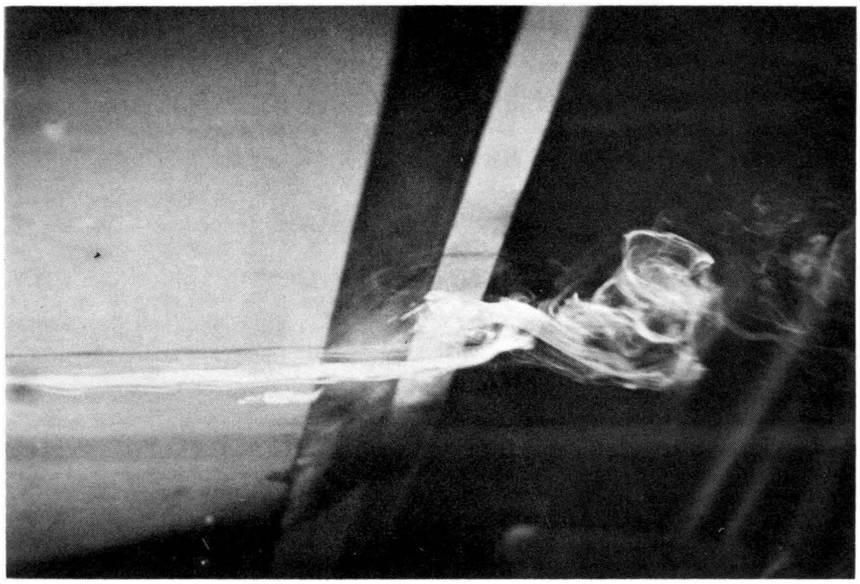

(α= 0°)

Fig. 30. Flow Visualization; Model Oscillating in Vertical Mode--Trailing Edge

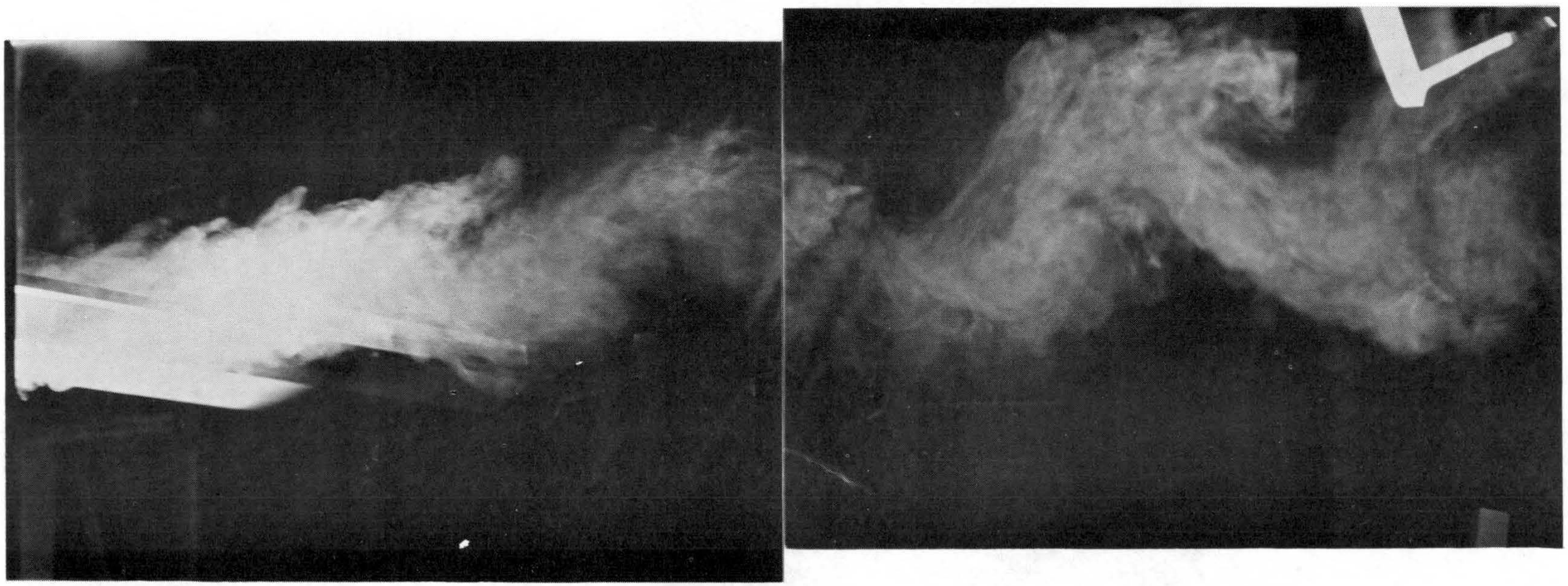

(α=0°)

Fig. 31. Flow Visualization; Model Oscillating in Vertical Mode--Wake behind Model

10. TABLES

Table 1. Parameters for Prototype and "Exact" Model

	Prototype (original deck)	"Exact" model (original deck)
Width (B)	48 ft - 10 in.	14.65 in.
Depth (h)	8 ft - 0 in.	2.40 in.
Mass per unit span (correspond. to total dead load)	$\frac{7.29 \times 10^3}{32.17} = 226.61 \frac{\text{slugs}}{\text{ft}}$	$0.1416 \frac{\text{slugs}}{\text{ft}}$
Frequency of vertical motion	1st mode 0.2940 cps	1.859 cps
Frequency of torsional motion	6th mode 0.9840 cps	6.223 cps

Table 2. Parameters for Actual Models

	Original Deck	Modified Deck	Smooth Deck
Deck width (B)	1.3375 ft (16.05")	1.4508 ft (17.45")	1.4508 ft (17.45")
Mass per unit span	0.1491 slugs/ft	0.1560 slugs/ft	0.1507 slugs/ft
Mass moment of inertia per unit span	0.0942 $\frac{\text{slugs ft}^2}{\text{ft}}$	0.1028 $\frac{\text{slugs ft}^2}{\text{ft}}$	0.0969 $\frac{\text{slugs ft}^2}{\text{ft}}$
Frequency for vert mot. (still air)	1.788 cps	1.748 cps	1.778 cps
Frequency for tors. mot. (still air)	4.310 cps	4.130 cps	4.250 cps
Model length	5.6667 ft	5.6667 ft	5.6667 ft
Average air density	0.0019 $\frac{\text{slugs}}{\text{ft}^3}$	0.0019 $\frac{\text{slugs}}{\text{ft}^3}$	0.0018 $\frac{\text{slugs}}{\text{ft}^3}$
Model scale	1:40	1:40	1:40

Table 3. Motion-Picture Scene Guide

Scene	Configuration	Model	Angle of Attack
1	MI B	still	$\alpha = 0°$
2	MII B	still	$\alpha = +3°$
3	MIII B	still	$\alpha = -3°$
4	MII BV	vertical oscillations	$\alpha = +3°$
5	MIII BV	vertical oscillations	$\alpha = -3°$
6	MI BV	vertical oscillations	$\alpha = 0°$

Wind velocity	10 fps
Movie length	470 ft
Running time	(24 ft/sec) 13 min.

11. APPENDICES

A. AERODYNAMIC CHARACTERISTICS

APPENDIX A.1

Aerodynamic Derivatives for Modified Bridge Deck

Modified Deck

(Dimensions for Model)
(Model Scale 1:40)

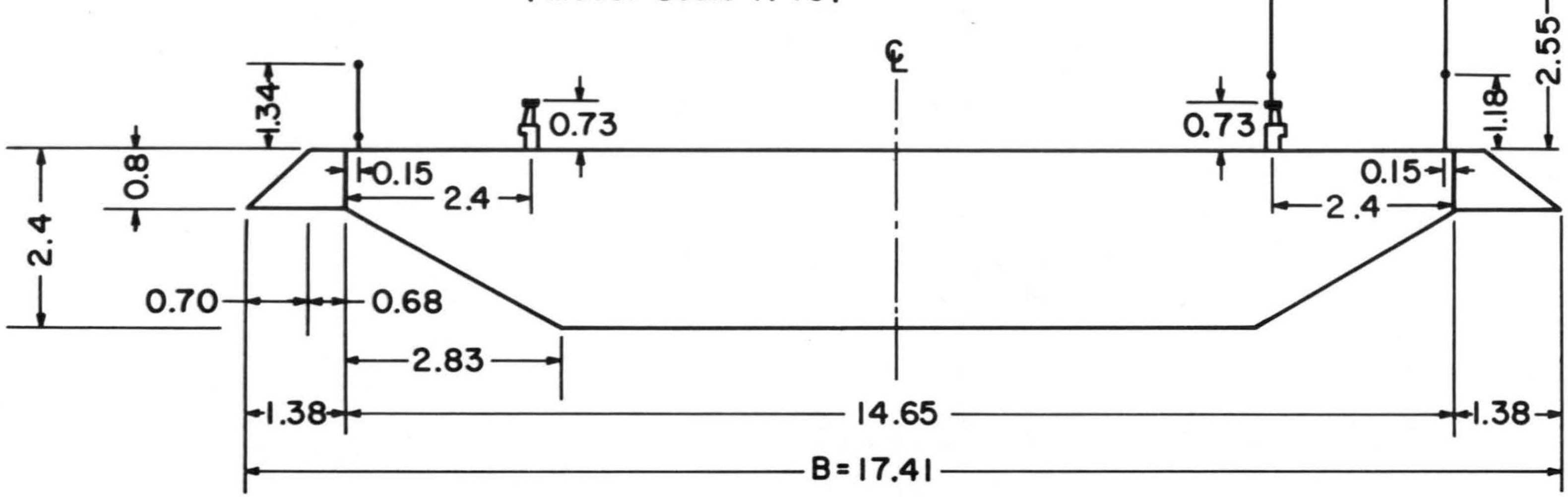

(All Dimensions in inches)

	M I	M II	M III
A	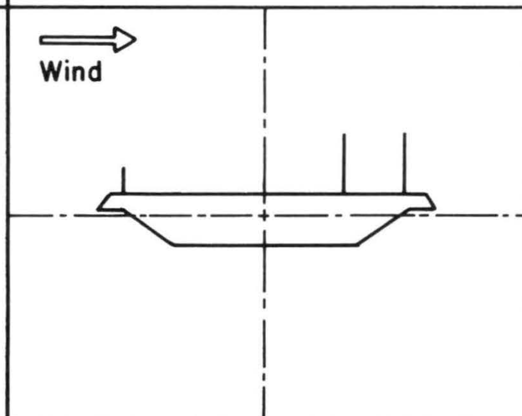	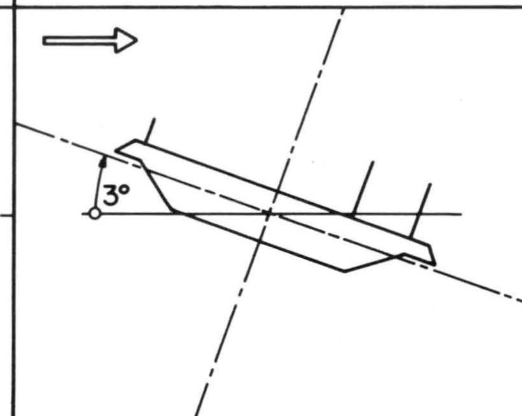	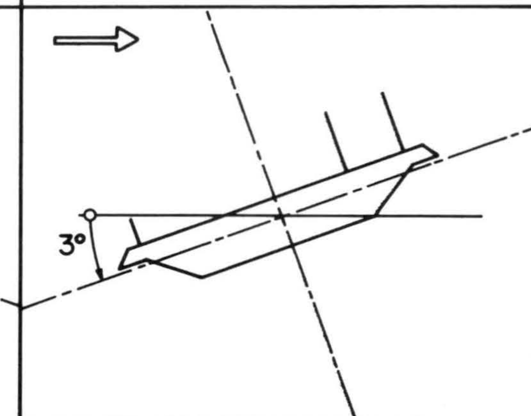
	Vertical MIA-V	Vertical MIIA-V	Vertical MIIIA-V
	Torsional MIA-T	Torsional MIIA-T	Torsional MIIIA-T
B	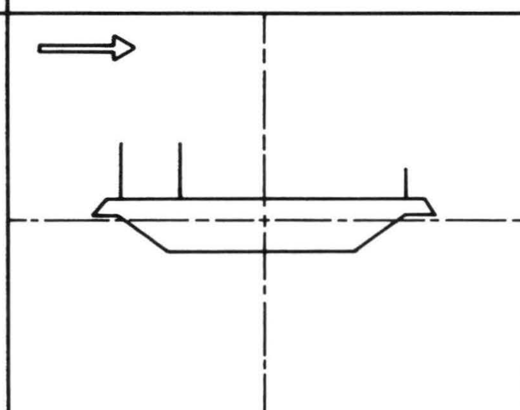	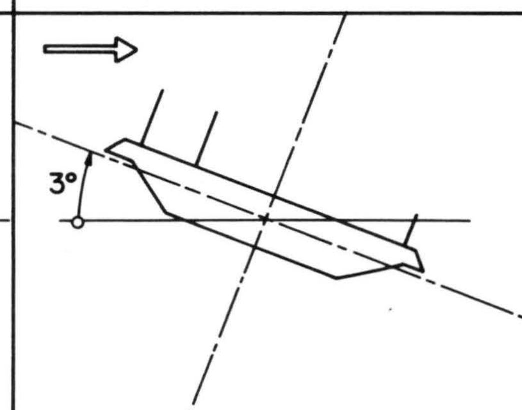	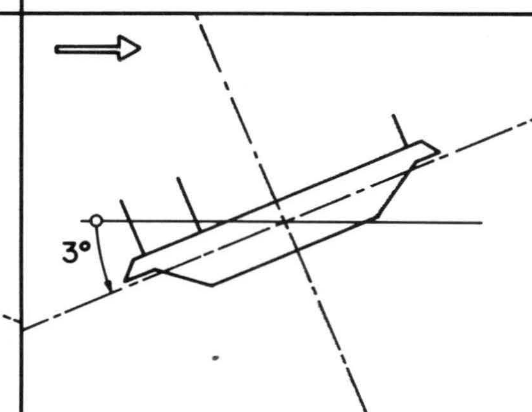
	Vertical MIB-V	Vertical MIIB-V	Vertical MIIIB-V
	Torsional MIB-T	Torsional MIIB-T	Torsional MIIIB-T

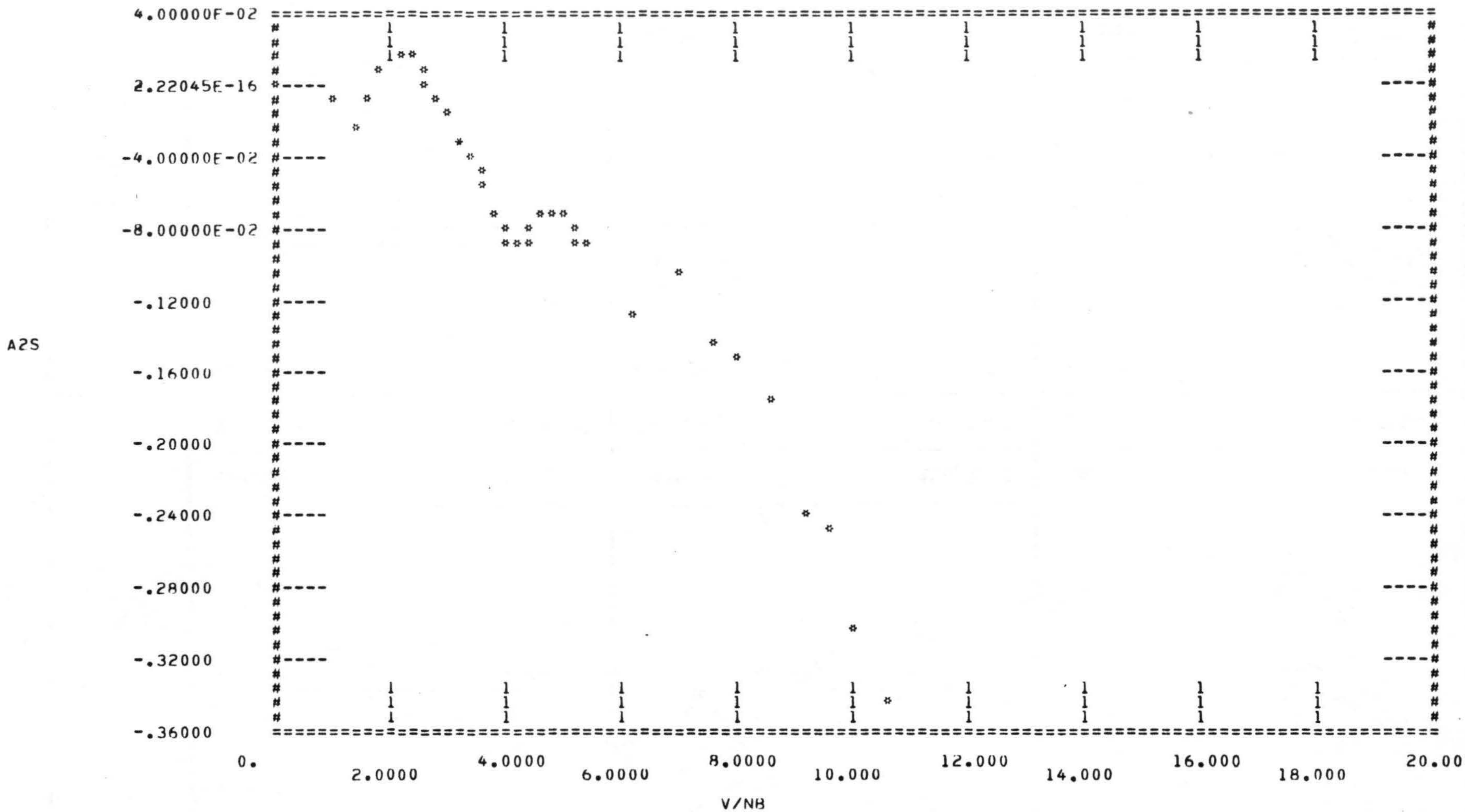

C O N F I G U R A T I O N   MIA-T

C O N F I G U R A T I O N   MIA-T

INDEX	V/NB	A2S
(1)	0.	2.42901E-04
(2)	.94791	-7.84491E-03
(3)	1.3406	-2.03550E-02
(4)	1.6418	-1.09436E-02
(5)	1.8958	4.21297E-03
(6)	2.1196	1.29787E-02
(7)	2.3219	1.47288E-02
(8)	2.5435	9.41403E-03
(9)	2.6811	3.01496E-03
(10)	2.8437	-6.84518E-03
(11)	2.9976	-1.86919E-02
(12)	3.1439	-2.87616E-02
(13)	3.2837	-3.55534E-02
(14)	3.3914	-4.10068E-02
(15)	3.5468	-4.93664E-02
(16)	3.6713	-5.87988E-02
(17)	3.7917	-7.04603E-02
(18)	3.9084	-8.23707E-02
(19)	4.0218	-8.99091E-02
(20)	4.1102	-9.13433E-02
(21)	4.2393	-8.88562E-02
(22)	4.3232	-8.68703E-02
(23)	4.4462	-8.16617E-02
(24)	4.5461	-7.49678E-02
(25)	4.6245	-7.11291E-02
(26)	4.7396	-6.86944E-02
(27)	4.8335	-6.84399E-02
(28)	4.9438	-7.05302E-02
(29)	5.0160	-7.33232E-02
(30)	5.1048	-7.79566E-02
(31)	5.1920	-8.21479E-02
(32)	5.2779	-8.45984E-02
(33)	5.3623	-8.55533E-02
(34)	5.4454	-8.67675E-02
(35)	6.2306	-.13006
(36)	6.9141	-.10648
(37)	7.5361	-.14553
(38)	8.0994	-.15389
(39)	8.6364	-.17568
(40)	9.1423	-.24008
(41)	9.6305	-.25001
(42)	10.078	-.30330
(43)	10.506	-.34192

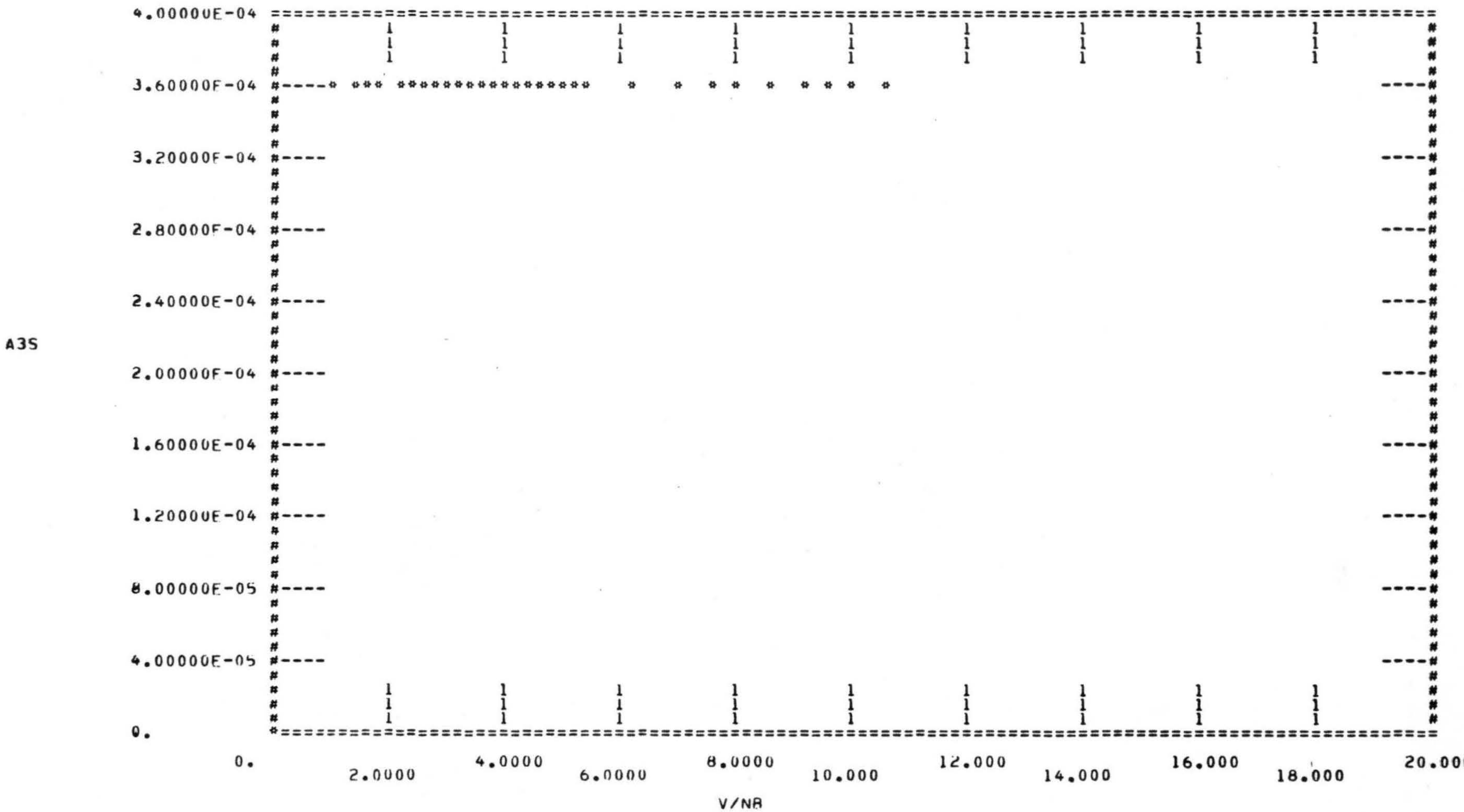

C O N F I G U R A T I O N   MIA-T

C O N F I G U R A T I O N   MIA-T

INDEX	V/NB	A3S
(1)	0.	0.
(2)	.94791	3.56645E-04
(3)	1.3406	3.56645E-04
(4)	1.6418	3.56645E-04
(5)	1.8958	3.56645E-04
(6)	2.1196	3.56645E-04
(7)	2.3219	3.56645E-04
(8)	2.5435	3.56645E-04
(9)	2.6811	3.56645E-04
(10)	2.8437	3.56645E-04
(11)	2.9976	3.56645E-04
(12)	3.1439	3.56645E-04
(13)	3.2837	3.56645E-04
(14)	3.3914	3.56645E-04
(15)	3.5468	3.56645E-04
(16)	3.6713	3.56645E-04
(17)	3.7917	3.56645E-04
(18)	3.9084	3.56645E-04
(19)	4.0218	3.56645E-04
(20)	4.1102	3.56645E-04
(21)	4.2393	3.56645E-04
(22)	4.3232	3.56645E-04
(23)	4.4462	3.56645E-04
(24)	4.5461	3.56645E-04
(25)	4.6245	3.56645E-04
(26)	4.7396	3.56645E-04
(27)	4.8335	3.56645E-04
(28)	4.9438	3.56645E-04
(29)	5.0160	3.56645E-04
(30)	5.1048	3.56645E-04
(31)	5.1920	3.56645E-04
(32)	5.2779	3.56645E-04
(33)	5.3623	3.56645E-04
(34)	5.4454	3.56645E-04
(35)	6.2306	3.56645E-04
(36)	6.9141	3.56645E-04
(37)	7.5361	3.56645E-04
(38)	8.0994	3.56645E-04
(39)	8.6364	3.56645E-04
(40)	9.1423	3.56645E-04
(41)	9.6305	3.56645E-04
(42)	10.078	3.56645E-04
(43)	10.506	3.56645E-04

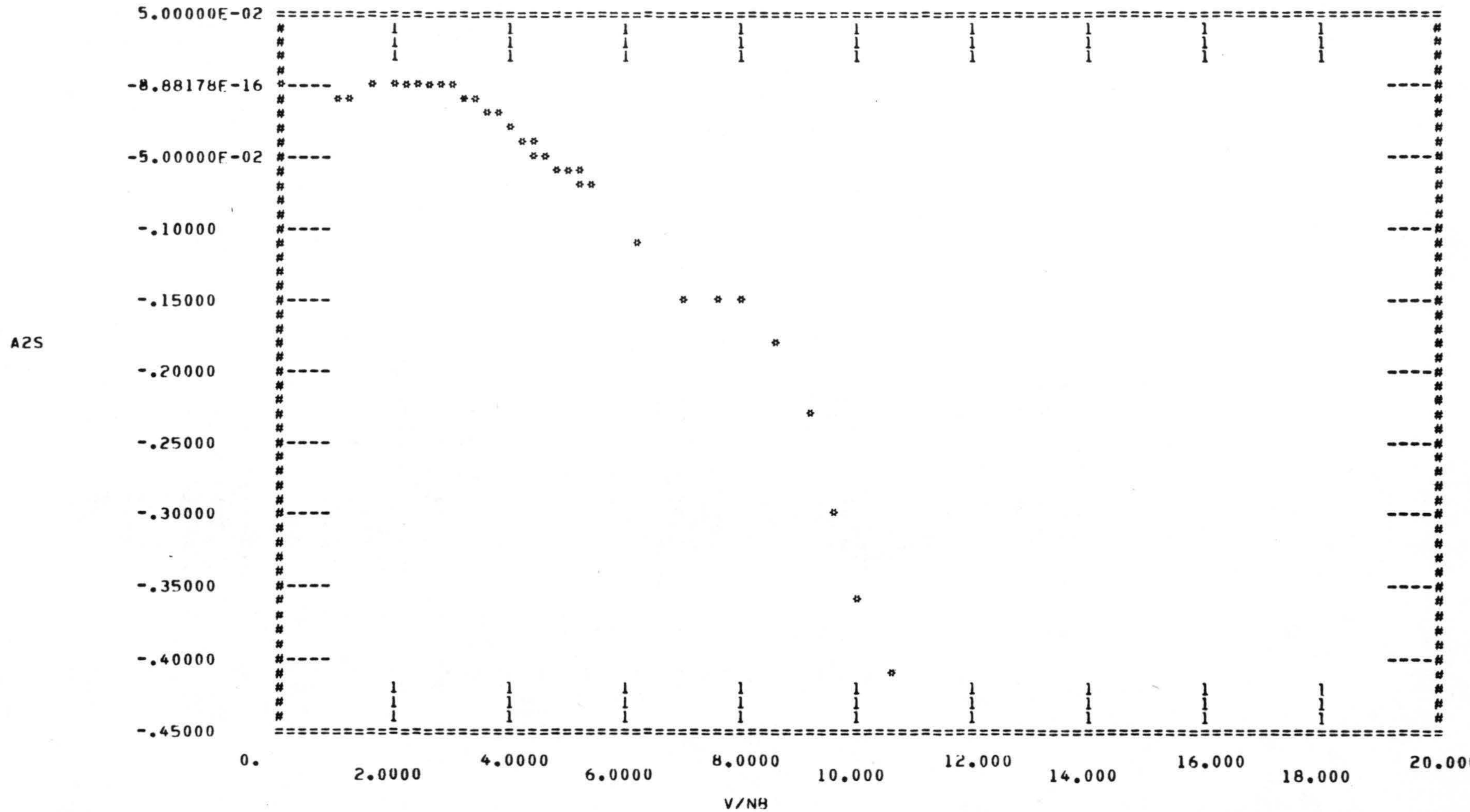

C O N F I G U R A T I O N   M1B-T

C O N F I G U R A T I O N   M18-T

INDEX	V/NB	A2S	INDEX	V/NB	A2S	INDEX	V/NB	A2S
(1)	0.	-9.53020E-04	(15)	3.5468	-1.63451E-02	(29)	5.0160	-6.16733E-02
(2)	.94791	-6.84694E-03	(16)	3.6713	-2.02370E-02	(30)	5.1048	-6.33535E-02
(3)	1.2718	-6.14787E-03	(17)	3.7917	-2.41672E-02	(31)	5.1920	-6.52059E-02
(4)	1.6418	-1.75098E-03	(18)	3.9084	-2.81441E-02	(32)	5.2778	-6.73765E-02
(5)	1.9426	2.18203E-03	(19)	4.0217	-3.22029E-02	(33)	5.3623	-6.99629E-02
(6)	2.1196	3.87756E-03	(20)	4.1319	-3.63259E-02	(34)	5.4455	-7.29805E-02
(7)	2.3219	4.54047E-03	(21)	4.2392	-4.04453E-02	(35)	6.2161	-.11349
(8)	2.5079	3.57249E-03	(22)	4.3439	-4.44520E-02	(36)	6.9143	-.14508
(9)	2.6811	1.63736E-03	(23)	4.4462	-4.82117E-02	(37)	7.5362	-.15277
(10)	2.8437	-7.70244E-04	(24)	4.5461	-5.15570E-02	(38)	8.0883	-.15377
(11)	2.9976	-3.40717E-03	(25)	4.6439	-5.43765E-02	(39)	8.6364	-.17817
(12)	3.1439	-6.21784E-03	(26)	4.7397	-5.66363E-02	(40)	9.1521	-.23258
(13)	3.2837	-9.24727E-03	(27)	4.8335	-5.84555E-02	(41)	9.6216	-.29719
(14)	3.4177	-1.26311E-02	(28)	4.9256	-6.00784E-02	(42)	10.079	-.35849
						(43)	10.515	-.40632

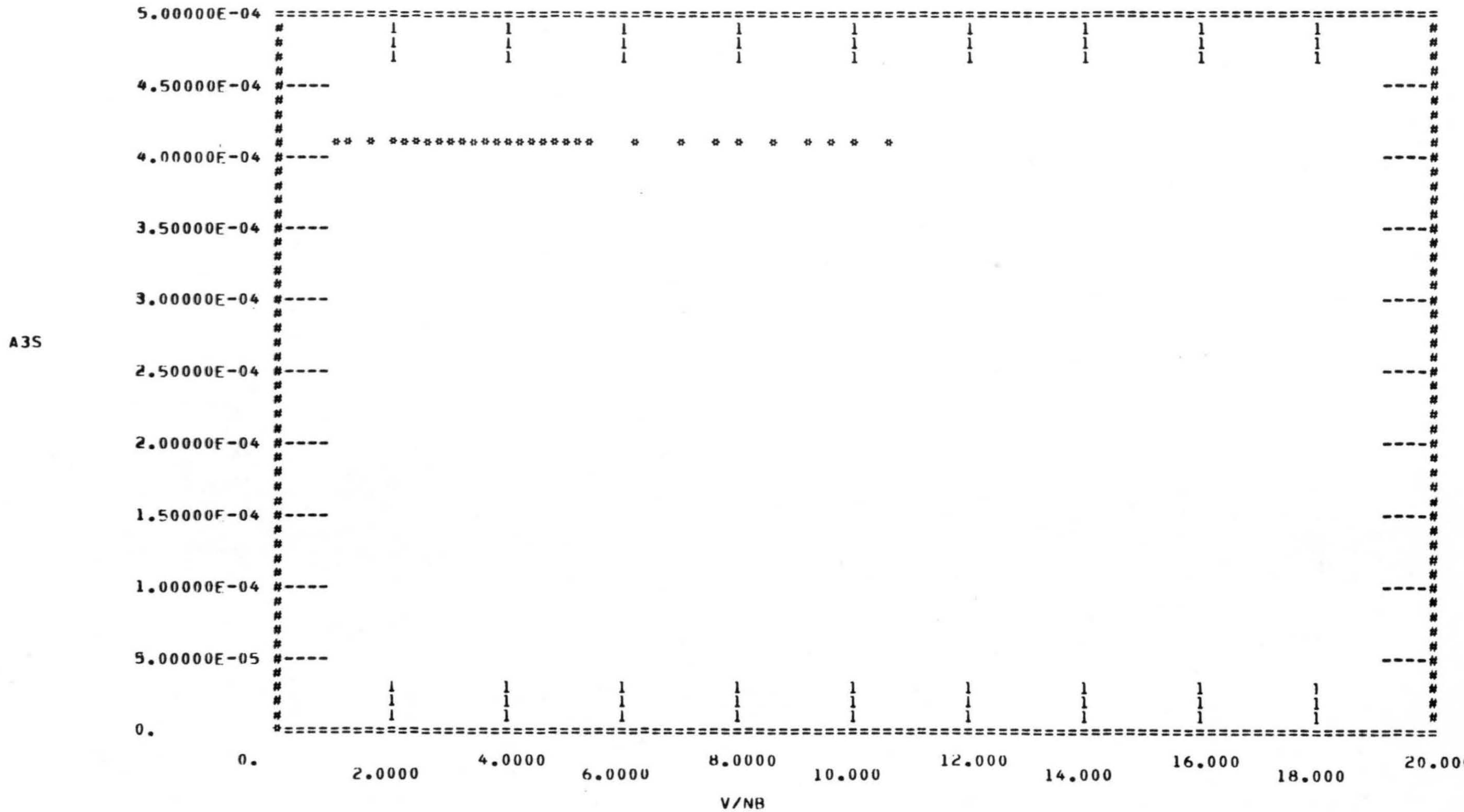

C O N F I G U R A T I O N   M1B-T

CONFIGURATION M1B-T

INDEX	V/NB	A3S	INDEX	V/NB	A3S	INDEX	V/NB	A3S
(1)	0.	6.61301E-14	(15)	3.5468	4.11372E-04	(29)	5.0160	4.11372E-04
(2)	.94791	4.11372E-04	(16)	3.6713	4.11372E-04	(30)	5.1048	4.11372E-04
(3)	1.2718	4.11372E-04	(17)	3.7917	4.11372E-04	(31)	5.1920	4.11372E-04
(4)	1.6418	4.11372E-04	(18)	3.9084	4.11372E-04	(32)	5.2778	4.11372F-04
(5)	1.9426	4.11372E-04	(19)	4.0217	4.11372E-04	(33)	5.3623	4.11372E-04
(6)	2.1196	4.11372E-04	(20)	4.1319	4.11372E-04	(34)	5.4455	4.11372E-04
(7)	2.3219	4.11372E-04	(21)	4.2392	4.11372E-04	(35)	6.2161	4.11372E-04
(8)	2.5079	4.11372E-04	(22)	4.3439	4.11372E-04	(36)	6.9143	4.11372E-04
(9)	2.6811	4.11372E-04	(23)	4.4462	4.11372E-04	(37)	7.5362	4.11372E-04
(10)	2.8437	4.11372E-04	(24)	4.5461	4.11372E-04	(38)	8.0883	4.11372E-04
(11)	2.9976	4.11372E-04	(25)	4.6439	4.11372E-04	(39)	8.6364	4.11372E-04
(12)	3.1439	4.11372E-04	(26)	4.7397	4.11372E-04	(40)	9.1521	4.11372E-04
(13)	3.2837	4.11372E-04	(27)	4.8335	4.11372E-04	(41)	9.6216	4.11372F-04
(14)	3.4177	4.11372E-04	(28)	4.9256	4.11372E-04	(42)	10.079	4.11372E-04
						(43)	10.515	4.11372E-04

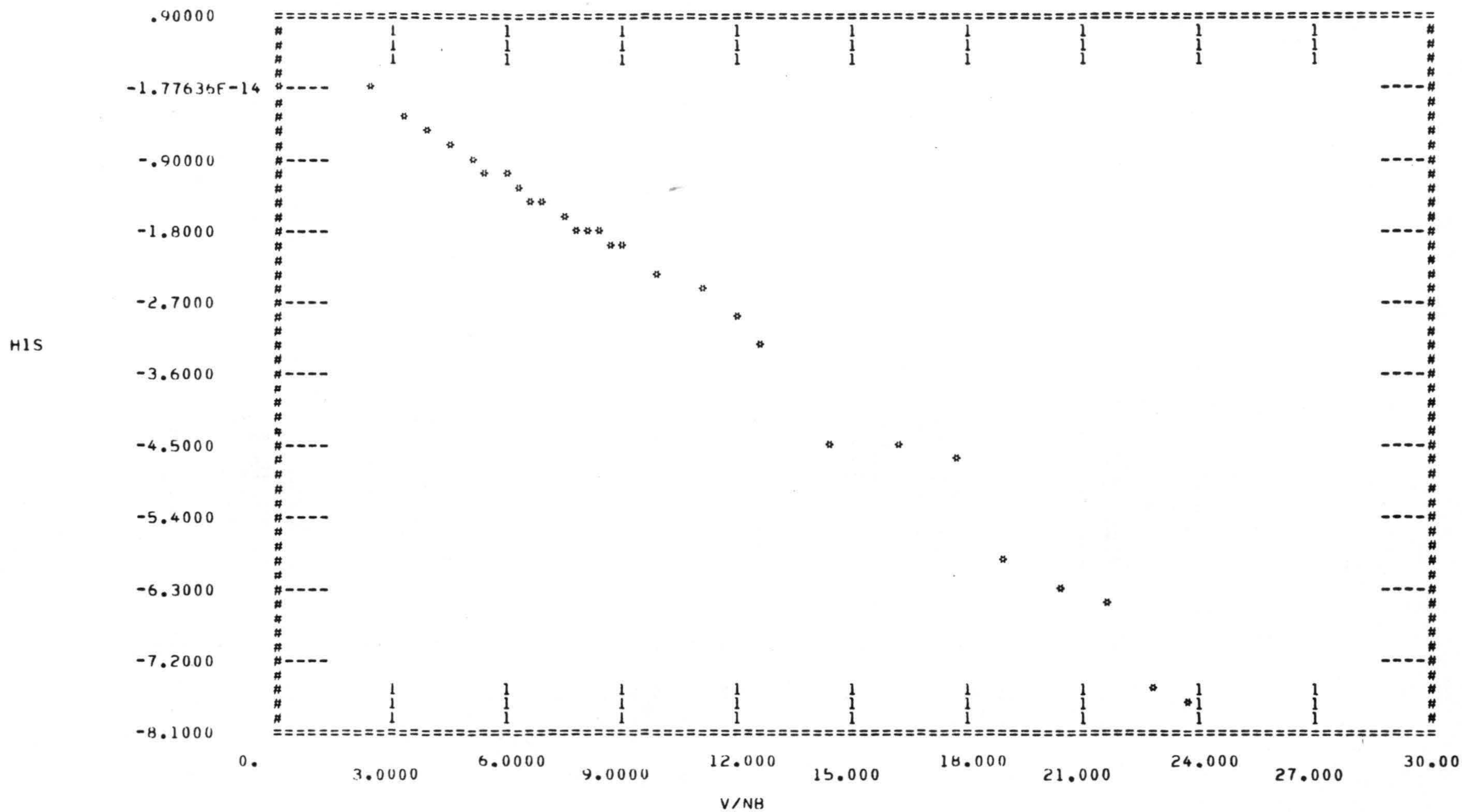

C O N F I G U R A T I O N MIA-V

C O N F I G U R A T I O N MIA-V

INDEX	V/NB	HIS	INDEX	V/NB	HIS	INDEX	V/NB	HIS
(1)	0.	4.59478E-03	(10)	6.7142	-1.3728	(19)	10.968	-2.4634
(2)	2.4512	-4.55963E-02	(11)	7.0067	-1.4792	(20)	11.852	-2.9694
(3)	3.1646	-.34394	(12)	7.4236	-1.6267	(21)	12.669	-3.1539
(4)	3.8760	-.60406	(13)	7.7538	-1.7174	(22)	14.390	-4.5200
(5)	4.3623	-.70326	(14)	8.0705	-1.7988	(23)	16.166	-4.5115
(6)	5.1031	-.86959	(15)	8.3759	-1.8820	(24)	17.682	-4.7159
(7)	5.4818	-.99929	(16)	8.6114	-1.9406	(25)	19.048	-5.9529
(8)	5.9212	-1.1509	(17)	8.9544	-2.0521	(26)	20.456	-6.2464
(9)	6.3302	-1.2650	(18)	10.013	-2.3819	(27)	21.542	-6.5261
						(28)	22.822	-7.4790
						(29)	23.804	-7.7538

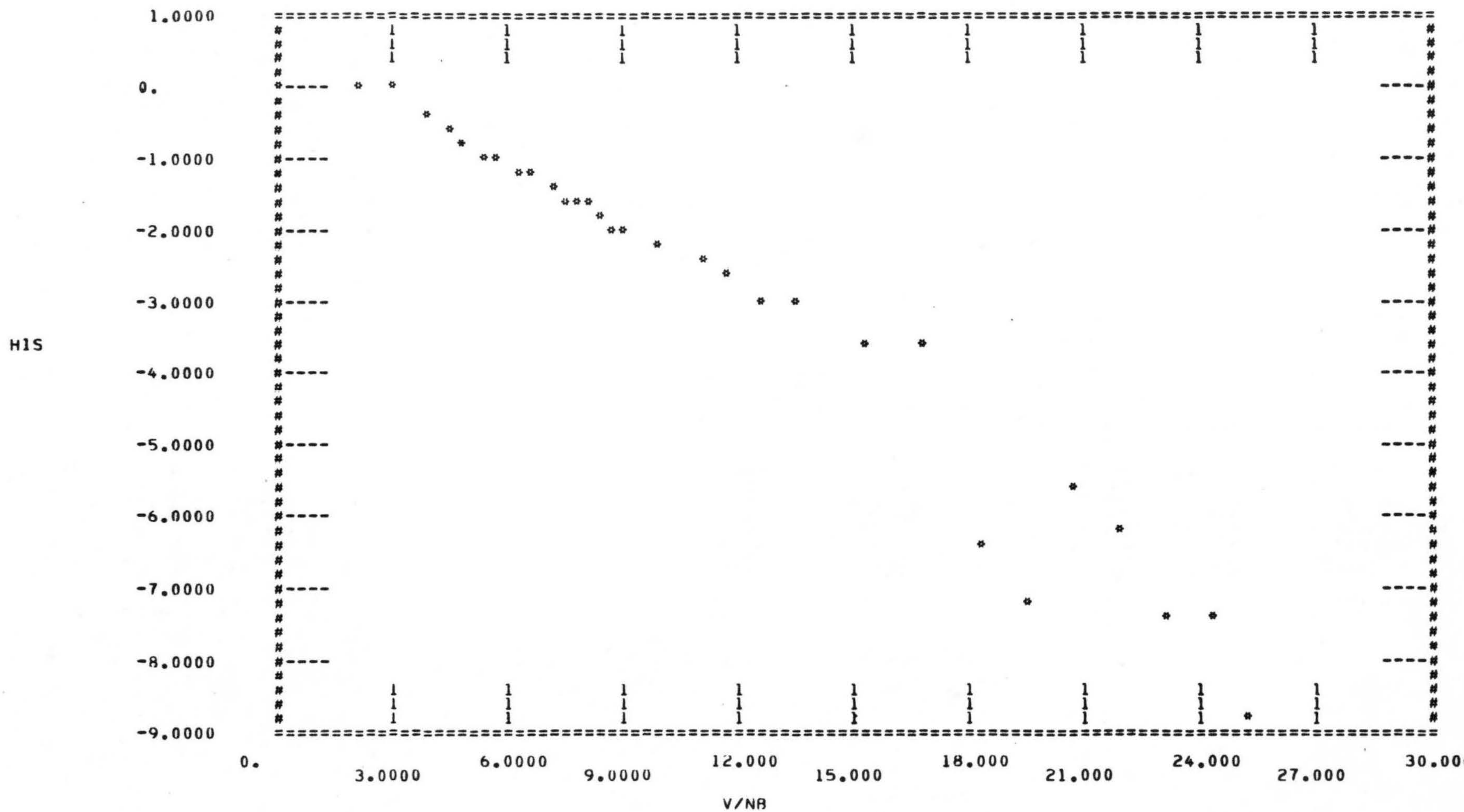

C O N F I G U R A T I O N M1B-V

C O N F I G U R A T I O N   M1B-V

INDEX	V/NB	HIS	INDEX	V/NB	HIS	INDEX	V/NB	HIS
(1)	0.	6.66973E-04	(11)	7.0777	-1.3825	(21)	12.669	-2.9059
(2)	2.2377	9.68529E-02	(12)	7.4232	-1.5065	(22)	13.438	-3.0966
(3)	3.0021	1.79676E-03	(13)	7.6890	-1.5905	(23)	15.195	-3.5611
(4)	4.0030	-.40338	(14)	8.1320	-1.6743	(24)	16.765	-3.6209
(5)	4.4756	-.63939	(15)	8.3753	-1.7871	(25)	18.243	-6.3097
(6)	4.9029	-.84513	(16)	8.6703	-1.9456	(26)	19.598	-7.1781
(7)	5.4820	-1.0775	(17)	8.9542	-2.0132	(27)	20.709	-5.5293
(8)	5.8359	-1.0882	(18)	10.012	-2.1111	(28)	22.000	-6.2352
(9)	6.2504	-1.1315	(19)	10.969	-2.3850	(29)	23.215	-7.3549
(10)	6.7142	-1.2525	(20)	11.848	-2.5284	(30)	24.210	-7.3017
						(31)	25.287	-8.7793

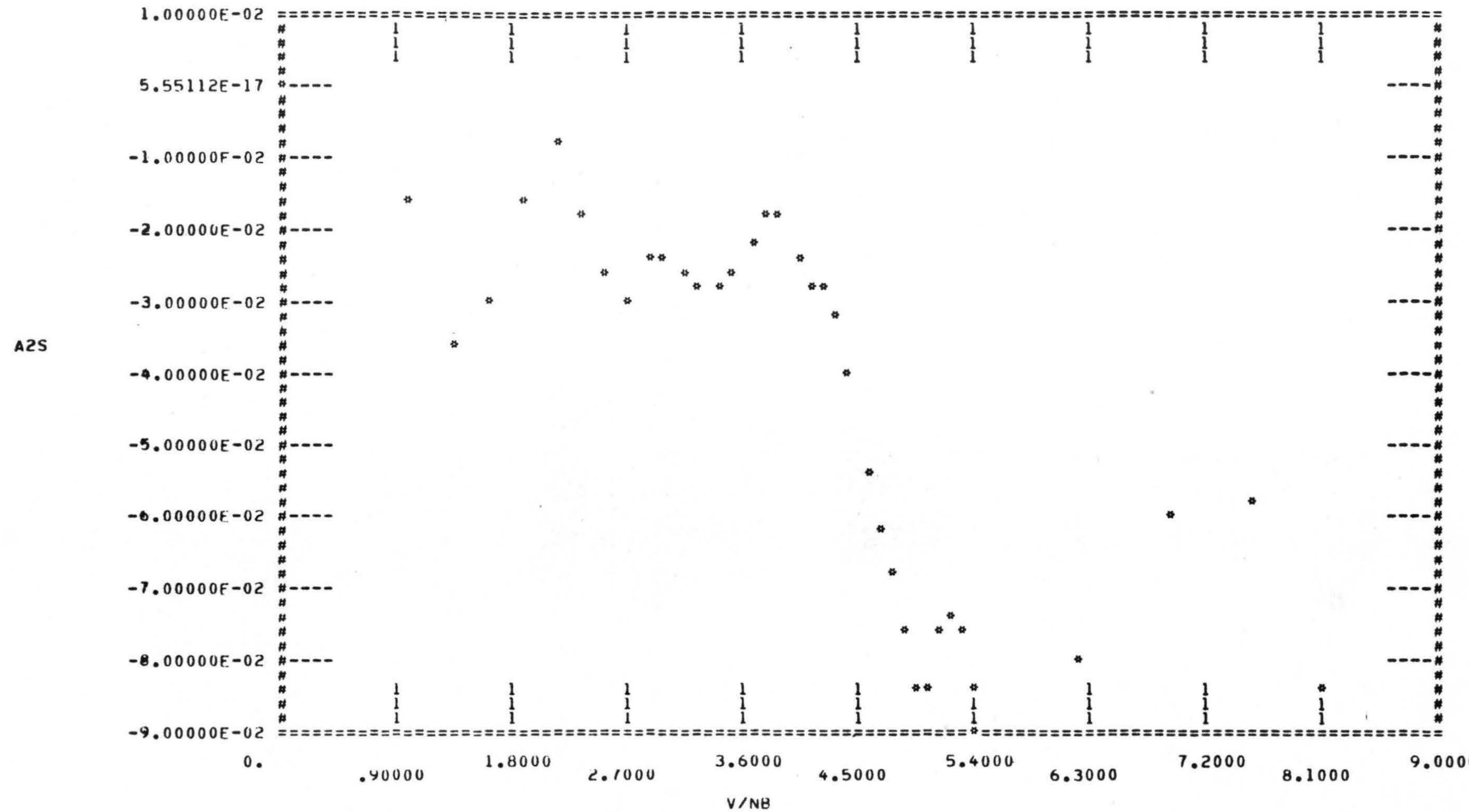

C O N F I G U R A T I O N   MIIA-T

C O N F I G U R A T I O N   MIIA-T

INDEX	V/NB	A2S
(1)	0.	1.42496E-04
(2)	.94793	-1.59042E-02
(3)	1.3406	-3.69358E-02
(4)	1.6419	-2.99035E-02
(5)	1.8959	-1.60555E-02
(6)	2.1616	-8.87371E-03
(7)	2.3220	-1.87263E-02
(8)	2.5080	-2.68675E-02
(9)	2.6812	-2.94124E-02
(10)	2.8438	-2.42779E-02
(11)	2.9976	-2.43253E-02
(12)	3.1152	-2.69939E-02

INDEX	V/NB	A2S
(13)	3.2563	-2.85803E-02
(14)	3.4178	-2.89221E-02
(15)	3.5468	-2.64658E-02
(16)	3.6713	-2.17656E-02
(17)	3.7917	-1.72418E-02
(18)	3.9084	-1.78571E-02
(19)	4.0218	-2.37691E-02
(20)	4.1320	-2.76935E-02
(21)	4.2393	-2.83145E-02
(22)	4.3233	-3.17728E-02
(23)	4.4260	-4.02224E-02
(24)	4.5462	-5.30251E-02

INDEX	V/NB	A2S
(25)	4.6440	-6.19256E-02
(26)	4.7397	-6.79501E-02
(27)	4.8336	-7.54727E-02
(28)	4.9258	-8.33302E-02
(29)	5.0162	-8.32758E-02
(30)	5.1049	-7.69449E-02
(31)	5.1921	-7.31214E-02
(32)	5.2780	-7.62367E-02
(33)	5.3625	-8.41275E-02
(34)	5.4291	-8.98354E-02
(35)	6.2017	-8.04515E-02
(36)	6.9012	-6.03594E-02
(37)	7.5241	-5.74230E-02
(38)	8.0883	-8.34555E-02

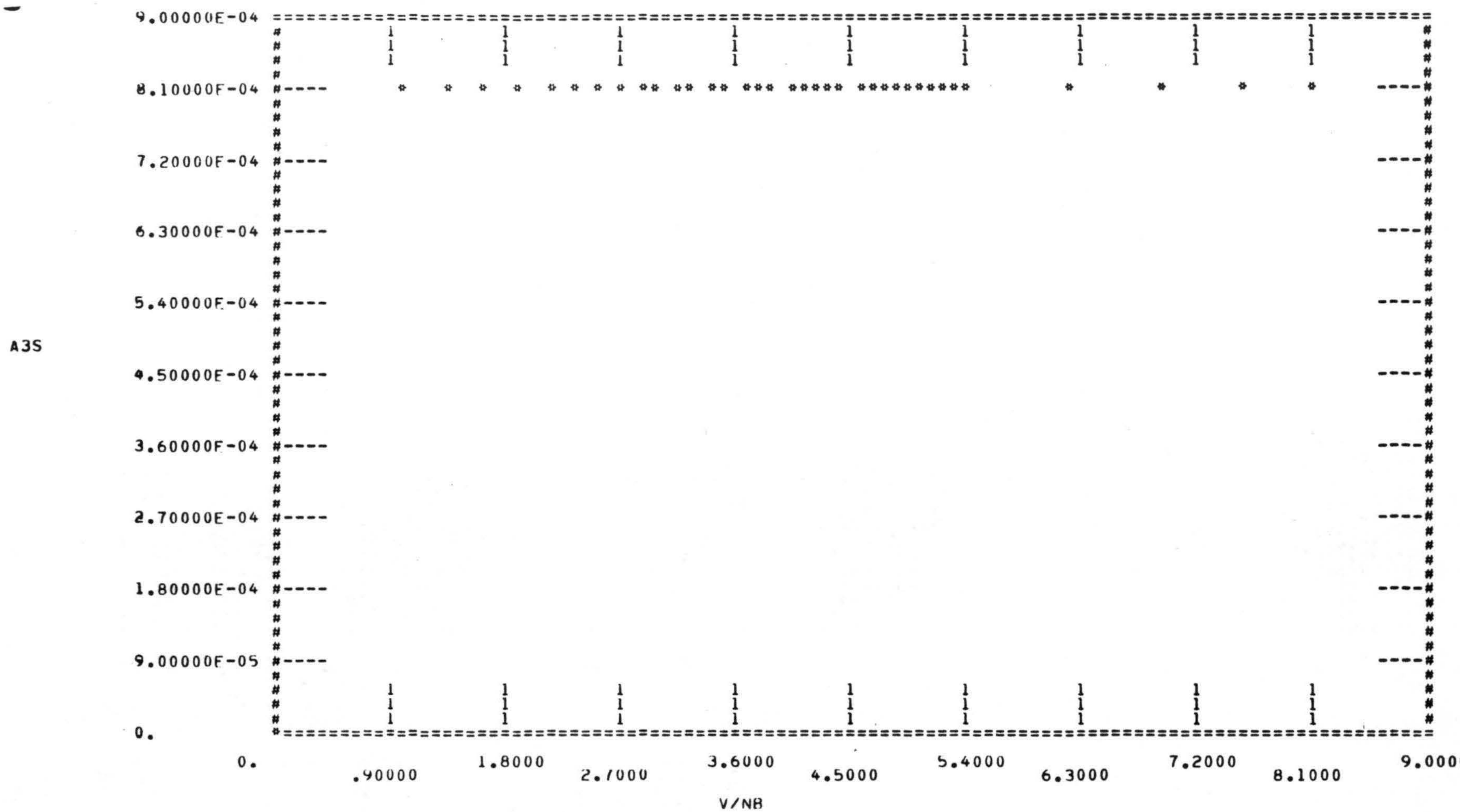

C O N F I G U R A T I O N   MIIA-T

CONFIGURATION MIIA-T

INDEX	V/NB	A3S	INDEX	V/NB	A3S	INDEX	V/NB	A3S
(1)	0.	0.	(13)	3.2563	8.02116E-04	(25)	4.6440	8.02116E-04
(2)	.94793	8.02116E-04	(14)	3.4178	8.02116E-04	(26)	4.7397	8.02116E-04
(3)	1.3406	8.02116E-04	(15)	3.5468	8.02116E-04	(27)	4.8336	8.02116E-04
(4)	1.6419	8.02116E-04	(16)	3.6713	8.02116E-04	(28)	4.9258	8.02116E-04
(5)	1.8959	8.02116E-04	(17)	3.7917	8.02116E-04	(29)	5.0162	8.02116E-04
(6)	2.1616	8.02116E-04	(18)	3.9084	8.02116E-04	(30)	5.1049	8.02116E-04
(7)	2.3220	8.02116E-04	(19)	4.0218	8.02116E-04	(31)	5.1921	8.02116E-04
(8)	2.5080	8.02116E-04	(20)	4.1320	8.02116E-04	(32)	5.2780	8.02116E-04
(9)	2.6812	8.02116E-04	(21)	4.2393	8.02116E-04	(33)	5.3625	8.02116E-04
(10)	2.8438	8.02116E-04	(22)	4.3233	8.02116E-04	(34)	5.4291	8.02116E-04
(11)	2.9976	8.02116E-04	(23)	4.4260	8.02116E-04	(35)	6.2017	8.02116E-04
(12)	3.1152	8.02116E-04	(24)	4.5462	8.02116E-04	(36)	6.9012	8.02116E-04
						(37)	7.5241	8.02116E-04
						(38)	8.0883	8.02116E-04

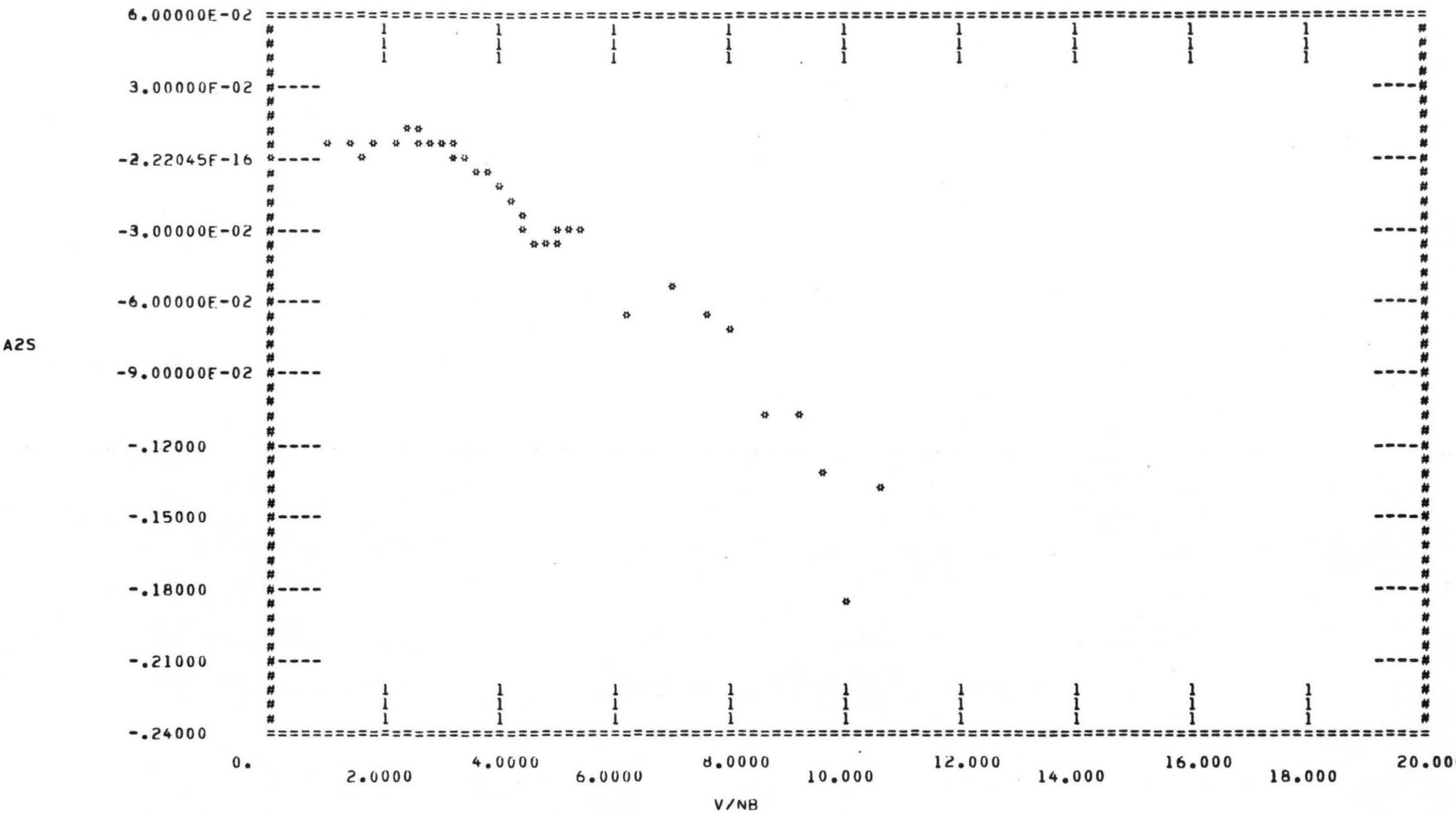

C O N F I G U R A T I O N   M11B-T

CONFIGURATION MIIB-T

INDEX	V/NB	A2S
(1)	0.	2.20477E-04
(2)	.94791	8.82165E-03
(3)	1.3406	4.86236E-03
(4)	1.6418	2.60095E-03
(5)	1.8958	4.35738E-03
(6)	2.1196	7.16909E-03
(7)	2.3219	1.01661E-02
(8)	2.5079	1.00831E-02
(9)	2.6811	8.61570E-03
(10)	2.8437	7.84757E-03
(11)	2.9976	6.99654E-03
(12)	3.1439	4.26797E-03
(13)	3.2837	1.13889E-03
(14)	3.4178	-2.19847E-03

INDEX	V/NB	A2S
(15)	3.5468	-4.71434E-03
(16)	3.6713	-6.64496E-03
(17)	3.7917	-8.66039E-03
(18)	3.9313	-1.08483E-02
(19)	4.0217	-1.26000E-02
(20)	4.1319	-1.55296E-02
(21)	4.2392	-1.97415E-02
(22)	4.3439	-2.54129E-02
(23)	4.4462	-3.14134E-02
(24)	4.5461	-3.54931E-02
(25)	4.6439	-3.75102E-02
(26)	4.7396	-3.79105E-02
(27)	4.8335	-3.65569E-02
(28)	4.9256	-3.41658E-02

INDEX	V/NB	A2S
(29)	5.0159	-3.21061E-02
(30)	5.1047	-3.09583E-02
(31)	5.1920	-3.06578E-02
(32)	5.2778	-3.07264E-02
(33)	5.3623	-3.11179E-02
(34)	5.4454	-3.26397E-02
(35)	6.2161	-6.63902E-02
(36)	6.9140	-5.22208E-02
(37)	7.5240	-6.40621E-02
(38)	8.0992	-7.42001E-02
(39)	8.6467	-.10549
(40)	9.1417	-.10562
(41)	9.6207	-.12949
(42)	10.086	-.18310
(43)	10.513	-.13844

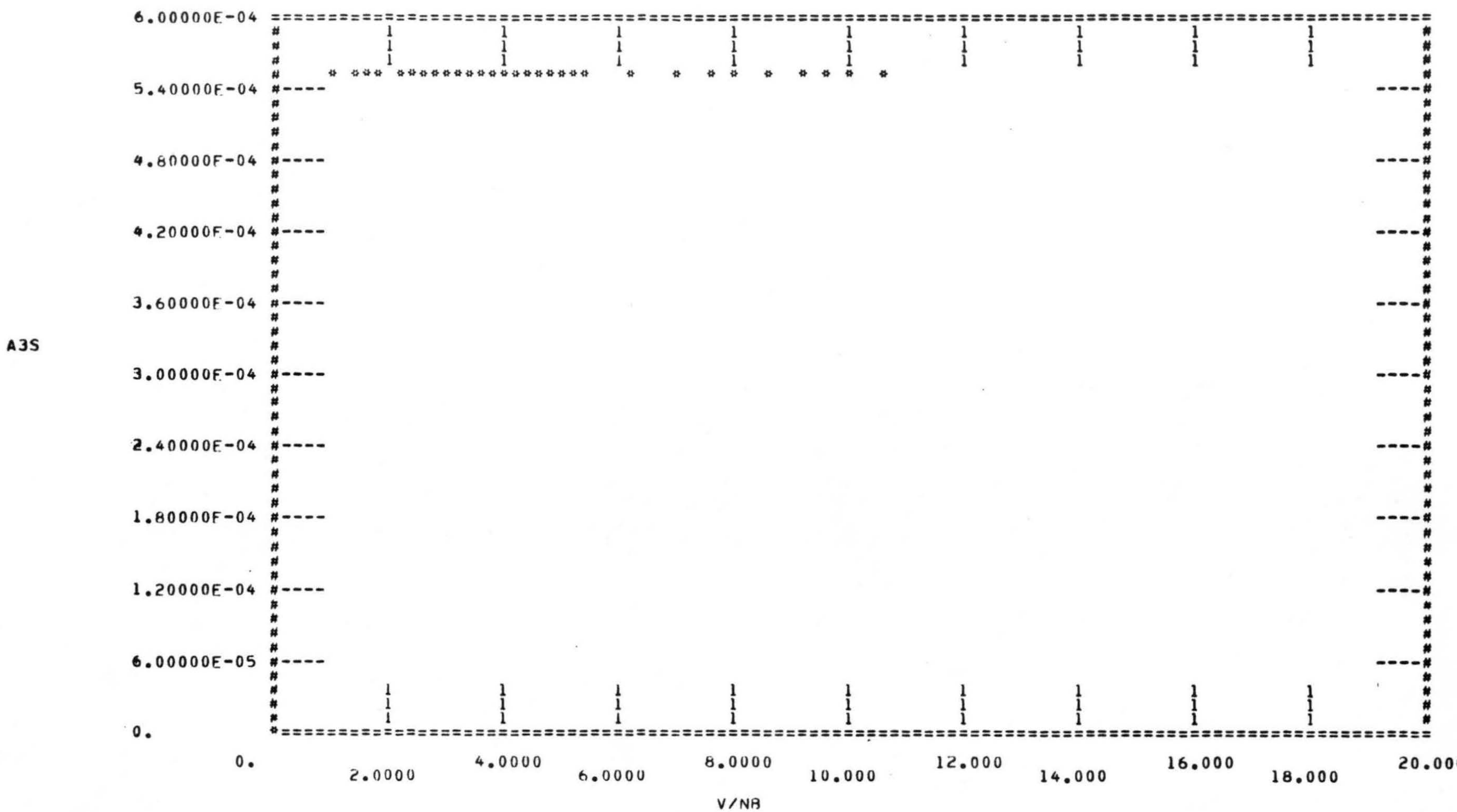

C O N F I G U R A T I O N   M118-T

C O N F I G U R A T I O N   M11B-T

INDEX	V/NB	A3S
(1)	0.	0.
(2)	.94791	5.56756E-04
(3)	1.3406	5.56756E-04
(4)	1.6418	5.56756E-04
(5)	1.8958	5.56756E-04
(6)	2.1196	5.56756E-04
(7)	2.3219	5.56756E-04
(8)	2.5079	5.56756E-04
(9)	2.6811	5.56756E-04
(10)	2.8437	5.56756E-04
(11)	2.9976	5.56756E-04
(12)	3.1439	5.56756E-04
(13)	3.2837	5.56756E-04
(14)	3.4178	5.56756E-04

INDEX	V/NB	A3S
(15)	3.5468	5.56756E-04
(16)	3.6713	5.56756E-04
(17)	3.7917	5.56756E-04
(18)	3.9313	5.56756E-04
(19)	4.0217	5.56756E-04
(20)	4.1319	5.56756E-04
(21)	4.2392	5.56756E-04
(22)	4.3439	5.56756E-04
(23)	4.4462	5.56756E-04
(24)	4.5461	5.56756E-04
(25)	4.6439	5.56756E-04
(26)	4.7396	5.56756E-04
(27)	4.8335	5.56756E-04
(28)	4.9256	5.56756E-04

INDEX	V/NB	A3S
(29)	5.0159	5.56756E-04
(30)	5.1047	5.56756E-04
(31)	5.1920	5.56756E-04
(32)	5.2778	5.56756E-04
(33)	5.3623	5.56756E-04
(34)	5.4454	5.56756E-04
(35)	6.2161	5.56756E-04
(36)	6.9140	5.56756E-04
(37)	7.5240	5.56756E-04
(38)	8.0992	5.56756E-04
(39)	8.6467	5.56756E-04
(40)	9.1417	5.56756E-04
(41)	9.6207	5.56756E-04
(42)	10.086	5.56756E-04
(43)	10.513	5.56756E-04

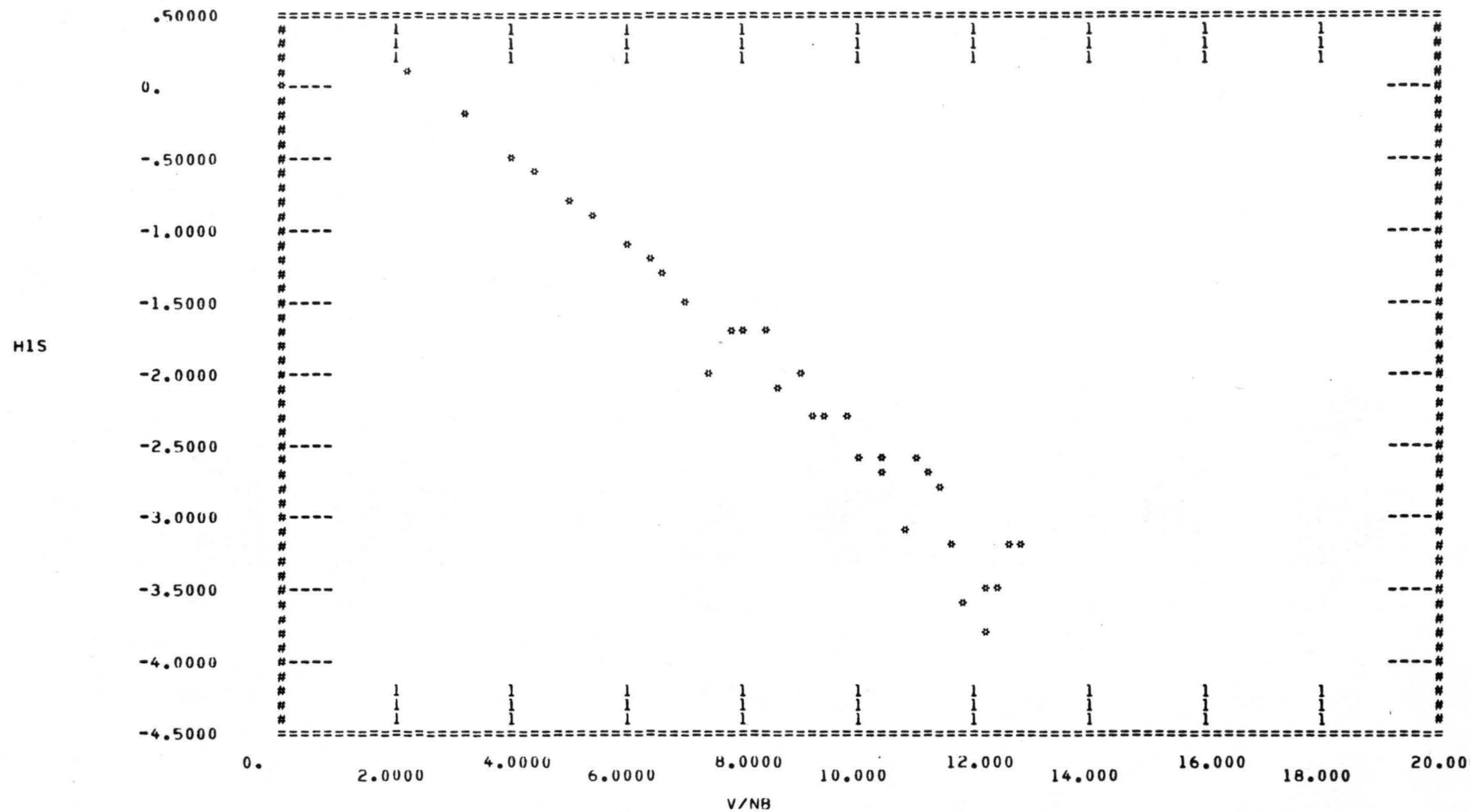

C O N F I G U R A T I O N   MIIA-V

CONFIGURATION MIIA-V

INDEX	V/NB	HIS
(1)	0.	4.15335E-05
(2)	2.2377	7.34110E-02
(3)	3.1646	-.15197
(4)	4.0030	-.45027
(5)	4.4756	-.60072
(6)	4.9028	-.75942
(7)	5.4817	-.91967
(8)	5.9211	-1.0818
(9)	6.3301	-1.2102
(10)	6.6392	-1.2964
(11)	7.0066	-1.4844

INDEX	V/NB	HIS
(12)	7.4918	-1.9938
(13)	7.7536	-1.6778
(14)	8.0705	-1.6920
(15)	8.3749	-1.6839
(16)	8.6703	-2.0558
(17)	8.9540	-1.9724
(18)	9.2854	-2.3404
(19)	9.4985	-2.3075
(20)	9.7072	-2.3017
(21)	10.014	-2.5878
(22)	10.309	-2.5563

INDEX	V/NB	HIS
(23)	10.455	-2.6943
(24)	10.742	-3.1057
(25)	11.014	-2.6016
(26)	11.197	-2.7051
(27)	11.418	-2.8199
(28)	11.638	-3.1698
(29)	11.855	-3.6468
(30)	12.108	-3.7528
(31)	12.269	-3.5230
(32)	12.473	-3.4548
(33)	12.670	-3.2237
(34)	12.828	-3.2243

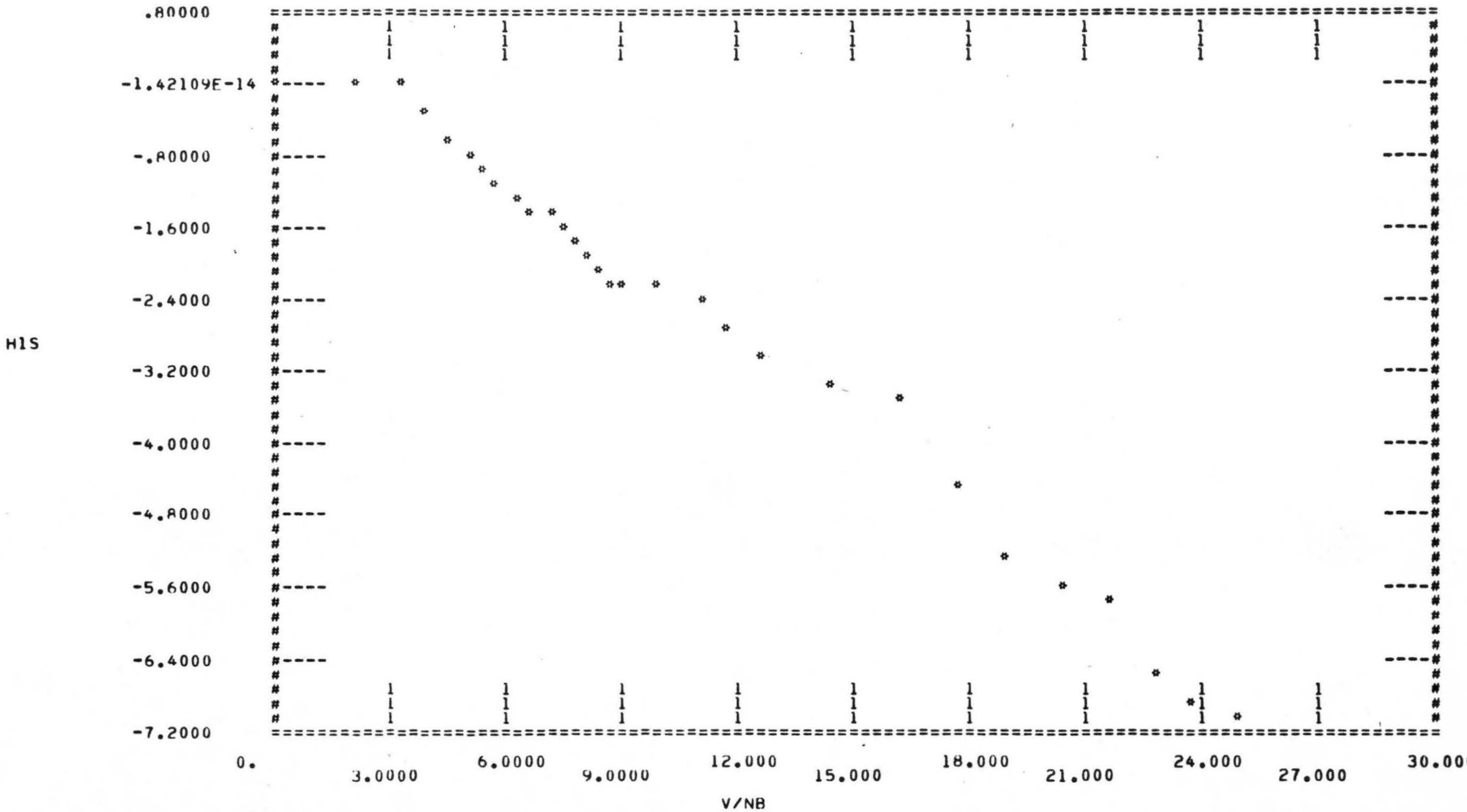

C O N F I G U R A T I O N   MIIB-V

C O N F I G U R A T I O N   MIIB-V

INDEX	V/NB	HIS	INDEX	V/NB	HIS	INDEX	V/NB	HIS
(1)	0.	7.86806E-04	(11)	7.0777	-1.4821	(21)	12.669	-2.9804
(2)	2.2377	7.15281E-02	(12)	7.3557	-1.5750	(22)	14.517	-3.3032
(3)	3.1645	-1.07570E-02	(13)	7.7538	-1.7233	(23)	16.155	-3.5745
(4)	3.8758	-.29543	(14)	8.0706	-1.8724	(24)	17.651	-4.4626
(5)	4.4756	-.57249	(15)	8.3760	-2.0411	(25)	19.036	-5.3077
(6)	5.0039	-.76908	(16)	8.7290	-2.2078	(26)	20.319	-5.5677
(7)	5.4817	-.93127	(17)	8.9550	-2.2634	(27)	21.525	-5.8191
(8)	5.8358	-1.0500	(18)	10.012	-2.3031	(28)	22.687	-6.5514
(9)	6.3302	-1.2291	(19)	10.969	-2.4685	(29)	23.777	-6.8315
(10)	6.7144	-1.3640	(20)	11.848	-2.6430	(30)	24.825	-7.0921

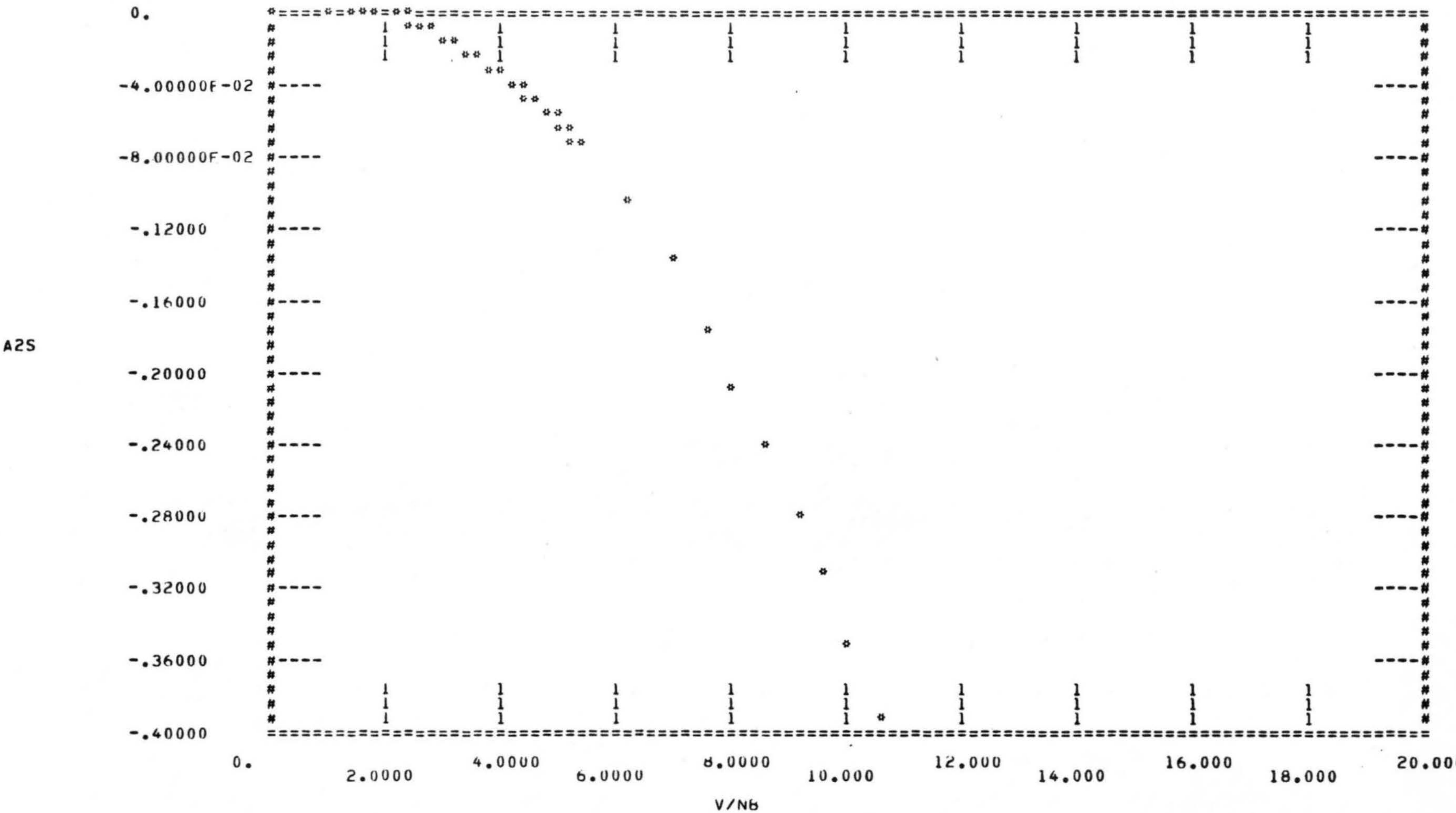

C O N F I G U R A T I O N   MIIIA-T

CONFIGURATION MIIIA-T

INDEX	V/NB	A2S	INDEX	V/NB	A2S	INDEX	V/NB	A2S
(1)	0.	-1.45001E-03	(15)	3.5213	-2.36603E-02	(29)	5.0160	-6.15585E-02
(2)	.94791	-3.89437E-03	(16)	3.6957	-2.76169E-02	(30)	5.1047	-6.43407E-02
(3)	1.3406	-3.76282E-03	(17)	3.7917	-2.98823E-02	(31)	5.1920	-6.71818E-02
(4)	1.6418	-2.86322E-03	(18)	3.8853	-3.21297E-02	(32)	5.2948	-7.06370E-02
(5)	1.8958	-2.11883E-03	(19)	3.9993	-3.48998E-02	(33)	5.3623	-7.29594E-02
(6)	2.1196	-2.27561E-03	(20)	4.1101	-3.75983E-02	(34)	5.4455	-7.58712E-02
(7)	2.3219	-3.41206E-03	(21)	4.2180	-4.02331E-02	(35)	6.2161	-.10536
(8)	2.4718	-4.87284E-03	(22)	4.3646	-4.38466E-02	(36)	6.9012	-.13720
(9)	2.6811	-7.67578E-03	(23)	4.4461	-4.58838E-02	(37)	7.5243	-.17436
(10)	2.8752	-1.08857E-02	(24)	4.5658	-4.89338E-02	(38)	8.0997	-.21031
(11)	2.9976	-1.31205E-02	(25)	4.6438	-5.09765E-02	(39)	8.6368	-.24370
(12)	3.1439	-1.59133E-02	(26)	4.7585	-5.40792E-02	(40)	9.1425	-.27653
(13)	3.2837	-1.86728E-02	(27)	4.8335	-5.61758E-02	(41)	9.6216	-.31174
(14)	3.4178	-2.14310E-02	(28)	4.9256	-5.88375E-02	(42)	10.078	-.35126
						(43)	10.515	-.39332

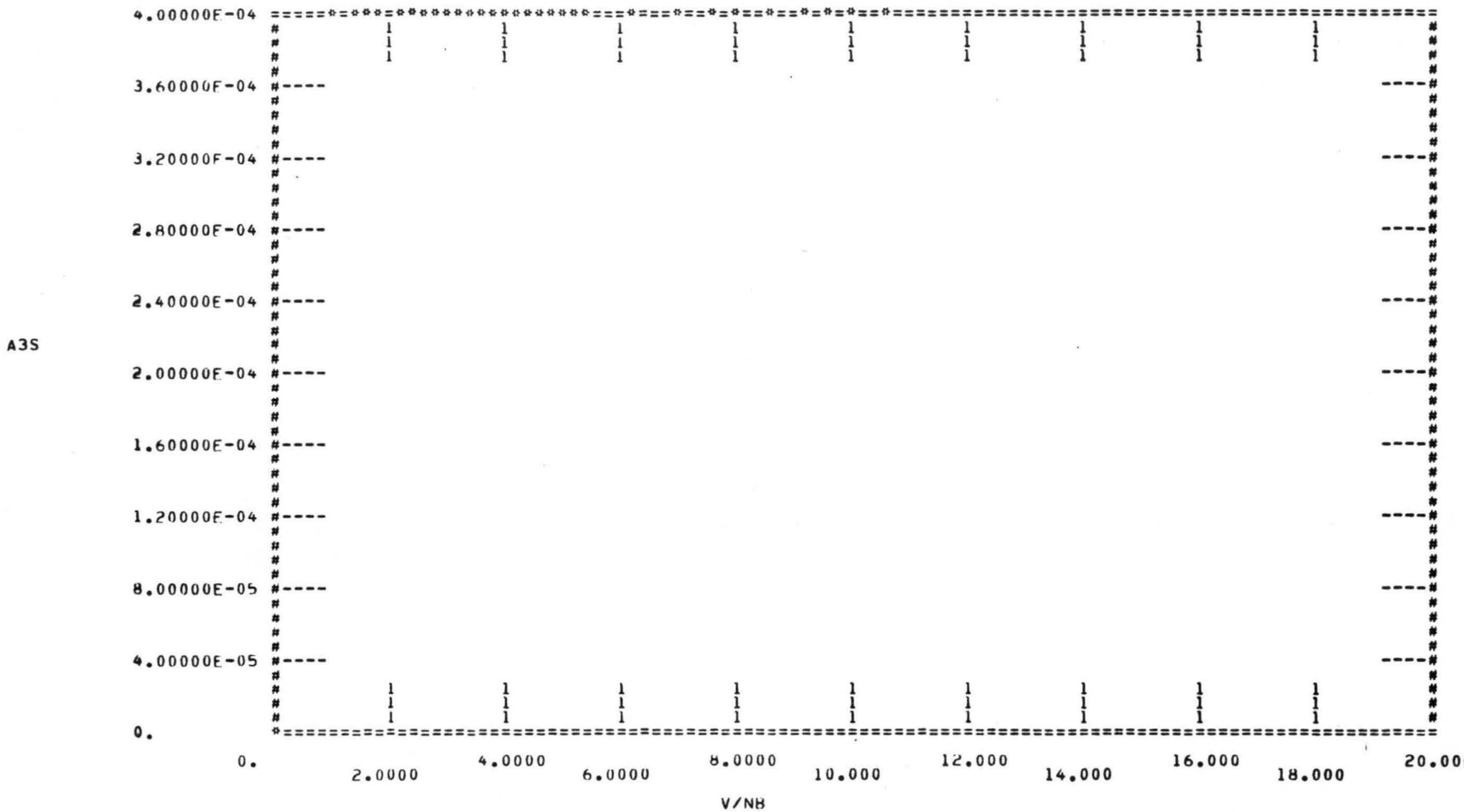

C O N F I G U R A T I O N   MIIIA-T

CONFIGURATION MIIIA-T

INDEX	V/NB	A3S
(1)	0.	0.
(2)	.94791	3.98917E-04
(3)	1.3406	3.98917E-04
(4)	1.6418	3.98917E-04
(5)	1.8958	3.98917E-04
(6)	2.1196	3.98917E-04
(7)	2.3219	3.98917E-04
(8)	2.4718	3.98917E-04
(9)	2.6811	3.98917E-04
(10)	2.8752	3.98917E-04
(11)	2.9976	3.98917E-04
(12)	3.1439	3.98917E-04
(13)	3.2837	3.98917E-04
(14)	3.4178	3.98917E-04

INDEX	V/NB	A3S
(15)	3.5213	3.98917E-04
(16)	3.6957	3.98917E-04
(17)	3.7917	3.98917E-04
(18)	3.8853	3.98917E-04
(19)	3.9993	3.98917E-04
(20)	4.1101	3.98917E-04
(21)	4.2180	3.98917E-04
(22)	4.3646	3.98917E-04
(23)	4.4461	3.98917E-04
(24)	4.5658	3.98917E-04
(25)	4.6438	3.98917E-04
(26)	4.7585	3.98917E-04
(27)	4.8335	3.98917E-04
(28)	4.9256	3.98917E-04

INDEX	V/NB	A3S
(29)	5.0160	3.98917E-04
(30)	5.1047	3.98917E-04
(31)	5.1920	3.98917E-04
(32)	5.2948	3.98917E-04
(33)	5.3623	3.98917E-04
(34)	5.4455	3.98917E-04
(35)	6.2161	3.98917E-04
(36)	6.9012	3.98917E-04
(37)	7.5243	3.98917E-04
(38)	8.0997	3.98917E-04
(39)	8.6368	3.98917E-04
(40)	9.1425	3.98917E-04
(41)	9.6216	3.98917E-04
(42)	10.078	3.98917E-04
(43)	10.515	3.98917E-04

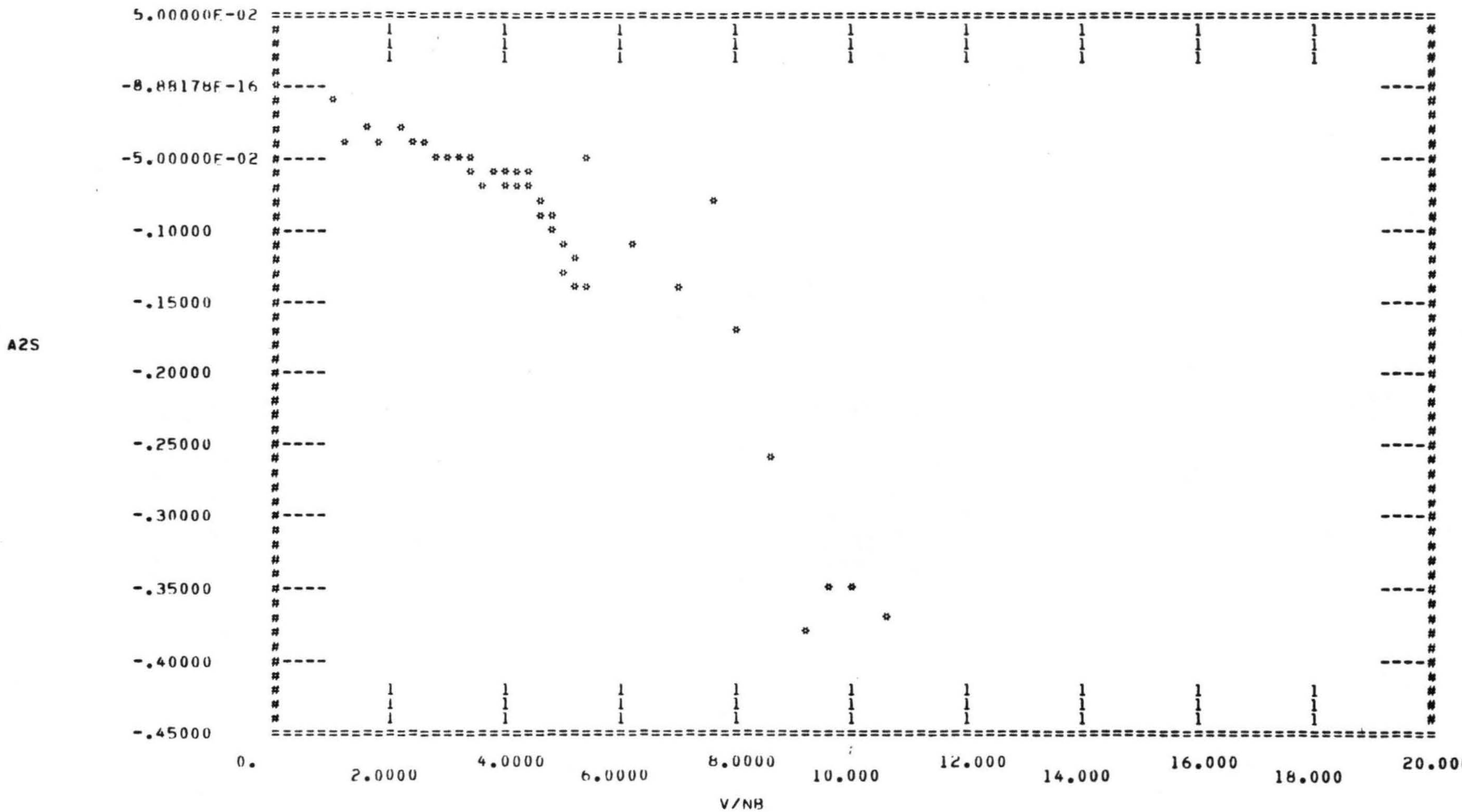

C O N F I G U R A T I O N   MIIIB-T

C O N F I G U R A T I O N   MIIIB-T

INDEX	V/NB	A2S	INDEX	V/NB	A2S	INDEX	V/NB	A2S
(1)	0.	6.92132E-06	(15)	3.5469	-6.78502E-02	(29)	5.0162	-.12758
(2)	.94793	-1.31431E-02	(16)	3.6714	-7.00506E-02	(30)	5.1226	-.13660
(3)	1.2718	-3.52589E-02	(17)	3.7918	-6.38668E-02	(31)	5.2781	-.11863
(4)	1.6419	-2.61484E-02	(18)	3.9085	-6.42132E-02	(32)	5.3623	-5.24270E-02
(5)	1.6959	-3.76373E-02	(19)	4.0218	-7.25913E-02	(33)	5.4458	-.13634
(6)	2.1196	-2.98403E-02	(20)	4.1537	-6.53581E-02	(34)	6.2162	-.10664
(7)	2.3220	-4.32915E-02	(21)	4.2181	-6.49177E-02	(35)	6.9144	-.14043
(8)	2.4719	-3.65874E-02	(22)	4.3647	-6.49283E-02	(36)	7.5122	-7.95482E-02
(9)	2.6812	-3.64034E-02	(23)	4.4463	-6.79086E-02	(37)	8.0775	-.17499
(10)	2.8438	-4.70073E-02	(24)	4.5462	-7.88899E-02	(38)	8.6267	-.25893
(11)	2.9976	-4.56885E-02	(25)	4.6440	-9.05958E-02	(39)	9.1436	-.37670
(12)	3.1724	-4.85670E-02	(26)	4.7398	-9.38999E-02	(40)	9.6317	-.35362
(13)	3.3110	-4.60017E-02	(27)	4.8337	-.10110	(41)	10.088	-.34727
(14)	3.4440	-5.78986E-02	(28)	4.9075	-.10927	(42)	10.524	-.37372

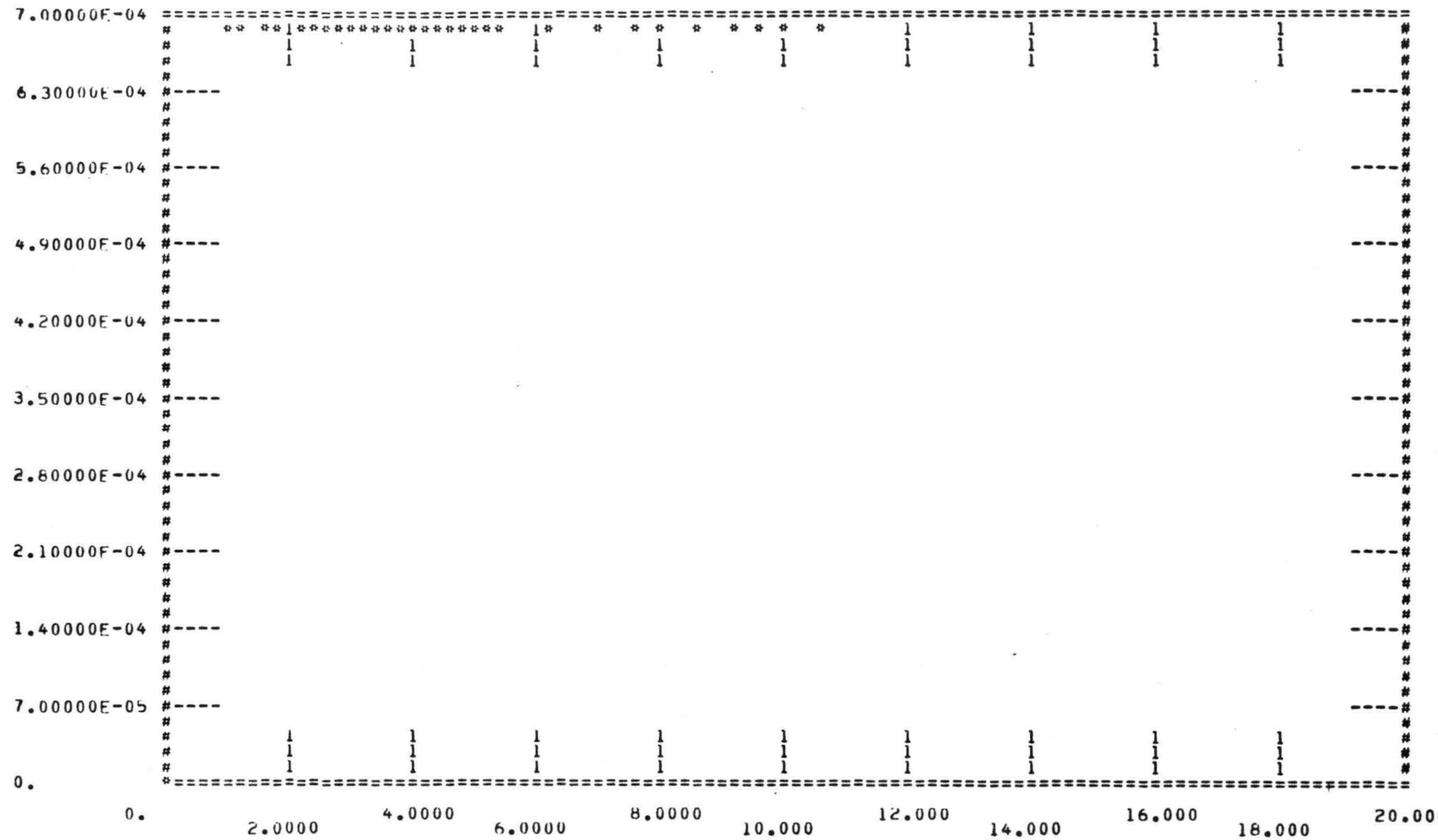

C O N F I G U R A T I O N MIIIB-T

CONFIGURATION MIIIB-T

INDEX	V/NB	A3S	INDEX	V/NB	A3S	INDEX	V/NB	A3S
(1)	0.	6.61301E-14	(15)	3.5469	6.90279E-04	(29)	5.0162	6.90279E-04
(2)	.94793	6.90279E-04	(16)	3.6714	6.90279E-04	(30)	5.1226	6.90279E-04
(3)	1.2718	6.90279E-04	(17)	3.7918	6.90279E-04	(31)	5.2781	6.90279E-04
(4)	1.6419	6.90279E-04	(18)	3.9085	6.90279E-04	(32)	5.3623	6.90279E-04
(5)	1.8959	6.90279E-04	(19)	4.0218	6.90279E-04	(33)	5.4458	6.90279E-04
(6)	2.1196	6.90279E-04	(20)	4.1537	6.90279E-04	(34)	6.2162	6.90279E-04
(7)	2.3220	6.90279E-04	(21)	4.2181	6.90279E-04	(35)	6.9144	6.90279E-04
(8)	2.4719	6.90279E-04	(22)	4.3647	6.90279E-04	(36)	7.5122	6.90279E-04
(9)	2.6812	6.90279E-04	(23)	4.4463	6.90279E-04	(37)	8.0775	6.90279E-04
(10)	2.8438	6.90279E-04	(24)	4.5462	6.90279E-04	(38)	8.6267	6.90279E-04
(11)	2.9976	6.90279E-04	(25)	4.6440	6.90279E-04	(39)	9.1436	6.90279E-04
(12)	3.1724	6.90279E-04	(26)	4.7398	6.90279E-04	(40)	9.6317	6.90279E-04
(13)	3.3110	6.90279E-04	(27)	4.8337	6.90279E-04	(41)	10.088	6.90279E-04
(14)	3.4440	6.90279E-04	(28)	4.9075	6.90279E-04	(42)	10.524	6.90279E-04

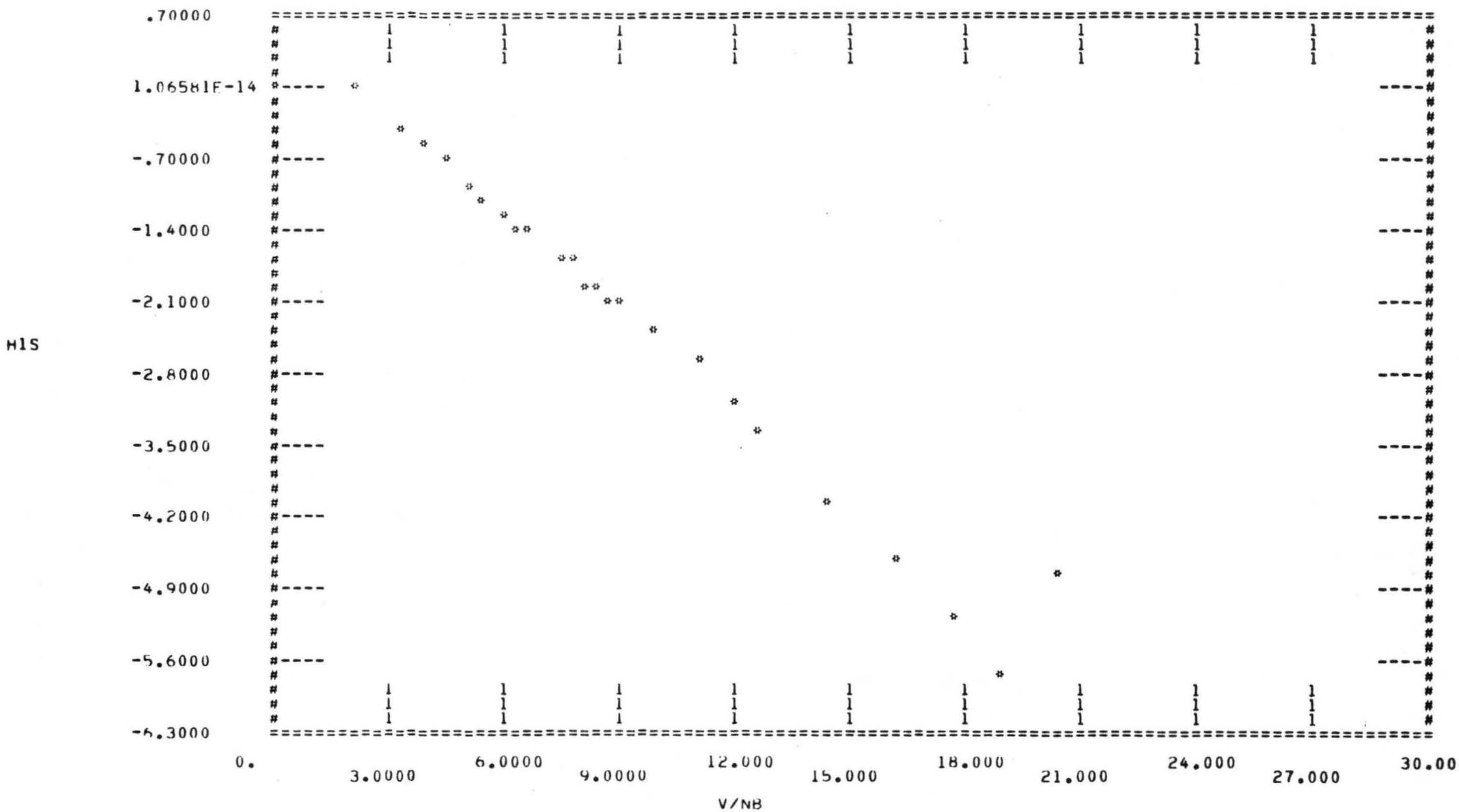

C O N F IG U R A T I O N MIIIA-V

CONFIGURATION MIIIA-V

INDEX	V/NB	HIS
(1)	0.	8.95823E-03
(2)	2.2377	-5.69269E-03
(3)	3.1646	-.36602
(4)	3.8760	-.60607
(5)	4.4757	-.76948
(6)	5.1032	-.93669
(7)	5.4818	-1.0667
(8)	6.0054	-1.2649
(9)	6.3304	-1.3657
(10)	6.7145	-1.4519
(11)	7.4233	-1.6194
(12)	7.7541	-1.7447
(13)	8.1326	-1.8905
(14)	8.3763	-1.9765
(15)	8.6700	-2.0567
(16)	8.9545	-2.1257
(17)	10.013	-2.3903
(18)	10.969	-2.6338
(19)	11.853	-3.1246
(20)	12.671	-3.3372
(21)	14.524	-4.0607
(22)	16.168	-4.6557
(23)	17.661	-5.1882
(24)	19.044	-5.6714
(25)	20.302	-4.7018

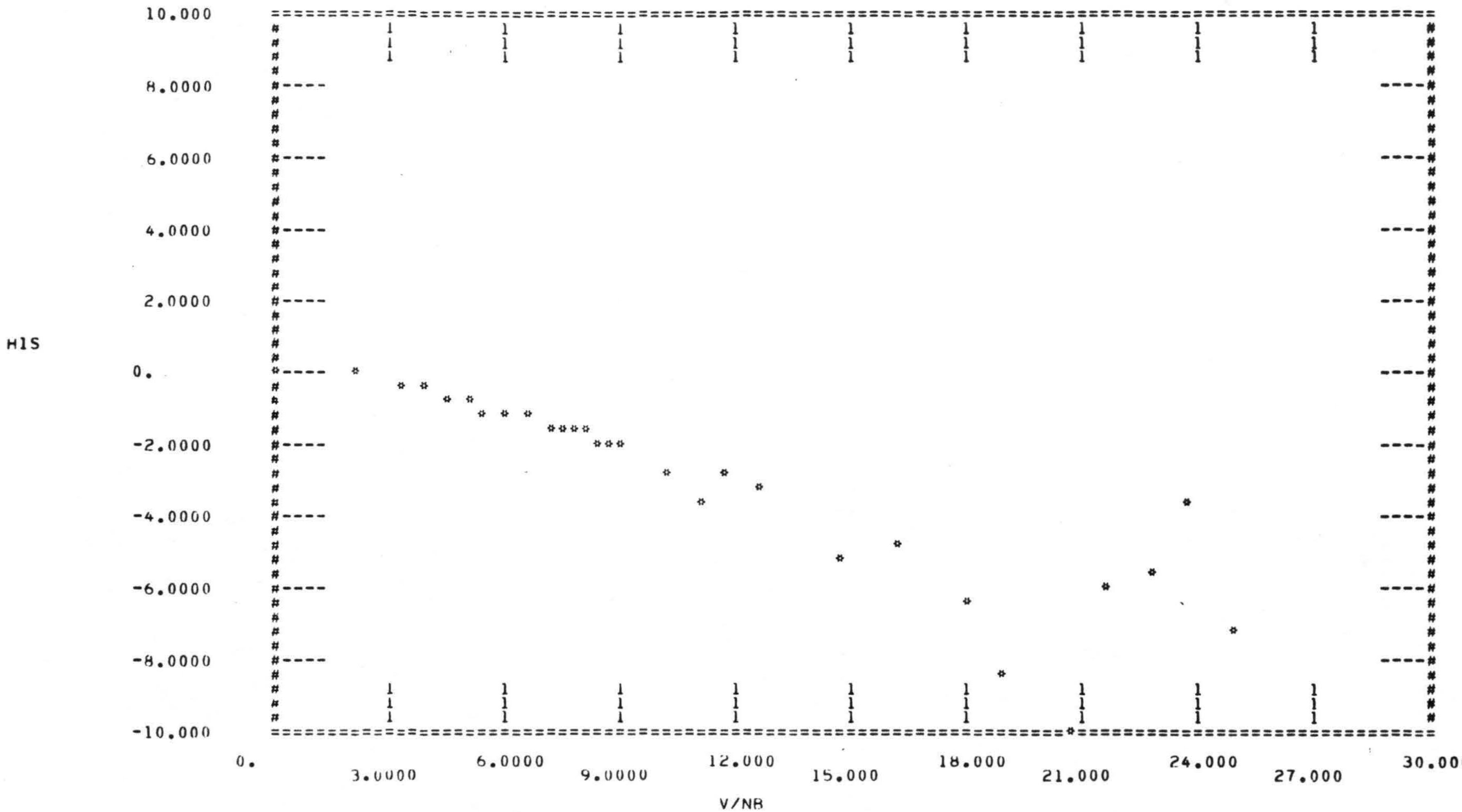

C O N F I G U R A T I O N   MIIIB-V

C O N F I G U R A T I O N   MIIIB-V

INDEX	V/NB	HIS	INDEX	V/NB	HIS	INDEX	V/NB	HIS
(1)	0.	5.63494E-04	(11)	7.0775	-1.4661	(21)	12.670	-3.1859
(2)	2.2377	-3.74409E-03	(12)	7.3560	-1.6543	(22)	14.569	-5.0538
(3)	3.1646	-.28106	(13)	7.7537	-1.6835	(23)	16.170	-4.9019
(4)	3.8759	-.55318	(14)	8.0702	-1.6918	(24)	17.854	-6.4381
(5)	4.4757	-.75053	(15)	8.4352	-1.8451	(25)	19.044	-8.2661
(6)	5.1031	-.86154	(16)	8.6694	-1.9568	(26)	20.582	-9.8073
(7)	5.4818	-1.0278	(17)	8.8986	-2.1133	(27)	21.480	-5.9538
(8)	5.9211	-1.1151	(18)	10.064	-2.7462	(28)	22.793	-5.4047
(9)	6.6391	-1.2525	(19)	10.975	-3.4916	(29)	23.665	-3.6034
(10)	6.6391	-1.2526	(20)	11.806	-2.7482	(30)	24.948	-7.1666

APPENDIX A.2

Aerodynamic Derivatives for Original Bridge Decks

Original Deck

(Dimensions for Model)
(Model Scale 1:40)

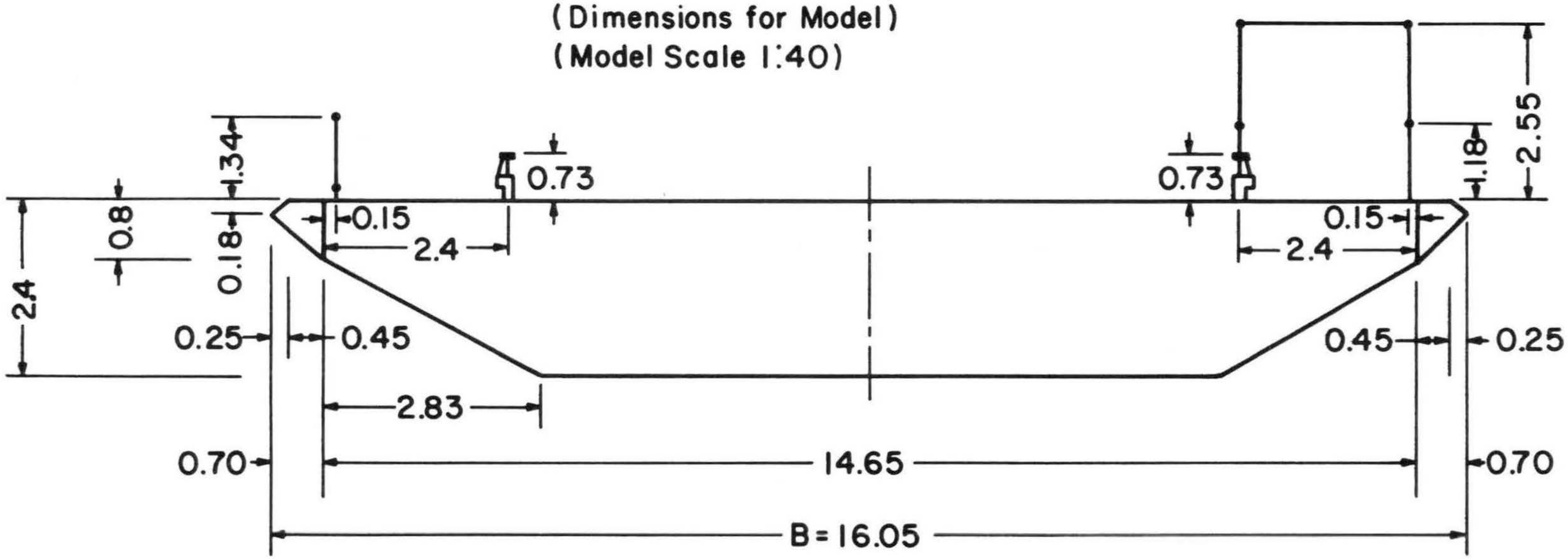

(All Dimensions in inches)

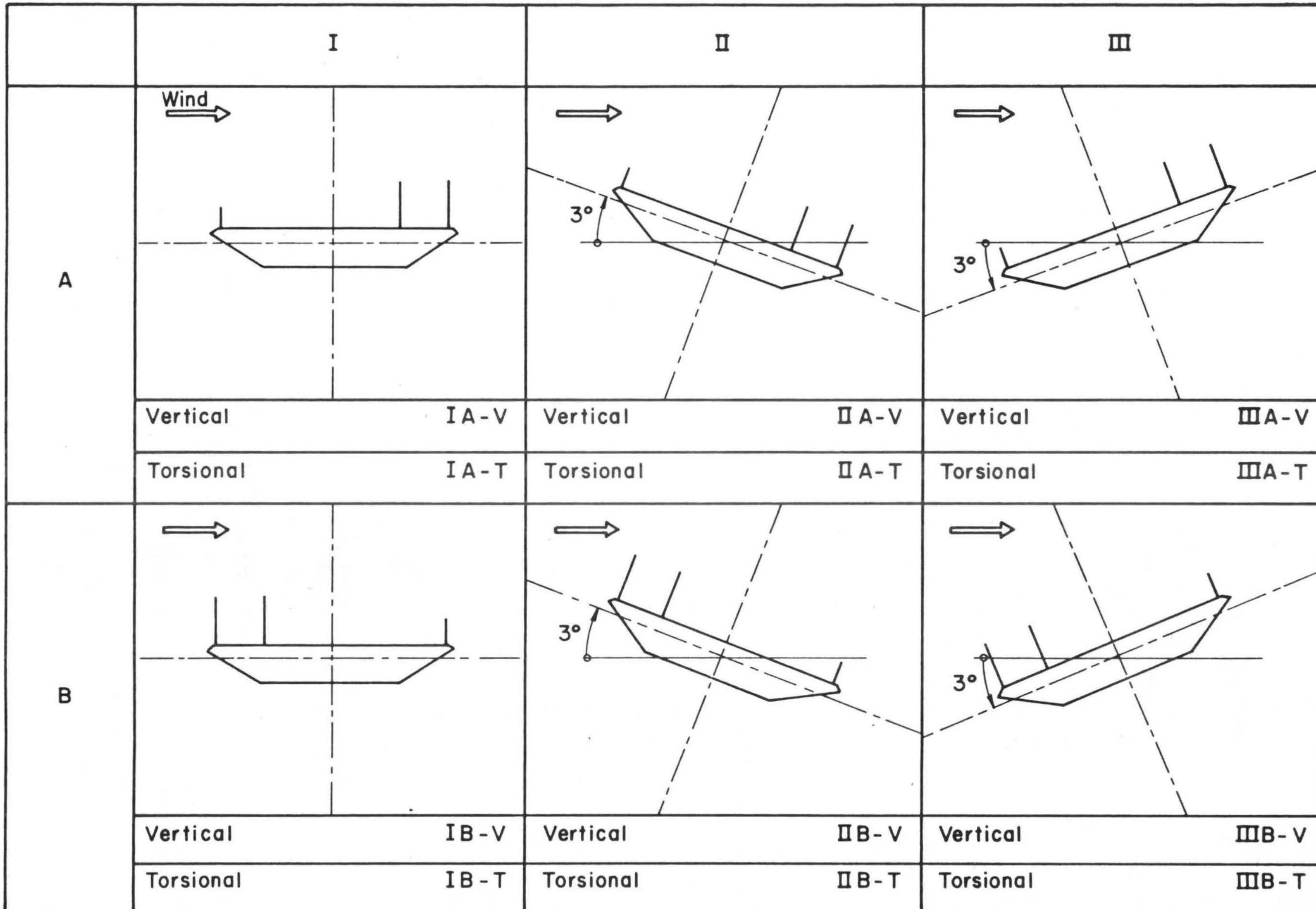
I
II
III
Wind
A
B
3°
Vertical IA-V
Torsional IA-T
Vertical IIA-V
Torsional IIA-T
Vertical IIIA-V
Torsional IIIA-T
Vertical IB-V
Torsional IB-T
Vertical IIB-V
Torsional IIB-T
Vertical IIIB-V
Torsional IIIB-T

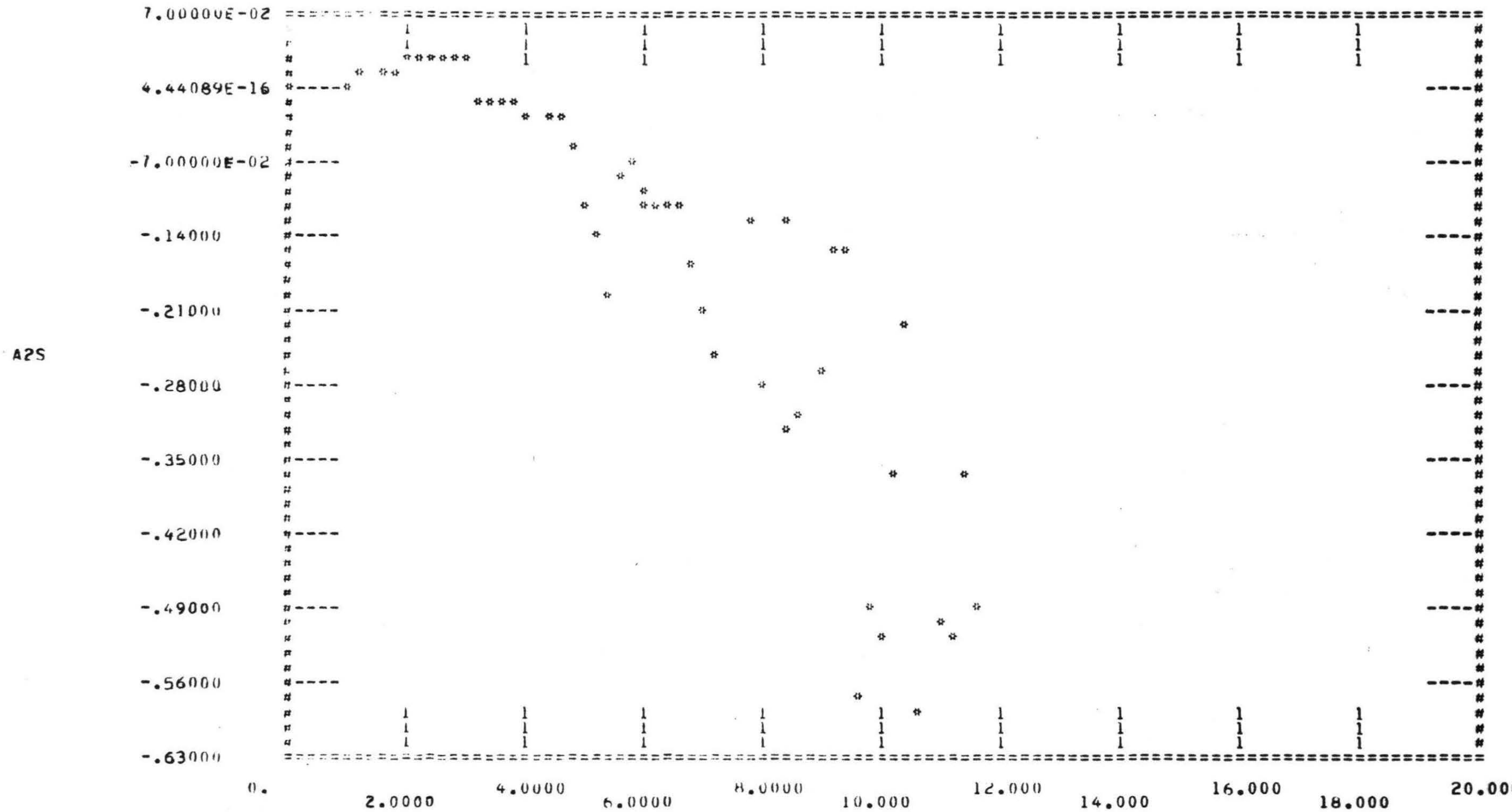

C O N F I G U R A T I O N   IA-T

CONFIGURATION IA-T

INDEX	V/NB	A2S
(1)	0.	-4.59486E-06
(2)	.98416	-5.68290E-04
(3)	1.2449	9.30775E-03
(4)	1.5247	2.08003E-02
(5)	1.7046	2.07162E-02
(6)	1.9185	3.22147E-02
(7)	2.2442	2.63423E-02
(8)	2.4107	2.42961E-02
(9)	2.6408	3.36001E-02
(10)	2.7836	3.40594E-02
(11)	2.9851	2.24518E-02
(12)	3.2042	-1.13038E-02
(13)	3.4092	-9.05747E-03
(14)	3.5485	-8.73634E-03
(15)	3.6824	-1.35604E-02
(16)	3.8117	-9.67667E-03
(17)	4.0578	-2.21084E-02
(18)	4.3124	-3.06420E-02
(19)	4.5100	-3.47605E-02
(20)	4.7199	-5.80938E-02
(21)	4.9209	-.11115
(22)	5.1892	-.14029
(23)	5.3908	-.19109
(24)	5.5674	-9.02754E-02
(25)	5.7723	-6.73624E-02
(26)	5.9542	-.11453
(27)	6.0988	-9.20232E-02
(28)	6.2556	-.11898
(29)	6.4086	-.11093
(30)	6.5727	-.11757
(31)	6.8188	-.16275
(32)	6.9595	-.20694
(33)	7.1789	-.25819
(34)	7.8612	-.13119
(35)	8.0444	-.28075
(36)	8.3054	-.32292
(37)	8.4892	-.13289
(38)	8.6929	-.31369
(39)	8.9453	-.26318
(40)	9.1165	-.14847
(41)	9.3576	-.14787
(42)	9.5446	-.56806
(43)	9.7745	-.48834
(44)	9.9517	-.52025
(45)	10.182	-.36189
(46)	10.435	-.22302
(47)	10.676	-.58125
(48)	10.908	-.50317
(49)	11.129	-.52261
(50)	11.326	-.36314
(51)	11.522	-.49621

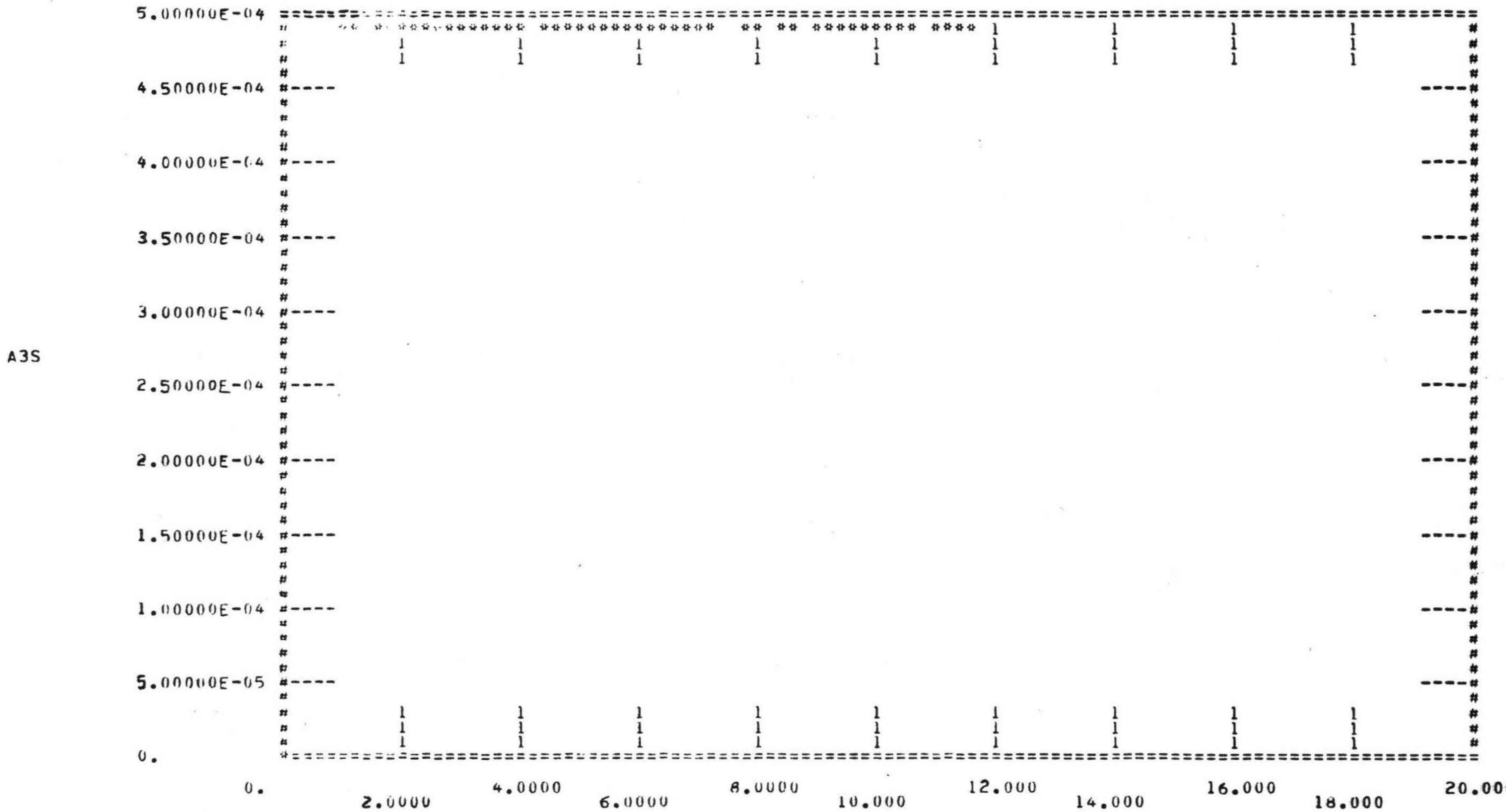

C O N F I G U R A T I O N 1A-T

CONFIGURATION IA-T

INDEX	V/NB	A3S
(1)	0.	-7.68573E-14
(2)	.98416	4.85579E-04
(3)	1.2449	4.85579E-04
(4)	1.5247	4.85579E-04
(5)	1.7046	4.85579E-04
(6)	1.9185	4.85579E-04
(7)	2.2442	4.85579E-04
(8)	2.4107	4.85579E-04
(9)	2.6408	4.85579E-04
(10)	2.7836	4.85579E-04
(11)	2.9851	4.85579E-04
(12)	3.2042	4.85579E-04
(13)	3.4092	4.85579E-04
(14)	3.5485	4.85579E-04
(15)	3.6424	4.85579E-04
(16)	3.8117	4.85579E-04
(17)	4.0578	4.85579E-04
(18)	4.3124	4.85579E-04
(19)	4.5100	4.85579E-04
(20)	4.7199	4.85579E-04
(21)	4.9209	4.85579E-04
(22)	5.1892	4.85579E-04
(23)	5.3908	4.85579E-04
(24)	5.5674	4.85579E-04
(25)	5.7723	4.85579E-04
(26)	5.9542	4.85579E-04
(27)	6.0988	4.85579E-04
(28)	6.2556	4.85579E-04
(29)	6.4086	4.85579E-04
(30)	6.5727	4.85579E-04
(31)	6.8188	4.85579E-04
(32)	6.9595	4.85579E-04
(33)	7.1789	4.85579E-04
(34)	7.8612	4.85579E-04
(35)	8.0444	4.85579E-04
(36)	8.3054	4.85579E-04
(37)	8.4892	4.85579E-04
(38)	8.6929	4.85579E-04
(39)	8.9453	4.85579E-04
(40)	9.1165	4.85579E-04
(41)	9.3576	4.85579E-04
(42)	9.5446	4.85579E-04
(43)	9.7745	4.85579E-04
(44)	9.9517	4.85579E-04
(45)	10.182	4.85579E-04
(46)	10.435	4.85579E-04
(47)	10.676	4.85579E-04
(48)	10.908	4.85579E-04
(49)	11.129	4.85579E-04
(50)	11.326	4.85579E-04
(51)	11.522	4.85579E-04

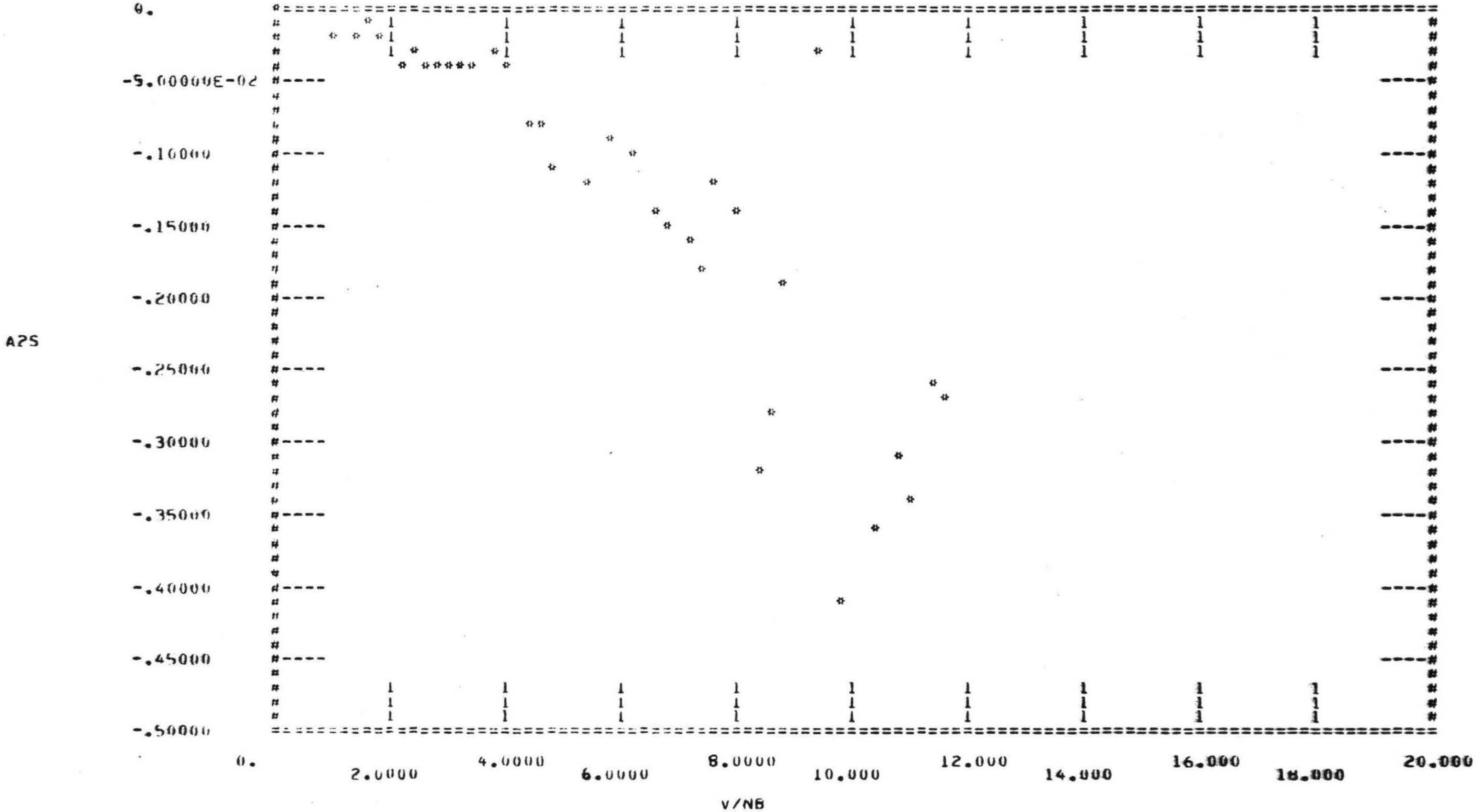

C O N F I G U R A T I O N 18-T

CONFIGURATION IB-T

INDEX	V/NB	A2S	INDEX	V/NB	A2S	INDEX	V/NB	A2S
(1)	0.	-1.06423E-05	(13)	3.7861	-3.23861E-02	(25)	7.6740	-.11816
(2)	.98416	-1.55526E-02	(14)	3.9655	-3.76995E-02	(26)	7.9347	-.13710
(3)	1.3418	-1.66096E-02	(15)	4.3124	-7.67509E-02	(27)	8.4554	-.31855
(4)	1.5869	-1.38952E-02	(16)	4.5314	-7.64563E-02	(28)	8.6589	-.27990
(5)	1.8673	-2.01429E-02	(17)	4.8813	-.10513	(29)	8.8905	-.18629
(6)	2.1562	-3.60071E-02	(18)	5.3182	-.12198	(30)	9.3676	-2.75681E-02
(7)	2.4897	-3.38171E-02	(19)	5.7048	-8.70335E-02	(31)	9.8233	-.40585
(8)	2.6772	-3.58491E-02	(20)	6.2555	-9.65648E-02	(32)	10.304	-.35575
(9)	2.7836	-3.99225E-02	(21)	6.5283	-.13567	(33)	10.809	-.31461
(10)	2.9525	-4.25214E-02	(22)	6.8044	-.14606	(34)	11.004	-.34106
(11)	3.2436	-4.43555E-02	(23)	7.1107	-.15750	(35)	11.359	-.25808
(12)	3.4092	-4.48087E-02	(24)	7.4175	-.18492	(36)	11.687	-.26629

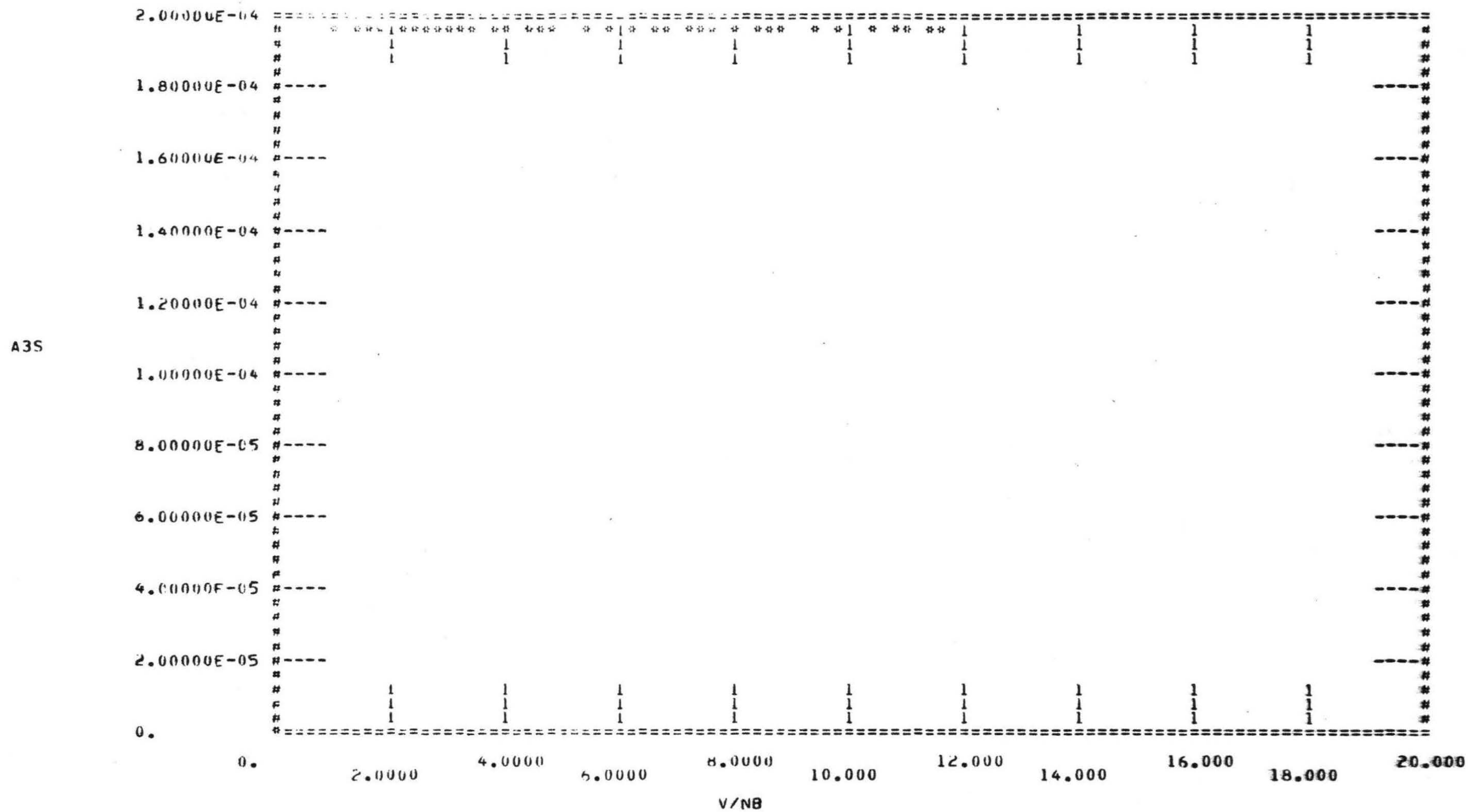

C O N F I G U R A T I O N IB-T

C O N F I G U R A T I O N   IB-T

INDEX	V/NB	A3S	INDEX	V/NB	A3S	INDEX	V/NB	A3S
(1)	0.	-7.68573E-14	(13)	3.7861	1.96827E-04	(25)	7.6740	1.96827E-04
(2)	.98416	1.96827E-04	(14)	3.9855	1.96827E-04	(26)	7.9347	1.96827E-04
(3)	1.3918	1.96827E-04	(15)	4.3124	1.96827E-04	(27)	8.4554	1.96827E-04
(4)	1.5869	1.96827E-04	(16)	4.5314	1.96827E-04	(28)	8.6589	1.96827E-04
(5)	1.8673	1.96827E-04	(17)	4.8813	1.96827E-04	(29)	8.8905	1.96827E-04
(6)	2.1562	1.96827E-04	(18)	5.3182	1.96827E-04	(30)	9.3676	1.96827E-04
(7)	2.4897	1.96827E-04	(19)	5.7048	1.96827E-04	(31)	9.8233	1.96827E-04
(8)	2.6772	1.96827E-04	(20)	6.2555	1.96827E-04	(32)	10.304	1.96827E-04
(9)	2.7836	1.96827E-04	(21)	6.5283	1.96827E-04	(33)	10.809	1.96827E-04
(10)	2.9525	1.96827E-04	(22)	6.8044	1.96827E-04	(34)	11.004	1.96827E-04
(11)	3.2936	1.96827E-04	(23)	7.1107	1.96827E-04	(35)	11.359	1.96827E-04
(12)	3.4092	1.96827E-04	(24)	7.4175	1.96827E-04	(36)	11.687	1.96827E-04

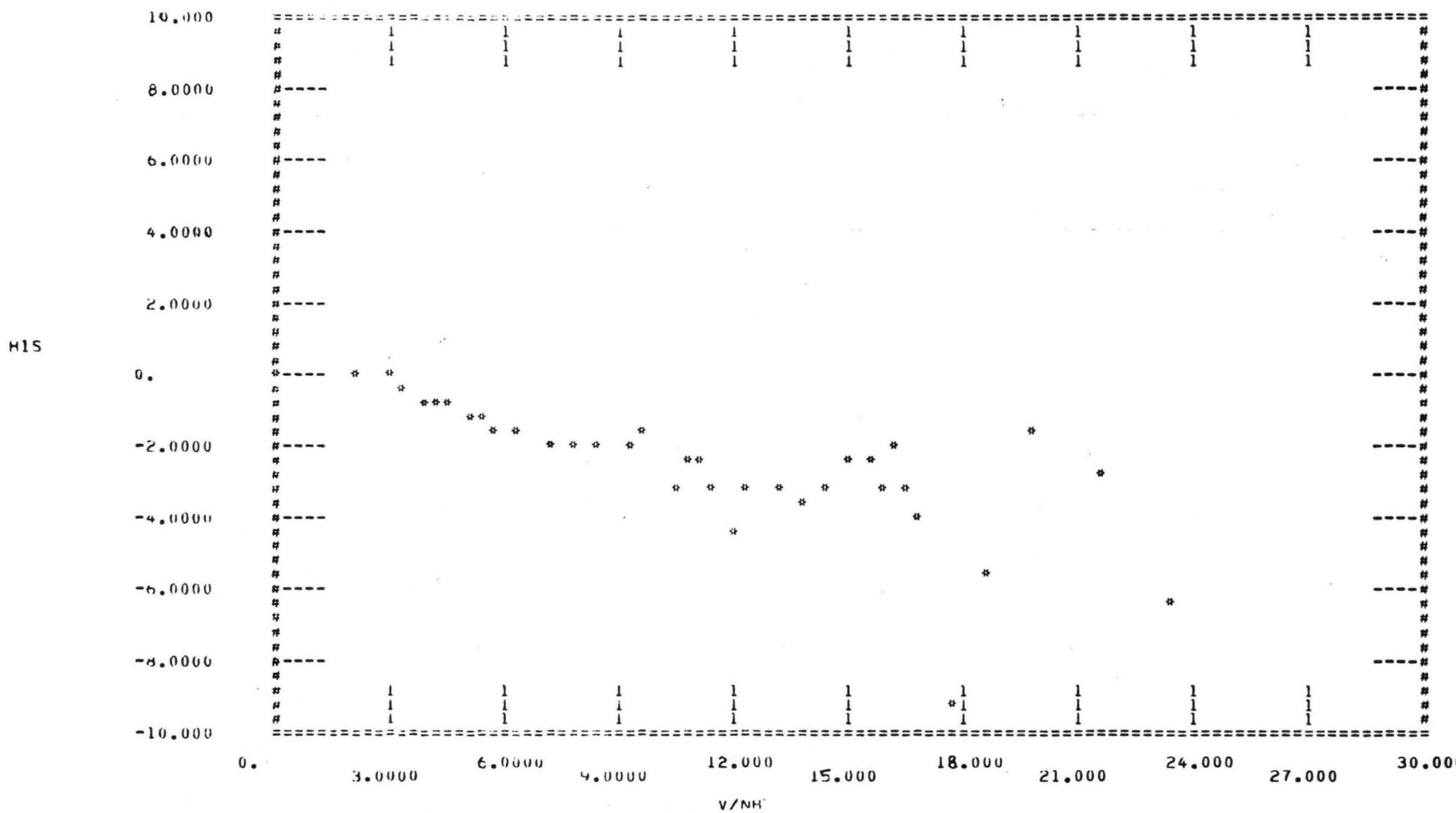

C O N F I G U R A T I O N   IA-V

C O N F I G U R A T I O N   IA-V

INDEX	V/NB	HIS
(1)	0.	-2.18648E-04
(2)	2.1226	4.46653E-03
(3)	3.0019	-3.65339E-03
(4)	3.1840	-.37669
(5)	3.8268	-.76554
(6)	4.2455	-.84318
(7)	4.5031	-.98949
(8)	4.9785	-1.1146
(9)	5.3073	-1.3194
(10)	5.8144	-1.7694
(11)	6.2801	-1.5627
(12)	7.2001	-1.9128

INDEX	V/NB	HIS
(13)	7.7285	-1.8737
(14)	8.3588	-1.8033
(15)	9.1936	-1.8236
(16)	9.7293	-1.7639
(17)	10.514	-3.1162
(18)	10.931	-2.2915
(19)	11.237	-2.3647
(20)	11.536	-3.0658
(21)	11.930	-4.3648
(22)	12.294	-3.1315
(23)	13.308	-3.2634
(24)	13.892	-3.7555

INDEX	V/NR	HIS
(25)	14.367	-3.1074
(26)	14.977	-2.2956
(27)	15.458	-2.2960
(28)	15.825	-3.1036
(29)	16.100	-2.1507
(30)	16.489	-3.1872
(31)	16.866	-4.0109
(32)	17.735	-9.3538
(33)	18.726	-5.6247
(34)	19.689	-1.7594
(35)	21.711	-2.8335
(36)	23.391	-6.4798

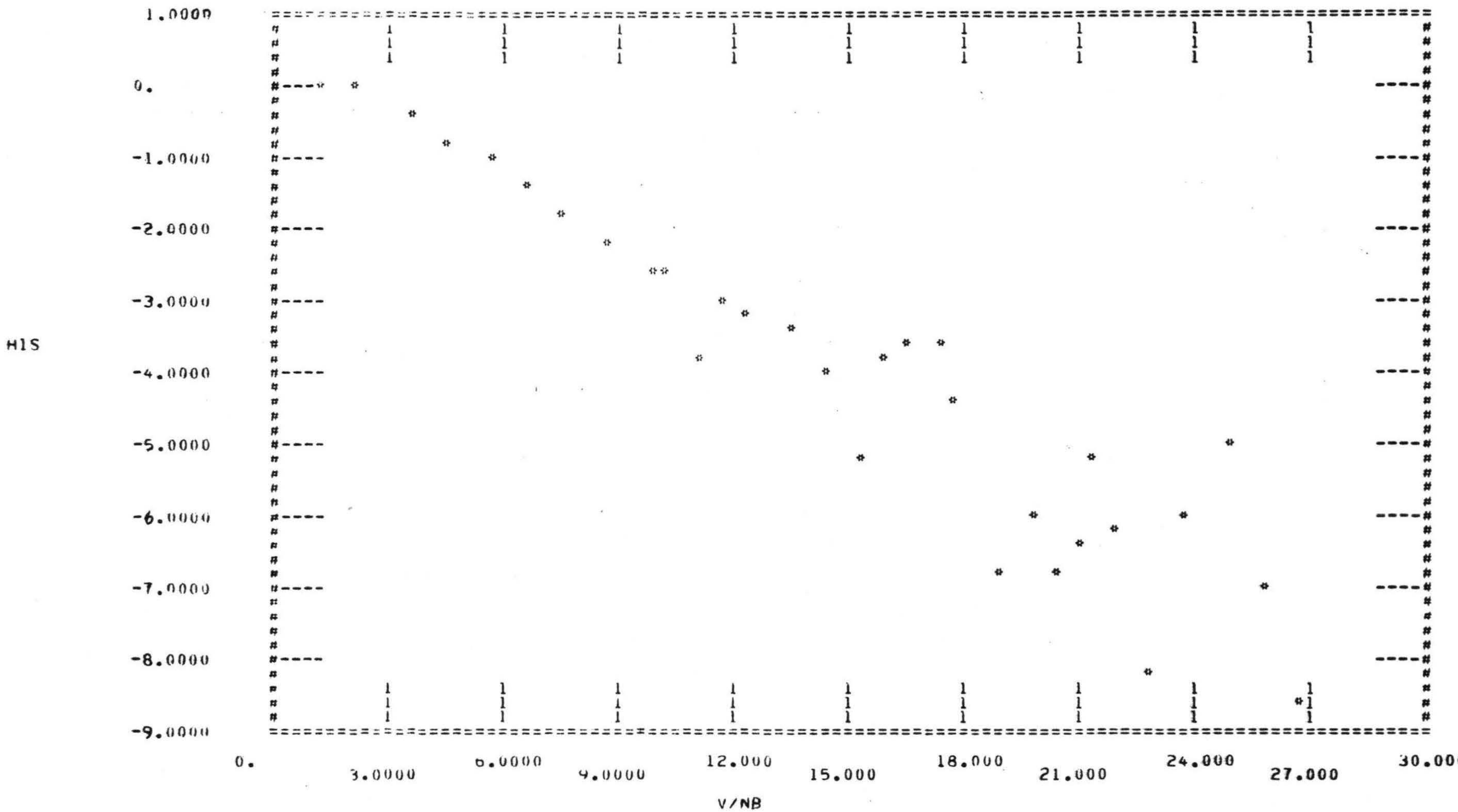

C O N F I G U R A T I O N IB-V

CONFIGURATION IB-V

INDEX	V/NB	HIS	INDEX	V/NB	HIS	INDEX	V/NB	HIS
(1)	1.0613	1.05444E-03	(11)	11.144	-3.8421	(21)	19.016	-6.7333
(2)	2.1226	7.41653E-02	(12)	11.730	-3.0539	(22)	19.732	-5.9784
(3)	3.5201	-.34328	(13)	12.387	-3.1928	(23)	20.454	-6.8194
(4)	4.5031	-.70327	(14)	13.352	-3.3706	(24)	20.886	-6.3994
(5)	5.6165	-1.0393	(15)	14.335	-4.0955	(25)	21.343	-5.2102
(6)	6.5436	-1.4764	(16)	15.263	-5.2349	(26)	21.862	-6.2521
(7)	7.5813	-1.7716	(17)	16.007	-3.8629	(27)	22.695	-8.2360
(8)	8.8190	-2.1037	(18)	16.423	-3.5651	(28)	23.720	-6.0470
(9)	9.8472	-2.5253	(19)	17.326	-3.6566	(29)	24.820	-5.0012
(10)	10.350	-2.6823	(20)	17.784	-4.3913	(30)	25.691	-7.0143
						(31)	26.836	-8.5957

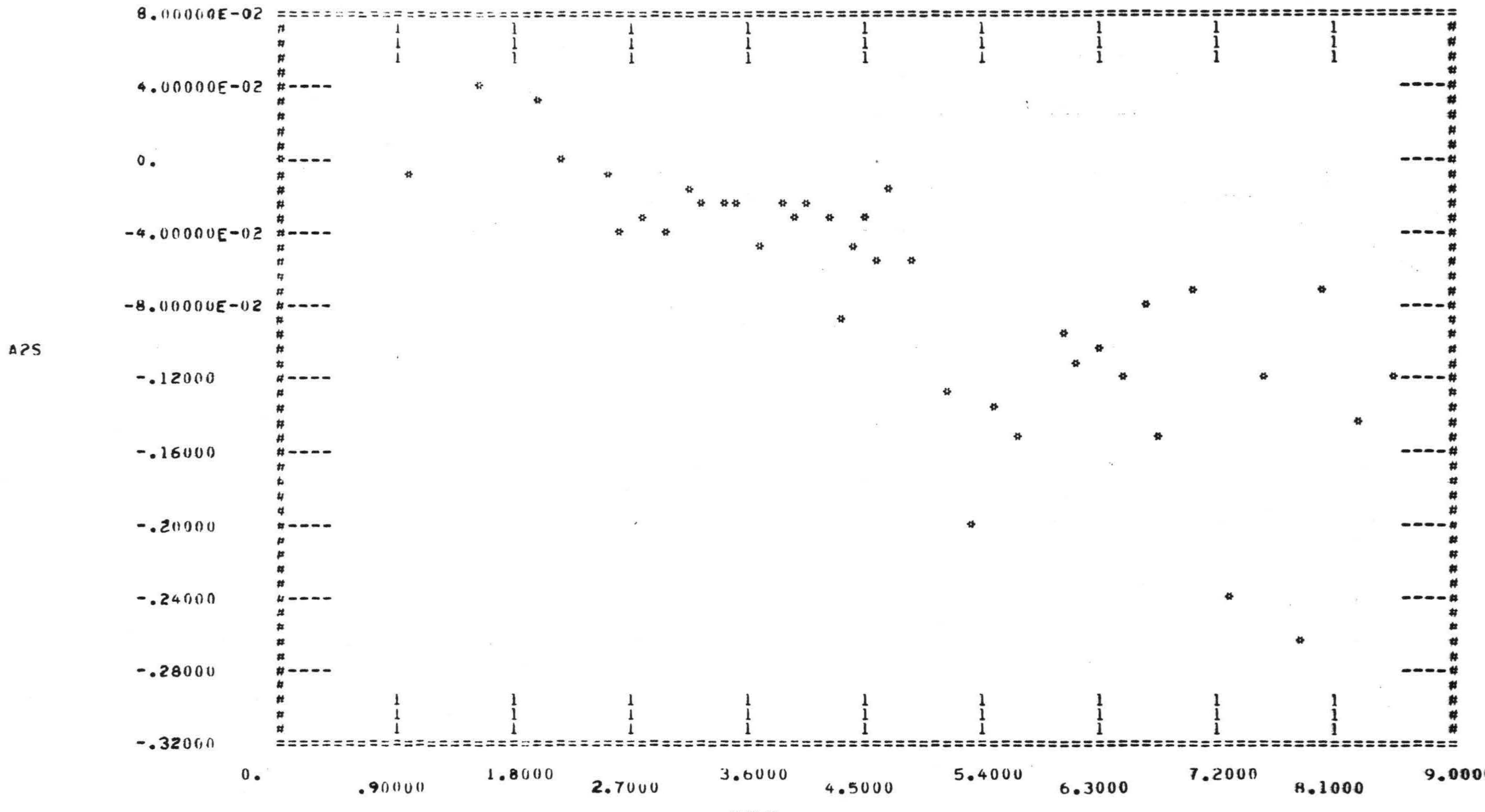

C O N F I G U R A T I O N   IIA-T

CONFIGURATION IIA-T

INDEX	V/NB	A2S
(1)	0.	-4.35917E-06
(2)	.98416	-4.98746E-03
(3)	1.5246	4.03734E-02
(4)	1.9683	2.85357E-02
(5)	2.2006	2.30673E-03
(6)	2.4897	-9.04982E-03
(7)	2.6408	-3.67883E-02
(8)	2.8182	-2.81825E-02
(9)	2.9525	-4.12233E-02
(10)	3.1122	-1.42332E-02
(11)	3.2641	-2.73741E-02
(12)	3.4092	-2.29644E-02
(13)	3.5210	-2.68875E-02
(14)	3.7086	-4.44715E-02
(15)	3.8370	-2.30512E-02
(16)	3.9612	-3.30360E-02
(17)	4.0816	-2.44983E-02
(18)	4.1986	-2.93099E-02
(19)	4.2899	-8.99721E-02
(20)	4.4233	-4.53159E-02
(21)	4.5314	-2.91843E-02
(22)	4.6162	-5.22509E-02
(23)	4.6993	-1.80147E-02
(24)	4.8414	-5.20394E-02
(25)	5.0950	-.12538
(26)	5.3001	-.19793
(27)	5.4973	-.13711
(28)	5.6537	-.15318
(29)	5.9865	-9.98226E-02
(30)	6.1619	-.11234
(31)	6.3171	-.10370
(32)	6.4537	-.11855
(33)	6.6166	-7.60398E-02
(34)	6.7329	-.15031
(35)	7.0283	-7.11962E-02
(36)	7.3124	-.24337
(37)	7.5596	-.11787
(38)	7.8121	-.26496
(39)	8.0437	-7.28860E-02
(40)	8.2812	-.14428
(41)	8.5119	-.12028

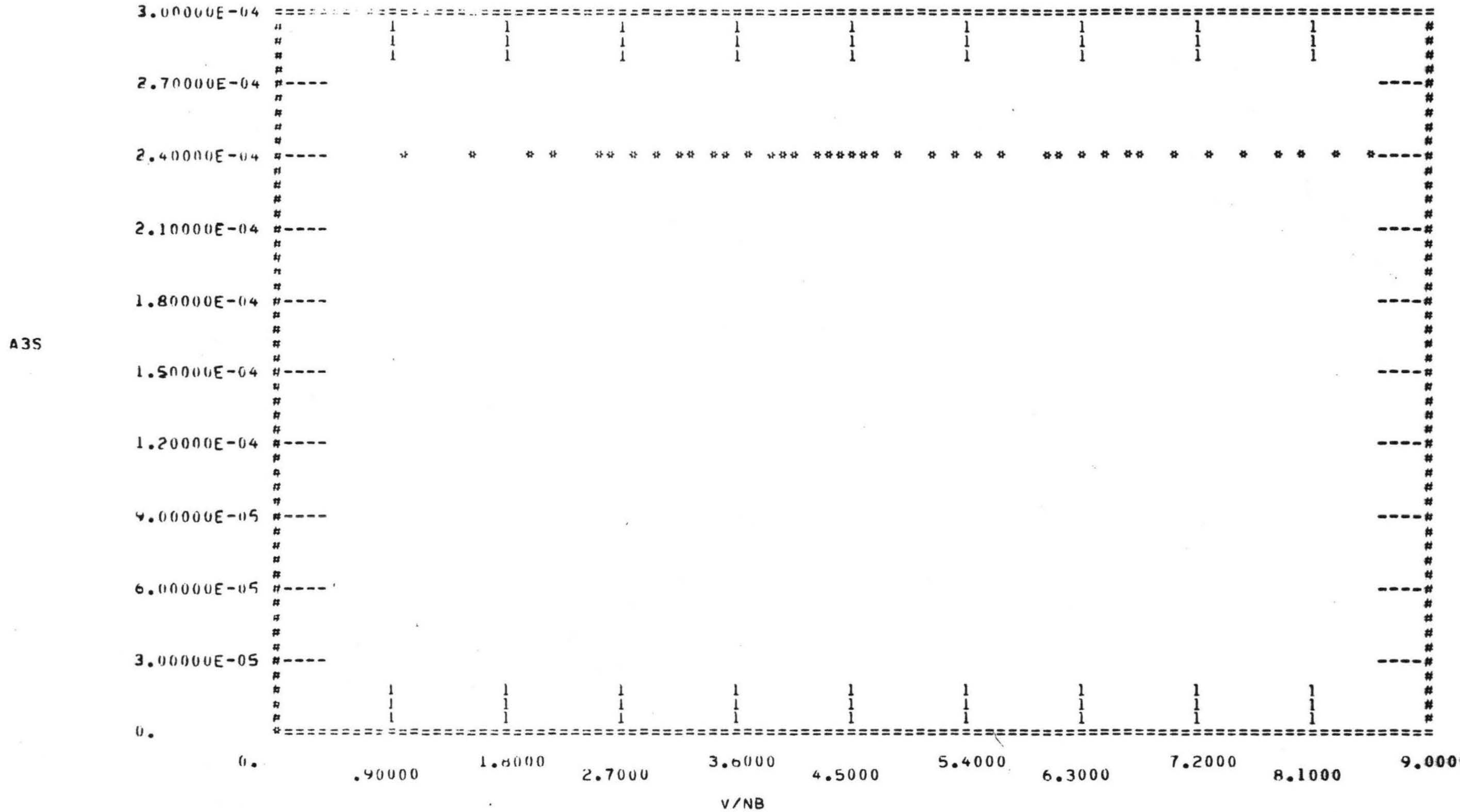

C O N F I G U R A T I O N   IIA-T

C O N F I G U R A T I O N   IIA-T

INDEX	V/NB	A3S	INDEX	V/NB	A3S	INDEX	V/NB	A3S
(1)	0.	-1.53715E-13	(14)	3.7086	2.37519E-04	(27)	5.4973	2.37519E-04
(2)	.98416	2.37519E-04	(15)	3.8370	2.37519E-04	(28)	5.6537	2.37519E-04
(3)	1.5246	2.37519E-04	(16)	3.9612	2.37519E-04	(29)	5.9865	2.37519E-04
(4)	1.9683	2.37519E-04	(17)	4.0816	2.37519E-04	(30)	6.1619	2.37519E-04
(5)	2.2006	2.37519E-04	(18)	4.1986	2.37519E-04	(31)	6.3171	2.37519E-04
(6)	2.4897	2.37519E-04	(19)	4.2899	2.37519E-04	(32)	6.4537	2.37519E-04
(7)	2.6408	2.37519E-04	(20)	4.4233	2.37519E-04	(33)	6.6166	2.37519E-04
(8)	2.8182	2.37519E-04	(21)	4.5314	2.37519E-04	(34)	6.7329	2.37519E-04
(9)	2.9525	2.37519E-04	(22)	4.6162	2.37519E-04	(35)	7.0283	2.37519E-04
(10)	3.1122	2.37519E-04	(23)	4.6993	2.37519F-04	(36)	7.3124	2.37519E-04
(11)	3.2641	2.37519E-04	(24)	4.8414	2.37519E-04	(37)	7.5596	2.37519E-04
(12)	3.4092	2.37519E-04	(25)	5.0950	2.37519E-04	(38)	7.8121	2.37519E-04
(13)	3.5210	2.37519E-04	(26)	5.3001	2.37519E-04	(39)	8.0437	2.37519E-04
						(40)	8.2812	2.37519E-04
						(41)	8.5119	2.37519E-04

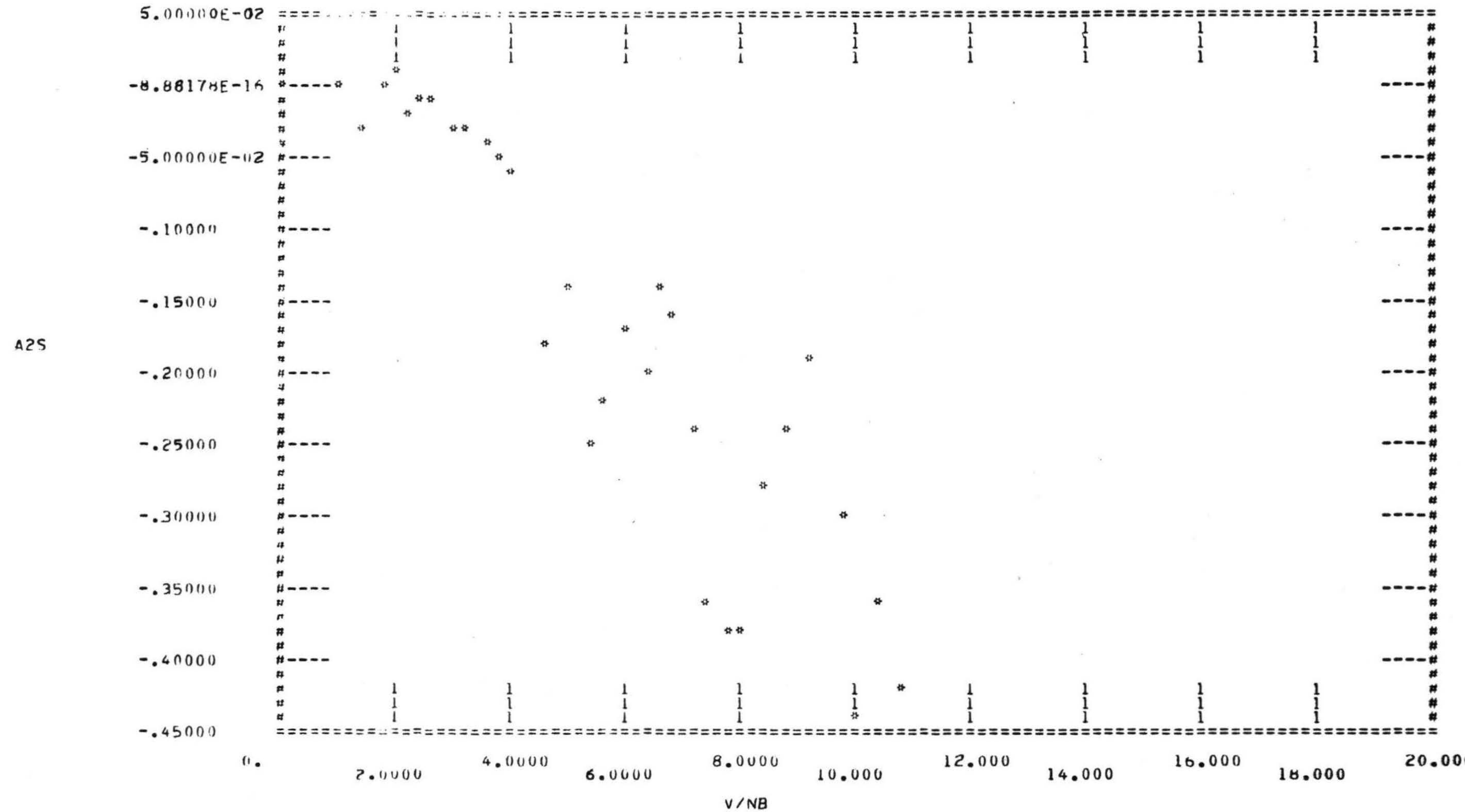

C O N F I G U R A T I O N   IIH-T

CONFIGURATION IIB-T

INDEX	V/NB	A2S
(1)	0.	2.01724E-04
(2)	.98416	7.38109E-04
(3)	1.3918	-2.82126E-02
(4)	1.7046	5.69927E-04
(5)	1.9683	6.43529E-03
(6)	2.2442	-1.52042E-02
(7)	2.4107	-1.07100E-02
(8)	2.5664	-1.46451E-02
(9)	2.9851	-2.75637E-02
(10)	3.2937	-3.28637E-02
(11)	3.5485	-3.76161E-02
(12)	3.8370	-4.63888E-02
(13)	4.0339	-6.47045E-02
(14)	4.5317	-.17906
(15)	4.9210	-.14439
(16)	5.3003	-.25318
(17)	5.6539	-.21804
(18)	5.9705	-.17069
(19)	6.3021	-.20309
(20)	6.6021	-.14052
(21)	6.8753	-.15988
(22)	7.1788	-.24076
(23)	7.4443	-.35792
(24)	7.7002	-.38180
(25)	7.9357	-.37582
(26)	8.4209	-.27780
(27)	8.8581	-.24238
(28)	9.2746	-.19486
(29)	9.7037	-.29619
(30)	10.096	-.43644
(31)	10.463	-.35715
(32)	10.837	-.42214

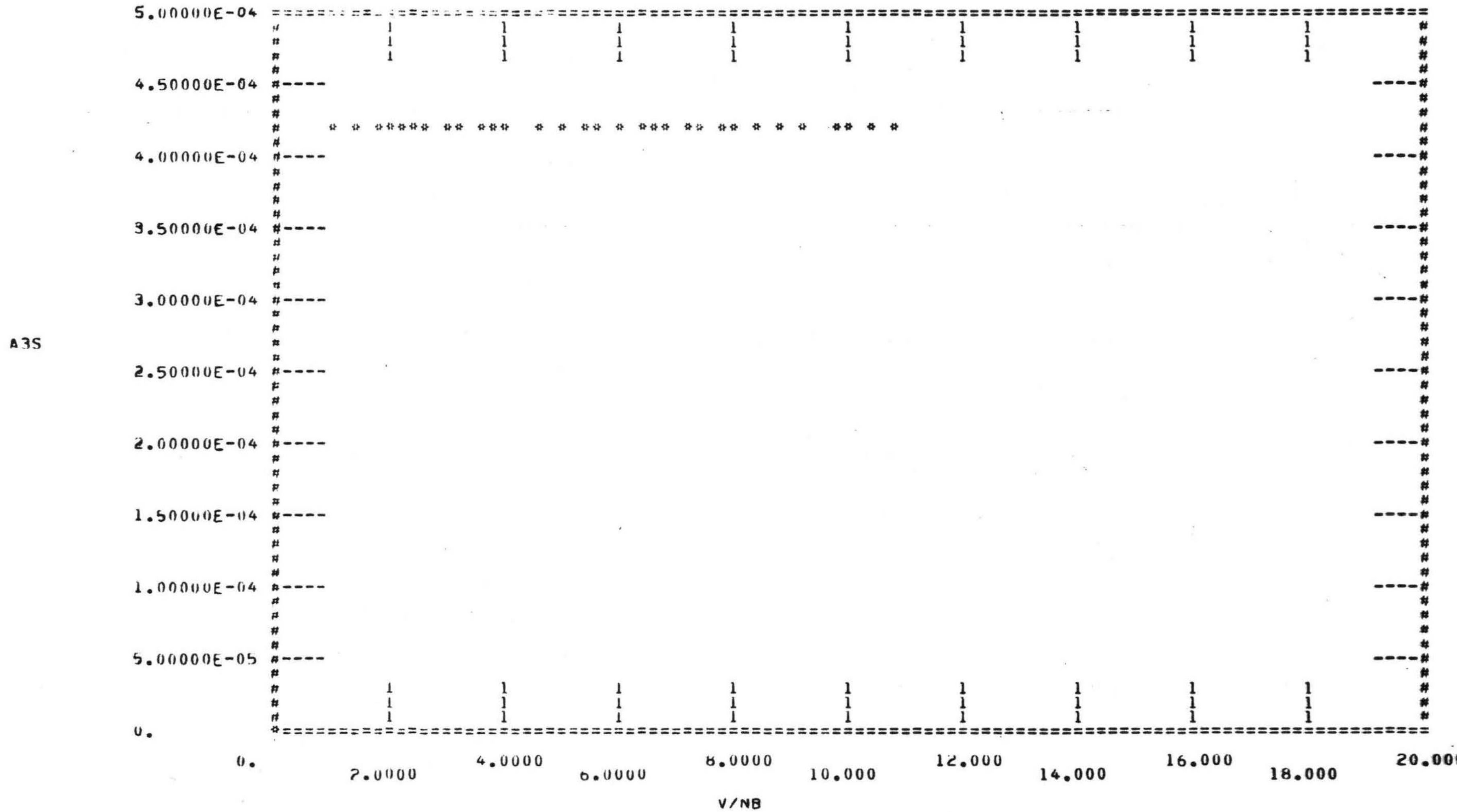

C O N F I G U R A T I O N IIB-T

C O N F I G U R A T I O N   IIB-T

INDEX	V/NB	A3S
(1)	0.	7.68573E-14
(2)	.98416	4.23335E-04
(3)	1.3918	4.23335E-04
(4)	1.7046	4.23335E-04
(5)	1.9683	4.23335E-04
(6)	2.2442	4.23335E-04
(7)	2.4107	4.23335E-04
(8)	2.5664	4.23335E-04
(9)	2.9851	4.23335E-04
(10)	3.2937	4.23335E-04
(11)	3.5485	4.23335E-04
(12)	3.8370	4.23335E-04
(13)	4.0339	4.23335E-04
(14)	4.5317	4.23335E-04
(15)	4.9210	4.23335E-04
(16)	5.3003	4.23335E-04
(17)	5.6539	4.23335E-04
(18)	5.9705	4.23335E-04
(19)	6.3021	4.23335E-04
(20)	6.6021	4.23335E-04
(21)	6.8753	4.23335E-04
(22)	7.1788	4.23335E-04
(23)	7.4443	4.23335E-04
(24)	7.7002	4.23335E-04
(25)	7.9357	4.23335E-04
(26)	8.4209	4.23335E-04
(27)	8.8581	4.23335E-04
(28)	9.2746	4.23335E-04
(29)	9.7037	4.23335E-04
(30)	10.096	4.23335E-04
(31)	10.463	4.23335E-04
(32)	10.837	4.23335E-04

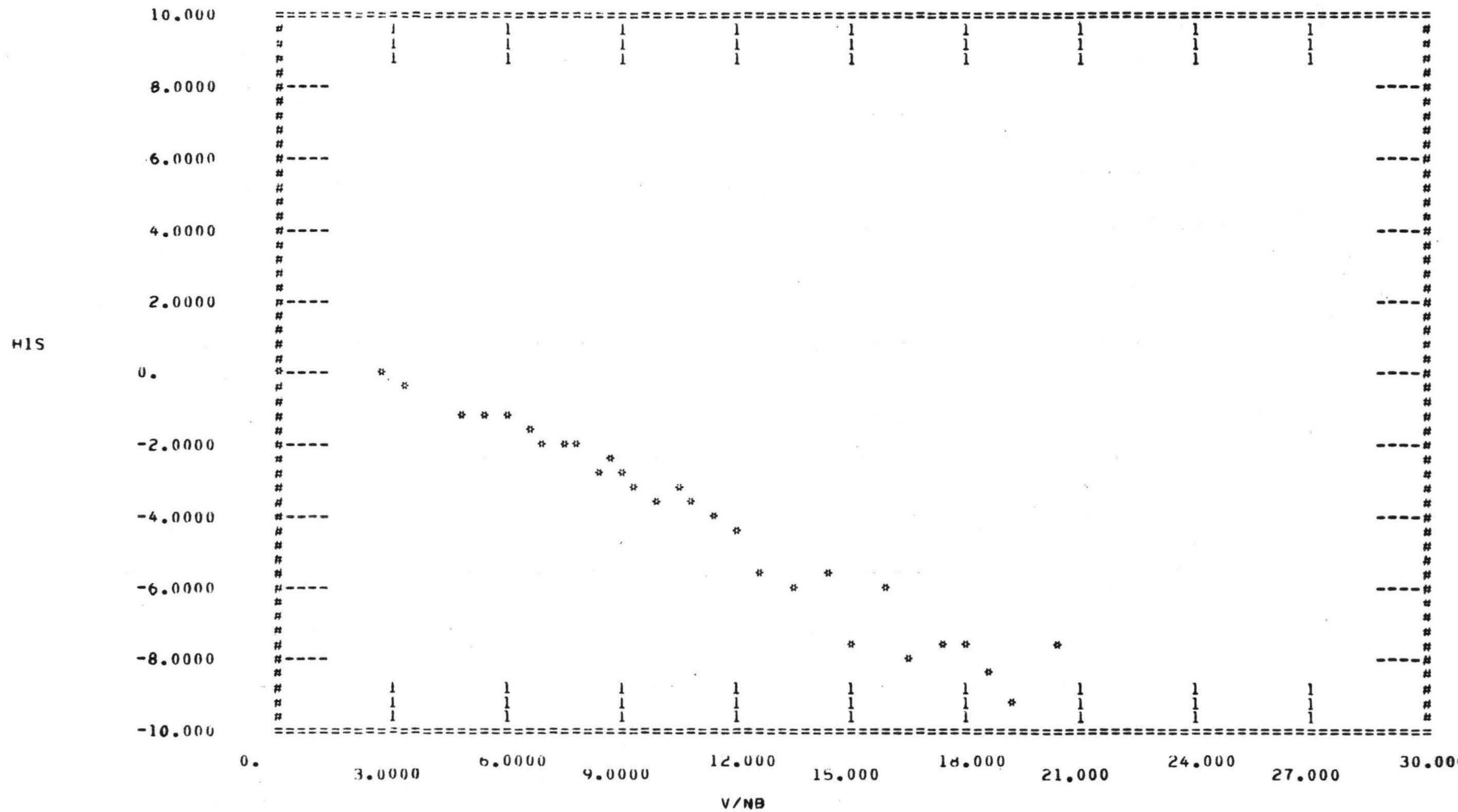

C O N F I G U R A T I O N   IIA-V

CONFIGURATION IIA-V

INDEX	V/NR	HIS
(1)	0.	1.10879E-04
(2)	2.5997	-.17512
(3)	3.3562	-.47493
(4)	3.3563	-.47500
(5)	4.7467	-1.0028
(6)	5.4124	-1.2700
(7)	5.9098	-1.1651
(8)	6.4569	-1.5336
(9)	6.8805	-2.1503
(10)	7.5819	-2.1417
(11)	7.9447	-2.1537
(12)	8.2937	-2.6355
(13)	8.6256	-2.4463
(14)	8.9477	-2.7388
(15)	9.3199	-3.2294
(16)	9.7933	-3.4927
(17)	10.406	-3.2578
(18)	10.834	-3.7432
(19)	11.493	-3.9948
(20)	11.976	-4.3282
(21)	12.719	-5.6537
(22)	13.542	-6.0572
(23)	14.309	-5.6580
(24)	15.144	-7.6061
(25)	15.887	-6.0525
(26)	16.614	-7.8589
(27)	17.309	-7.4992
(28)	17.957	-7.7018
(29)	18.620	-8.2812
(30)	19.246	-9.3989
(31)	20.353	-7.5050

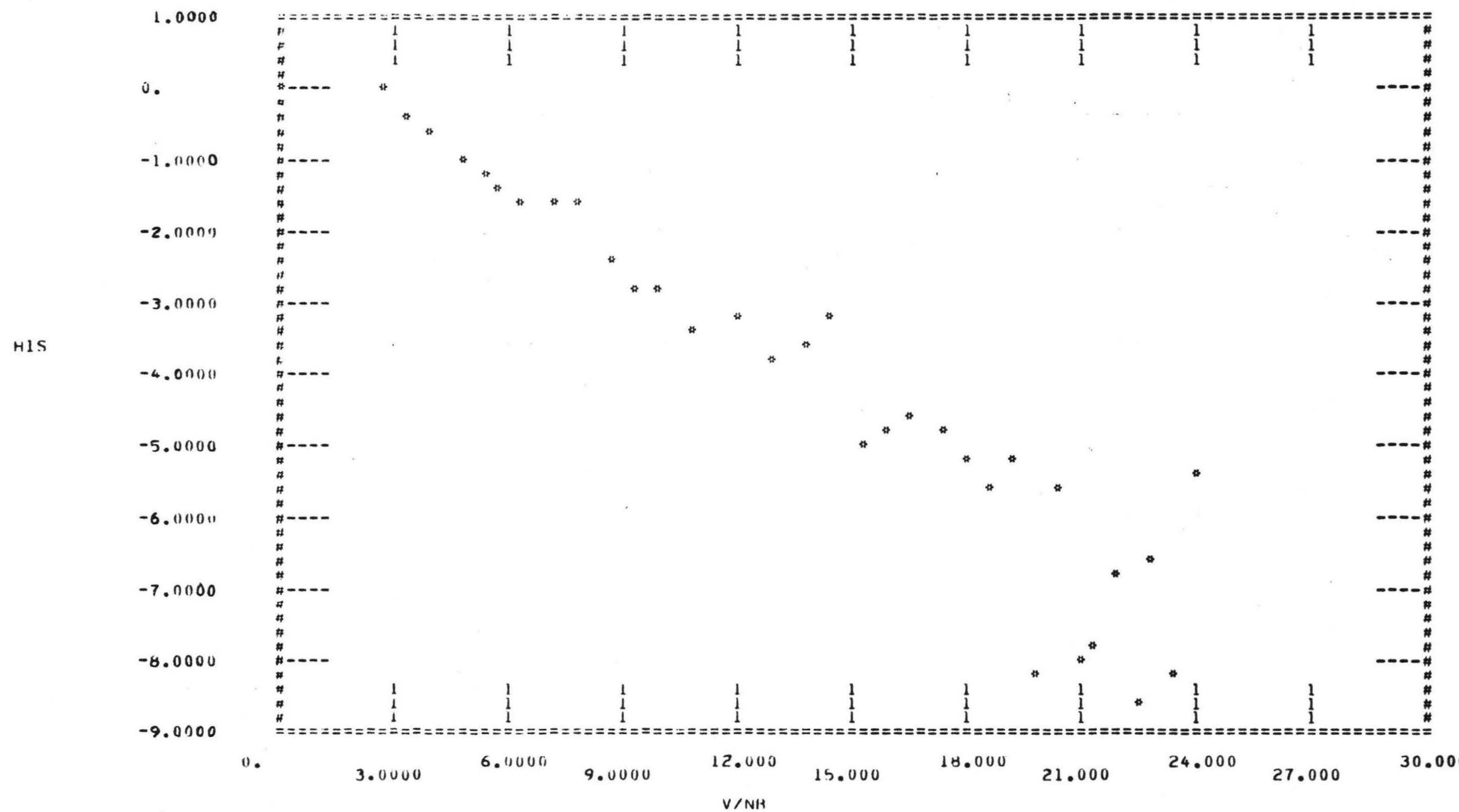

C O N F I G U R A T I O N IIB-V

117

CONFIGURATION IIB-V

INDEX	V/NB	H1S
(1)	0.	1.66675E-04
(2)	2.5997	5.14280E-02
(3)	3.3563	-.48736
(4)	3.9713	-.67799
(5)	4.8640	-1.0342
(6)	5.3072	-1.2017
(7)	5.8140	-1.4189
(8)	6.3692	-1.5837
(9)	7.1211	-1.6920
(10)	7.8726	-1.6522
(11)	8.6258	-2.3592
(12)	9.1966	-2.8104
(13)	9.8478	-2.7863
(14)	10.884	-3.3088
(15)	11.875	-3.2883
(16)	12.838	-3.8850
(17)	13.686	-3.5448
(18)	14.485	-3.1660
(19)	15.259	-4.9497
(20)	15.909	-4.7022
(21)	16.603	-4.5835
(22)	17.305	-4.7834
(23)	17.919	-5.1786
(24)	18.608	-5.6920
(25)	19.197	-5.1528
(26)	19.807	-8.2545
(27)	20.345	-5.5435
(28)	20.915	-7.9378
(29)	21.423	-7.8964
(30)	21.921	-6.8009
(31)	22.528	-8.5146
(32)	22.928	-6.6906
(33)	23.482	-8.1652
(34)	23.921	-5.4042

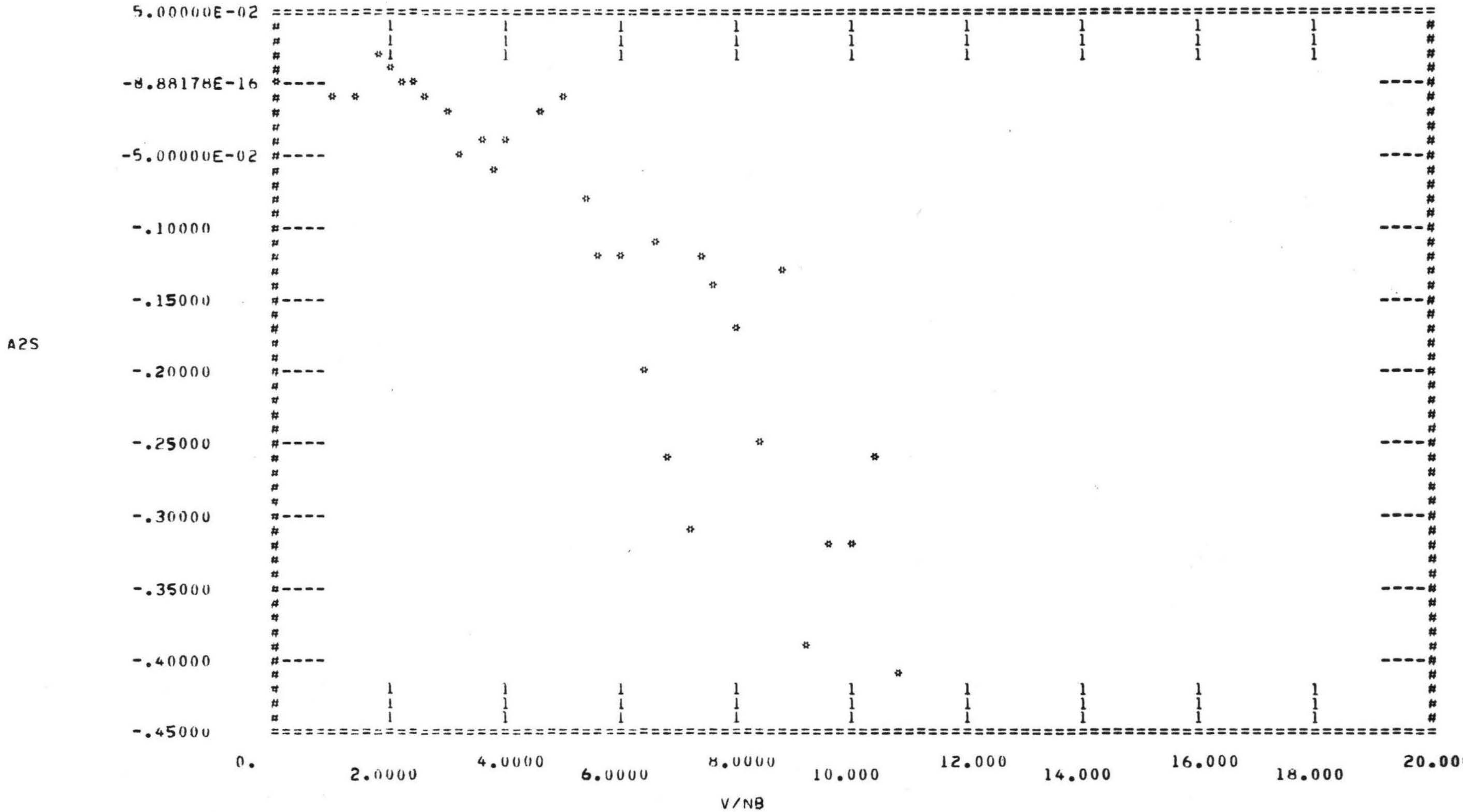

C O N F I G U R A T I O N   IIIA-T

CONFIGURATION IIIA-T

INDEX	V/NB	A2S
(1)	0.	5.85572E-06
(2)	.98417	-1.35499E-02
(3)	1.3204	-1.05915E-02
(4)	1.7046	2.18712E-02
(5)	1.9683	9.77856E-03
(6)	2.2007	3.81394E-04
(7)	2.4107	-3.54284E-03
(8)	2.6408	-1.36764E-02
(9)	2.9852	-2.11559E-02
(10)	3.2642	-4.85974E-02
(11)	3.5485	-3.67853E-02
(12)	3.8371	-5.67654E-02
(13)	4.0579	-4.11000E-02
(14)	4.5315	-2.36863E-02
(15)	4.9011	-1.10017E-02
(16)	5.3183	-7.83856E-02
(17)	5.6536	-.12126
(18)	6.0028	-.11656
(19)	6.3023	-.20374
(20)	6.6168	-.10989
(21)	6.8899	-.26316
(22)	7.1658	-.30547
(23)	7.4435	-.11934
(24)	7.6996	-.13784
(25)	7.9228	-.17207
(26)	8.3980	-.25310
(27)	8.8578	-.12979
(28)	9.2967	-.39291
(29)	9.6841	-.32314
(30)	10.086	-.32460
(31)	10.454	-.26375
(32)	10.837	-.40894

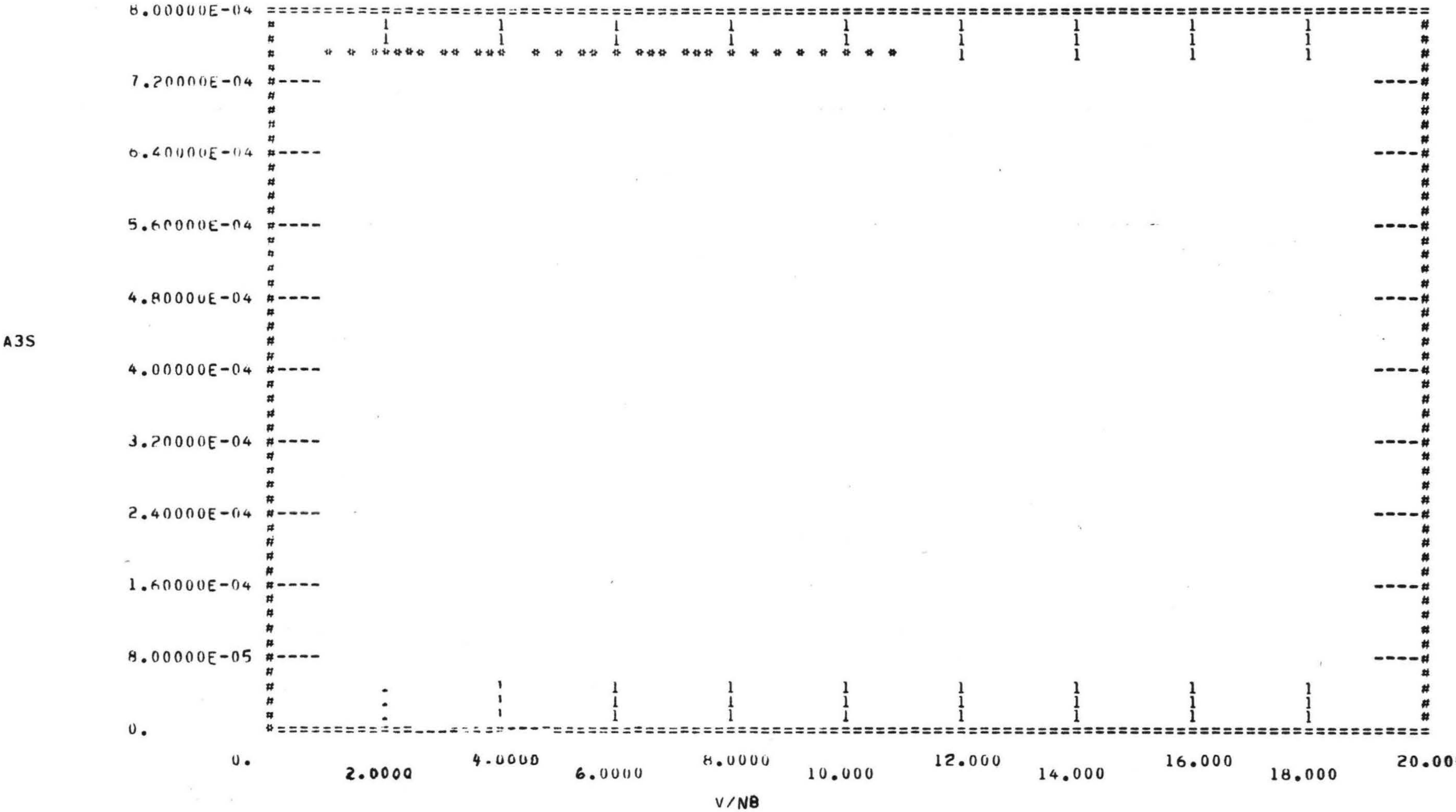

C O N F I G U R A T I O N IIIA-T

CONFIGURATION IIIA-T

INDEX	V/NB	A3S
(1)	0.	0.
(2)	.98417	7.45055E-04
(3)	1.3204	7.45055E-04
(4)	1.7046	7.45055E-04
(5)	1.9683	7.45055E-04
(6)	2.2007	7.45055E-04
(7)	2.4107	7.45055E-04
(8)	2.6408	7.45055E-04
(9)	2.9852	7.45055E-04
(10)	3.2642	7.45055E-04
(11)	3.5485	7.45055E-04
(12)	3.8371	7.45055E-04
(13)	4.0579	7.45055E-04
(14)	4.5315	7.45055E-04
(15)	4.9011	7.45055E-04
(16)	5.3183	7.45055E-04
(17)	[illegible].6538	7.45055E-04
(18)	[illegible].0028	7.45055E-04
(19)	[illegible].3023	7.45055E-04
(20)	[illegible].[illegible]168	7.45055E-04
(21)	6.8899	7.45055E-04
(22)	7.1658	7.45055E-04
(23)	7.4435	7.45055E-04
(24)	7.6996	7.45055E-04
(25)	7.9228	7.45055E-04
(26)	8.3980	7.45055E-04
(27)	8.8578	7.45055E-04
(28)	9.2967	7.45055E-04
(29)	9.6841	7.45055E-04
(30)	10.086	7.45055E-04
(31)	10.454	7.45055E-04
(32)	10.837	7.45055E-04

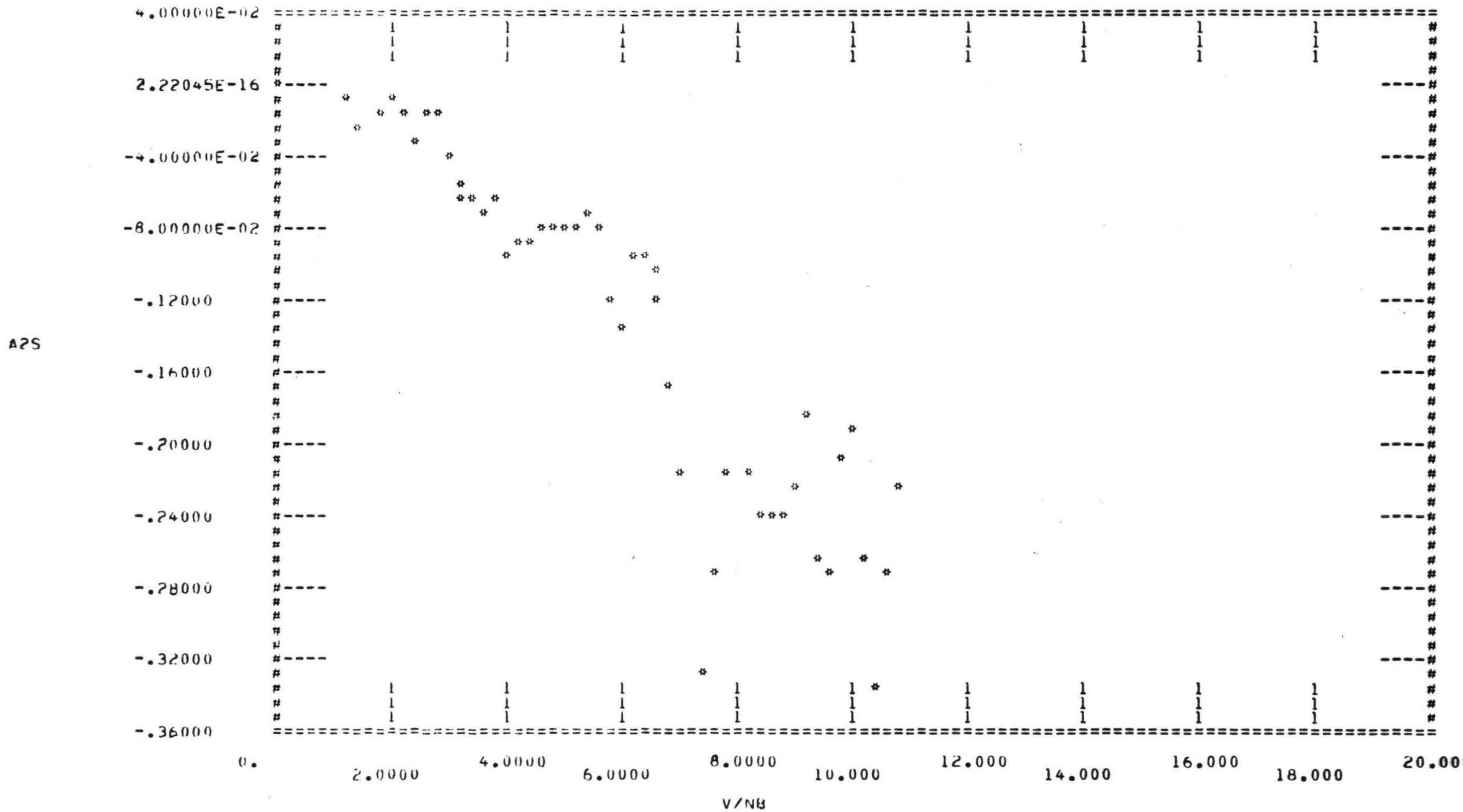

C O N F I G U R A T I O N   IIIB-T

CONFIGURATION IIIB-T

INDEX	V/NB	A2S
(1)	0.	6.11759E-05
(2)	1.2449	-1.01634E-02
(3)	1.3918	-2.55276E-02
(4)	1.7046	-1.38630E-02
(5)	1.9683	-4.15066E-03
(6)	2.2442	-1.70208E-02
(7)	2.3702	-2.87705E-02
(8)	2.6038	-1.71784E-02
(9)	2.7486	-1.58258E-02
(10)	2.9195	-3.97258E-02
(11)	3.1122	-5.42925E-02
(12)	3.2641	-6.61144E-02
(13)	3.4092	-6.70651E-02
(14)	3.5484	-7.15387E-02
(15)	3.7086	-6.44040E-02
(16)	3.7861	-6.76148E-02
(17)	3.9856	-9.22472E-02
(18)	4.1754	-8.44688E-02
(19)	4.4013	-8.86930E-02
(20)	4.5951	-8.13532E-02
(21)	4.8214	-8.01265E-02
(22)	5.0183	-7.94666E-02
(23)	5.2077	-7.75751E-02
(24)	5.4263	-6.82628E-02
(25)	5.5673	-8.32428E-02
(26)	5.7386	-.11692
(27)	5.9050	-.13938
(28)	6.0569	-.13341
(29)	6.2554	-9.96572E-02
(30)	6.3781	-9.92939E-02
(31)	6.5726	-.10127
(32)	6.6604	-.11928
(33)	6.8186	-.17025
(34)	7.0971	-.21968
(35)	7.3522	-.32819
(36)	7.6110	-.27125
(37)	7.8489	-.21370
(38)	8.1278	-.21688
(39)	8.3628	-.24266
(40)	8.5575	-.23819
(41)	8.8030	-.24183
(42)	9.0203	-.22008
(43)	9.2429	-.18546
(44)	9.4505	-.26027
(45)	9.6433	-.27575
(46)	9.8419	-.21022
(47)	10.037	-.18966
(48)	10.228	-.26180
(49)	10.426	-.33269
(50)	10.600	-.27537
(51)	10.781	-.22228

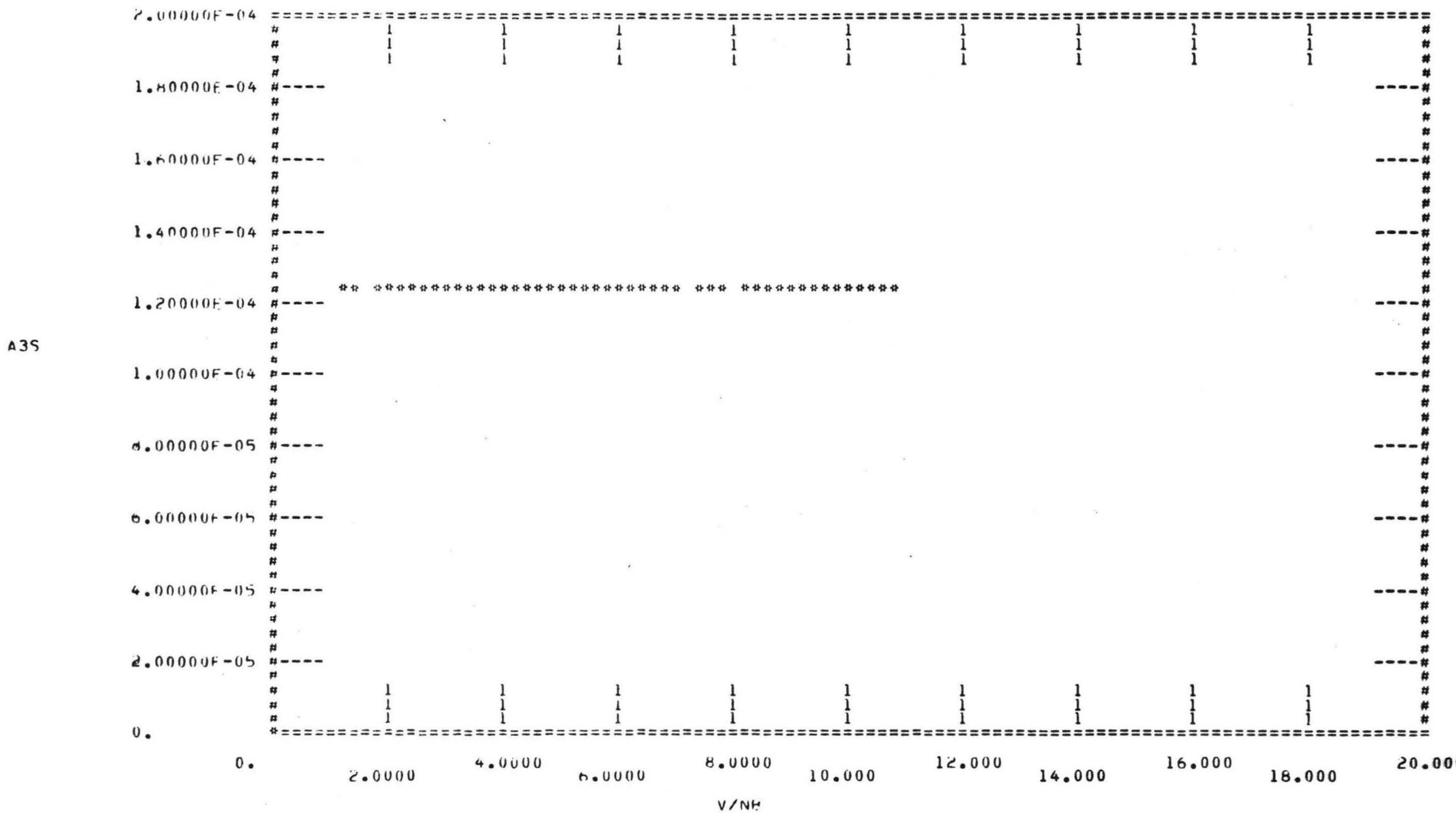

C O N F I G U R A T I O N IIIB-T

C O N F I G U R A T I O N IIIB-T

INDEX	V/NB	A3S
(1)	0.	-7.68573E-14
(2)	1.2449	1.23603E-04
(3)	1.3918	1.23603E-04
(4)	1.7046	1.23603E-04
(5)	1.9683	1.23603E-04
(6)	2.2442	1.23603E-04
(7)	2.3702	1.23603E-04
(8)	2.6038	1.23603E-04
(9)	2.7486	1.23603E-04
(10)	2.9195	1.23603E-04
(11)	3.1122	1.23603E-04
(12)	3.2641	1.23603E-04
(13)	3.4092	1.23603E-04
(14)	3.5484	1.23603E-04
(15)	3.7086	1.23603E-04
(16)	3.7861	1.23603E-04
(17)	3.9856	1.23603E-04
(18)	4.1754	1.23603E-04
(19)	4.4013	1.23603E-04
(20)	4.5951	1.23603E-04
(21)	4.8214	1.23603E-04
(22)	5.0183	1.23603E-04
(23)	5.2077	1.23603E-04
(24)	5.4263	1.23603E-04
(25)	5.5673	1.23603E-04
(26)	5.7386	1.23603E-04
(27)	5.9050	1.23603E-04
(28)	6.0665	1.23603E-04
(29)	6.2554	1.23603E-04
(30)	6.3761	1.23603E-04
(31)	6.5726	1.23603E-04
(32)	6.6604	1.23603E-04
(33)	6.8186	1.23603E-04
(34)	7.0971	1.23603E-04
(35)	7.3522	1.23603E-04
(36)	7.6110	1.23603E-04
(37)	7.8489	1.23603E-04
(38)	8.1278	1.23603E-04
(39)	8.3628	1.23603E-04
(40)	8.5575	1.23603E-04
(41)	8.8030	1.23603E-04
(42)	9.0203	1.23603E-04
(43)	9.2429	1.23603E-04
(44)	9.4505	1.23603E-04
(45)	9.6433	1.23603E-04
(46)	9.8419	1.23603E-04
(47)	10.037	1.23603E-04
(48)	10.228	1.23603E-04
(49)	10.426	1.23603E-04
(50)	10.600	1.23603E-04
(51)	10.781	1.23603E-04

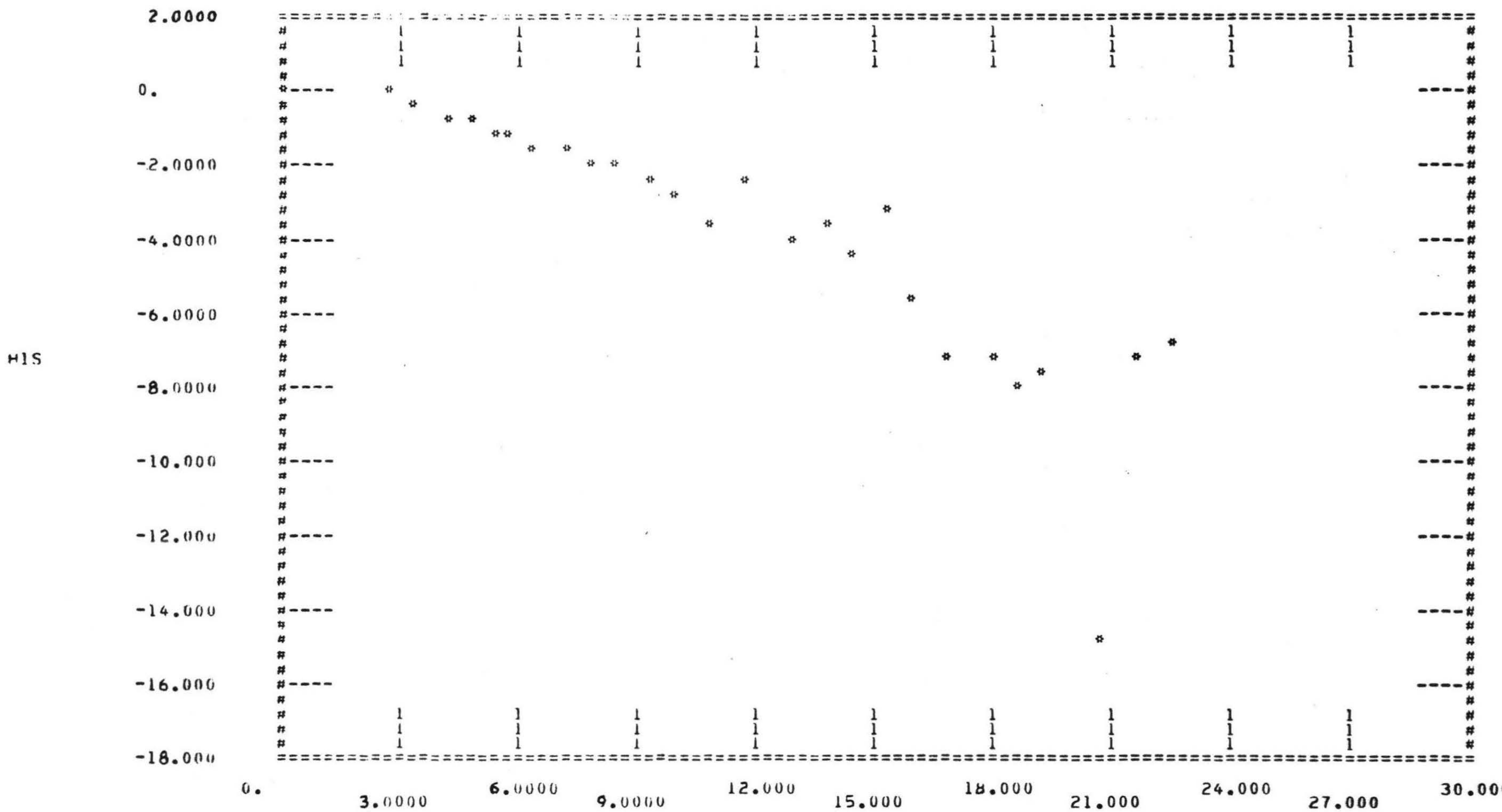

C O N F I G U R A T I O N   IIIA-V

CONFIGURATION IIIA-V

INDEX	V/NB	HIS	INDEX	V/NB	HIS	INDEX	V/NB	HIS
(1)	0.	5.50154E-04	(10)	7.9443	-1.8700	(19)	15.244	-3.2852
(2)	2.5997	7.03429E-02	(11)	8.4932	-2.0474	(20)	15.920	-5.6438
(3)	3.3563	-.46228	(12)	9.1954	-2.4496	(21)	16.708	-7.3605
(4)	4.1107	-.74945	(13)	9.7906	-2.8552	(22)	17.982	-7.3402
(5)	4.7466	-.82503	(14)	10.885	-3.4416	(23)	18.646	-7.8859
(6)	5.3973	-1.2005	(15)	11.824	-2.5591	(24)	19.177	-7.6676
(7)	5.8137	-1.1436	(16)	12.839	-3.9733	(25)	20.612	-14.974
(8)	6.2800	-1.4953	(17)	13.686	-3.6027	(26)	21.458	-7.2205
(9)	7.1998	-1.6680	(18)	14.493	-4.2141	(27)	22.488	-6.9402

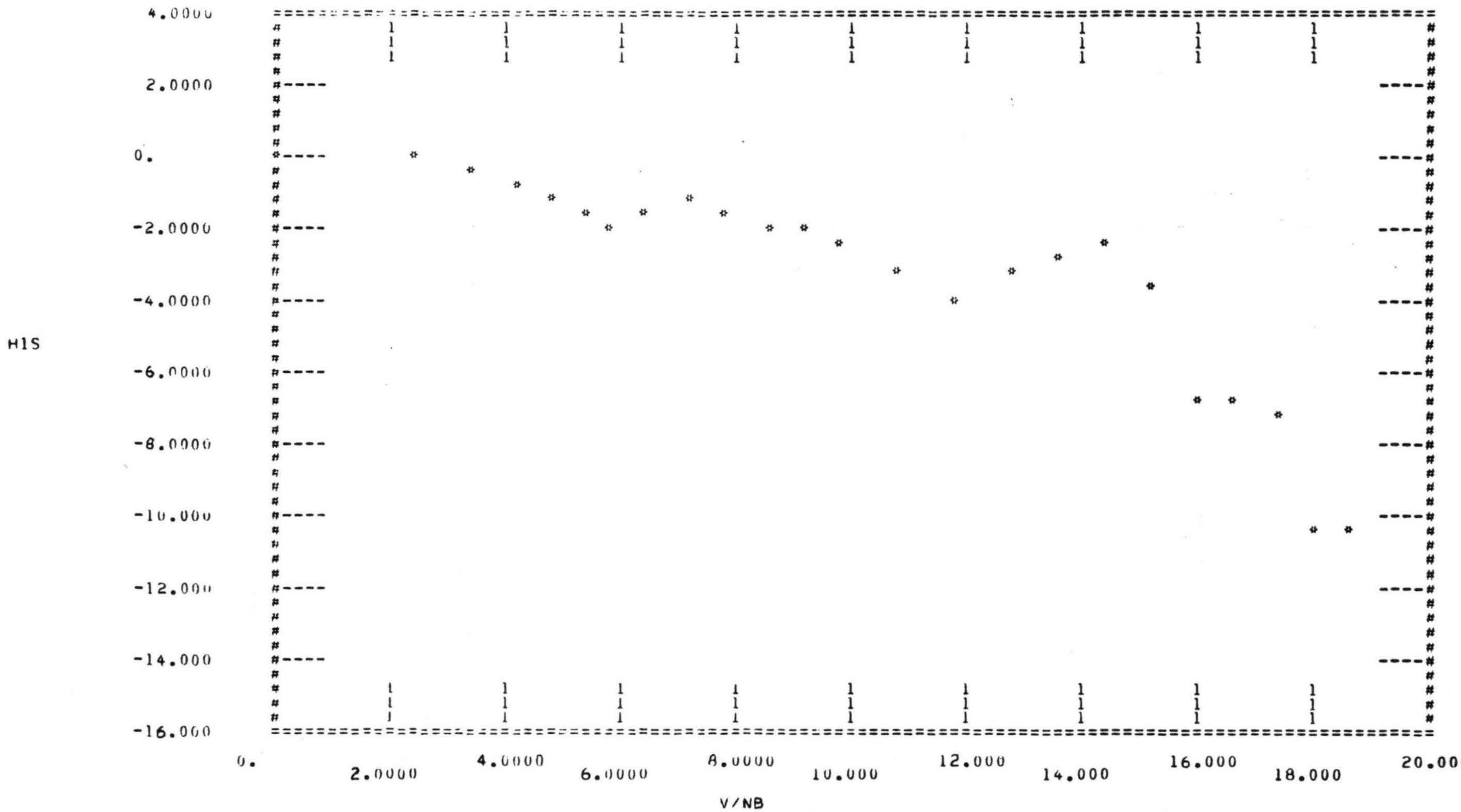

C O N F I G U R A T I O N IIIB-V

CONFIGURATION IIIB-V

INDEX	V/NB	HIS	INDEX	V/NB	HIS	INDEX	V/NB	HIS
(1)	0.	8.77523E-04	(9)	7.1993	-1.3456	(17)	13.683	-2.9294
(2)	2.3732	9.26154E-03	(10)	7.8006	-1.5553	(18)	14.403	-2.4877
(3)	3.3563	-.44383	(11)	8.5569	-1.8187	(19)	15.210	-3.6803
(4)	4.1106	-.64865	(12)	9.1939	-1.9645	(20)	15.938	-6.8140
(5)	4.7468	-1.0370	(13)	9.7898	-2.5589	(21)	16.630	-6.7496
(6)	5.4127	-1.5914	(14)	10.884	-3.2632	(22)	17.337	-7.2934
(7)	5.8150	-1.9804	(15)	11.879	-3.9458	(23)	18.085	-10.418
(8)	6.3694	-1.7539	(16)	12.834	-3.2853	(24)	18.639	-10.476

APPENDIX A.3

Aerodynamic Derivatives for Smooth Bridge Deck

Smooth Deck

(Dimensions for Model)
(Model Scale 1:40)

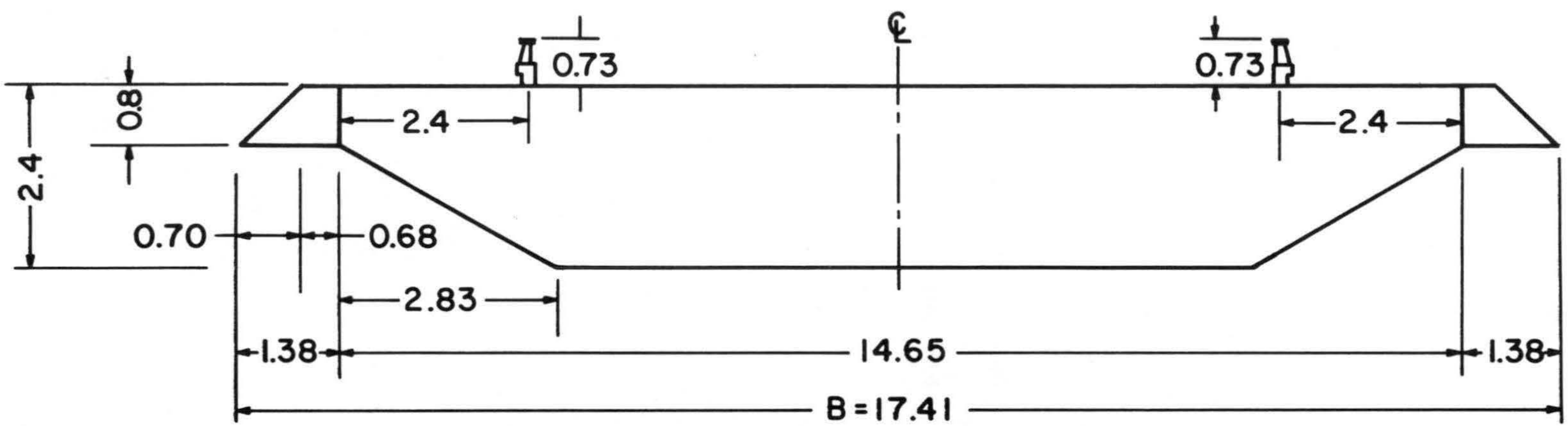

(All Dimensions in inches)

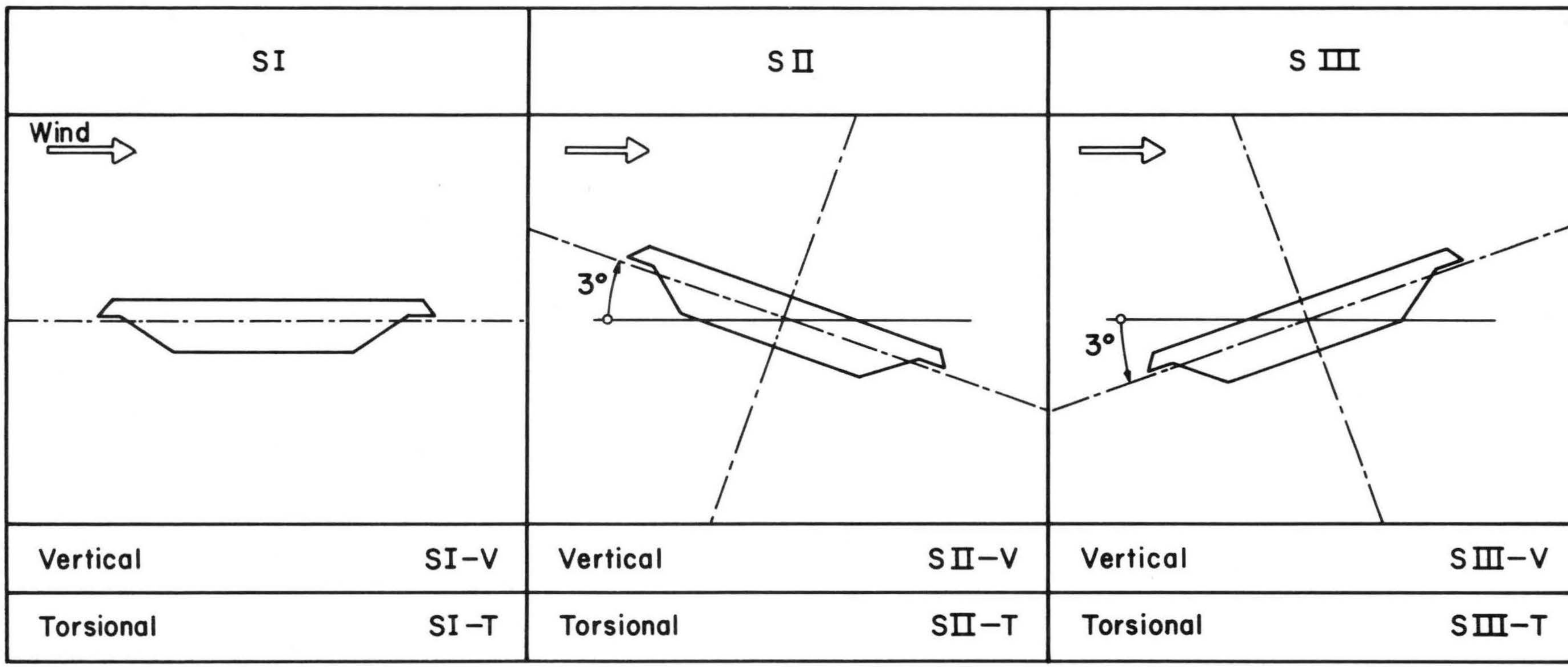
S I
S II
S III
Wind
3°
3°
Vertical
SI-V
Vertical
SII-V
Vertical
SIII-V
Torsional
SI-T
Torsional
SII-T
Torsional
SIII-T

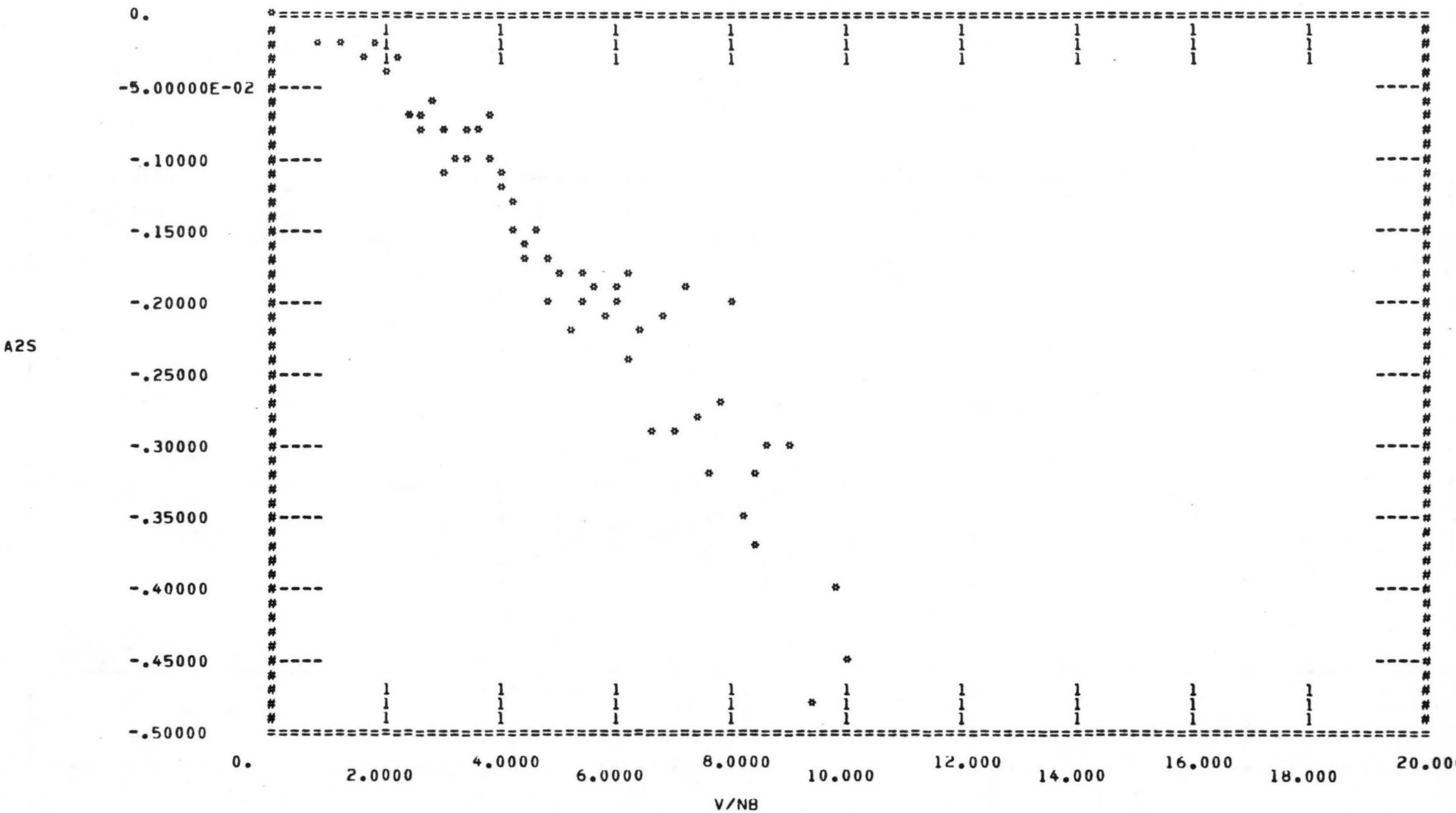

C O N F I G U R A T I O N SI-T

CONFIGURATION SI-T

INDEX	V/NB	A2S	INDEX	V/NB	A2S	INDEX	V/NB	A2S
(1)	0.	-5.96529E-07	(20)	3.8806	-9.62442E-02	(39)	6.1682	-.18055
(2)	.89023	-1.61834E-02	(21)	3.9814	-.11425	(40)	6.2958	-.23900
(3)	1.2590	-2.31492E-02	(22)	4.0797	-.11758	(41)	6.4817	-.21696
(4)	1.5419	-2.69576E-02	(23)	4.1758	-.13291	(42)	6.6631	-.29302
(5)	1.7805	-1.86635E-02	(24)	4.2882	-.15262	(43)	6.8387	-.20704
(6)	1.9906	-3.75485E-02	(25)	4.3615	-.15613	(44)	6.9997	-.28524
(7)	2.1806	-3.10762E-02	(26)	4.4516	-.16966	(45)	7.1889	-.19030
(8)	2.3554	-6.90513E-02	(27)	4.5396	-.14953	(46)	7.3423	-.28459
(9)	2.5180	-7.57238E-02	(28)	4.6261	-.15447	(47)	7.5027	-.31982
(10)	2.6409	-7.18176E-02	(29)	4.7112	-.20466	(48)	7.7109	-.26840
(11)	2.8152	-5.61819E-02	(30)	4.8764	-.17412	(49)	7.9133	-.20092
(12)	2.9526	-7.53042E-02	(31)	5.0364	-.18419	(50)	8.1124	-.35161
(13)	3.0582	-.11180	(32)	5.1915	-.21521	(51)	8.3052	-.32141
(14)	3.2099	-9.62934E-02	(33)	5.3270	-.18401	(52)	8.4945	-.36899
(15)	3.3310	-8.49563E-02	(34)	5.4883	-.19524	(53)	8.6877	-.30487
(16)	3.4480	-.10217	(35)	5.6309	-.19376	(54)	9.0366	-.30418
(17)	3.5610	-7.99228E-02	(36)	5.7563	-.21285	(55)	9.3828	-.48127
(18)	3.6706	-7.76155E-02	(37)	5.9057	-.20200	(56)	9.7059	-.40081
(19)	3.7560	-7.49115E-02	(38)	6.0384	-.18518	(57)	10.036	-.44656

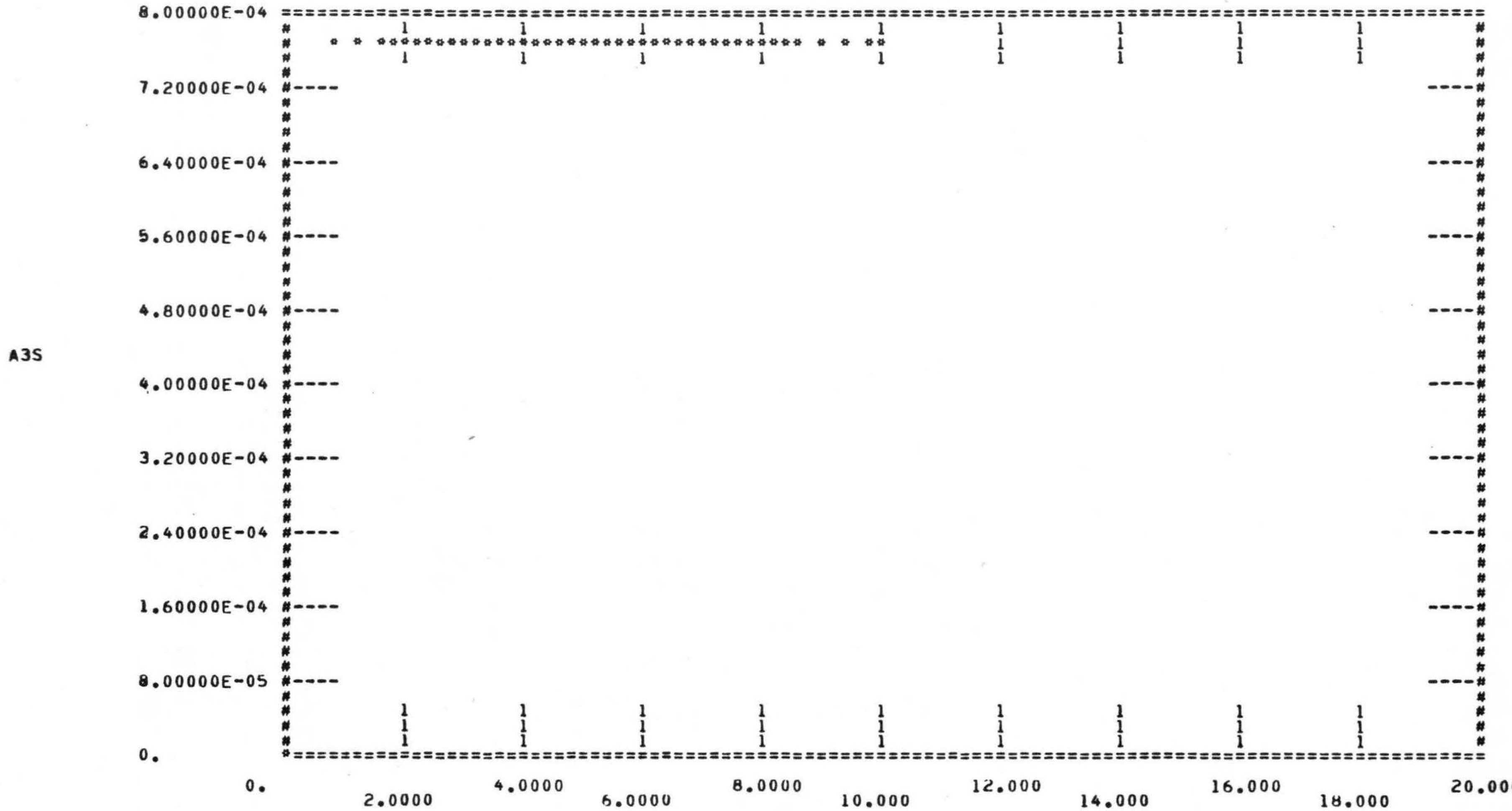

C O N F I G U R A T I O N   SI-T

C O N F I G U R A T I O N   SI-T

INDEX	V/NB	A3S	INDEX	V/NB	A3S	INDEX	V/NB	A3S
(1)	0.	0.	(20)	3.8806	7.68032E-04	(39)	6.1682	7.68032E-04
(2)	.89023	7.68032E-04	(21)	3.9814	7.68032E-04	(40)	6.2958	7.68032E-04
(3)	1.2590	7.68032E-04	(22)	4.0797	7.68032E-04	(41)	6.4817	7.68032E-04
(4)	1.5419	7.68032E-04	(23)	4.1758	7.68032E-04	(42)	6.6631	7.68032E-04
(5)	1.7805	7.68032E-04	(24)	4.2882	7.68032E-04	(43)	6.8387	7.68032E-04
(6)	1.9906	7.68032E-04	(25)	4.3615	7.68032E-04	(44)	6.9997	7.68032E-04
(7)	2.1806	7.68032E-04	(26)	4.4516	7.68032E-04	(45)	7.1889	7.68032E-04
(8)	2.3554	7.68032E-04	(27)	4.5396	7.68032E-04	(46)	7.3423	7.68032E-04
(9)	2.5180	7.68032E-04	(28)	4.6261	7.68032E-04	(47)	7.5027	7.68032E-04
(10)	2.6409	7.68032E-04	(29)	4.7112	7.68032E-04	(48)	7.7109	7.68032E-04
(11)	2.8152	7.68032E-04	(30)	4.8764	7.68032E-04	(49)	7.9133	7.68032E-04
(12)	2.9526	7.68032E-04	(31)	5.0364	7.68032E-04	(50)	8.1124	7.68032E-04
(13)	3.0582	7.68032E-04	(32)	5.1915	7.68032E-04	(51)	8.3052	7.68032E-04
(14)	3.2099	7.68032E-04	(33)	5.3270	7.68032E-04	(52)	8.4945	7.68032E-04
(15)	3.3310	7.68032E-04	(34)	5.4883	7.68032E-04	(53)	8.6877	7.68032E-04
(16)	3.4480	7.68032E-04	(35)	5.6309	7.68032E-04	(54)	9.0366	7.68032E-04
(17)	3.5610	7.68032E-04	(36)	5.7563	7.68032E-04	(55)	9.3828	7.68032E-04
(18)	3.6706	7.68032E-04	(37)	5.9057	7.68032E-04	(56)	9.7059	7.68032E-04
(19)	3.7560	7.68032E-04	(38)	6.0384	7.68032E-04	(57)	10.036	7.68032E-04

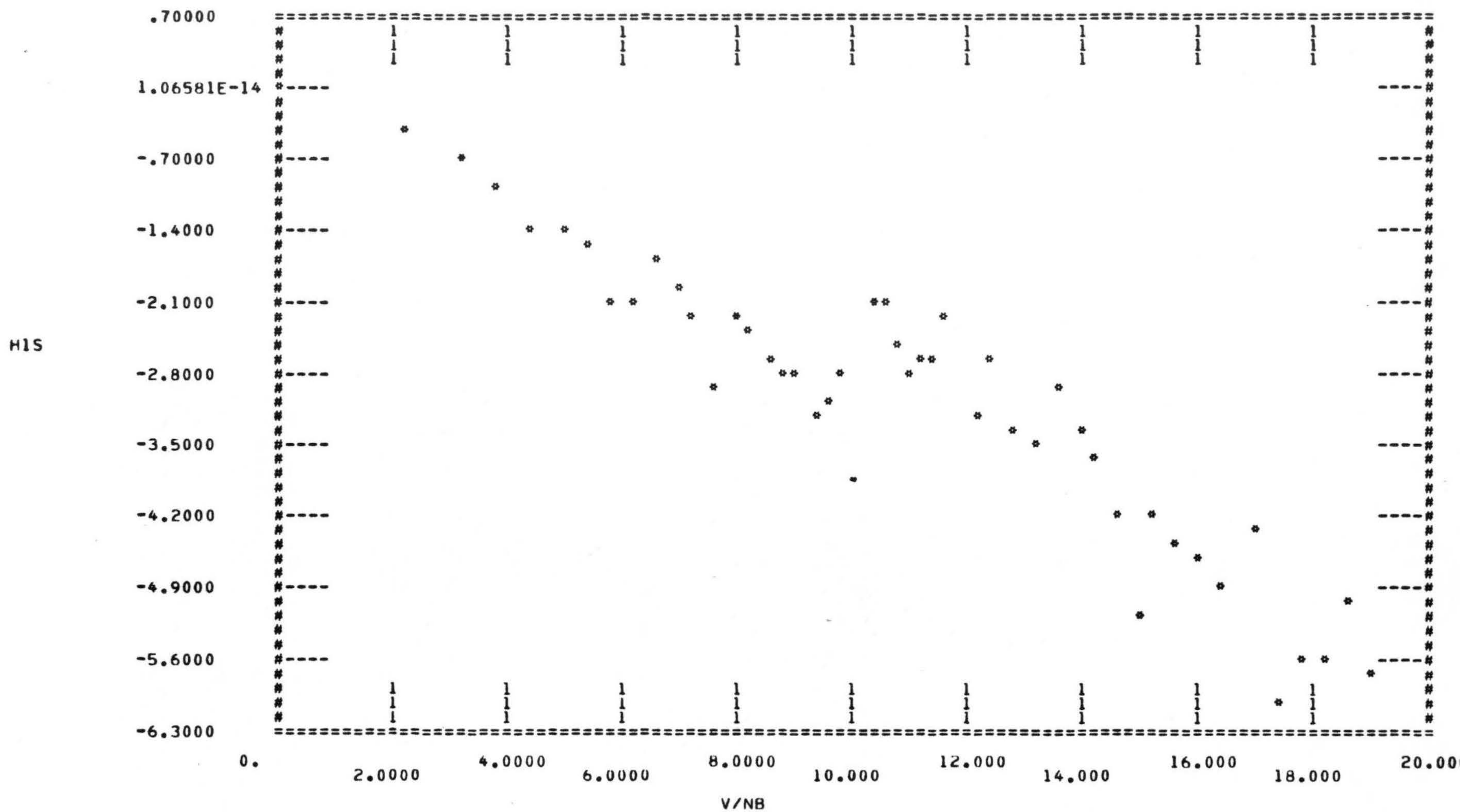

C O N F I G U R A T I O N   SI-V

CONFIGURATION SI-V

INDEX	V/NB	HIS
(1)	0.	3.24291E-05
(2)	2.1996	-.36998
(3)	3.1109	-.72394
(4)	3.8102	-.95770
(5)	4.4001	-1.3410
(6)	4.9194	-1.3585
(7)	5.3893	-1.5834
(8)	5.8222	-2.1063
(9)	6.2241	-2.0337
(10)	6.6007	-1.6761
(11)	6.9587	-1.9981
(12)	7.2322	-2.2353
(13)	7.6895	-2.9061
(14)	7.9347	-2.2808
(15)	8.2349	-2.3848

INDEX	V/NB	HIS
(16)	8.5249	-2.6453
(17)	8.8052	-2.7770
(18)	9.0763	-2.8650
(19)	9.3417	-3.2267
(20)	9.5968	-3.1078
(21)	9.8442	-2.7472
(22)	10.322	-2.1585
(23)	10.553	-2.0560
(24)	10.782	-2.4675
(25)	11.007	-2.8293
(26)	11.223	-2.6571
(27)	11.439	-2.7050
(28)	11.644	-2.1997
(29)	12.101	-3.2376
(30)	12.451	-2.6393

INDEX	V/NB	HIS
(31)	12.840	-3.3164
(32)	13.213	-3.4536
(33)	13.570	-2.9204
(34)	13.926	-3.3018
(35)	14.274	-3.6788
(36)	14.614	-4.1589
(37)	14.924	-5.1365
(38)	15.264	-4.2317
(39)	15.584	-4.5021
(40)	16.046	-4.6438
(41)	16.498	-4.8983
(42)	16.925	-4.3546
(43)	17.379	-6.0443
(44)	17.785	-5.5879
(45)	18.191	-5.5364
(46)	18.577	-4.9985
(47)	19.083	-5.7827

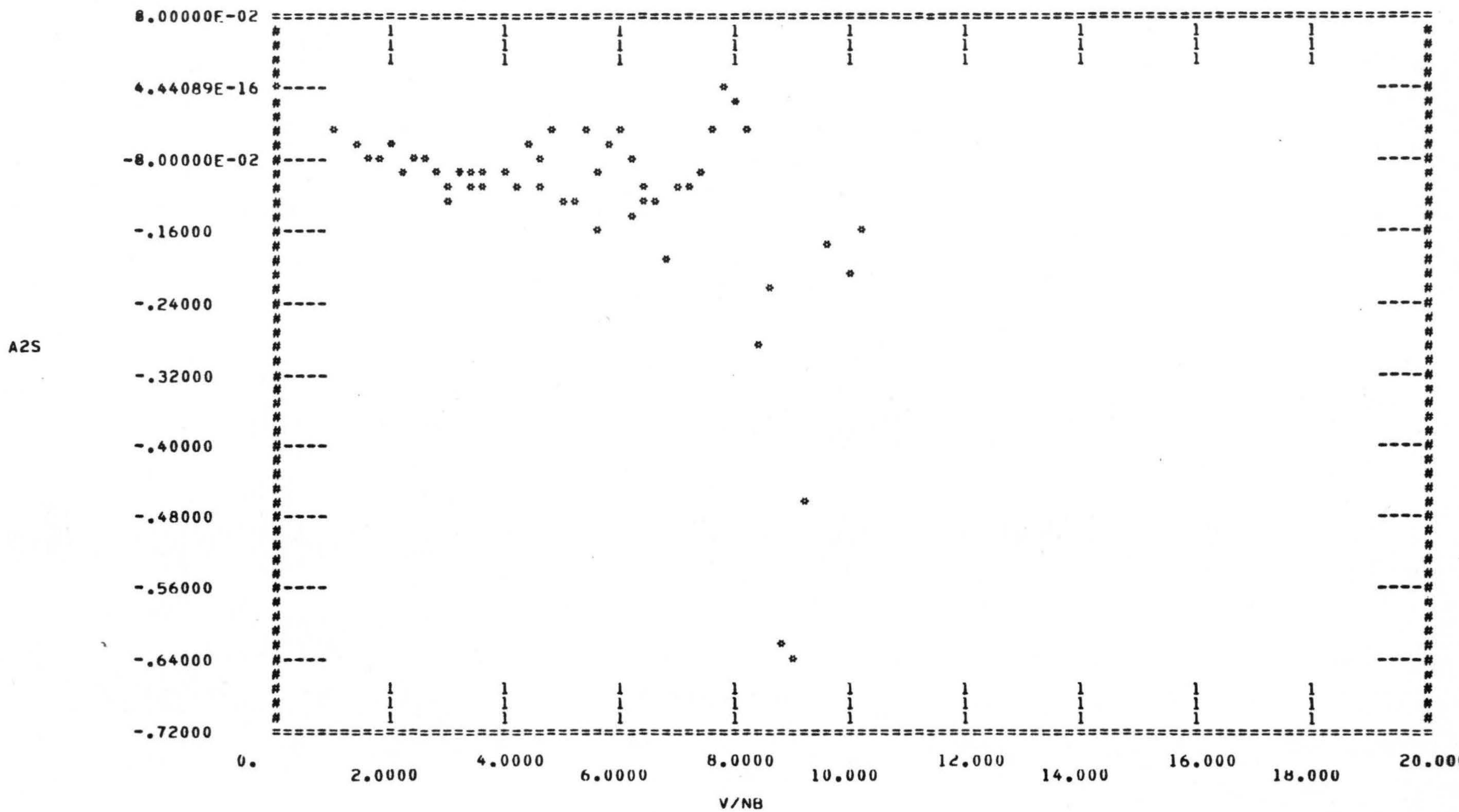

C O N F I G U R A T I O N   SII-T

CONFIGURATION SII-T

INDEX	V/NB	A2S	INDEX	V/NB	A2S	INDEX	V/NB	A2S
(1)	0.	-9.67224E-07	(18)	3.9043	-9.62842E-02	(35)	6.6997	-.13502
(2)	.92024	-5.50233E-02	(19)	4.1156	-.10846	(36)	6.8870	-.18547
(3)	1.3650	-7.16353E-02	(20)	4.3163	-6.88626E-02	(37)	7.0687	-.11955
(4)	1.5939	-7.55881E-02	(21)	4.5083	-8.02787E-02	(38)	7.2462	-.10957
(5)	1.8405	-7.85734E-02	(22)	4.6744	-.11810	(39)	7.4194	-.10306
(6)	2.0577	-5.82812E-02	(23)	4.8694	-4.36723E-02	(40)	7.5885	-5.54808E-02
(7)	2.2542	-9.17150E-02	(24)	5.0237	-.12395	(41)	7.8084	6.55668E-03
(8)	2.4348	-8.53590E-02	(25)	5.1732	-.12050	(42)	8.0224	-1.19265E-02
(9)	2.5701	-7.83604E-02	(26)	5.3659	-5.24066E-02	(43)	8.2206	-5.35709E-02
(10)	2.7608	-9.30474E-02	(27)	5.5215	-9.43235E-02	(44)	8.4355	-.29178
(11)	2.9102	-.12800	(28)	5.6731	-.15736	(45)	8.6334	-.22707
(12)	3.0243	-.11628	(29)	5.8202	-6.82406E-02	(46)	8.8219	-.62008
(13)	3.1612	-9.07571E-02	(30)	5.9638	-5.03906E-02	(47)	9.0215	-.64271
(14)	3.3181	-.10319	(31)	6.1045	-.14874	(48)	9.2054	-.46053
(15)	3.4433	-.11726	(32)	6.2414	-7.21241E-02	(49)	9.5640	-.17242
(16)	3.5642	-.11143	(33)	6.3758	-.11908	(50)	9.9036	-.20313
(17)	3.6810	-9.43972E-02	(34)	6.4943	-.12464	(51)	10.248	-.15935

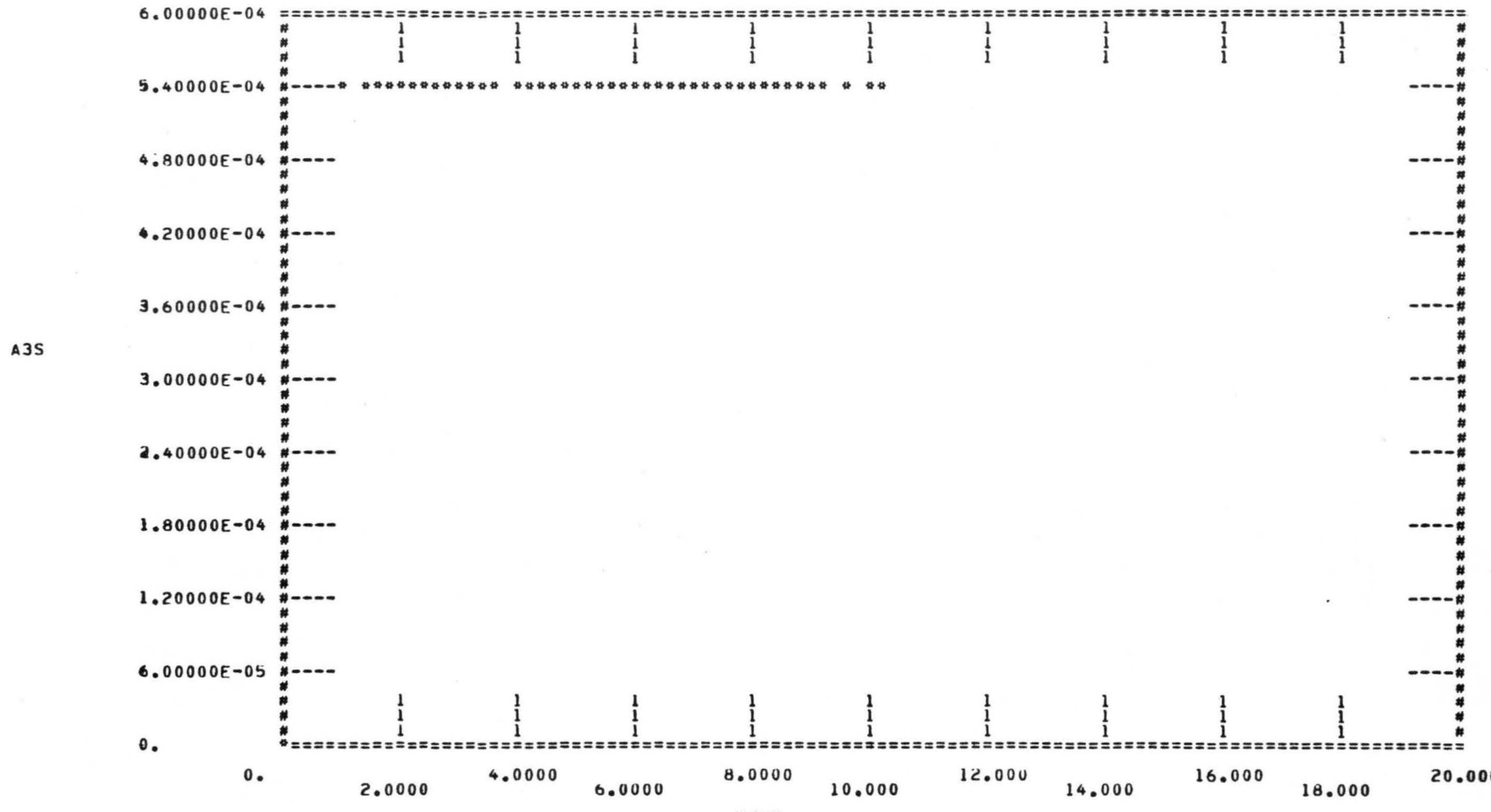

C O N F I G U R A T I O N   SII-T

CONFIGURATION SII-T

INDEX	V/NB	A3S	INDEX	V/NB	A3S	INDEX	V/NB	A3S
(1)	0.	-5.87459E-14	(18)	3.9043	5.41151E-04	(35)	6.6997	5.41151E-04
(2)	.92024	5.41151E-04	(19)	4.1156	5.41151E-04	(36)	6.8870	5.41151E-04
(3)	1.3650	5.41151E-04	(20)	4.3163	5.41151E-04	(37)	7.0687	5.41151E-04
(4)	1.5939	5.41151E-04	(21)	4.5083	5.41151E-04	(38)	7.2462	5.41151E-04
(5)	1.8405	5.41151E-04	(22)	4.6744	5.41151E-04	(39)	7.4194	5.41151E-04
(6)	2.0577	5.41151E-04	(23)	4.8694	5.41151E-04	(40)	7.5885	5.41151E-04
(7)	2.2542	5.41151E-04	(24)	5.0237	5.41151E-04	(41)	7.8084	5.41151E-04
(8)	2.4348	5.41151E-04	(25)	5.1732	5.41151E-04	(42)	8.0224	5.41151E-04
(9)	2.5701	5.41151E-04	(26)	5.3659	5.41151E-04	(43)	8.2206	5.41151E-04
(10)	2.7608	5.41151E-04	(27)	5.5215	5.41151E-04	(44)	8.4355	5.41151E-04
(11)	2.9102	5.41151E-04	(28)	5.6731	5.41151E-04	(45)	8.6334	5.41151E-04
(12)	3.0243	5.41151E-04	(29)	5.8202	5.41151E-04	(46)	8.8219	5.41151E-04
(13)	3.1612	5.41151E-04	(30)	5.9638	5.41151E-04	(47)	9.0215	5.41151E-04
(14)	3.3181	5.41151E-04	(31)	6.1045	5.41151E-04	(48)	9.2054	5.41151E-04
(15)	3.4433	5.41151E-04	(32)	6.2414	5.41151E-04	(49)	9.5640	5.41151E-04
(16)	3.5642	5.41151E-04	(33)	6.3758	5.41151E-04	(50)	9.9036	5.41151E-04
(17)	3.6810	5.41151E-04	(34)	6.4943	5.41151E-04	(51)	10.248	5.41151E-04

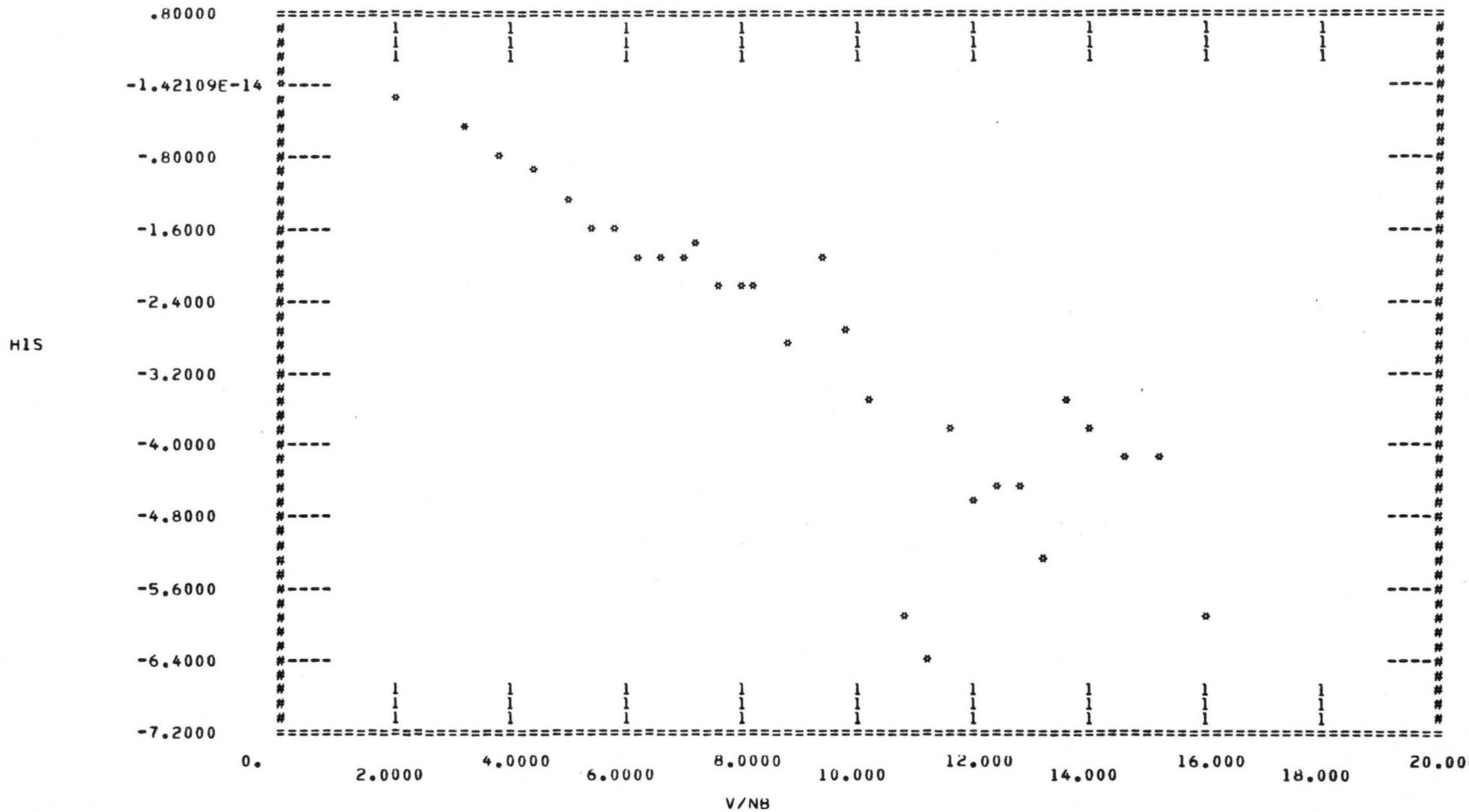

C O N F I G U R A T I O N   SII-V

C O N F I G U R A T I O N   SII-V

INDEX	V/NB	H1S	INDEX	V/NB	H1S	INDEX	V/NB	H1S
(1)	0.	9.88215E-06	(11)	6.9586	-1.9677	(21)	11.259	-6.3227
(2)	1.9674	-.23381	(12)	7.2307	-1.7262	(22)	11.655	-3.8973
(3)	3.1108	-.53065	(13)	7.6235	-2.2200	(23)	12.072	-4.5799
(4)	3.8101	-.83877	(14)	7.9351	-2.3147	(24)	12.466	-4.4612
(5)	4.3996	-.92098	(15)	8.2340	-2.1983	(25)	12.849	-4.4914
(6)	4.9193	-1.2169	(16)	8.8057	-2.8589	(26)	13.234	-5.2851
(7)	5.3892	-1.5203	(17)	9.3358	-1.9935	(27)	13.575	-3.5959
(8)	5.8213	-1.6613	(18)	9.8440	-2.6744	(28)	13.931	-3.7631
(9)	6.2237	-1.8673	(19)	10.282	-3.5658	(29)	14.582	-4.2170
(10)	6.5275	-1.9215	(20)	10.811	-5.9790	(30)	15.295	-4.0848
						(31)	15.914	-5.9442

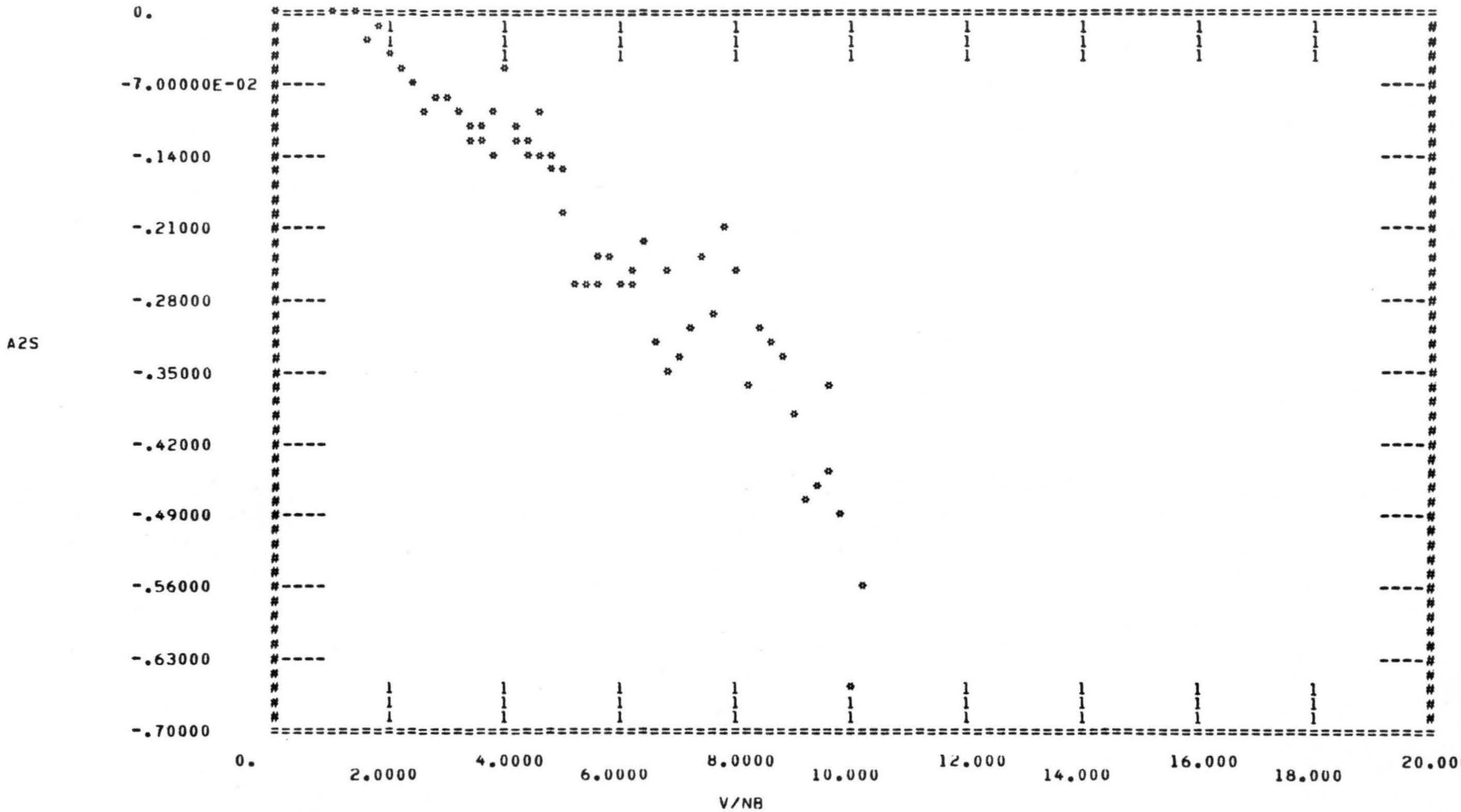

C O N F I G U R A T I O N   SIII-T

CONFIGURATION SIII-T

INDEX	V/NB	A2S
(1)	0.	-4.36244E-06
(2)	.92022	-6.27767E-03
(3)	1.3014	-4.65950E-03
(4)	1.5939	-2.93089E-02
(5)	1.8404	-1.83992E-02
(6)	2.0577	-4.42358E-02
(7)	2.2541	-5.43144E-02
(8)	2.4347	-6.86212E-02
(9)	2.6029	-9.38126E-02
(10)	2.7607	-8.64160E-02
(11)	2.9101	-8.54147E-02
(12)	3.0521	-8.48722E-02
(13)	3.1878	-9.53811E-02
(14)	3.3180	-.11401
(15)	3.4433	-.12230
(16)	3.5641	-.11286
(17)	3.6810	-.12441
(18)	3.7944	-.13391
(19)	3.8825	-9.72592E-02
(20)	4.0323	-5.99572E-02
(21)	4.1155	-.10687
(22)	4.2172	-.12295
(23)	4.3164	-.13219
(24)	4.4134	-.13385
(25)	4.5084	-.13668
(26)	4.6012	-.10059
(27)	4.7105	-.13611
(28)	4.7819	-.14999
(29)	4.8696	-.14690
(30)	4.9559	-.15918
(31)	5.0407	-.18981
(32)	5.2062	-.25922
(33)	5.3665	-.26102
(34)	5.5221	-.25951
(35)	5.6732	-.23140
(36)	5.8207	-.24137
(37)	5.9645	-.26266
(38)	6.1048	-.24973
(39)	6.2421	-.25976
(40)	6.3761	-.22910
(41)	6.5082	-.31723
(42)	6.7001	-.25315
(43)	6.8878	-.35233
(44)	7.0816	-.33249
(45)	7.2470	-.30405
(46)	7.4199	-.24215
(47)	7.5895	-.28905
(48)	7.7546	-.20705
(49)	7.9703	-.24591
(50)	8.1810	-.36939
(51)	8.3850	-.30711
(52)	8.5848	-.31982
(53)	8.7800	-.33698
(54)	8.9714	-.39244
(55)	9.1591	-.47319
(56)	9.3422	-.46098
(57)	9.5208	-.36039
(58)	9.6981	-.44516
(59)	9.8717	-.49299
(60)	10.044	-.66047
(61)	10.210	-.55696

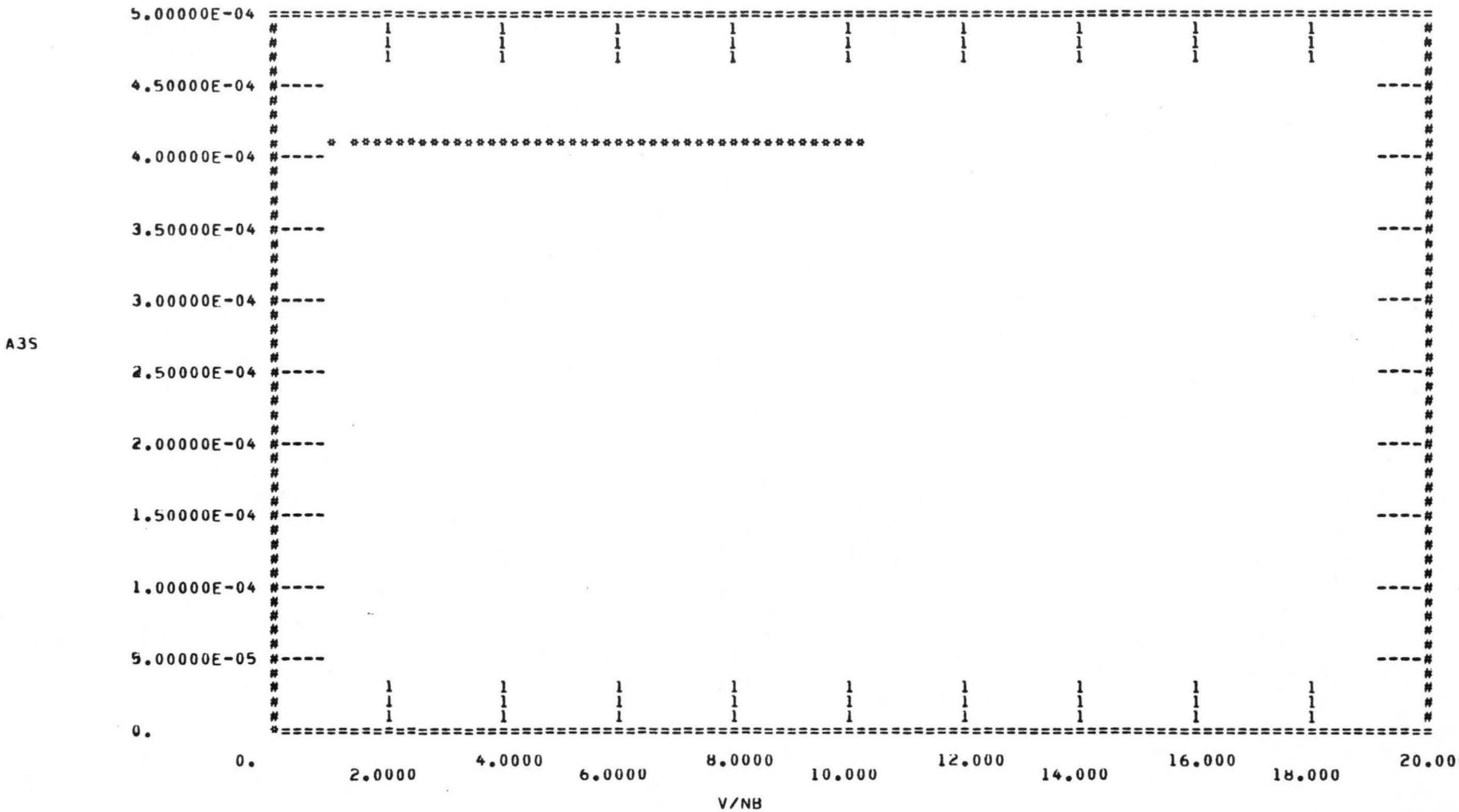

C O N F I G U R A T I O N   SIII-T

C O N F I G U R A T I O N   SIII-T

INDEX	V/NB	A3S
(1)	0.	-1.17492E-13
(2)	.92022	4.12671E-04
(3)	1.3014	4.12671E-04
(4)	1.5939	4.12671E-04
(5)	1.8404	4.12671E-04
(6)	2.0577	4.12671E-04
(7)	2.2541	4.12671E-04
(8)	2.4347	4.12671E-04
(9)	2.6029	4.12671E-04
(10)	2.7607	4.12671E-04
(11)	2.9101	4.12671E-04
(12)	3.0521	4.12671E-04
(13)	3.1878	4.12671E-04
(14)	3.3180	4.12671E-04
(15)	3.4433	4.12671E-04
(16)	3.5641	4.12671E-04
(17)	3.6810	4.12671E-04
(18)	3.7944	4.12671E-04
(19)	3.8825	4.12671E-04
(20)	4.0323	4.12671E-04

INDEX	V/NB	A3S
(21)	4.1155	4.12671E-04
(22)	4.2172	4.12671E-04
(23)	4.3164	4.12671E-04
(24)	4.4134	4.12671E-04
(25)	4.5084	4.12671E-04
(26)	4.6012	4.12671E-04
(27)	4.7105	4.12671E-04
(28)	4.7819	4.12671E-04
(29)	4.8696	4.12671E-04
(30)	4.9559	4.12671E-04
(31)	5.0407	4.12671E-04
(32)	5.2062	4.12671E-04
(33)	5.3665	4.12671E-04
(34)	5.5221	4.12671E-04
(35)	5.6732	4.12671E-04
(36)	5.8207	4.12671E-04
(37)	5.9645	4.12671E-04
(38)	6.1048	4.12671F-04
(39)	6.2421	4.12671E-04
(40)	6.3761	4.12671E-04

INDEX	V/NB	A3S
(41)	6.5082	4.12671E-04
(42)	6.7001	4.12671E-04
(43)	6.8878	4.12671E-04
(44)	7.0816	4.12671E-04
(45)	7.2470	4.12671E-04
(46)	7.4199	4.12671E-04
(47)	7.5895	4.12671E-04
(48)	7.7546	4.12671E-04
(49)	7.9703	4.12671E-04
(50)	8.1810	4.12671E-04
(51)	8.3850	4.12671E-04
(52)	8.5848	4.12671E-04
(53)	8.7800	4.12671E-04
(54)	8.9714	4.12671E-04
(55)	9.1591	4.12671E-04
(56)	9.3422	4.12671E-04
(57)	9.5208	4.12671E-04
(58)	9.6981	4.12671E-04
(59)	9.8717	4.12671E-04
(60)	10.044	4.12671E-04
(61)	10.210	4.12671E-04

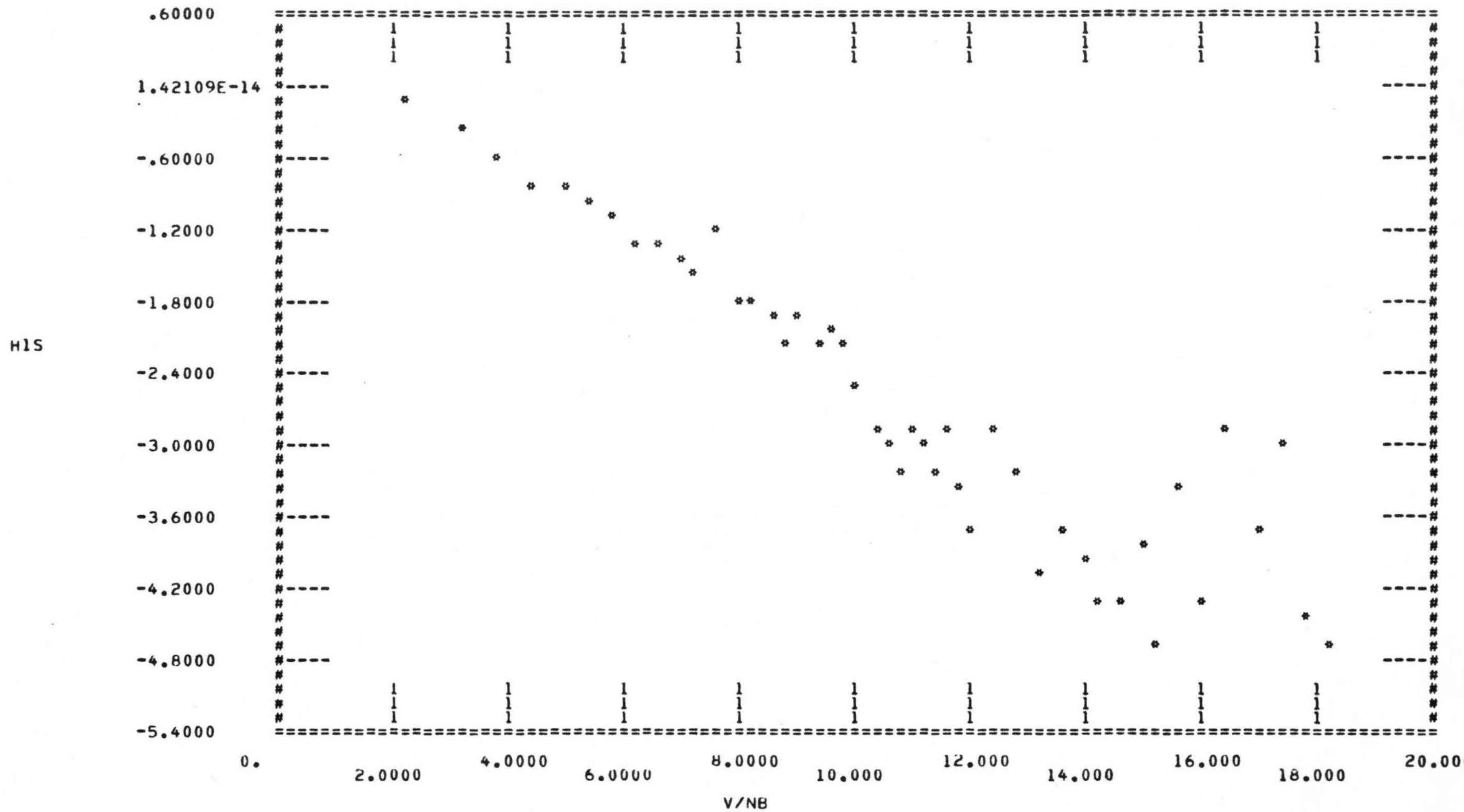

C O N F I G U R A T I O N SIII-V

C O N F I G U R A T I O N   SIII-V

INDEX	V/NB	HIS
(1)	0.	2.42959E-05
(2)	2.1996	-9.30195E-02
(3)	3.1108	-.36682
(4)	3.8101	-.64616
(5)	4.3997	-.88885
(6)	4.9190	-.85811
(7)	5.3887	-.99821
(8)	5.8207	-1.1393
(9)	6.2228	-1.3037
(10)	6.6004	-1.3556
(11)	6.9576	-1.4388
(12)	7.2975	-1.5389
(13)	7.6209	-1.1495
(14)	7.9340	-1.8120
(15)	8.2335	-1.8528

INDEX	V/NB	HIS
(16)	8.5227	-1.9426
(17)	8.8035	-2.2089
(18)	9.0729	-1.9292
(19)	9.3375	-2.2040
(20)	9.5419	-2.0691
(21)	9.8419	-2.1107
(22)	10.087	-2.4908
(23)	10.326	-2.8600
(24)	10.513	-3.0023
(25)	10.788	-3.1818
(26)	11.007	-2.8215
(27)	11.226	-2.9829
(28)	11.442	-3.1836
(29)	11.607	-2.8965
(30)	11.859	-3.3191

INDEX	V/NB	HIS
(31)	12.065	-3.7042
(32)	12.454	-2.8673
(33)	12.840	-3.2220
(34)	13.221	-4.1141
(35)	13.578	-3.6876
(36)	13.934	-3.9878
(37)	14.282	-4.3272
(38)	14.619	-4.3630
(39)	14.940	-3.8621
(40)	15.274	-4.6592
(41)	15.571	-3.3761
(42)	16.044	-4.2898
(43)	16.445	-2.8746
(44)	16.921	-3.7556
(45)	17.336	-2.9825
(46)	17.769	-4.4183
(47)	18.177	-4.6303

APPENDIX A.4

Typical Results before and after Smoothing

Results have been slightly smoothed by FORTRAN LIBRARY SUBROUTINE ICSSCU*, with control parameter:

SM = 0.010 for A2S, HIS
     0.000 for A3S

*IMSL-International Mathematical and Statistical Library.

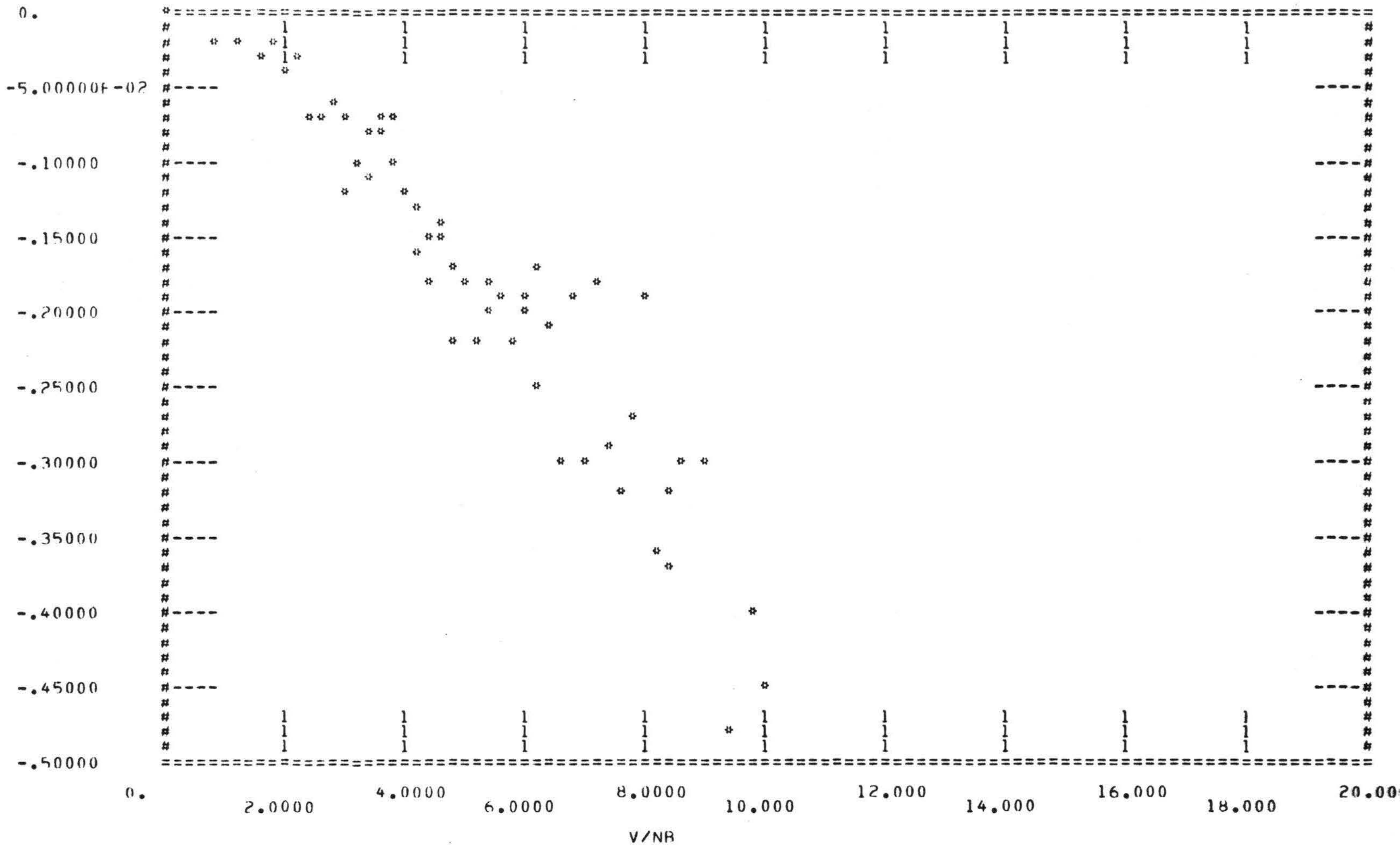

C O N F I G U R A T I O N   XX-X
U N S M O O T H E D

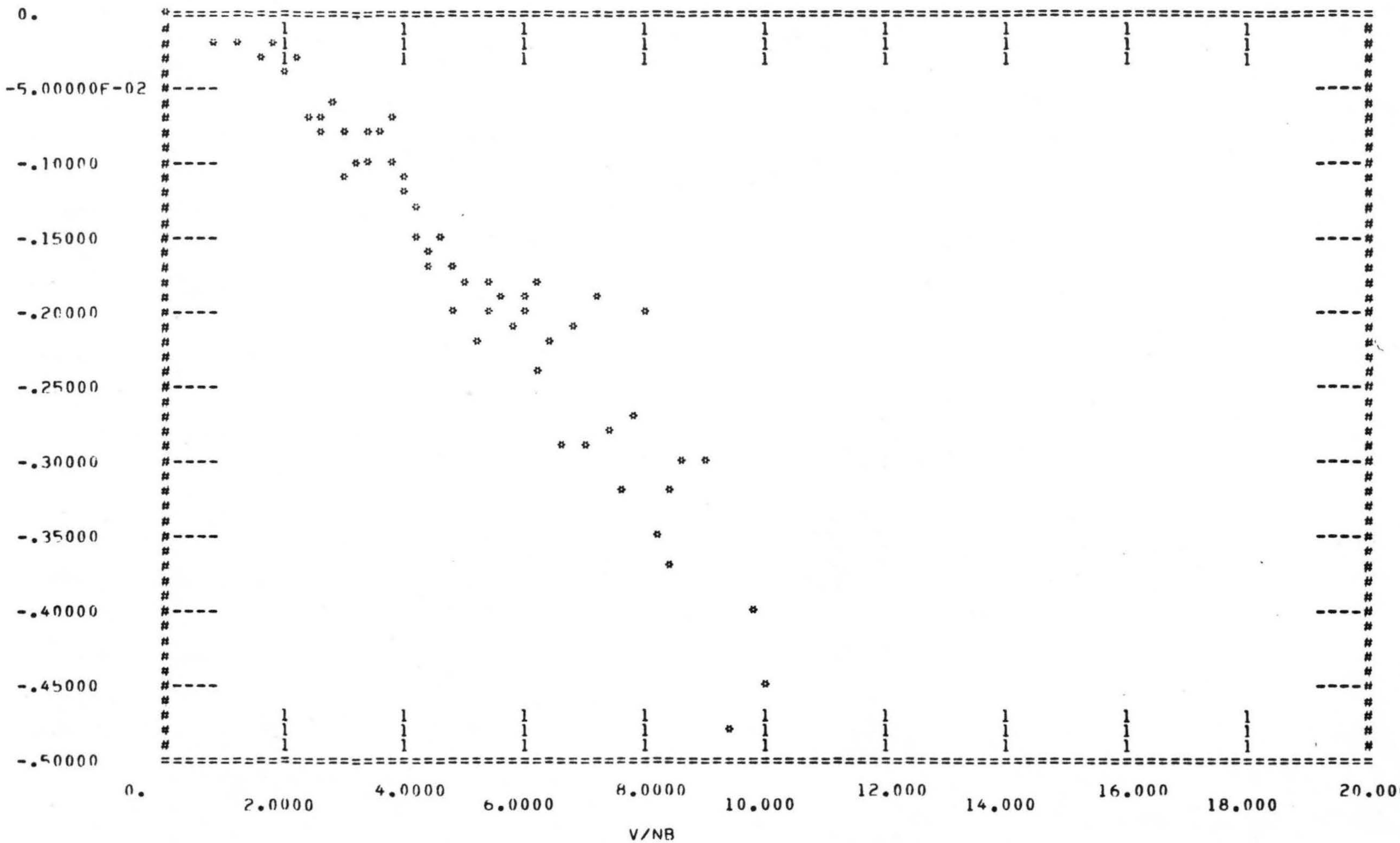

CONFIGURATION XX-X
SMOOTHED

APPENDIX B

WIND CHARACTERISTICS OF BRIDGE SITE

TABLE OF CONTENTS

LIST OF FIGURES

Appendix B

WIND CHARACTERISTICS OF BRIDGE SITE

B.1 Topographic Model

The Ruck-A-Chucky Bridge location is schematically shown in Fig. 1. Topography of the area surrounding the bridge site is rather complex. Accordingly, an investigation of wind characteristics in this area by means of physical modeling in a wind tunnel was recommended and accomplished. Certain similarity criteria must be fulfilled in order to obtain similar flow fields for model and prototype. These criteria are implied by governing physical conservation laws and have been discussed in detail by Cermak (1,2). Basically they provide geometric, dynamic and kinematic similarity. In addition, similarity of upwind flow characteristics and ground boundary conditions must be achieved.

In the study presented, geometric similarity is satisfied by an undistorted model of length ratio 1:1920. This scale was chosen to enable significant topography surrounding the site to be included in the model and to provide a representative upwind fetch necessary for appropriate boundary-layer growth. Topography was modeled by thin styrofoam layers cut to match contour lines of a topographic map (enlarged to the 1:1920 scale) and glued together. Overall view of the model in the environmental wind tunnel (EWT) is shown in Fig. 2.

The model terrain surface was made rough to represent estimated roughness of the site which was sufficient to achieve Reynolds number independence of flow over the model surface.

Sections of modeled topography were constructed for regions upwind and downwind of the topography mounted on the 12-ft (3.66 m) diameter turntable.

The EWT, in which the whole, described herein, wind study was conducted is schematically presented in Fig. 3.

B.2 Vertical Profiles of Mean Velocity and Turbulence

Velocity profiles and turbulence intensities were measured at the bridge deck center for several different wind directions. The most extreme conditions were expected for wind blowing along and across the canyon centerline at the bridge site. These directions, respectively $\alpha = 300°$ and $\alpha = 30°$, are shown in Fig. 4. Also certain intermediate wind directions ($\alpha = 105°$, $\alpha = 270°$) were chosen for measurements.

Vertical profiles of the longitudinal mean velocity component and turbulence intensities were measured for the configurations indicated. The velocity profiles are plotted in Figs. 5-8. Corresponding turbulence intensity graphs are shown in Figs. 9-12. Similar data were taken for a representative point located on top of one of the ridges near the bridge site. These results are compared with measurements taken at the bridge center in Fig. 5 and Fig. 9.

The above graphs show that, for wind along the canyon ($\alpha = 300°$) the mean longitudinal velocity at the center of the bridge deck level equals approximately 40% of its value above the boundary layer, Fig. 6. This magnitude reduces as the wind direction approaches $\alpha = 30°$ and its lower limit is approximately 15%, Fig. 5. The extreme magnitude of turbulence intensity at the bridge center equals approximately 50% for flow across the canyon, i.e., $\alpha = 30°$, Fig. 9.

The effects of wind direction on the overall flow pattern are shown by Figs. 13a, 13b and 14. No large-scale organized swirling flow was observed at the bridge site by flow visualization. Furthermore, no such motion was detected by a rotated, yawed hot-film probe--a technique which is capable of detecting organized vorticity (3). More detail of the flow pattern is provided by a motion picture that supplements this report.

B.3 Turbulence Spectra

Turbulence spectra were calculated for the longitudinal* U and vertical W velocity components at two different points of the bridge deck, located 1/3 bridge span apart. These points are schematically shown in Fig. 1. Again two representative wind directions ($\alpha = 30°$, $\alpha = 300°$) were chosen (see Fig. 4).

The spectra computed for the foregoing configurations are plotted in Figs. 15-22. They are normalized in such a way that mean-square-value (the area under a spectrum graph) is equal to one.

Basically the spectra for point No. 1 and No. 2 are almost identical. Comparison of the spectrum of the vertical velocity component for flows along ($\alpha = 300°$) and across the canyon ($\alpha = 30°$) shows that the later flow has relatively more turbulent energy in the low-frequency range.

B.4 Space Correlations

Two-point velocity correlations for the longitudinal* and vertical velocity components were measured for the two locations and wind directions described in the Section B.3. The results of the measurements are shown in Table I. The vertical component is practically uncorrelated for both wind directions. However, the correlation coefficient for the longitudinal component is substantial and is higher for $\alpha = 300°$ than for $\alpha = 30°$. This is a reasonable result since for $\alpha = 300°$ the wind blows parallel to the canyon axis while if $\alpha = 30°$ the flow is perpendicular to the canyon.

*Parallel to canyon axis

REFERENCES

1. Cermak, J. E., "Laboratory Simulation of the Atmospheric Boundary Layer," AIAA Jnl., Vol. 9, No. 9, Sept. 1971, pp. 1746-1754.

2. Cermak, J. E., "Applications of Fluid Mechanics to Wind Engineering--A Freeman Scholar Lecture," ASME, Jnl. of Fluid Engrg., Vol. 97, Series 1, No. 1, March 1975.

3. Marsh, G. L., and Peterka, J. A., "Measurement of Turbulent Flows with a Rotated Hot-Film Anemometer," Fluid Mechanics and Diffusion Laboratory Report, CER76-77GLM-JAP64, Colorado State University, 1977.

FIGURES

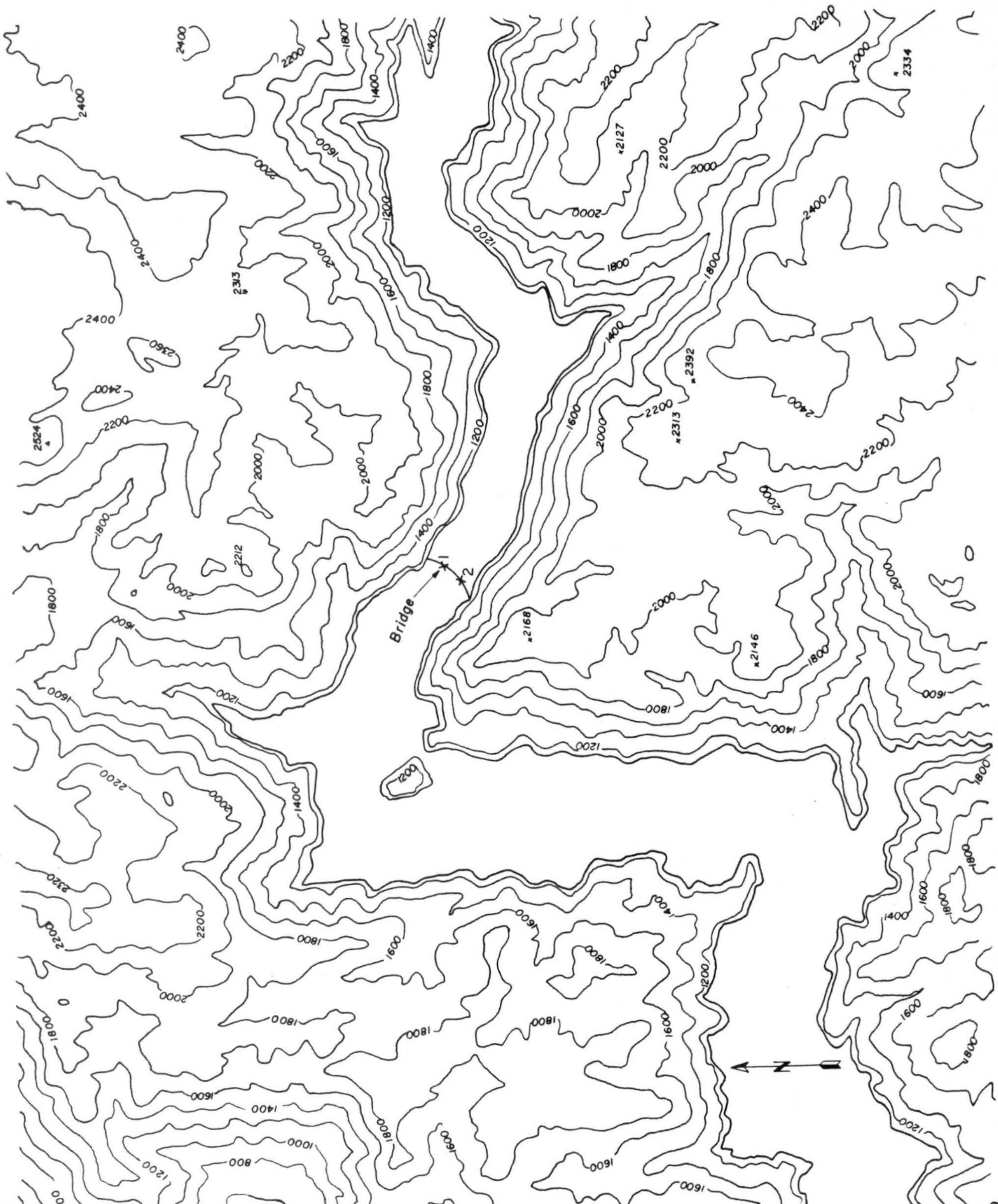

Fig. 1. Schematic of Bridge Location

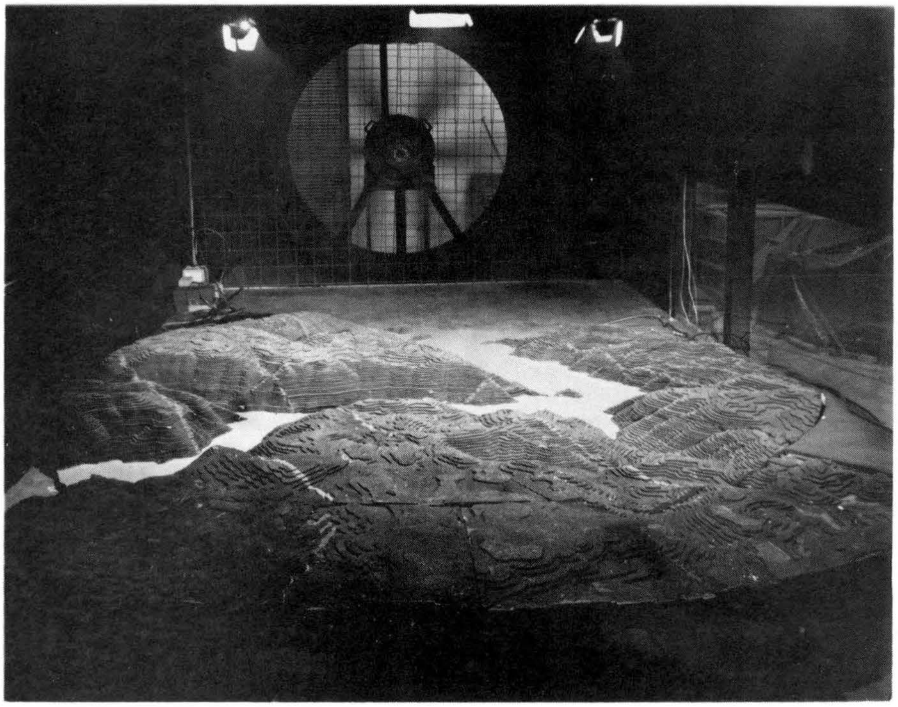

Fig. 2. Topographic Model in Wind Tunnel

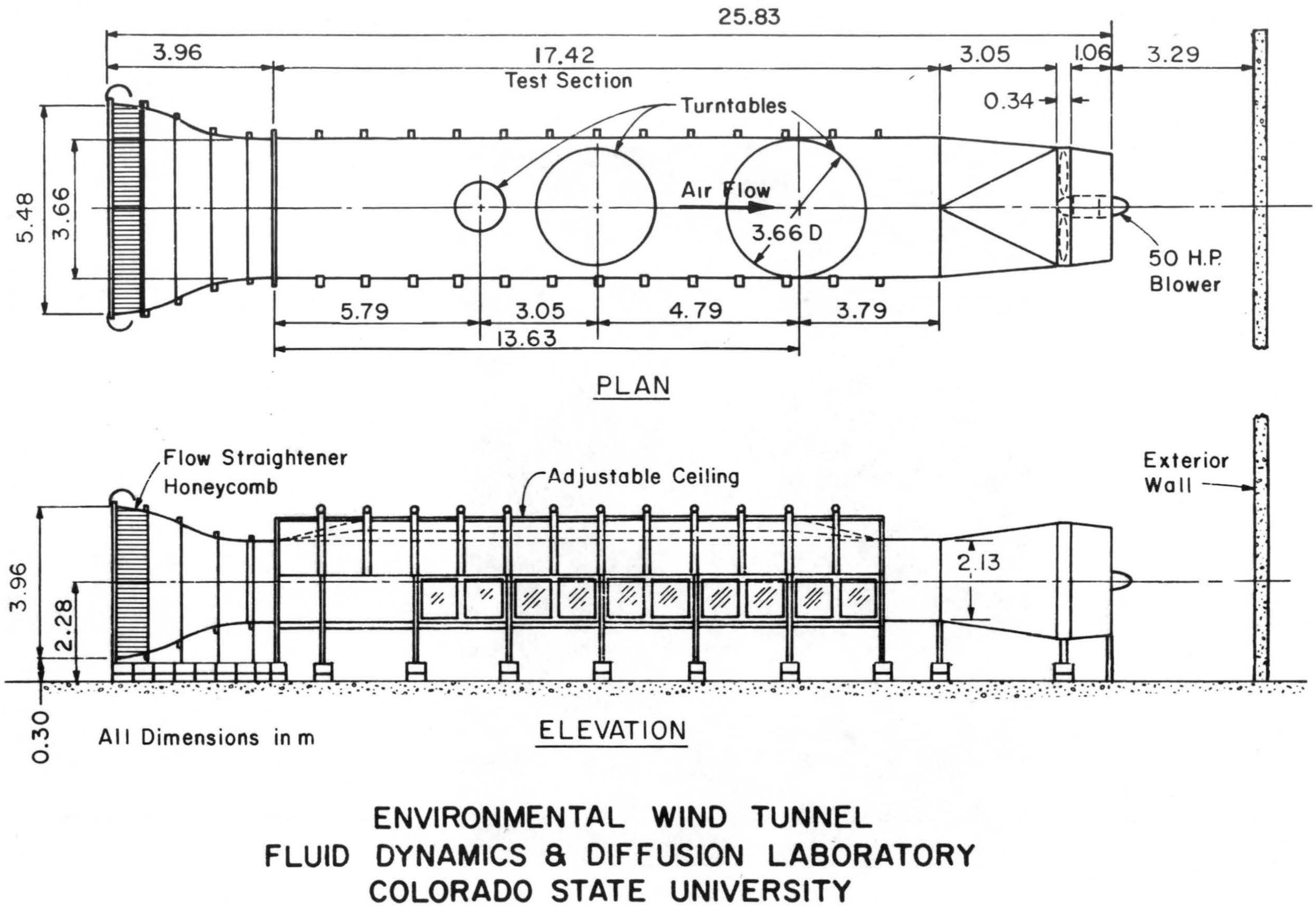

Fig. 3. Environmental Wind Tunnel

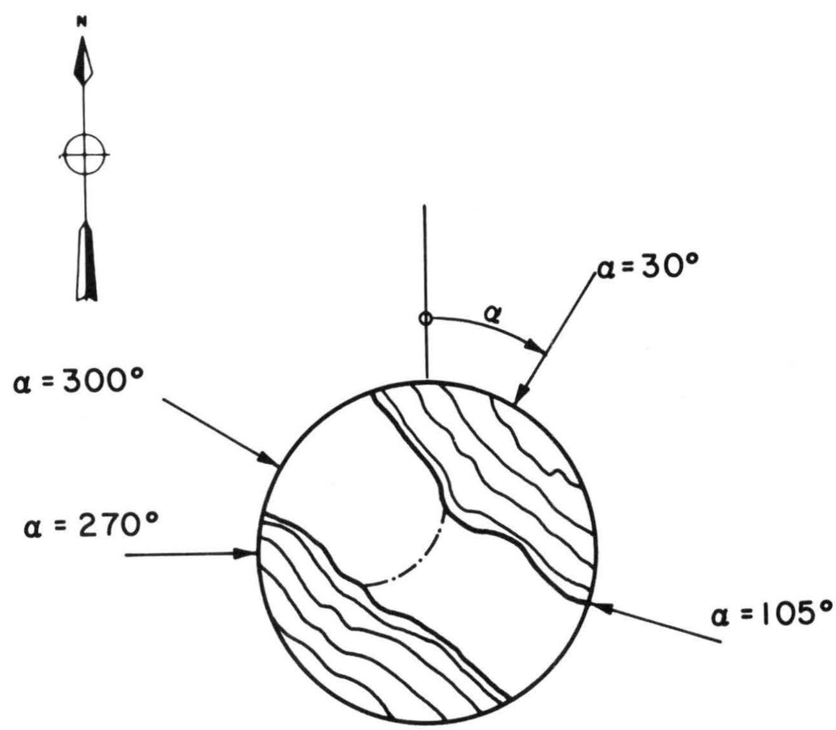

Fig. 4. Basic Wind Directions Considered in Study

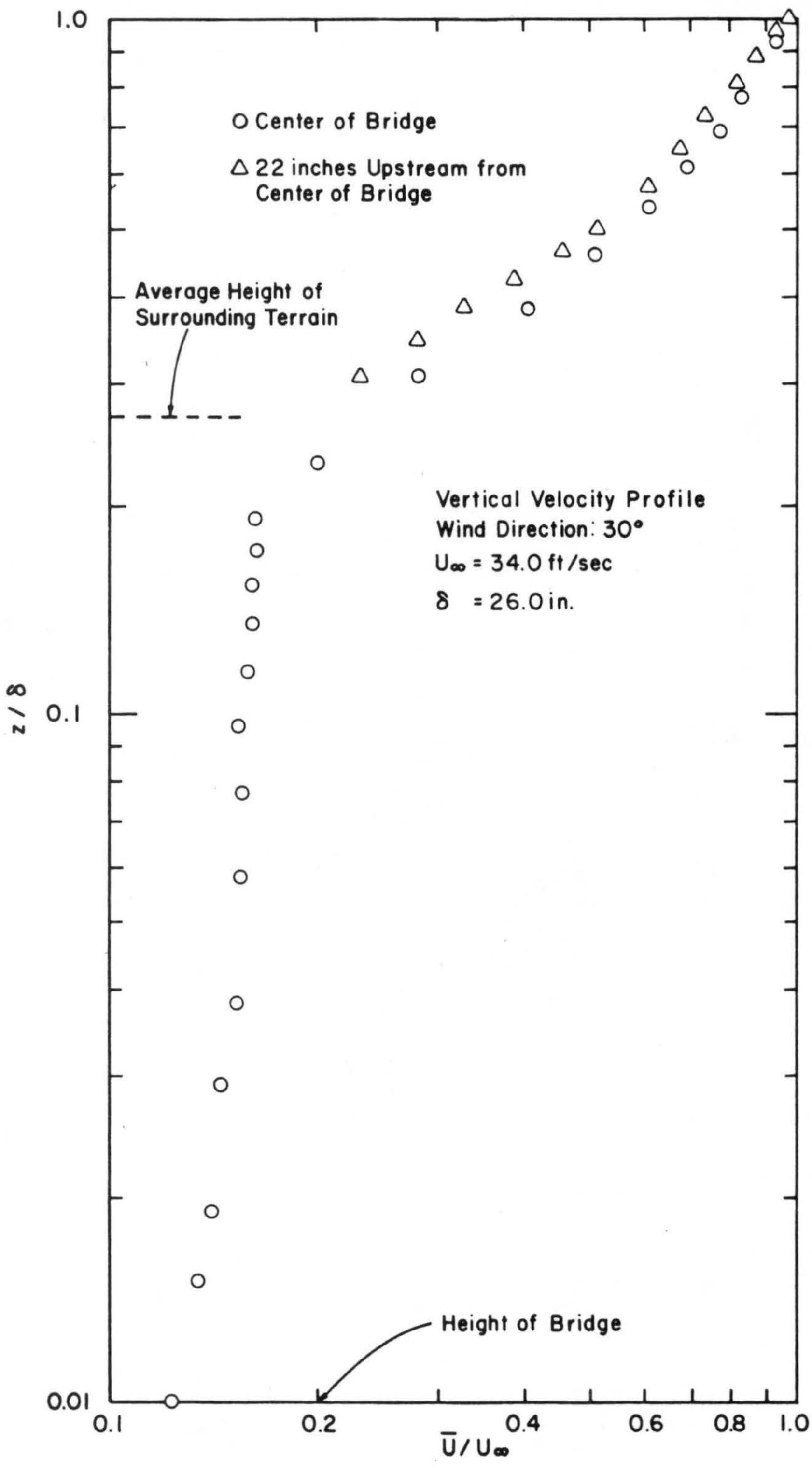

Fig. 5. Mean Velocity Profile $\alpha = 30°$

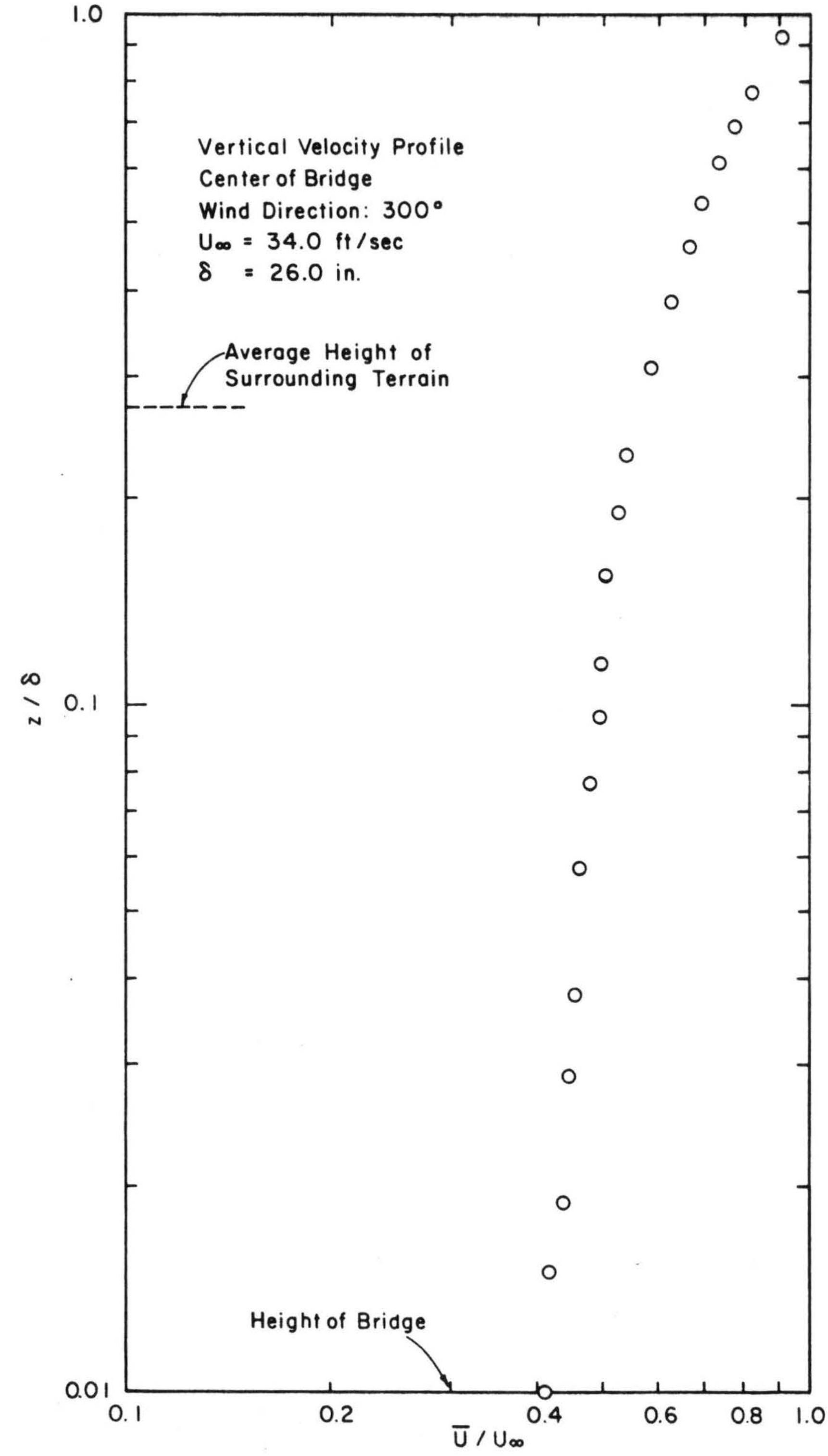

Fig. 6. Mean Velocity Profile α = 300°

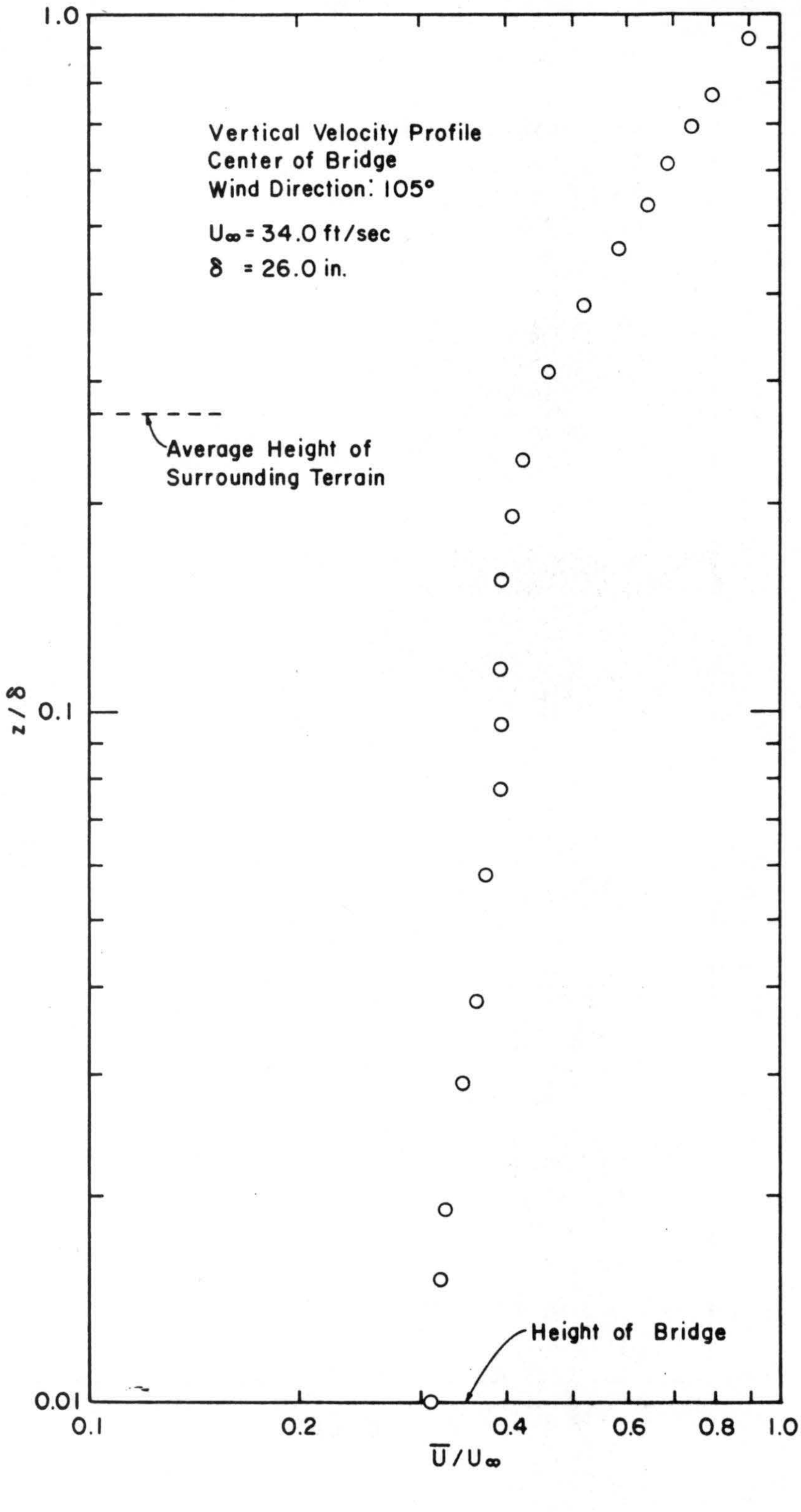

Fig. 7. Mean Velocity Profile α = 105°

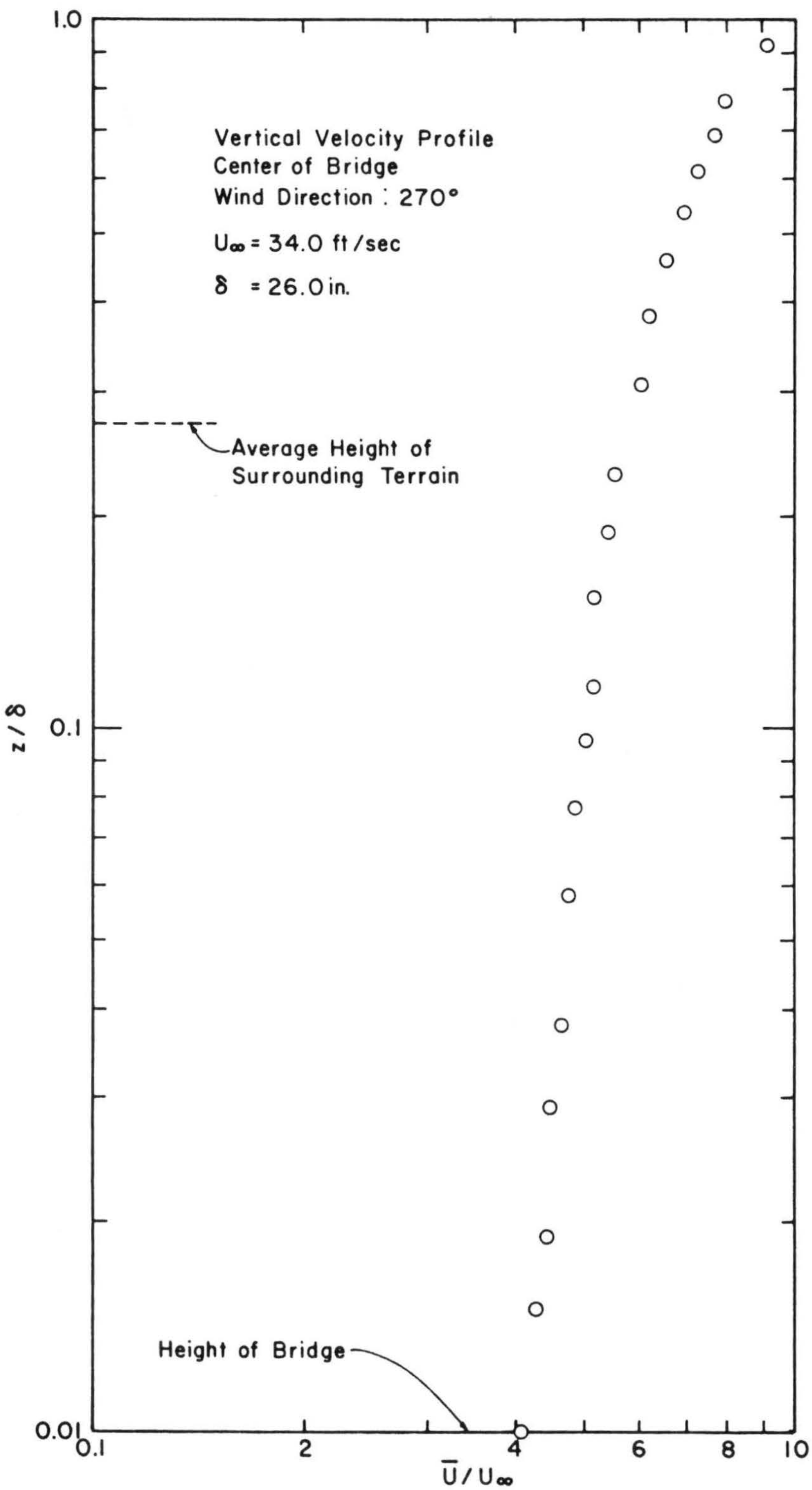

Fig. 8. Mean Velocity Profile $\alpha = 270°$

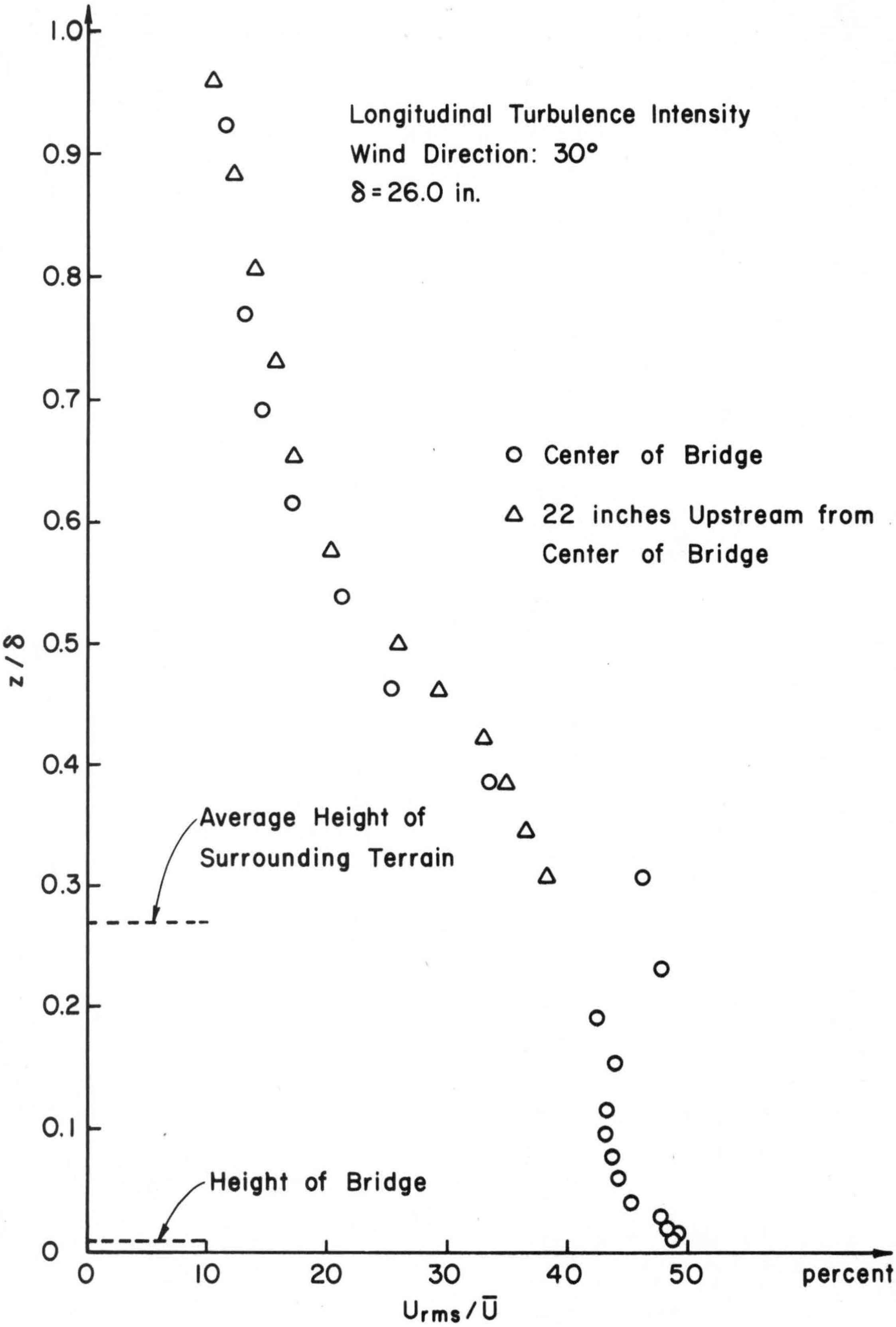

Fig. 9. Turbulence Intensity $\alpha = 30°$

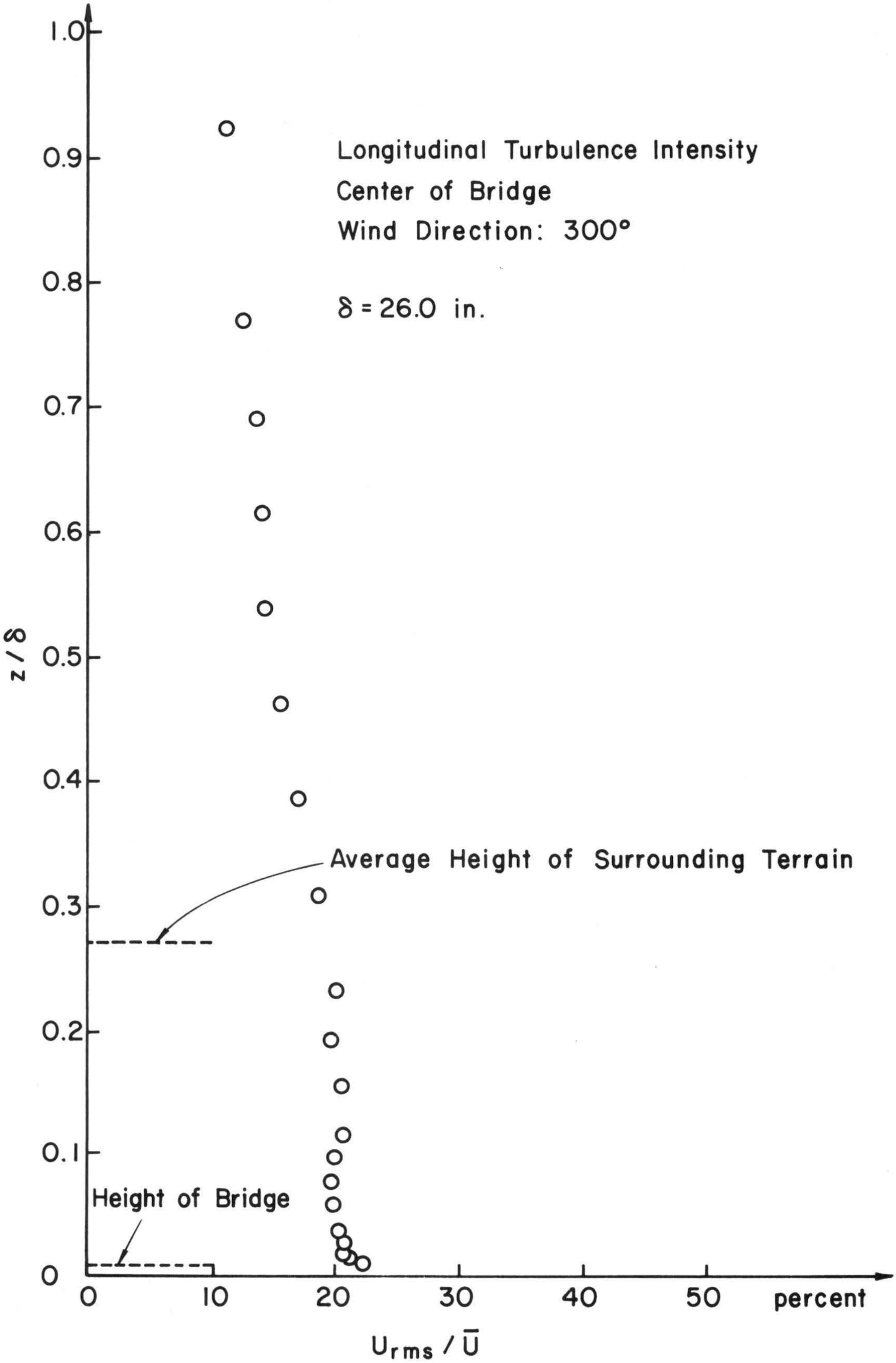

Fig. 10. Turbulence Intensity α = 300°

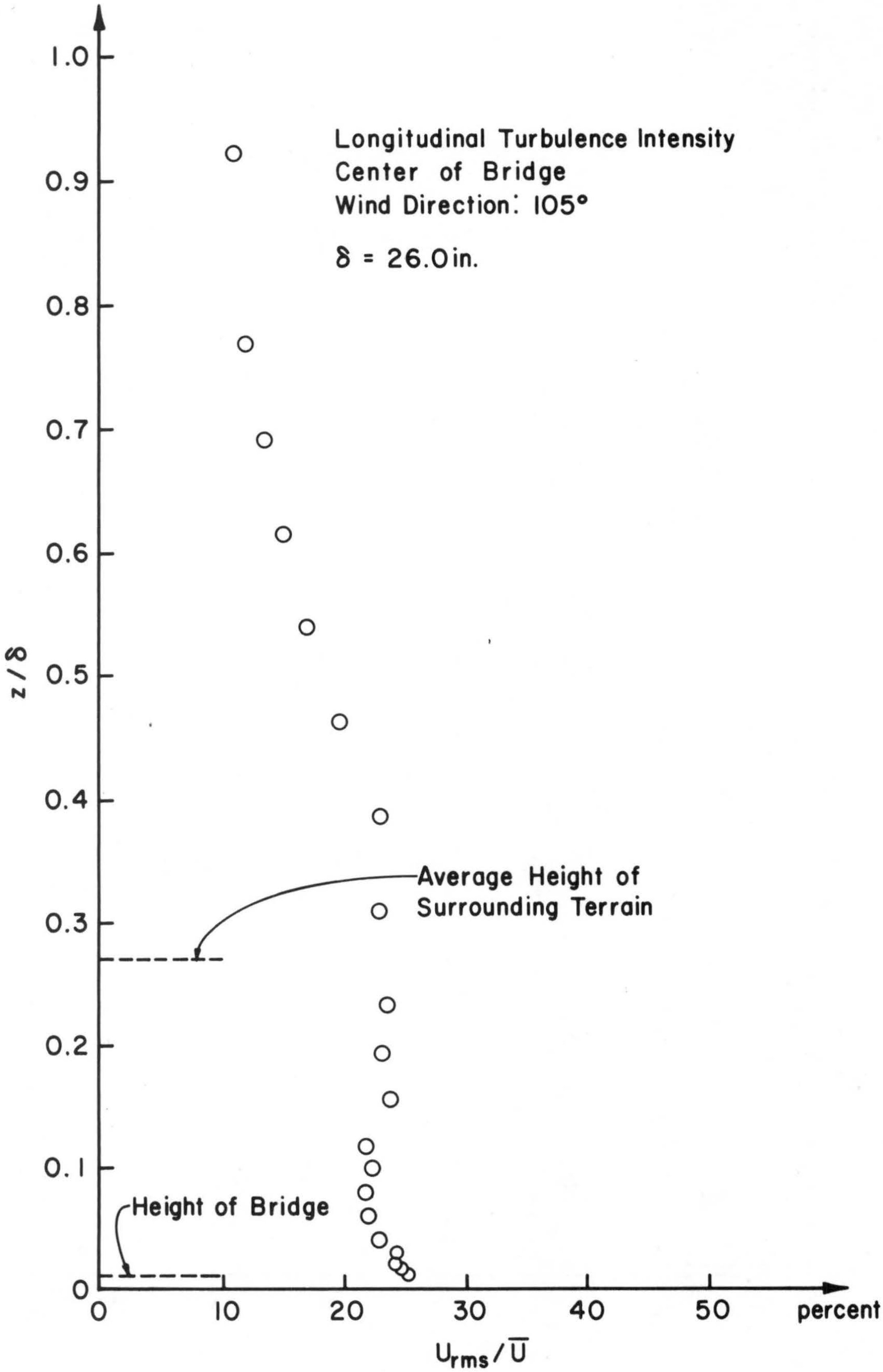

Fig. 11. Turbulence Intensity α = 105°

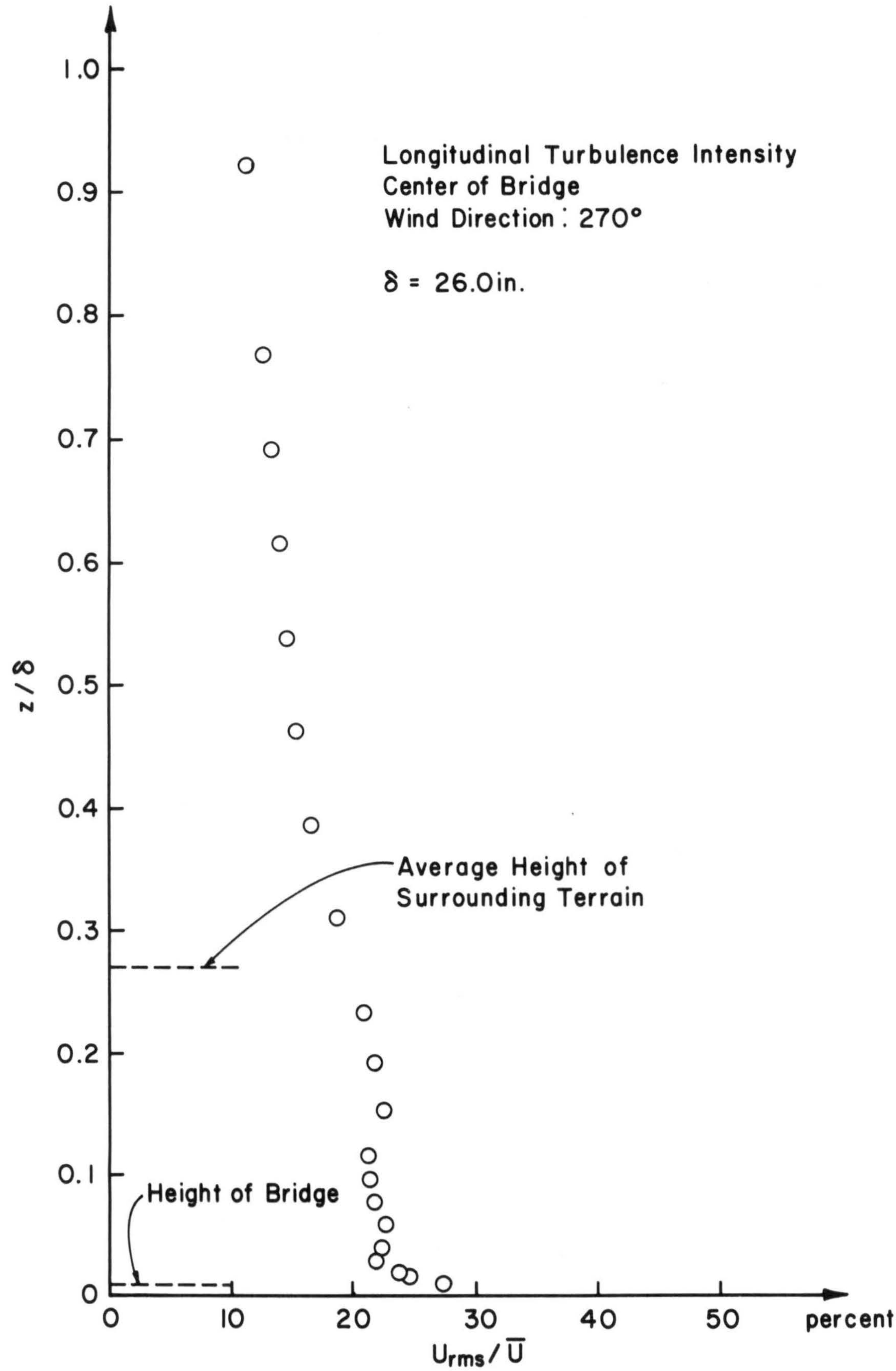

Fig. 12. Turbulence Intensity α = 270°

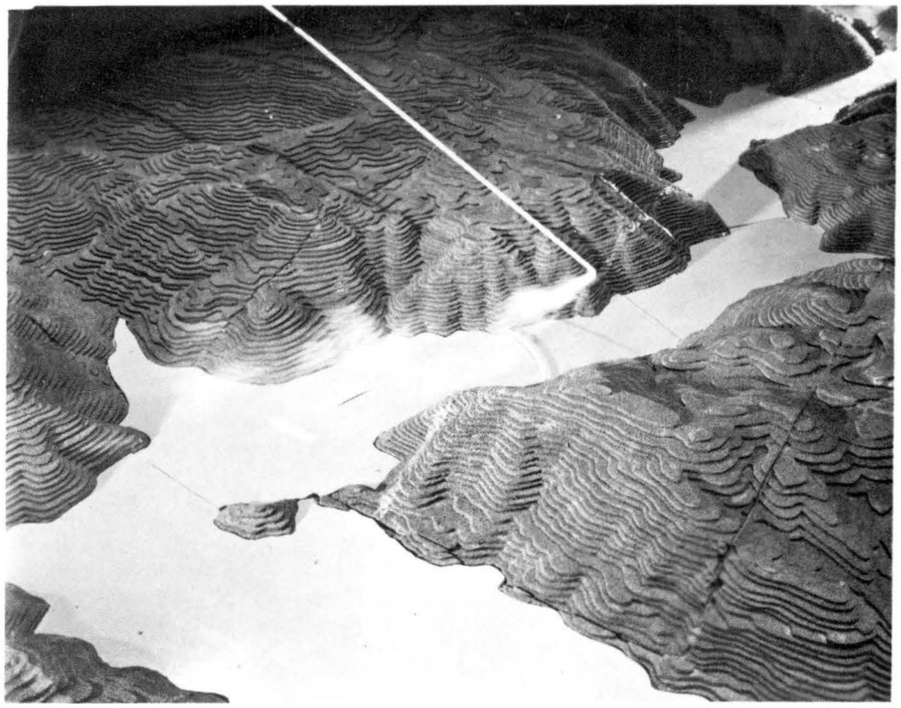

(a)

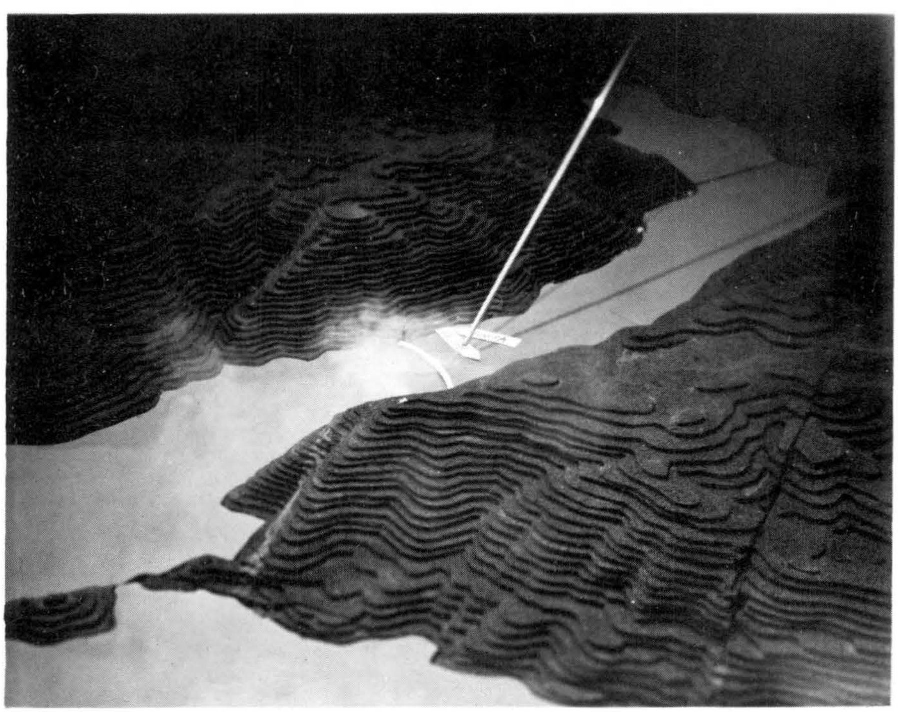

(b)

Fig. 13. Wind Visualization (a) along canyon, (b) across canyon

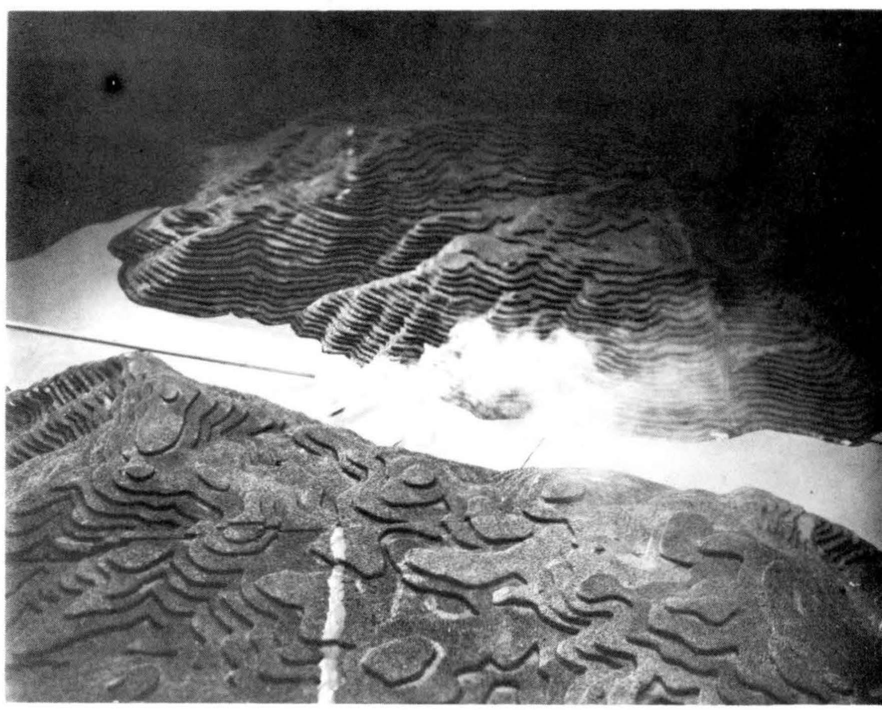

Fig. 14. Unsteady Vortex Formation Associated with North Wind ($\alpha=0°$)

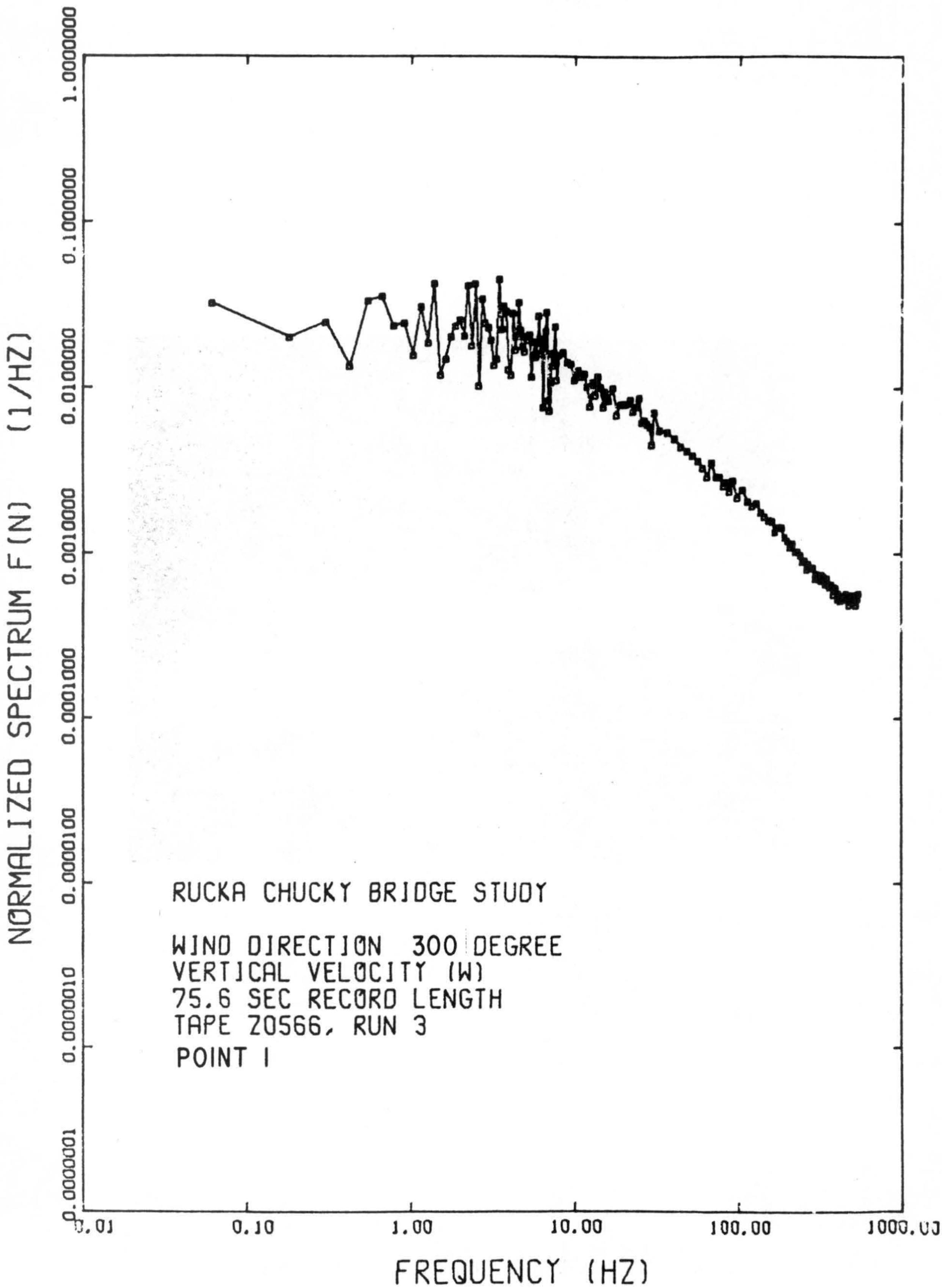
NORMALIZED SPECTRUM F(N) (1/HZ)
1.0000000
0.1000000
0.0100000
0.0010000
0.0001000
0.0000100
0.0000010
0.0000001
0.01
0.10
1.00
10.00
100.00
1000.00
FREQUENCY (HZ)
RUCKA CHUCKY BRIDGE STUDY
WIND DIRECTION 300 DEGREE
VERTICAL VELOCITY (W)
75.6 SEC RECORD LENGTH
TAPE 20566, RUN 3
POINT I

Fig. 15

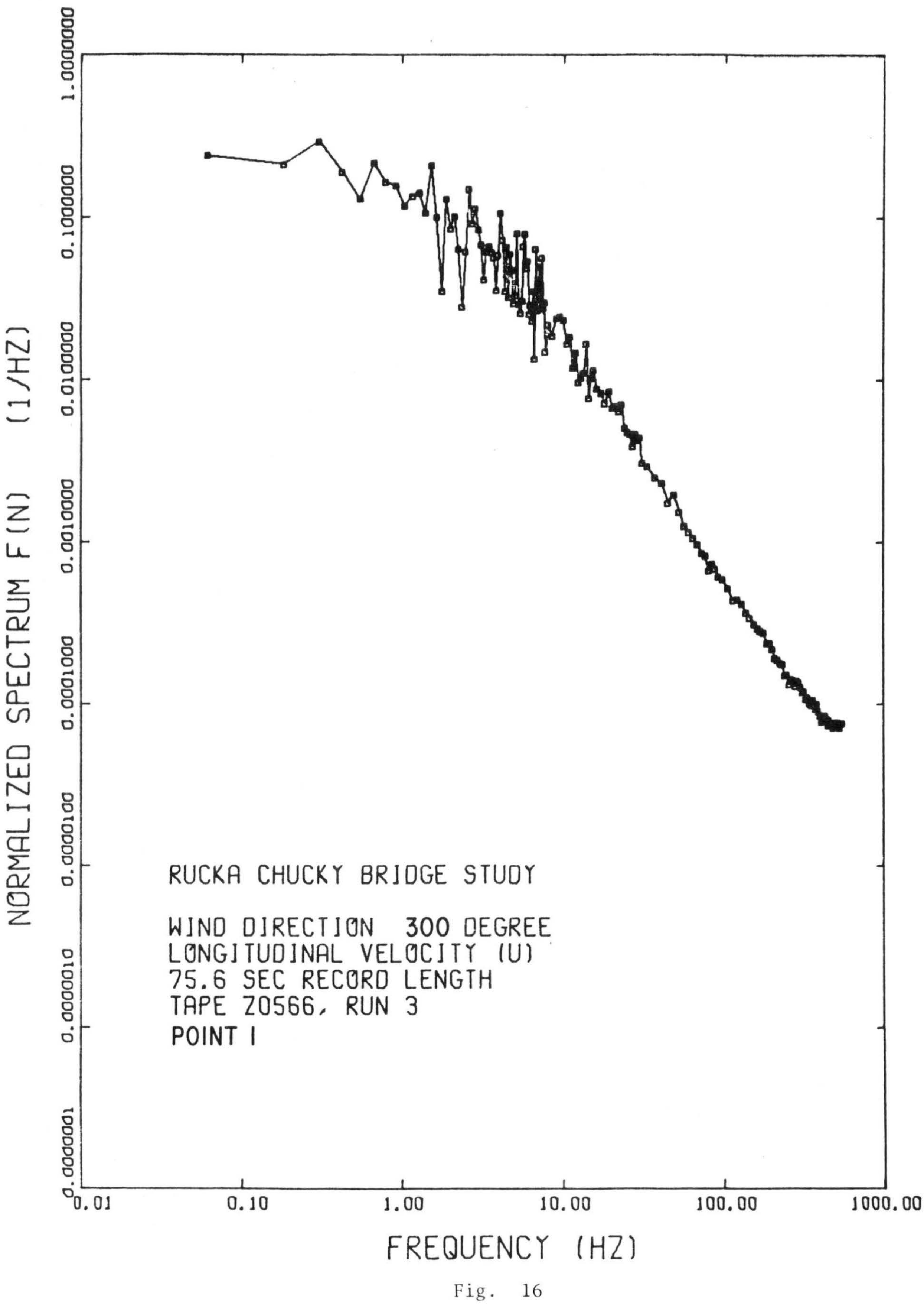
1.0000000
0.1000000
0.0100000
0.0010000
0.0001000
0.0000100
0.0000010
0.0000001
NORMALIZED SPECTRUM F(N) (1/HZ)
0.01
0.10
1.00
10.00
100.00
1000.00
FREQUENCY (HZ)
RUCKA CHUCKY BRIDGE STUDY
WIND DIRECTION 300 DEGREE
LONGITUDINAL VELOCITY (U)
75.6 SEC RECORD LENGTH
TAPE Z0566, RUN 3
POINT I

Fig. 16

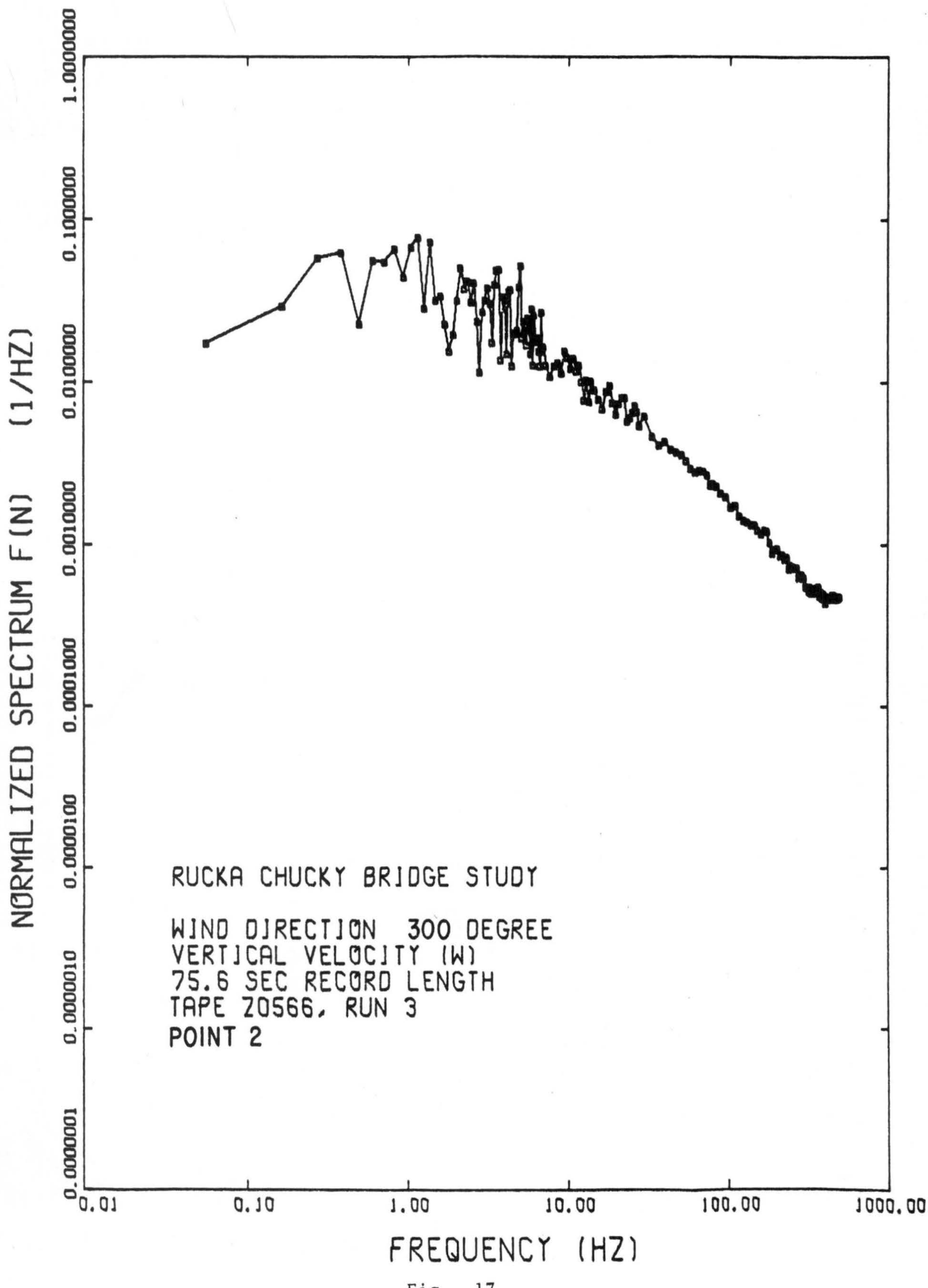
NORMALIZED SPECTRUM F(N) (1/HZ)
1.0000000
0.1000000
0.0100000
0.0010000
0.0001000
0.0000100
0.0000010
0.0000001
0.01
0.10
1.00
10.00
100.00
1000.00
FREQUENCY (HZ)
RUCKA CHUCKY BRIDGE STUDY
WIND DIRECTION 300 DEGREE
VERTICAL VELOCITY (W)
75.6 SEC RECORD LENGTH
TAPE Z0566, RUN 3
POINT 2

Fig. 17

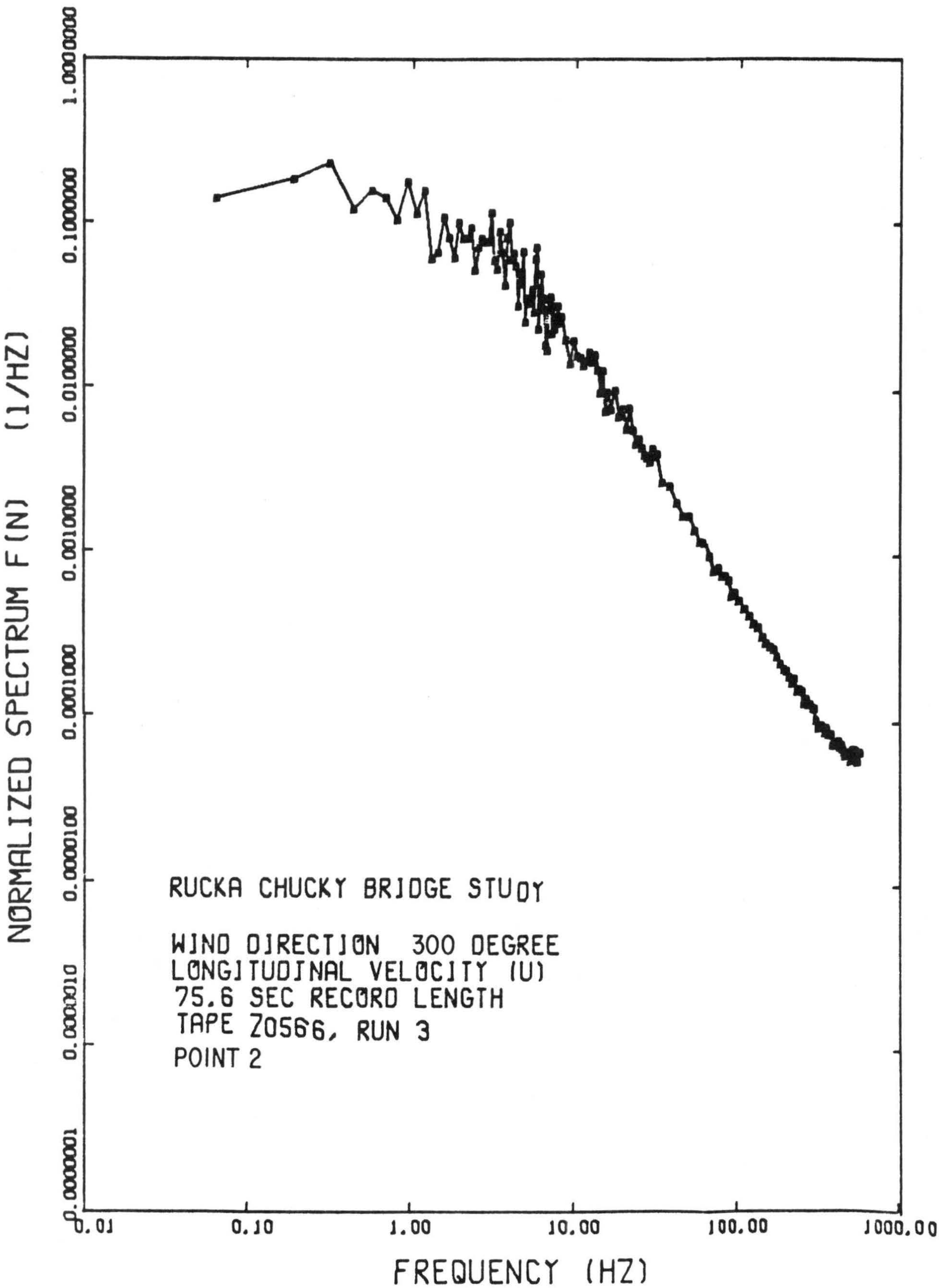
NORMALIZED SPECTRUM F(N) (1/HZ)
1.0000000
0.1000000
0.0100000
0.0010000
0.0001000
0.0000100
0.0000010
0.0000001
0.01
0.10
1.00
10.00
100.00
1000.00
FREQUENCY (HZ)
RUCKA CHUCKY BRIDGE STUDY
WIND DIRECTION 300 DEGREE
LONGITUDINAL VELOCITY (U)
75.6 SEC RECORD LENGTH
TAPE Z0566, RUN 3
POINT 2

Fig. 18

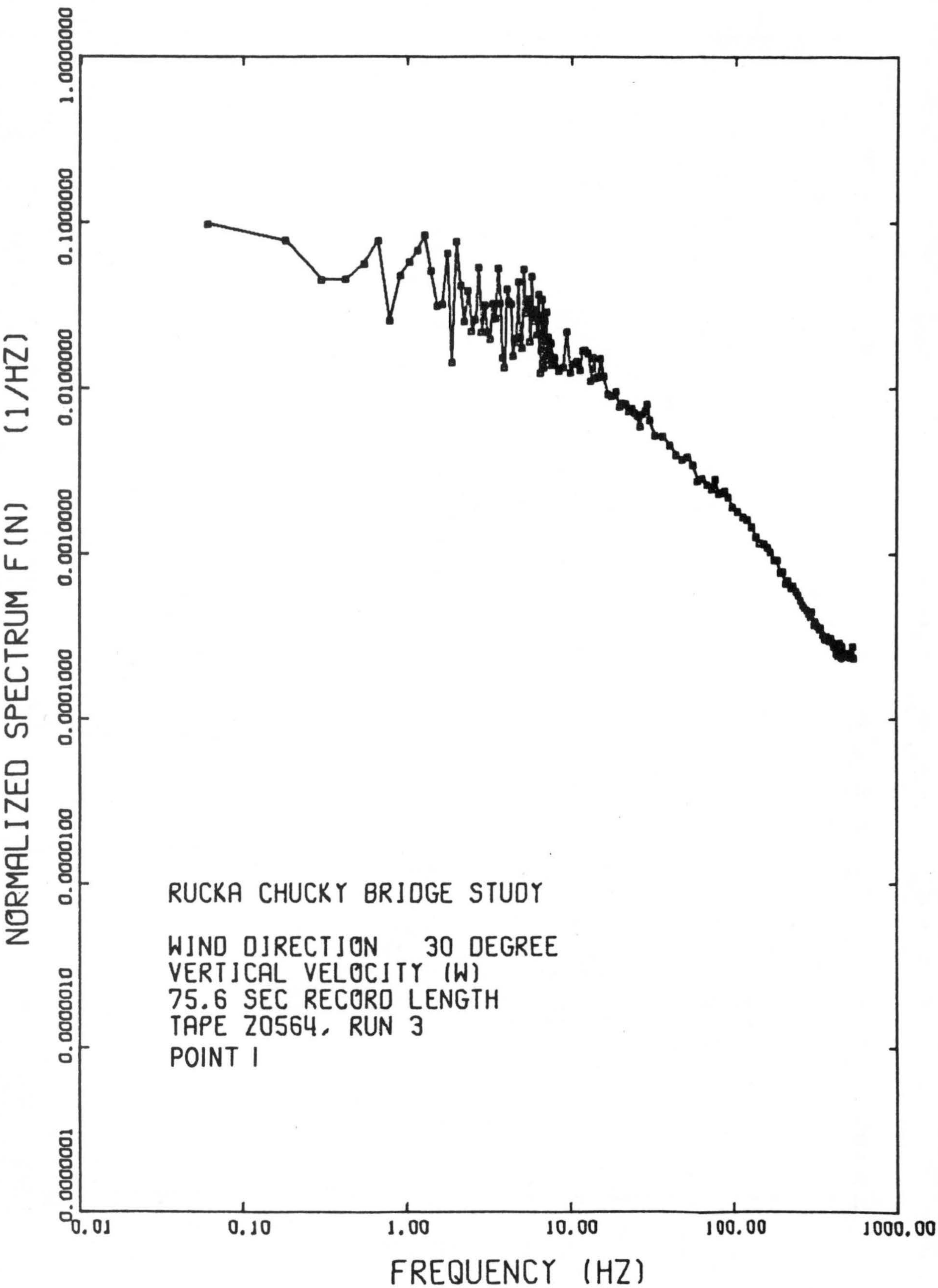

1.0000000
0.1000000
0.0100000
0.0010000
0.0001000
0.0000100
0.0000010
0.0000001
NORMALIZED SPECTRUM F(N) (1/HZ)
0.01
0.10
1.00
10.00
100.00
1000.00
FREQUENCY (HZ)
RUCKA CHUCKY BRIDGE STUDY
WIND DIRECTION 30 DEGREE
VERTICAL VELOCITY (W)
75.6 SEC RECORD LENGTH
TAPE 20564, RUN 3
POINT I

Fig. 19

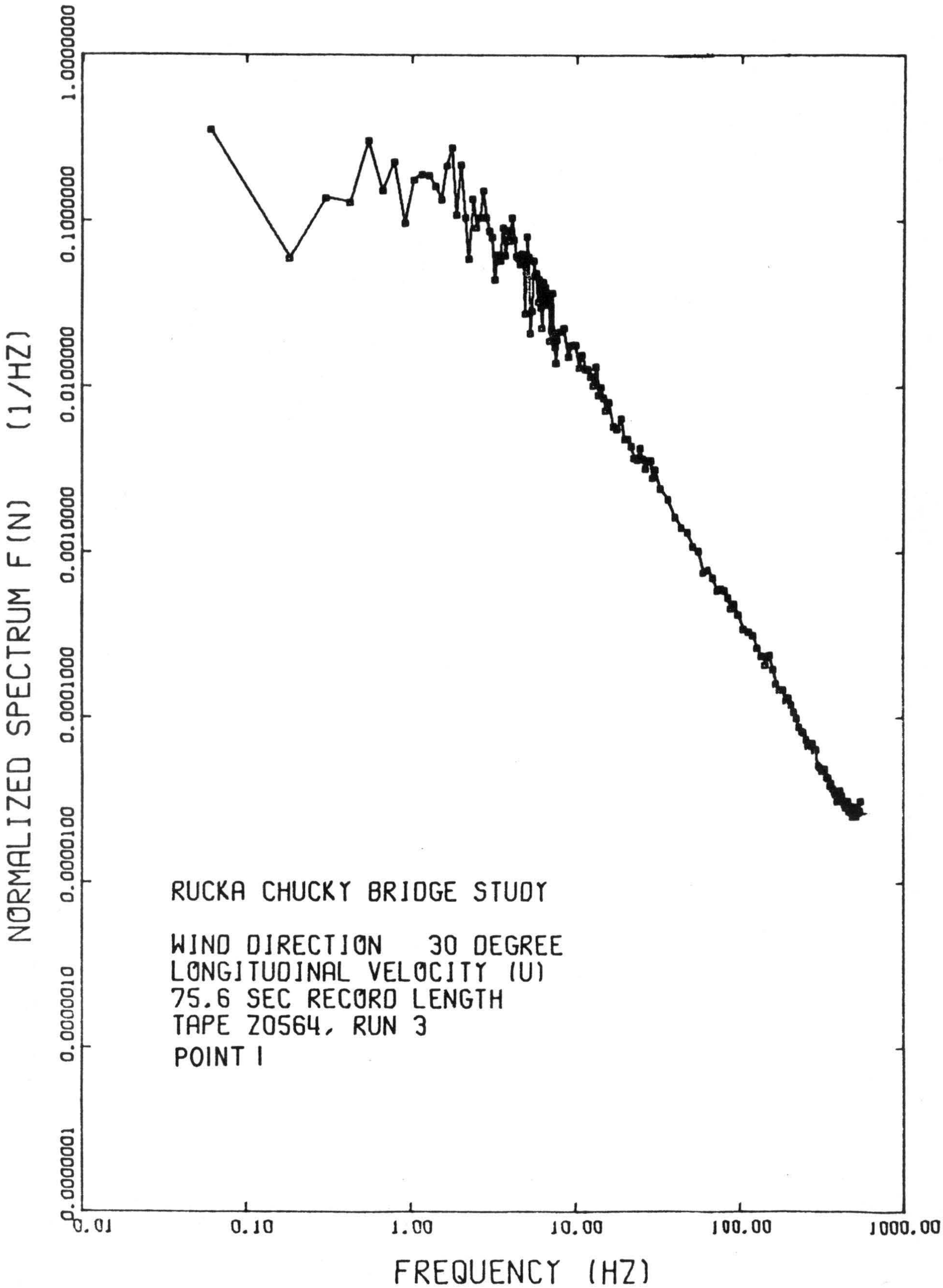

1.0000000
0.1000000
0.0100000
0.0010000
0.0001000
0.0000100
0.0000010
0.0000001
NORMALIZED SPECTRUM F(N) (1/HZ)
0.01
0.10
1.00
10.00
100.00
1000.00
FREQUENCY (HZ)
RUCKA CHUCKY BRIDGE STUDY
WIND DIRECTION 30 DEGREE
LONGITUDINAL VELOCITY (U)
75.6 SEC RECORD LENGTH
TAPE Z0564, RUN 3
POINT I

Fig. 20

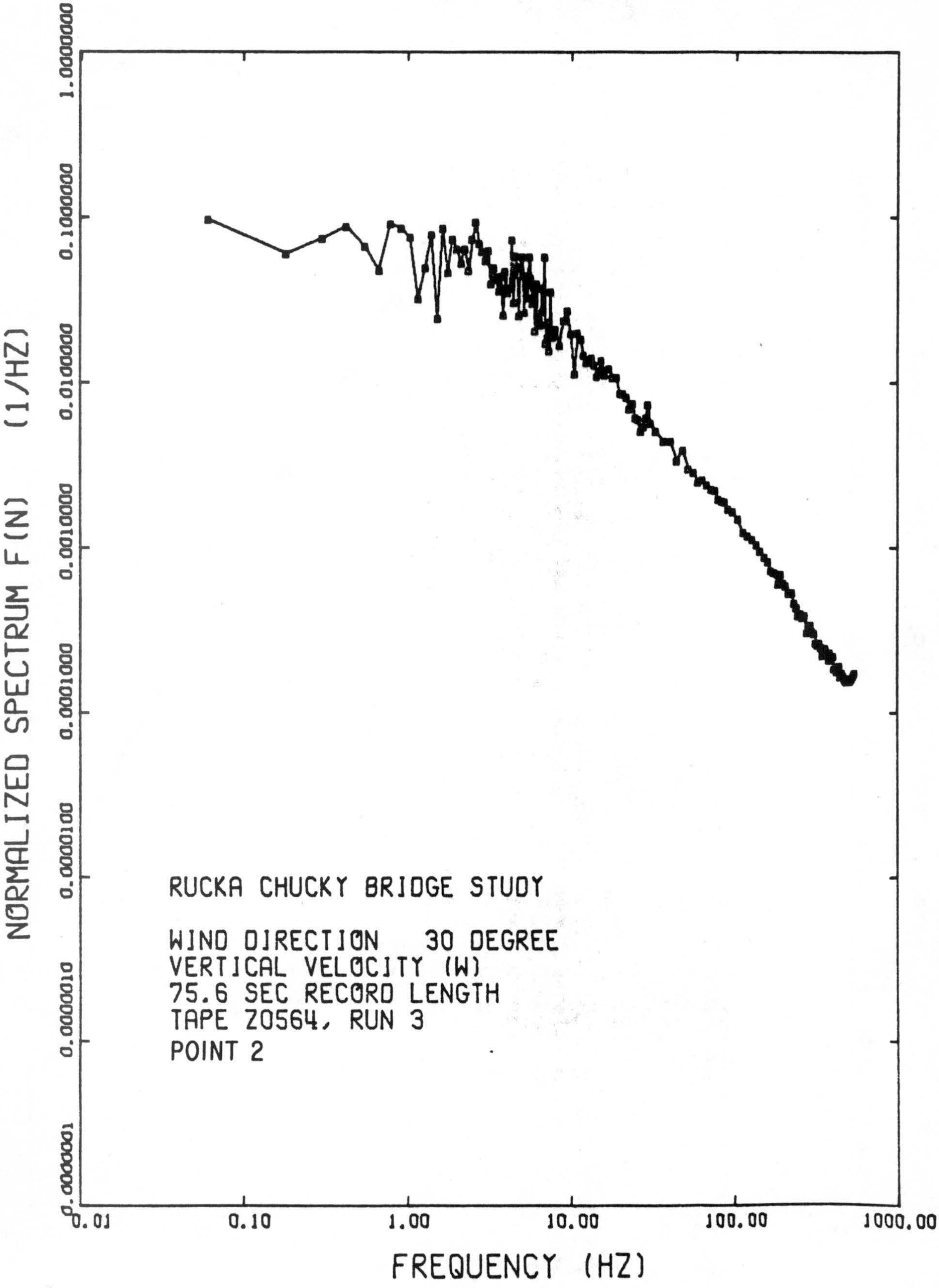
NORMALIZED SPECTRUM F(N) (1/HZ)
1.0000000
0.1000000
0.0100000
0.0010000
0.0001000
0.0000100
0.0000010
0.0000001
0.01
0.10
1.00
10.00
100.00
1000.00
FREQUENCY (HZ)
RUCKA CHUCKY BRIDGE STUDY
WIND DIRECTION 30 DEGREE
VERTICAL VELOCITY (W)
75.6 SEC RECORD LENGTH
TAPE Z0564, RUN 3
POINT 2

Fig. 21

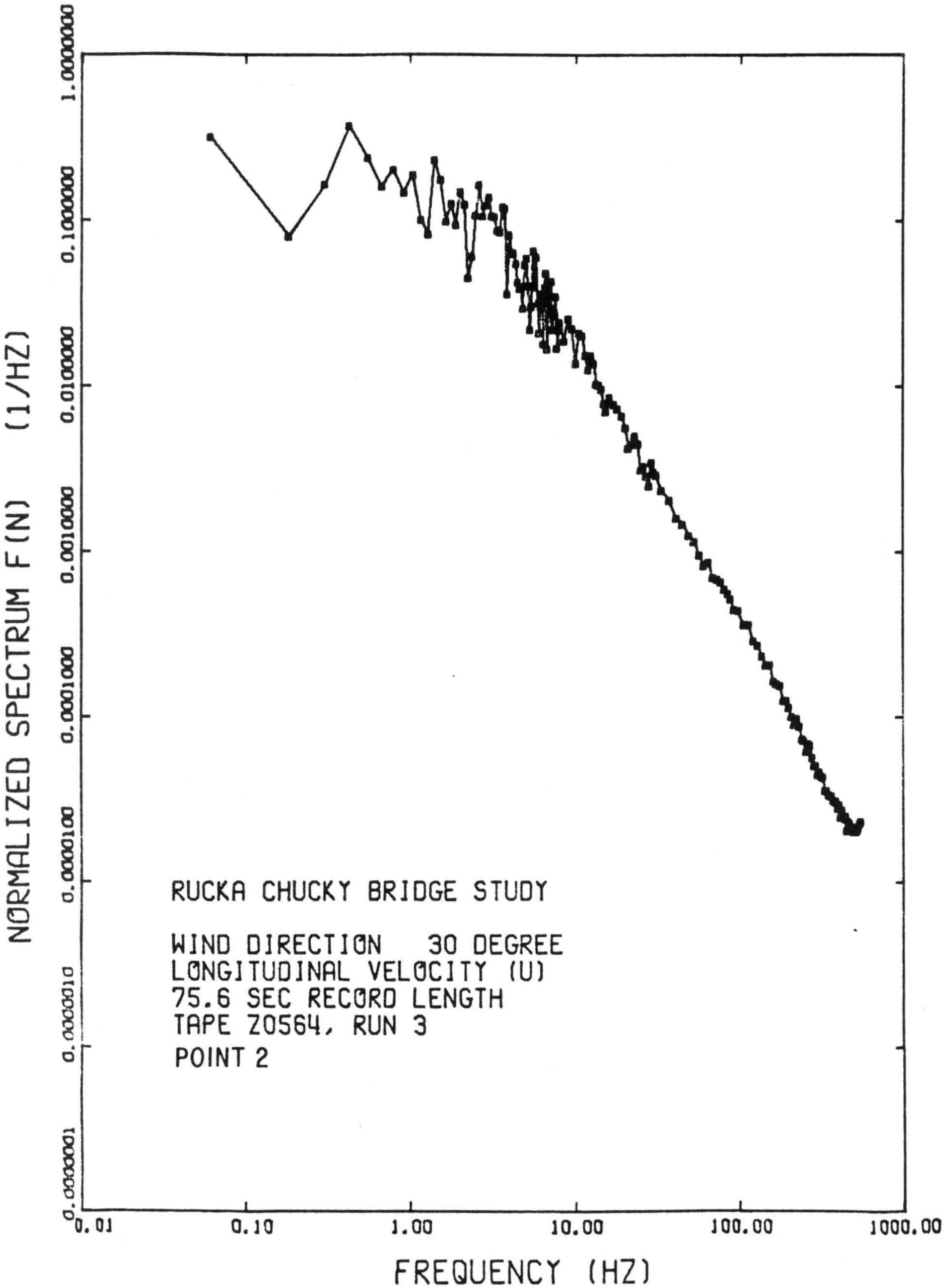

1.0000000
0.1000000
0.0100000
0.0010000
0.0001000
0.0000100
0.0000010
0.0000001
0.0000000
NORMALIZED SPECTRUM F(N) (1/HZ)
0.01
0.10
1.00
10.00
100.00
1000.00
FREQUENCY (HZ)
RUCKA CHUCKY BRIDGE STUDY
WIND DIRECTION 30 DEGREE
LONGITUDINAL VELOCITY (U)
75.6 SEC RECORD LENGTH
TAPE Z0564, RUN 3
POINT 2

Fig. 22

Table I. Two-Point Space Correlations

α	Velocity component	Correlation Coefficient
30°	U(Parallel to canyon axis)	0.297
30°	W (Vertical)	0.001
300°	U (Parallel to canyon axis)	0.390
300°	W (Vertical	-0.017